



MASTER'S THESIS

Design and construction of a prototype segment for a wind tower based on a new construction method

executed in partial fulfilment of the requirements for the degree of
Master of Science in Civil Engineering

under the supervision of
O.Univ.Prof. Dipl.-Ing. Dr.-Ing. Johann Kollegger, M.Eng.
Dipl.-Ing. Ilja Fischer
Dipl.-Ing. Charlotte Schönweger

E 212 - Institute for Structural Engineering

submitted at the Vienna University of Technology
Faculty of Civil Engineering

by

Vjekoslav Janjić

Matr. Nr.: 1329484
Ive Vojnovića 1G
51 000 Rijeka, Croatia

Vienna, September 2014

Acknowledgements

I am using this opportunity to express my gratitude to everyone who supported me throughout the work on this thesis.

I would like to thank to my supervisor O.Univ.Prof. Dipl.-Ing. Dr.techn. Johann Kollegger for the useful advices, remarks and academic support through the learning process of this master thesis. Furthermore, I would like to thank Dipl.-Ing. Ilja Fischer and Dipl.-Ing. Charlotte Schönweger for their enthusiastic approach, invaluable constructive criticism and enlightening guidance.

Special thanks are given to the Institute for Structural Engineering at Vienna University of Technology for providing me the great opportunity to participate in this project.

Moreover, I would like to express my special thanks to Austria Wirtschaftsservice, the main sponsor, and the following companies for their support in the project: Oberndorfer, Doka, StekoX and Hilti.

Finally, I wish to thank my family and my girlfriend for their support and encouragement throughout my studies.

Abstract

A significant growth in the size of wind turbines has led to the development of precast concrete wind towers that overcome limitations of the current technologies of steel towers. The precast concrete wind towers are frequently confronted with the complicated transport of long precast elements to the construction sites that are mostly difficult to reach. A new approach for the construction of concrete wind turbine towers out of hollow double wall elements is currently being developed at the Vienna University of Technology. The main idea is to combine the advantages of precast elements (e.g. no formwork needed) and in-situ concrete (e.g. better fatigue behaviour). The single and plane double wall elements, which can be easily transported to the construction site, are firstly connected to polygonal rings and then assembled into an elegant tapered tower. Once a ring segment is pre-assembled, it can be placed on top of the preceding segment enabling the tower to grow by e.g. 13 m at a time. To create a monolithic structure the separate segments are then filled with in-situ concrete. This process of lifting one segment on top of the other and filling of the double wall elements with in-situ concrete is repeated until the final height of the tower is reached. The continuous filling of the segments with in-situ concrete allows the structure to rise without any joints in the core of the hollow elements, and thus providing a higher structural integrity and bearing capacity. In order to examine this new tower building technique in its feasibility and to show that this method allows economical, faster and more profound construction in comparison to the conventional construction methods the mock-up tower segment has been designed, built and tested. The experiments and evaluation of the mock-up confirmed claims about the functionality and feasibility of the proposed construction method and revealed new technical challenges that have to be addressed for the construction of the following tower segments.

Contents

1	Introduction and scope of the work	1
2	State of the art in the construction of wind towers	3
2.1	Tower configurations	3
2.2	Steel towers	7
2.2.1	Free-standing steel tubular towers	7
2.2.2	Guyed steel tubular towers	9
2.2.3	Lattice towers	9
2.3	Concrete Towers	12
2.3.1	In-situ slip form towers	12
2.3.2	Precast Concrete Towers	13
2.3.3	Semi-precast concrete towers	17
2.4	Hybrid Towers	18
2.5	Comparison of the different tower designs	19
2.6	Overview of wind tower patents	23
2.6.1	Assembly structure and procedure for concrete towers used in wind turbines (EP1889988A2)	23
2.6.2	Sectional smokestack (D4US5038540)	24
2.6.3	Prefabricated modular tower (EP1876316A1)	25
2.6.4	Method for producing concrete pre-finished parts (WO2009/121581A2)	27
2.6.5	Tower structure (DE4023465A1)	28
3	Double wall element tower construction developed at Vienna University of Technology	29
3.1	Overview of the new construction method	29
3.2	Description of a proposed prototype	31
3.3	Construction and technological challenges	35

3.3.1	Technological challenges during prefabrication of double wall elements	37
3.3.1.1	Common interconnections of double wall shells	37
3.3.1.2	Geometry	37
3.3.2	Transportation	38
3.3.3	Pre-assembling of ring segments	38
3.3.3.1	Arrangement of elements	38
3.3.3.2	Reinforcement in the last two vertical joints	39
3.3.3.3	Connection of elements in order to fix set up geometry . .	42
3.3.3.4	Sealing of internal and external vertical joints	44
3.3.4	Assembly of the tower	49
3.3.4.1	Lifting and placing of the ring segment	50
3.3.4.2	Horizontal joints	51
3.3.4.3	Proposal of scaffold and crane arrangement	52
3.3.4.4	Installation of prestressed tendons in vertical direction . .	54
3.4	Innovations and comparison	55
3.4.1	Advantages of the proposed construction method	55
3.4.2	Disadvantages of the proposed construction method	56
4	Structural analysis, production and assembly of the mock-up tower segment	57
4.1	Description of the mock-up	57
4.2	Structural analysis of the mock-up	68
4.2.1	Estimation of the required concrete cover	68
4.2.2	Estimation of normal forces in the concrete shells due to concrete pressure	71
4.2.2.1	Analytical analysis	75
4.2.2.2	Approval of analytical solution using the FEM	80
4.2.3	Structural analysis of the mock-up	82
4.2.3.1	Concrete pressure	83
4.2.3.2	Internal forces of vertical element strip	84
4.2.3.3	Internal forces of the most loaded horizontal element strip	85
4.2.4	Proofs for reinforced-concrete shells	90
4.2.4.1	Concrete shells bending proof	91
4.2.4.2	Shear resistance	95
4.2.5	Proofs for interconnection of concrete shells	98
4.3	Production of double wall elements	100
4.3.1	Positioning of formwork	100

4.3.2	Placing of the reinforcement	103
4.3.3	Concreting and aftertreatment	105
4.3.4	Connection of both shells	107
4.3.5	Concrete curing and storage of the double wall elements	110
4.4	Assembly of the mock-up	111
4.4.1	Foundation	111
4.4.2	Marking and measuring of the bottom ring segment geometry . . .	113
4.4.3	Arrangement of the double wall elements	115
4.5	Lifting and concreting of the mock-up	128
5	Evaluation and discussion	135
5.1	Comparison of planned and achieved geometry of the double wall elements	135
5.1.1	Element width	137
5.1.2	Element height	138
5.1.3	Shell thickness	138
5.1.4	Element thickness	140
5.1.5	Horizontal displacement between shells	141
5.1.6	Element weight	143
5.1.6.1	Theoretical weight of the elements	143
5.1.6.2	Measuring of the element weight	144
5.2	Evaluation of the achieved mock-up segment geometry	146
5.2.1	Segment geometry before lifting, after lifting and after concreting .	146
5.2.1.1	Observation of the deformation between concrete blocks .	146
5.2.1.2	Deformation of the segment after concreting	148
5.2.2	Joint widths before lifting, after lifting and after concreting	149
5.3	Evaluation of vertical joints	153
5.3.1	Evaluation of different joint types	154
5.3.2	Evaluation of mortar cracks in joints	159
5.3.3	Joint deformation measurement during the concreting of the segment	163
6	Summary, conclusions and outlook	169
	List of Figures	171
	List of Tables	180
	Bibliography	185

Chapter 1

Introduction and scope of the work

The wind power has been recognized as a clean, affordable, domestic and sustainable renewable source of electrical energy. The operation of wind energy gaining facilities is only accompanied by a possible visual disturbance and some other more or less negligible emissions which allow to preserve the air and water clean. Furthermore, it helps to maintain low electric rates and protects the energy market against fossil fuel price volatility. Therefore, the European Commission embraced wind energy as a reliable and cost-effective investment for the future. Their long-term ambitious target for 2050 is to reduce greenhouse gas emissions by 80 to 95% compared to 1990 levels, which requires a power sector with zero carbon emission [1]. In order to achieve this goal, wind turbine technology has become one of the most commercially developed and rapidly growing renewable energy industries worldwide.

Wind turbines capture the kinetic wind energy from the atmosphere and convert it into mechanical energy and afterwards electricity. Whereby, the energy amount depends on the observed air volume and its speed, which increases with rising height. Consequently, to provide the production of more electricity, the wind industry identified the need of increased turbine sizes, rotor diameters and tower heights. The change in size and capacity imposes special requirements for conventional wind turbine components, especially for steel towers. This trend revealed the limitations of the current technologies and led to the development of precast concrete wind towers of high performances which reduce carbon emissions and overcome heights that were not achievable for steel towers.

Based on these market requirements, a new construction method for wind towers is currently being developed at the Institute for Structural Engineering at Vienna University of Technology. This approach offers innovative solutions in the field of onshore concrete

wind tower constructions out of precast double wall elements. Wherein, the main idea is to effectively combine advantages of precast double wall elements and in-situ poured concrete. The outcome tower structure should result in lower construction costs in comparison to nowadays conventional towers out of full bodied precast elements.

The aim of this thesis is to examine the feasibility of the new construction method and to evaluate the proposed tower structure. Therefore, the mock-up tower segment is designed, built and tested. Herein, the mock-up model has to provide the evaluation of the proposed building technique and identification of technical challenges that will be confronted with a future construction of a prototype tower.

The work in the thesis is organized as follows. Section 2 refers to the state of the art in construction of conventional types of wind towers which are nowadays present in the market. Herein is presented an overview of different tower types, building techniques and patents, which are relevant for this thesis. Section 3 is devoted to the descriptions of the new construction method and the possible prototype structure out of double wall elements with accompanying technical challenges and proposed solutions. Section 4 contains a description of the mock-up structure and its structural analysis. This is followed by an overview of the production process of the double wall elements and their assembly into a ring segment. Section 5 presents and discusses the results from the experiments performed on the mock-up and an assessment of the used technical solutions. Finally, Section 6 provides a summary and conclusions with suggestions of improvements for the future ring segments.

Chapter **2**

State of the art in the construction of wind towers

A great variety of wind turbine constructions were developed in the last 30 years. This evolution was governed by the rising demand for energy and led to the construction of new types of on-shore and off-shore wind turbines. The most important construction methods for support tower structures of on-shore wind turbines is described in the following section. Consequently, the different construction types and building techniques are compared. This is followed by an overview of the patents that propose wind tower designs based on prefabricated concrete elements.

2.1 Tower configurations

The modern use of renewable wind energy demands the construction of taller and stronger towers (Fig. 2.1). New developments in turbine technology have caused the evolution of new tower designs that have started to replace conventional solutions out of steel. The wind industry recognized concrete, as a competitive option, in order to construct sophisticated wind farms.

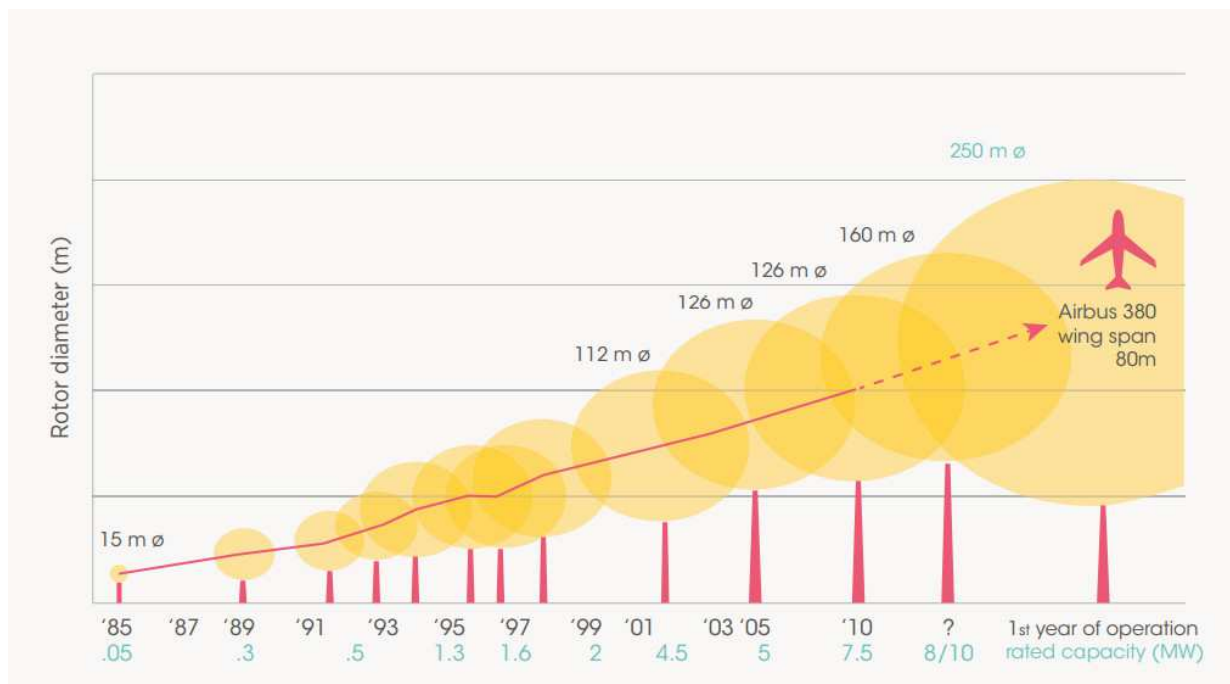


Figure 2.1: Growth in the size of the wind turbines since 1985, taken from [2]

Wind turbines consist of four main parts: foundation, tower, nacelle and blades (Fig. 2.2). The tower shaft, which is an essential component of a wind turbine, consists of numerous different elements. These elements have to satisfy the requirements of strength, stiffness, fabrication and erection.

The foundation is designed according to the local ground conditions and the size of the wind turbine. Depending on geological conditions, like depth and soil layers, either slab or pile foundations are used. Whereby the size of the wind turbine defines the size of the tower, and therefore, the loading of the foundation. Furthermore, big loaded towers are equipped with pre-stressed strands that use the foundation as an abutment.

The nacelle is the housing of all energy generating components, including generator, gearbox, drive train and brake assembly. These are the highest stressed components of wind turbines because all forces and moments are concentrated around the rotation axis. The mentioned dynamic loadings of the nacelle, like breaking deceleration or vibration during the generation of electricity are of importance for the structural analysis.

The wind turbines usually operate with two or three blades. They are typically produced from fiberglass-reinforced polyester and epoxy resin. The rotor hub connects the blades with the rotor shaft, which has a spin rate of 10 to 25 revolutions per minute [2]. The radius of the wind turbine blades has increased over time (Fig. 2.1) and depends on a variety of aerodynamic conditions.

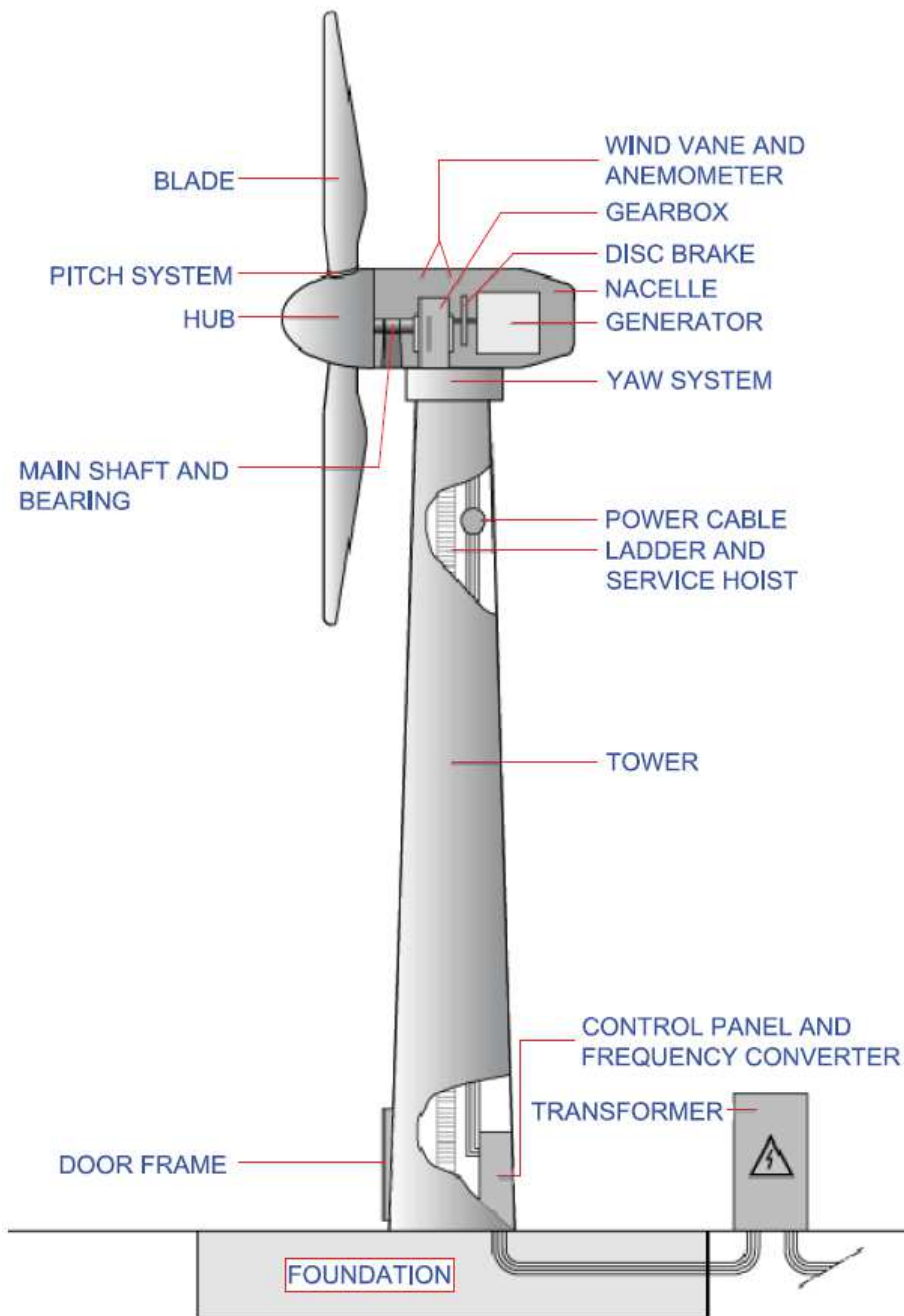


Figure 2.2: Components of a horizontal-axis wind turbine, taken from [3]

The effective overall wind turbine costs are governed by the energy yield compared to the costs of the erection at the foreseen location. The cost of the tower itself is estimated to be 20% of the overall turbine costs [4]. Wherein, the costs are sensitive to the complexity of transport and assembly. There is no universal rule for the optimal tower height because the most important parameters are individual for each project.

To realize an economic construction it is necessary to achieve the desired tower height with the required stiffness, at the lowest possible construction costs. The stiffness and the economical achievable height is depending on the used materials and design of the tower. Nowadays, the most common materials used for tower designs are structural steel, reinforced or pre-stressed concrete and combination of both– hybrid configurations. As a result, these tower designs are described in the following sections.

Steel towers are used for heights up to 100 m, while hybrid and concrete towers are used for taller wind turbines. Therefore, it can be easily shown that there is a correlation between the used construction types (Fig. 2.3) and the tower height, which corresponds with the energy output capacity (Fig. 2.4). Besides previously mentioned designs, there are various special designs, but the wind market has recognized the following types presented in the Fig. 2.3 as the most rational and effective.

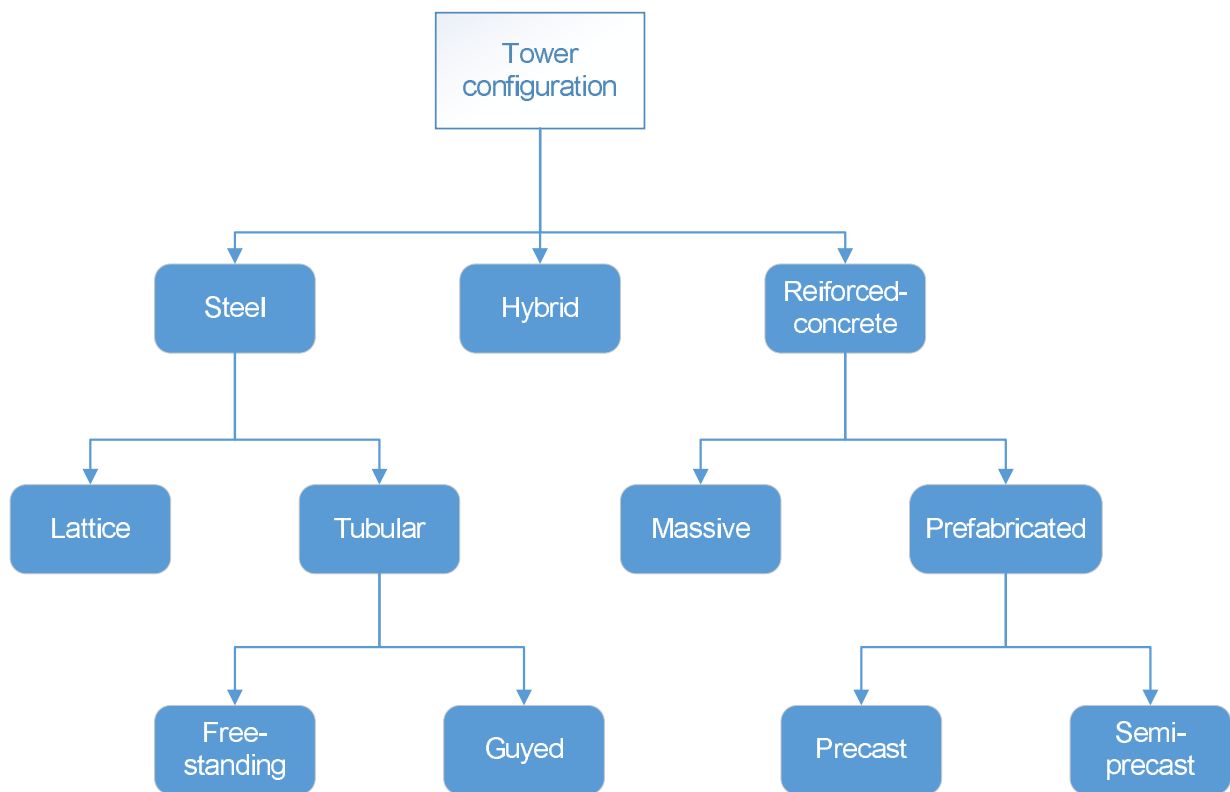


Figure 2.3: Configuration of the most important tower designs

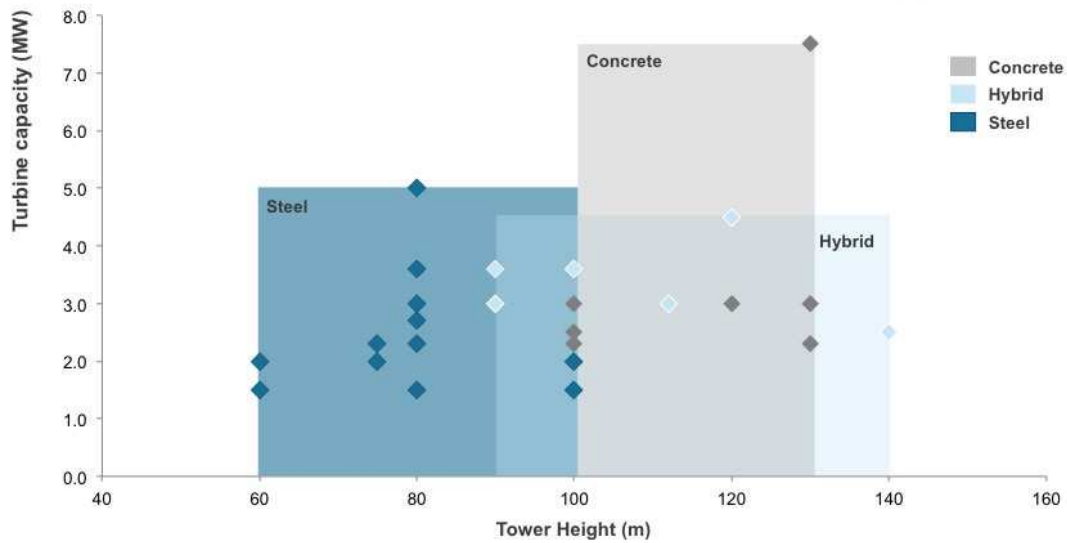


Figure 2.4: Relation between height and output capacity of a wind turbine, taken from [5]

2.2 Steel towers

2.2.1 Free-standing steel tubular towers

Free-standing tubular towers are the most preferred type of construction for wind turbine installations due to their short assembly and erection time. They have a tapered form that gradually narrows with the increase of height. Small towers, with a height up to 20 m, are usually prefabricated as one piece and connected with the foundation at the site. On the contrary, high towers up to 100 m, consist of several sections that are connected by bolts so that no on-site welding is required. The structural analysis of the tower has to satisfy numerous requirements like: breaking strength, fatigue demands, stiffness, and buckling strength [4].

The construction consists of prefabricated steel ring segments with a length up to 30 m. The ring segments are produced from steel sheets with a thickness that varies from 8 mm at the top to 65 mm at the base [6]. The steel sheets are rolled into the required cylindrical shape. The resulting vertical gap is welded by automatic welding machines (Fig. 2.5(a)). The diameters up to 4 m do not have special requirements for traditional steel manufacturers. At greater heights the tower base diameter becomes wider than 4.5 m and the required thickness of steel exceeds 40 mm. The production of such geometries demands special roll bending machines, which are rare and expensive (Fig. 2.5(b)).

Due to high loading, high steel grades are used. Usually, the tower is made out of steel St 52 (S 355), while higher strength materials are used for detail constructions and for the segments at the bottom near the foundation.



Figure 2.5: Steel tower; (a) bolt connection between segments, taken from [7]; and (b) rolled 40 mm thick steel sheet, taken from [8]

A very important factor for the maintenance of steel towers is the need of a special surface treatment, especially for off-shore wind towers. The corrosion protection is achieved with a thermally applied zinc coating and two or three different paint coatings.

The transport of the complete tube segments is usually performed by road (Fig. 2.6). This results in restraints for the geometry and the maximum transportable mass. A diameter of 4.3 m, a mass of about 60 t and a length of 25 m should not be exceeded.



Figure 2.6: Transportation of a steel tower segment, taken from [9]

2.2.2 Guyed steel tubular towers

Guyed turbines are characterized by the usage of guy steel cables or stiff trusses, which ensure the required bending stiffness (Fig. 2.7(a) and 2.7(b)). These towers are mainly constructed as steel tubular towers. Not so common are guyed towers out of concrete or with a steel lattice structure.

With respect to the material usage, towers with bracings represent the most efficient structures. Therefore, such structures are very slender and cast a very small shadow. The big downside is that the whole structure requires a large area to accommodate the guy cables and anchors with foundations, which is a problem in agricultural areas. Due to the high price of the complicated anchoring of cables in the foundations these towers are not cost-efficient.

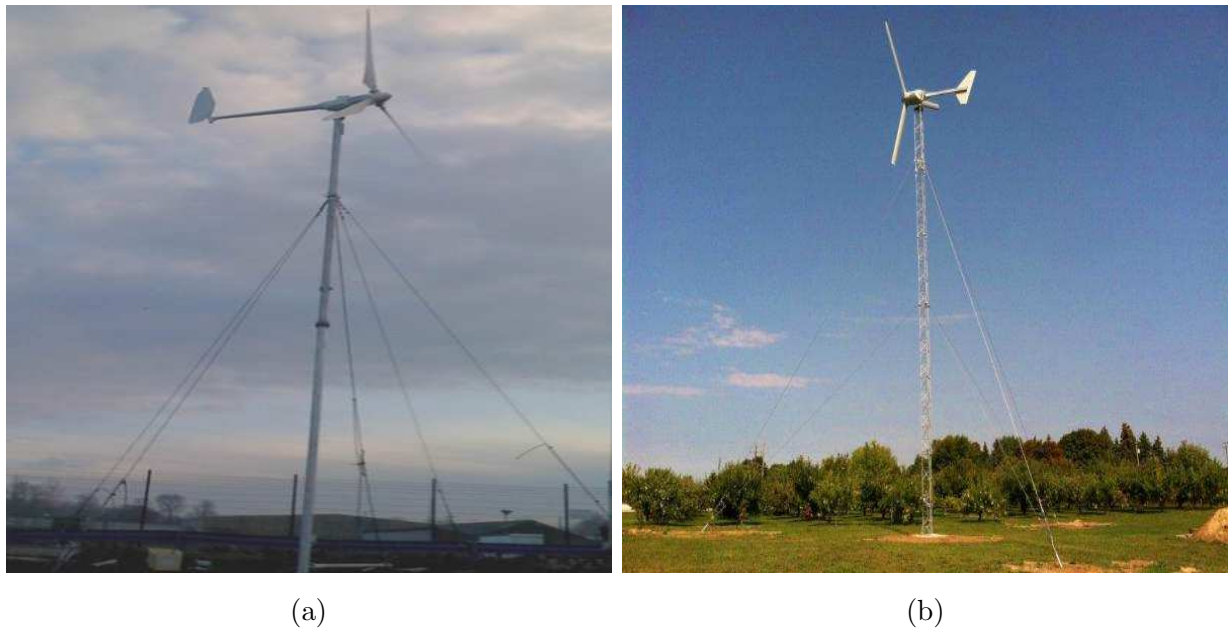


Figure 2.7: Guyed steel towers; (a) with a tubular design, taken from [10]; or (b) with a lattice design, taken from [11]

2.2.3 Lattice towers

Lattice or truss towers are constructed from steel profiles, which are connected by bolts or welds (Fig. 2.8(a) and 2.8(b)). Throughout history they were widely used for small turbines, but as their size increased they were displaced by tubular towers. Nowadays, lattice towers are considered mostly for a turbine with hub height higher than 100 m or as a segment of a hybrid structure [4].

The lattice configuration offer cost and structural advantages over conical tubular towers. The wind loading can be significantly reduced because of the large open space between the members. Truss constructions represent a material saving way to build tower structures. Up to 40% of mass can be reduced in comparison to fully bodied steel forms. Therefore, foundations can also be designed less massive. Another considerable advantage is the easy transport of the single members by regular construction vehicles [4].



(a)

(b)

Figure 2.8: Steel lattice towers; (a) Fuhrländer Wind Turbine Laasow, taken from [12]; and (b) one bolted connection in Wind Turbine Laasow, taken from [13]

The main reason for minor use of this tower design is their unpleasant visual appearance, although from greater distance they begin to merge with the background. Moreover, the assembly process of truss towers is more complex and requires more time. In addition they demand a huge amount of maintenance, especially in cold or offshore regions, [4]. Despite all of that, the world's tallest wind tower is a steel lattice tower, Fuhrländer Wind Turbine Laasow in Germany, with a hub height of 160 m (Fig. 2.9), stated by [14].



Figure 2.9: Fuhrländer Wind Turbine Laasow in Germany, taken from [14]

2.3 Concrete Towers

Concrete structures offer the possibility to design towers of great height at low maintenance costs. A greater height also means that a greater structural strength and self-weight is needed to resist wind- and therefore bending loads. In addition, higher loads from larger rotors and blades, which can cause damaging resonance effects, need to be deflected. Therefore, a bigger cross-section diameter is needed. This results in a transportation problem for usual tubular steel segments. For these reasons concrete, as a versatile material, represents an economical solution for both onshore and offshore wind turbines [15].

Structural concrete can be used without reinforcement, with reinforced steel bars or other appropriate materials and pre-stressed (with tensioned steel bars or tendons). Its structural performances can be designed from normal to very high structural grade, depending on desired properties. According to the place of production it can be site-mixed or delivered in liquid form with special vehicles or prefabricated.

All of the mentioned methods have a significant impact on the needed construction technology, as well as on the required building time. In-situ concrete techniques with slip-form and self-climbing formwork provide valuable solutions in case of limited site access where transportation of large construction elements is problematic. On the other hand, precast towers offer considerably shorter building time independent of unfavourable weather conditions [4].

2.3.1 In-situ slip form towers

A slip form is an in-situ casting method where formwork is raised vertically in a continuous process (Fig. 2.10). It is suitable for very high-rise structures with various shapes of sections [16]. Slip formwork systems enable the vertical extension of reinforced concrete elements by using hydraulic jacks to climb, making heavy cranes unnecessary for tower erection. It can be an entirely crane independent process, therefore the height of the tower is not limited by crane capabilities. Another advantage is the absence of vertical and horizontal joints, which is usually the biggest challenge of precast construction techniques [15].

The minimum achievable wall thickness is in the range of 150 to 175 mm for normal concrete grades and conditions, without the use of additives. Smaller thicknesses would cause the growth of horizontal cracks during the elevation of the slip form on higher levels. This construction method enables output rates of 4 to 6 m height per day [15].



Figure 2.10: In-situ slip form method, taken from [17]; (a) concrete tower; (b) slip formwork; and (c) working platform in slip formwork

2.3.2 Precast Concrete Towers

The manufacturing process of elements prefabricated in the factory offer a high degree of accuracy during erection with minimal dimensional tolerances. The elements are usually piled up on each other on site and connected with concrete/resin mixture or with dry joints [4]. The precast elements can be easily delivered on site by road with usual construction vehicles. One of the most successful manufacturers of concrete towers are Enercon from Germany and Inneo Torres from Spain.

Inneo Torres is the biggest Spanish manufacturer of precast concrete towers for onshore and offshore wind turbines. It was founded in 2004 and has installed more than 150 towers. They offer concrete towers for heights between 80 and 140 m, which can support wind generators from 1,5 MW to 5 MW. Inneo has developed a fast and reliable assembly process where the erection of the tower sections can be completed in one working day [18]. These towers consist of segments with a length up to 20 m. Such precast elements can be easily transported to the building site, sparing special transport permissions (Fig. 2.11(a)).

The first assembly phase consist of the unloading of the precast elements from the truck, lifting and placing of the elements on the top of the foundation by ensuring the required geometry (Fig. 2.11(b)). The process ends with the filling of the vertical joints. The rest of the segments are placed to the ground near the tower where they are assembled and prepared for erection (Fig. 2.11(c)) [18].

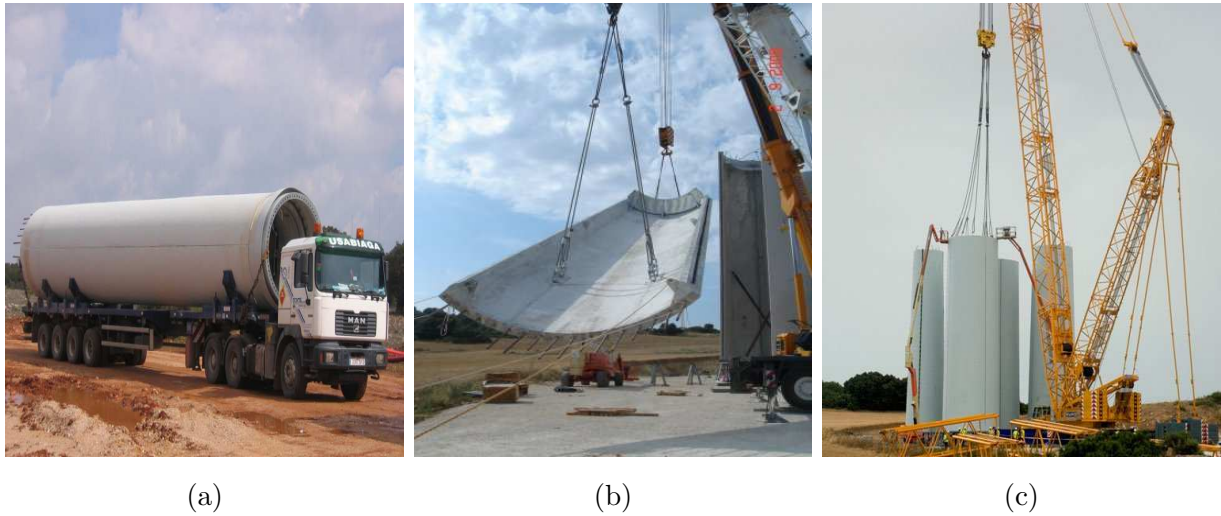


Figure 2.11: Inneo towers, taken from [18]; (a) transportation of precast elements; (b) erection of precast elements; and (c) the first assembly phase of a concrete tower

In the tower erection process each tube section is raised and placed on the top of the tower until the final height is reached (Fig. 2.12(a) and 2.12(b)). The capacity of the cranes that are required for the erection of the segment is lesser than 300 t. Horizontal joints are constructed with embedded bars that provide a stable and monolithic structure with a good dynamic behaviour and fatigue strength. When this process is over, the tower is ready for the assembling of the nacelle and blades. These tower structures are constructed without any need for vertical and horizontal post-tensioning (Fig. 2.12(c)) [18].

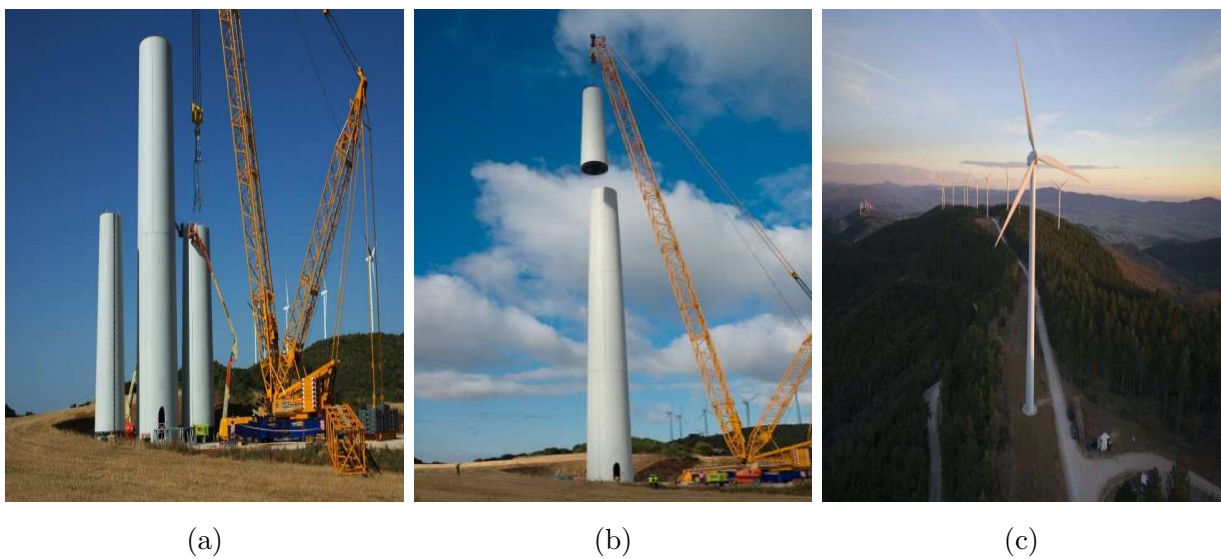


Figure 2.12: Inneo towers in assembly process, taken from [18]; (a) working environment; (b) tower erection; and (c) assembled wind turbine

The company Enercon is one of the leading manufacturers of steel and concrete wind turbines on an international level. In its 30 years of existence Enercon has installed more than 22,000 wind turbines providing a power of 32.9 GW in over 30 countries worldwide (Figure 2.13).

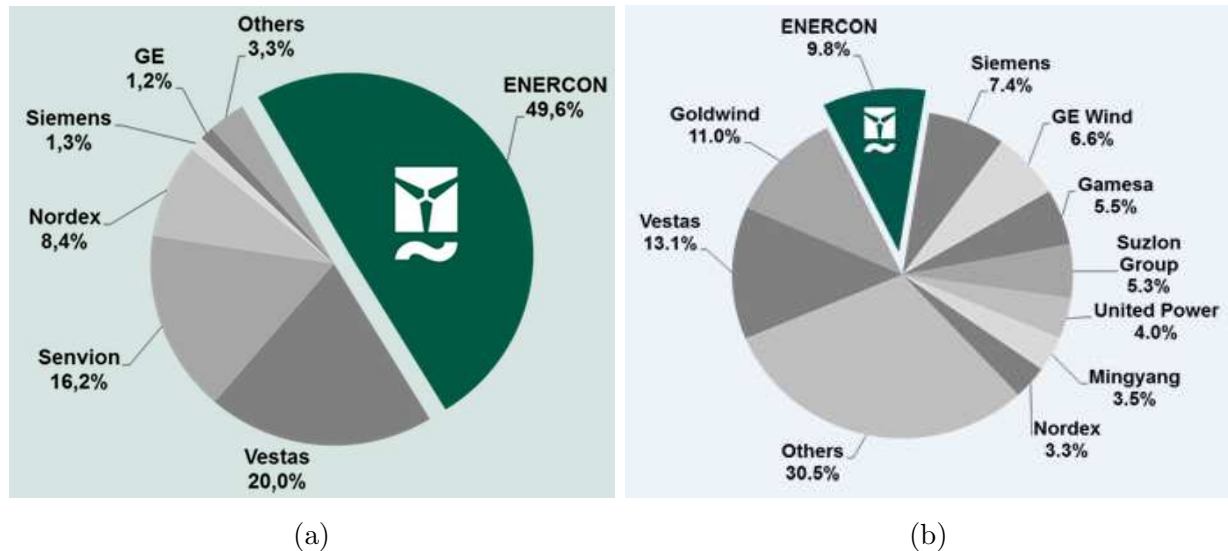


Figure 2.13: Enercon market share, taken from [19]; (a) in Germany 2013; and (b) worldwide 2013

This concrete tower pioneer manufactures pre-fabricated concrete towers with diameters up to 14.5 m. All elements are produced under controlled industrial conditions. Segments with a large diameter are manufactured in two half shells so that they can be easier transported to locations that are difficult to reach.

The assembly of the segments is performed on a construction site with the assistance of cranes. Afterwards, the precast concrete shells are connected into an inseparable unit by means of pre-stressing tendons. Tendons are passing through embedded ducts in the walls and they are grouted to provide effective corrosion protection. The joints between individual elements are sealed with epoxy resin in order to ensure a transmission of compressive stresses [20].

The wind turbine Enercon E-126 is the largest concrete onshore wind turbine type in the world (Fig. 2.14). The concrete tower has a hub height of 138 m, and rotor diameter of 127 m. It is also the most powerful wind turbine type in the world that generates 7.58 MW of power and its list price is \$14 million plus costs of installation [21].

The prototype of this turbine was installed in Emden, Germany in 2007. Until June 2012, Enercon has already installed more than 147 of these turbines. The total weight of E-126 is about 6000 t. Whereby, the weight distribute 2500 t to the foundation, 2800 t

to the tower, 128 t to the machine housing, 220 t to the generator and 364 t to the ring including the blades [21].



Figure 2.14: Enercon E-126, taken from [22]

The prefabricated tower E-126 consists of 35 concrete rings, with walls up to 45 cm thick, and one steel bearing connector (Fig. 2.15), [23]. The diameter of the ring is 14.5 m at foundation and narrows to a slender 4.1 m at the top. The lowest rings are composed of

three 120 degree sections, the middle ones of two 180 degree halves, while the upper rings are manufactured in one circular piece. The joints between the segments have the form of pockets which are filled with rapid hardening high-strength mortar after each segment has been aligned and after the vertical reinforcement has been installed [24].

All tower elements are pre-tensioned with steel tendons that pass through holes in the precast concrete walls. Afterwards, all spaces between the cables in the walls are sealed with concrete grout. An elevator capable of transporting up to four persons to the nacelle is situated in the tower [24]. The erection crew consists of the installation team that counts between 100 to 120 workers [25].

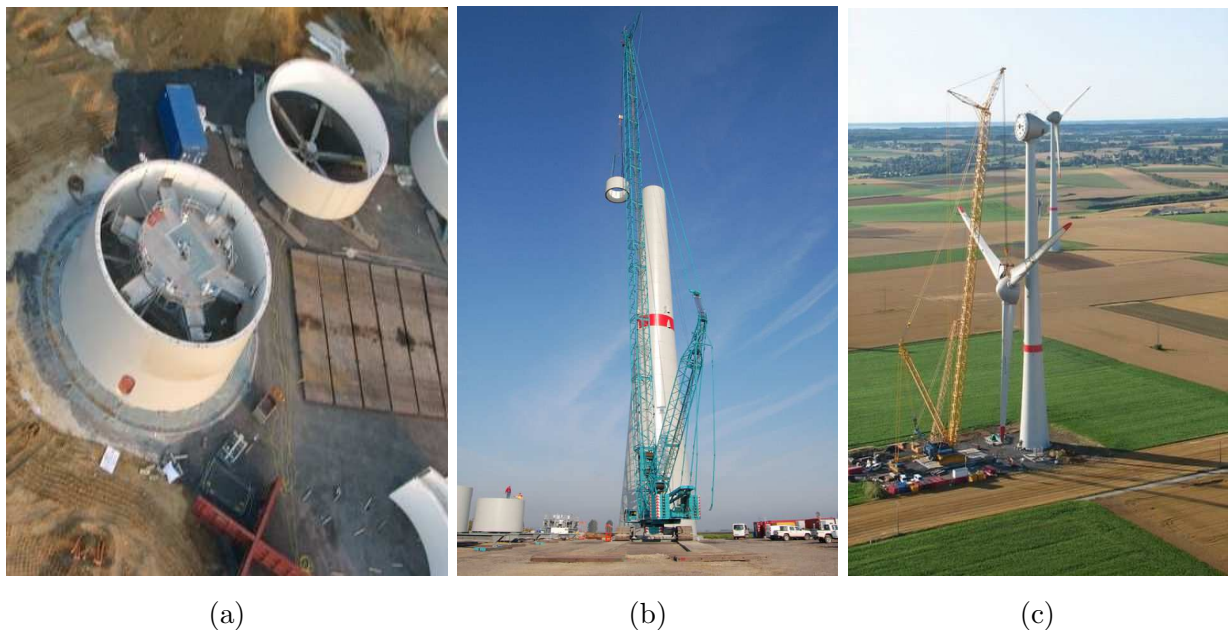


Figure 2.15: Enercon E-126 during construction, taken from [18]; (a) concrete ring segments from the air; (b) assembly process; and (c) erection of the nacelle

2.3.3 Semi-precast concrete towers

Semi-precast concrete towers consist of precast concrete elements and in-situ poured concrete. This innovative technology is being developed at Vienna University of Technology and it will be described in the Chapter 3.

2.4 Hybrid Towers

Hybrid wind towers are composed of concrete and steel elements which participate together to provide the total load bearing capacity, trying to implement benefits of both materials. Concrete elements are positioned in the lower sections of the tower, while steel segments constitute the upper parts that are connected with the nacelle [23]. Companies that produce and install hybrid towers are Advanced Tower System, Max Boegl, Nordex, Repower, ect.

In order to construct the highest hybrid wind turbine tower three companies; Mecal, Hurks beton and JUWI launched a mutual pilot project and established the company Advanced Tower Systems (ATS). They built the hybrid tower with a hub height of 133 m and rotor diameter of 93 m, which generates the power of 2.3 MW at the wind power test site Grevenbroich near Düsseldorf, Germany (Fig. 2.16). The project took place in 2008 and it was finished in 2009 when the tower was connected to the electricity net [26].



Figure 2.16: ATS wind tower during construction, taken from [18]; (a) assembling process; (b) placing of the nacelle; and (c) assembled tower

The lower part of the tower is 74 m high and consists of precast concrete elements, while the upper part is a 55 m high steel tower (Fig. 2.16(a)) [26]. These individual parts are joined together with a 50 t reinforced concrete adapter that is 2.5 m high [27]. The precast concrete segments of the tower include plane and round shaped elements. The

corner elements are rounded and they have the same geometry over the whole height of the tower. Whereby, the flat elements wide is linearly changing with height [26].

Each of the 40 individual height strength concrete elements is 15 m tall, which enables their easy transport by conventional trucks. The segments are pre-assembled and temporarily connected by bolts, and later on post-tensioned with Dywidag tendons at each corner of the tower. After installation of the tendons all ducts are subsequently grouted and sealed to assure an appropriate corrosion protection [26].

2.5 Comparison of the different tower designs

This section provides an overview and comparison of the relative advantages and disadvantages of steel and concrete towers. Hybrid towers can incorporate the advantages from both concrete and steel towers, by implying in general higher costs due to material and structural diversity.

- **Fabrication**

Steel towers are manufactured by a well-established technology in a factory under controlled conditions. They are prefabricated in large sections and connected with bolts or welded at the site, which may cause imperfections during execution. For larger diameters and higher wall thickness special manufacturing equipment is required [15].

Concrete towers can achieve larger diameters without a disproportionate increase of cost. Slip formed concrete towers can accommodate section changes relatively easy even during the construction process. They require a high initial investment in formwork that can be reused and therefore it is profitable only for a large amount of tower units or segments of precast towers (Fig. 2.3) [15].

- **Transportation**

Small segments of steel towers are lightweight and can be easily transported to the site. For diameters larger than 4 m transportation by road is difficult or sometimes impossible which is not the case for lattice towers that are constructed from steel profiles.

Precast concrete elements can be easily adjusted to transportation requirements, while in-situ slip-formed concrete towers do not require transportation at all. However, precast constructions are sometimes not feasible when there is no local manufacturer due to the high cost of transportation to long distances.

- **Installation**

Tubular and lattice steel towers are assembled and erected with cranes. Tubular towers, which are transported as a whole tube, can be constructed in a relatively short period of time. On the opposite, lattice tower demand longer assembling time due to a large number of joints.

Precast concrete towers are usually pre-assembled on a construction site and then erected with cranes. Slip-formed concrete towers are crane independent because they use hydraulic jacks for the erection of formwork and working platform.

- **Maintenance over design life**

Steel constructions have to ensure appropriate corrosion protection which consists of zinc coating and paint coats. A significant problem for both tubular and lattice constructions is the low fatigue resistance of the connections. Therefore, the typical design life of steel towers amounts to about 20 to 30 years. Afterwards, steel towers can be dismantled and recycled [15].

Concrete towers are highly durable constructions with very little maintenance requirements. The design life of concrete can be estimated to range between 50 to 100 years, so when the turbine needs to be replaced, it is possible to dismantle the old-one and mount a new turbine. The dismantling process of a concrete wind tower is more complicated and request more time than for steel towers [15].

- **Costs**

Steel tubular towers are produced at a specific cost less than \$1.5/kg, while concrete towers have specific cost of about \$240 to 400/tonne (values from the year 2006) [4]. The specified price ranges can not be directly compared because concrete towers have a greater mass for the same height. The cost of the lattice design is approximately 20% less than the cost of steel tubular towers, but with higher assembly and maintenance costs. It should be taken into consideration that these values are outdated, because the price of steel has increased in recent years, while the price of concrete remained almost the same. Generally, concrete towers are the most cost-effective, particularly the precast concrete solutions. Wherein, the economic optimum can be only reached by choosing a tower design that suits to the to the conditions at the site.

- **Environmental impact**

One of the basic reasons of operating wind towers is to decrease CO_2 emissions and make a contribution to a more sustainable future. The comparison of quantities of

CO_2 embodied in structural steel and reinforced concrete is presented in the Table 2.1.

Table 2.1: Embodied mass of CO_2 by mass of material $kgCO_2/t$, taken from [15]

Structural material	Reinforcement content			
	none	low	high	average
Concrete (C32/40)	140	150	156	153
Structural steel	1932	-	-	-

The obtained values can not be directly compared because, for the same height, mass of a concrete tower is considerably greater than the mass of a steel tower. Therefore, the Table 2.2 shows a comparison of embodied CO_2 for a 70 m tall tower.

Table 2.2: Embodied mass of CO_2 for 70 m tall tower, taken from [15]

Wind tower option	Mass of construction materials		Mass of embodied CO_2 (t)
	Structural steel (t)	Reinforced concrete (t)	
70 m steel tower	125	-	242
70 m concrete tower	2	550	88

Embodied levels of CO_2 in concrete towers can be remarkably lower than for the steel towers (64 %) (Table 2.2). During carbonation process concrete consummates CO_2 from the atmosphere especially if we use recycled or crushed concrete. The British Cement Association state that for all types of concrete, the average consumption is 20 % of the CO_2 emitted from its cement manufacture.

From an environmental aspect it is important to mention that concrete towers generate less noise from rotating blades due to the concrete damping effect [28].

• Performance

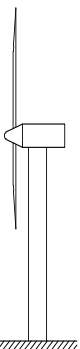
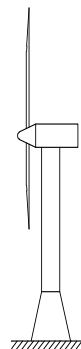




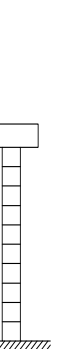
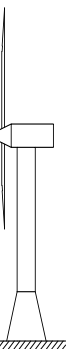
Structural characteristics of various types of tower designs depend on the used material, diameter, height, wall thickness, mass, and rotor speed. Performance like stiffness and dynamic behavior of the overall tower structure depends upon the features of the pylon-tower and foundation. [4]

Steel tubular and pre-stressed precast concrete towers are usually dimensioned as soft towers with a first natural bending frequency of approximately 0.67 Hz. In-situ

reinforced concrete towers without pre-stressing have higher stiffness of approximately 0.4 Hz. Concrete can offer higher material damping properties than steel, while pre-cast concrete has a high fatigue resistance and therefore reduced dynamical effects [4].

Although a free-standing cylindrical tube with a constant wall thickness may be simple to manufacture, mass comparison of the tower reveals that other configurations enable lighter towers. Guyed towers provide a significantly reduced diameter and wall thickness, but they require additional foundations what makes them cost-inefficient. The conical geometry is optimal, and therefore, this design can be found in most wind turbines.

Table 2.3: Comparison of steel and concrete tower designs, taken from [4]

Wind turbine		Steel				Concrete			
Rotor: 3 blade		Cylindrical	Cylindrical with conical base	Conical	Cylindrical with guys	Lattice	Prefabricated prestressed	Reinforced	Prestressed
Blades diameter: 60 m									
Rotor speed: 23 rpm									
Towerhead mass: 180 t									
Hub height: 50 m									
Tower height: 46.6 m									
1st bending eigenfrequency Hz		0.567	0.577	0.570	0.551	0.600	0.650	0.941	0.947
Multiple of rated rotor speed P		1.48	1.51	1.49	1.44	1.57	1.70	2.45	2.47
Upper tower diameter	m	3.5	3.5	3.5	2.5	3.5	3.5	3.5	3.5
Lower tower diameter	m	3.5	7.1	4.4	2.5	11.6	3.5	8.4	5.5
Wall thickness	mm	55 + 15 staged	25/15 staged	30/15 staged	20/15 staged	16/10	520/250 staged	300	300
Mass									
-Tower structure	t	150	120	111	40	110	465	485	477
-Equipment	t	22	22.5	22.8	20	22.5	21	22.5	22.5
Total mass	t	172	142.5	133.8	60 + guys	ca. 120	486	507.5	499.5
Approximate const relation	%	100	90	85	95	70	60	75	75

2.6 Overview of wind tower patents for prefabricated concrete elements

An overview of the most important patents for wind towers in conjunction with prefabricated concrete elements, which are of interest for this thesis, is given in the following subsections. Some of them describe new construction techniques, while other ones suggest the usage of new materials, erection technologies and innovative shapes. The description of each patent is accompanied with the main features of the innovation that ensures exclusive rights assigned by the International Intellectual Property Office.

2.6.1 Assembly structure and procedure for concrete towers used in wind turbines (EP1889988A2)

The structure and procedure for the erection of a wind concrete tower that is put together by sections, which are composed of various elements is the object of the following patent [29]. The procedure includes two construction cycles, which can be performed simultaneously: the pre-assembly of one tower section and the assembly of the tower. The sections are pre-assembled on the ground with the assistance of bracings and mechanical jacks (Fig. 2.17(a) and 2.17(b)). Afterwards, all the pre-assembled segments are stacked on each other until the complete tower is formed (Fig. 2.17(c)).

Features of the patent:

- The first segment can be pre-assembled directly on the tower foundation, while other sections are pre-assembled on mounting bases, which are placed on the ground in close proximity to the tower.
- The following tower sections are positioned with the crane and connected with the underlying ones. Two neighbouring segments are connected by reinforcement that protrudes through the upper segment into openings at the top of the lower segment.
- The final section can be pre-assembled at the factory and erected directly from a transportation vehicle.
- Pre-assembly and erection cycles culminate with the execution of the vertical and horizontal joints with an appropriate mortar that together with corresponding reinforcement achieves an effective connection between the different segments.

- The correct positioning of the segments and sections is secured by transmitters or with a self-levelling vertical laser beam. Whereby the stability of the first two elements is achieved with adjustable struts.

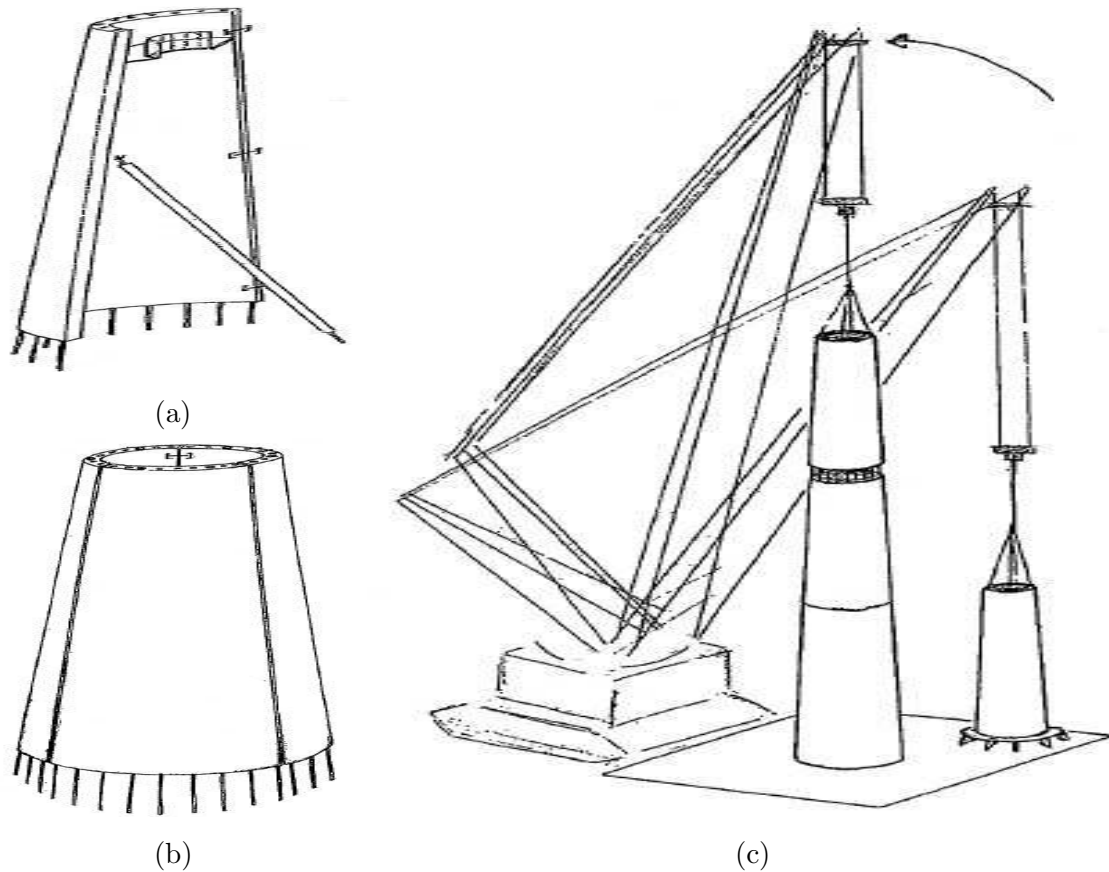


Figure 2.17: Prefabricated modular tower, taken from [29]; (a) element with strut; (b) pre-assembled tower segment; and (c) tower assembling

2.6.2 Sectional smokestack (D4US5038540)

The assembly of multiple precast concrete segments that are stacked axially one upon the other and aligned with vertical ribs, is the object of the sectional smokestack patent [30]. Each rib contains concentrated reinforcement that is extended vertically through apertures over the entire height of the smokestack (Fig. 2.18(a) and 2.18(b)). Every segment has embedded structural tie rods which are extended laterally into the aperture on the opposite sides of the concentrated reinforcement to transfer wind and heat stress loads to the reinforcement in vertical ribs. The precast segments are assembled at the construction site.

Features of the patent:

- The smokestack consist of precast sections that are axially stacked one upon the other (Fig. 2.18(c)).
- Each section has vertical rib members integrally formed in the segments (Fig. 2.18(d)).
- Each rib member has an aperture for concentrated reinforcement which extend longitudinally in an axial direction of the smokestack.
- Structural tie rods, which are extended outwardly from each segment, are used to tie adjoining segment together and form the integral section.

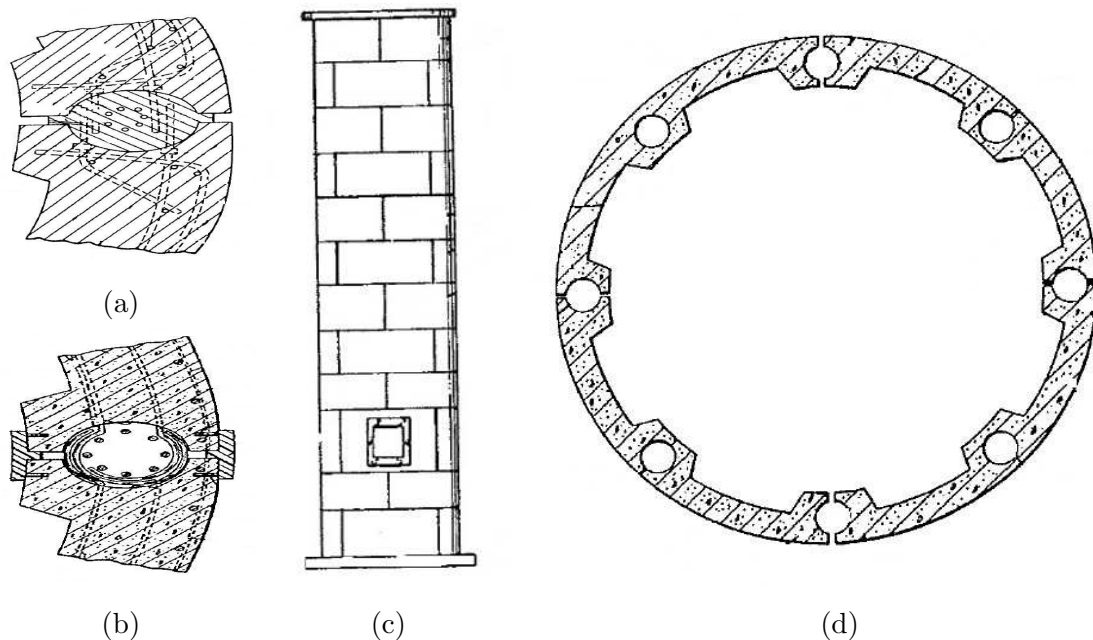


Figure 2.18: Prefabricated modular tower, taken from [30]; (a) and (b) proposed details of vertical joint; (c) assembled tower; and (d) cross-section

2.6.3 Prefabricated modular tower (EP1876316A1)

A prefabricated modular concrete tower, characterized by slim or loading optimized cross-sections, is presented in this patent (Fig. 2.19) [31]. Every element is reinforced and tensioned in vertical and horizontal direction. This tower is divided into a small number of tapered parts that are laterally connected from identical prefabricated modular elements. The patent proposes an exemplary tower, which is 100 m tall, composed of only 13 prefabricated modular elements, produced with only three different manufacturing moulds. The

tower is divided into three tapered parts with a height of approximately 35 m each. The lower and the intermediate parts of the tower are formed of five identical prefabricated modular elements, while the upper part is formed by three elements.

Features of the patent:

- Enables a fast construction of very high towers using a limited number of relatively lightweight elements that can be easily transported.
- The external wall is smooth, while the internal wall has numerous prominent horizontal and vertical reinforcement stiffeners that allow the reduced thickness of the elements with high rigidity and resistance.
- The approximate height of the elements is 35 m, while the maximum width is 4.5 m in order to satisfy transportation requirements.
- The vertical cables are integrated in the tower walls and subsequently filled with mortar.
- Horizontally arranged reinforcement stiffeners in each of the elements have a central longitudinal tube to provide space for horizontal tensioning cables, which span the elements together.
- Vertical joints between each element of the sections are executed right after the elements are arranged: firstly they are sealed from outside and inside and then filled with liquid cement sealant.

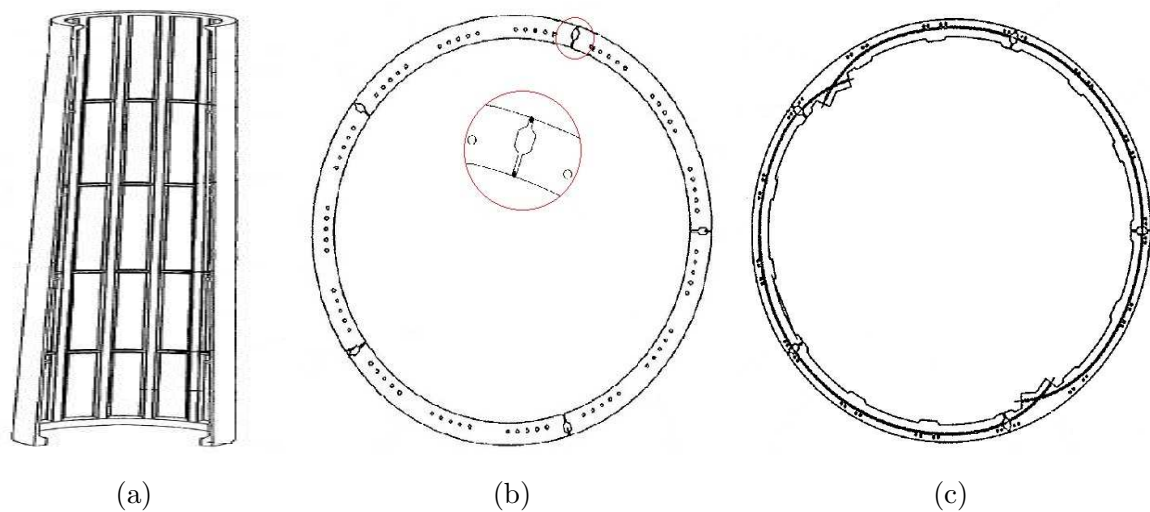


Figure 2.19: Prefabricated modular tower, taken from [31]; (a) longitudinal cross-section; (b) and (c) proposed horizontal cross-sections of ring segment

2.6.4 Method for producing concrete pre-finished parts (WO2009/121581A2)

A new way to produce pre-finished concrete elements with a reduction of tolerances, applicable for the tower structures is described in this patent (Fig. 2.20) [32]. To achieve the wanted accuracy special moulds and equalizing layers are used. The concrete is poured into a mould with a planar bottom. When the concrete reaches a defined strength the equalization layer out of mortar or synthetic resin can be applied to the side opposing the planar surface of the mould. After equalization layer reaches the predetermined minimum strength, the precast concrete wall segment is placed on a horizontally oriented surface and the equalization layer on the top side is polished until the top and the bottom side is parallel to each other. All working steps are preferably performed in a factory under controlled conditions.

Features of the patent:

- Easier and faster erection of a tower from precast concrete parts.
- Polishing of the equalization layer is carried out with a milling device that has a milling head, which can be precisely navigated in all directions.
- The method provides uniform quality of the precast concrete parts with very small tolerances, thus excluding an imperfect geometry.

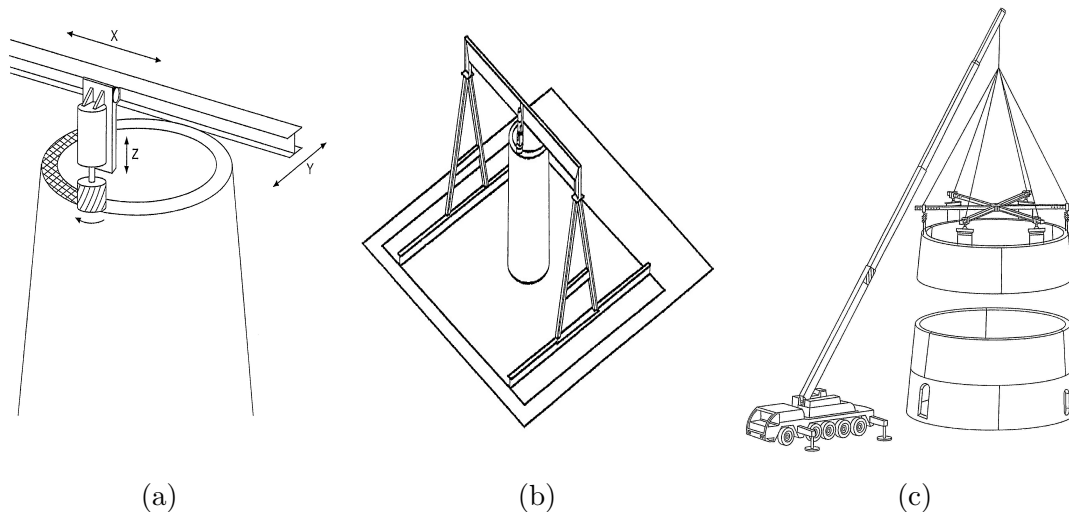


Figure 2.20: Method for producing concrete pre-finished parts, taken from [32];
(a) milling head in operation; (b) working platform for the polishing; and
(c) tower assembly process

2.6.5 Tower structure (DE4023465A1)

This innovation describes a tower structure with polygonal cross-sections, built from composite concrete-steel elements [33]. The elements are made of prefabricated double wall panels that are arranged one above another and filled with in-situ mixed concrete. Vertical supports of the elements are placed in the middle of the core layer or on the vertical edges as edge supports that connects adjacent wall elements.

The proposed method enables a construction of a tapered tower shape because there is no need for formwork. The feasibility of this method is questionable because there is no description of the construction process. Herein, one could ask how it is geometrically possible to position the vertical columns and the conical plane double wall elements. (Fig. 2.21)

Features of the patent:

- The polygonal horizontal cross section are composed of easy transportable double wall elements that are filled with in-situ mixed concrete.
- Vertical columns, which are embedded in the in-situ concrete, are extended over the entire height of the tower and they connect inner with the outer side of the double wall elements.
- Edge supports can be designed as steel profiles, prefabricated reinforced concrete parts or as welded composite elements. These supports connect adjacent wall elements and they can be extended to the outer shell surface and/or to the inner shell surface.

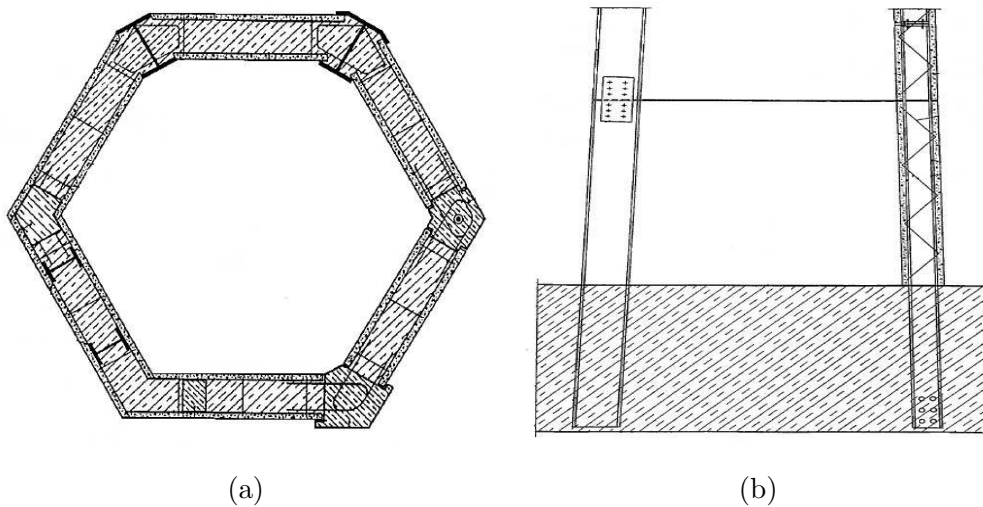


Figure 2.21: Tower structure, taken from [33]; (a) cross-section of a ring segment; and (b) longitudinal section of the tower

Double wall element tower construction developed at Vienna University of Technology

A new construction method, developed at the Institute for Structural Engineering at Vienna University of Technology, offers innovative solutions in the field of wind tower constructions. This method is currently being under development, although the basic concept is already protected and can be found under the patent number DE WO 2014067884 A1 in the Austrian Patent Office [34]. To evaluate the feasibility and cost effectiveness of this new tower building technique, a mock-up and a prototype will be built. The concept of fabrication and construction process of the tower structure is the object of the following chapter.

3.1 Overview of the new construction method

The main idea of this new approach for the construction of towers is to combine the advantages of precast double wall elements and in-situ concrete. Therefore, standard and plane double wall elements are used. Precast double wall elements have already demonstrated their advantages in the previous projects, for example in the balanced lift method, developed at the Institute for Structural Engineering at Vienna University of Technology [35].

The light-weight double wall elements can be easily transported to the construction site by usual construction vehicles, where they can be connected to form a polygonal ring segment (Fig. 3.1). This construction out of hollow double wall elements allows installation of continuous reinforcement through the whole tower structure. During pre-assembling, the elements have to be arranged in the accurate position and, if required, angled to form a tapered geometry. When the required ring segment geometry is set up, the elements are mutually connected. In the last phase all vertical joints are sealed to prevent leakage during concreting.

The height of one ring segment is limited to a maximum length of the double wall elements, which usually amounts to be around 13 m. After the assembly of the ring segments, they can be placed on top of each other, enabling the tower to grow by 13 m at a time. The segments are subsequently filled out with in-situ poured concrete after each lift, until the desired tower height is reached. The filling of the tower segments with concrete allows the structure to rise without horizontal and vertical joints in the core of the hollow elements. As a result, a monolithic structure with considerable structural integrity is obtained. When the entire concrete structure is built, it has to be pre-stressed with tendons in the vertical direction. The entire building process, as well as the geometry of the tower, is confronted with many technological challenges that are described in the following sections.

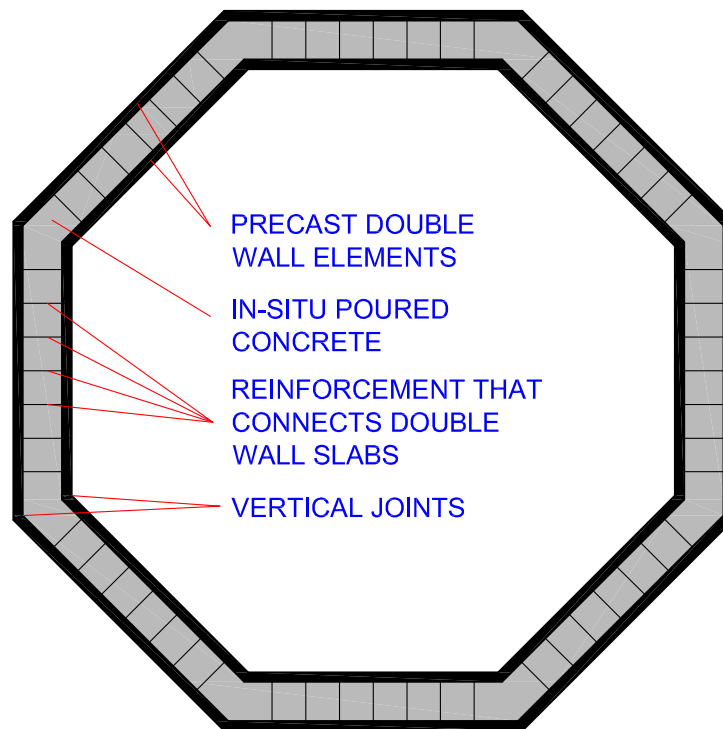


Figure 3.1: Horizontal section through a schematic polygonal ring segment

3.2 Description of a proposed prototype

One possible variant for a prototype structure is a tapered tower with a height of 21.4 m, composed of three various polygonal segments. With these dimensions, the prototype represents the middle segment of a 130 m tall wind turbine (Fig. 3.2).

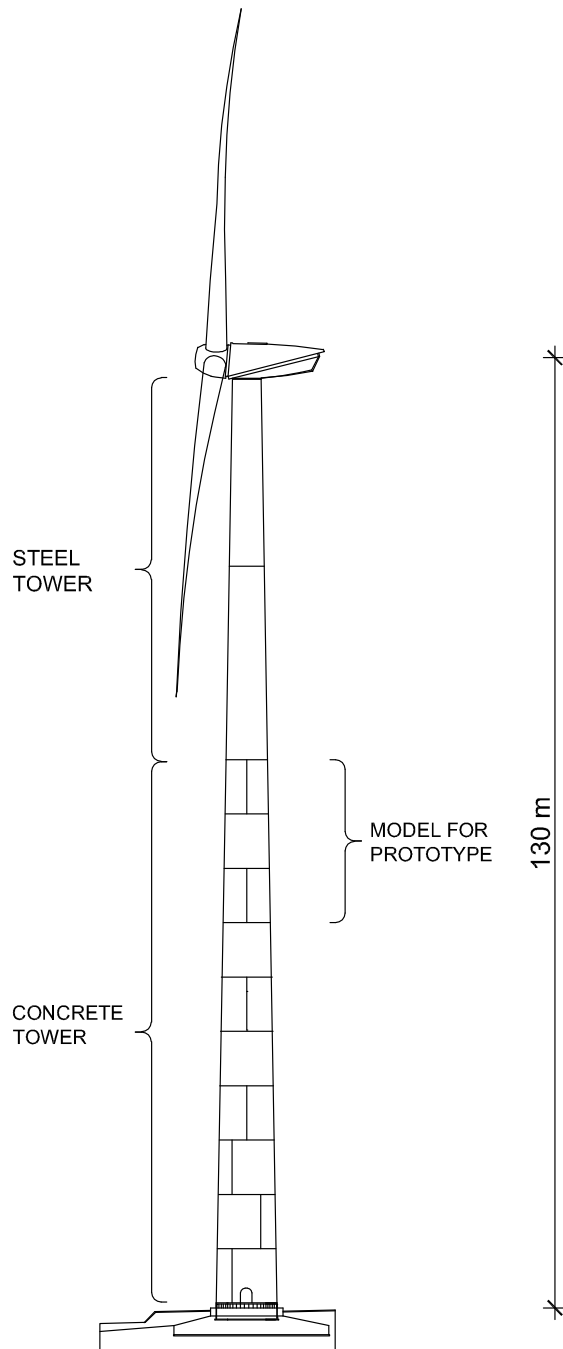


Figure 3.2: Model for prototype- 130 m tall wind tower

The first prototype segment has a diameter of approximately 6 m and a height of 3.6 m, while the two upper segments have a height of 8.9 m (Fig. 3.3). The double wall segments are angled by 1° referred to the vertical tower axis.

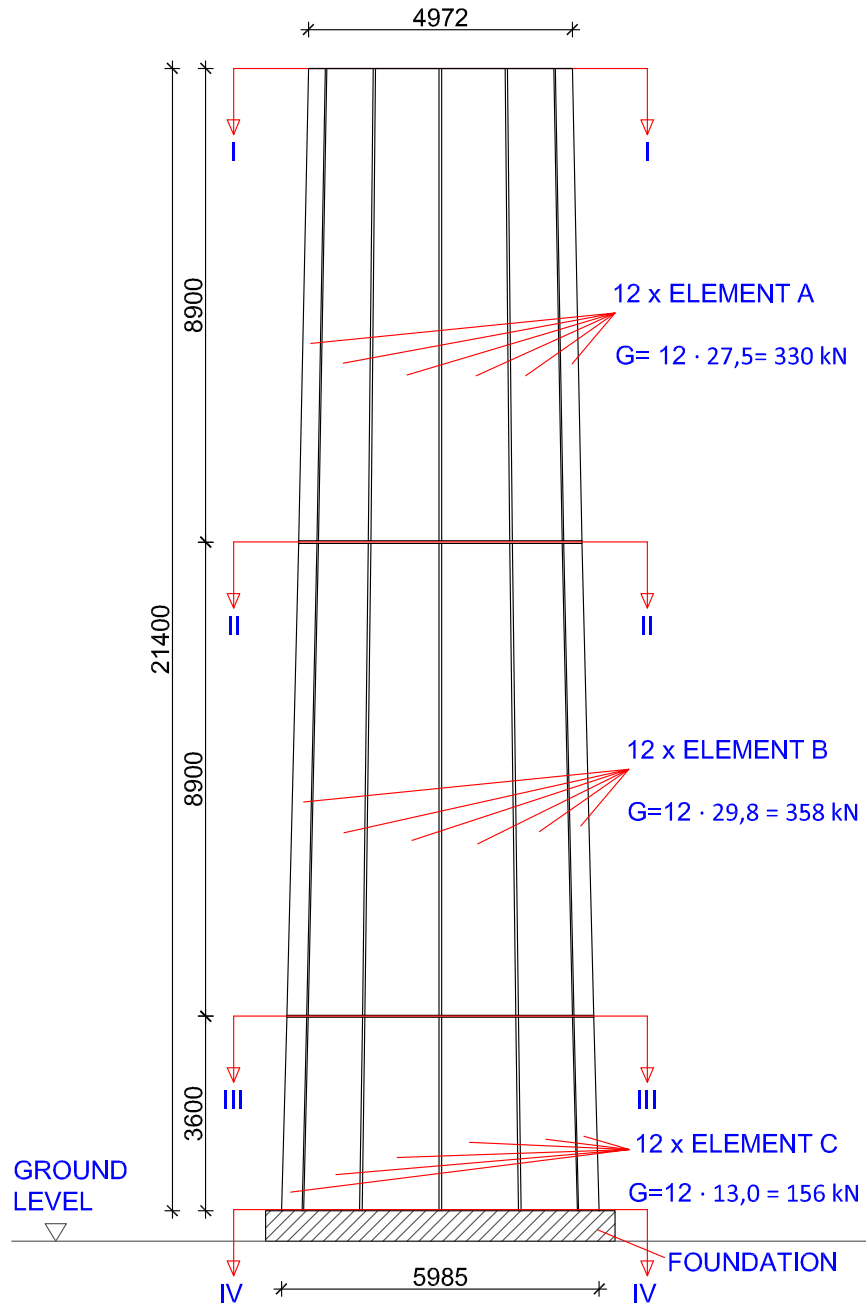
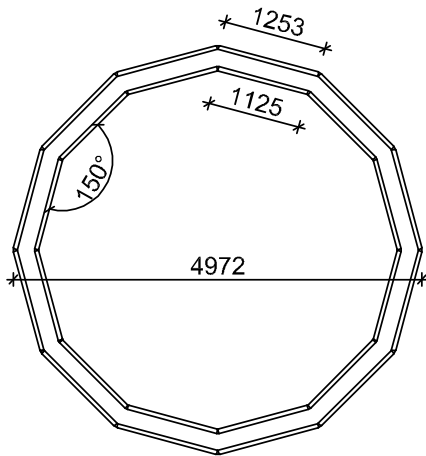


Figure 3.3: Front elevation of the prototype [mm]

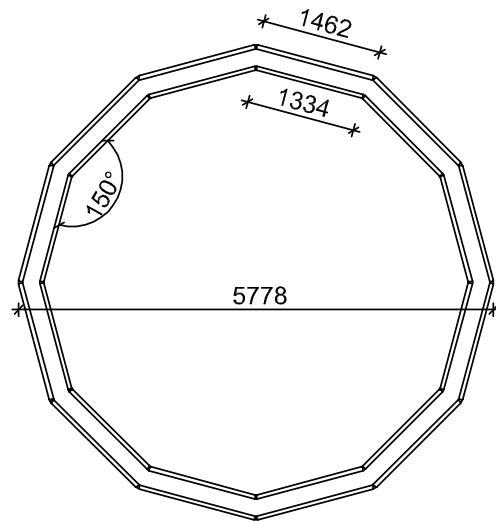
The prototype cross-section is a polygonal ring that consists of 12 double wall elements with an equal length (dodecagon) and an angle of 150° in between (Fig. 3.4). The structure

has two horizontal joints between the three segments that can be implemented in various ways. The dimensions of the prototype are shown in the accompanying figures (Fig. 3.3 and 3.4).

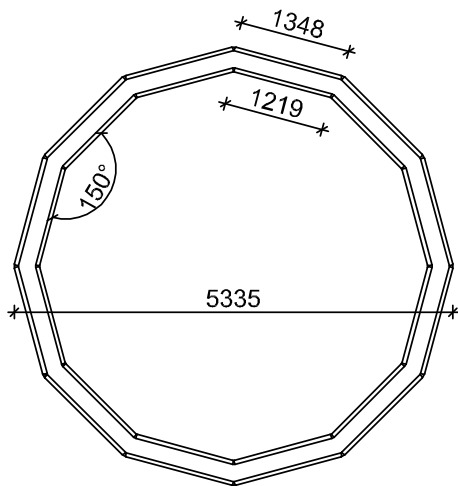
SECTION I-I



SECTION III-III



SECTION II-II



SECTION IV-IV

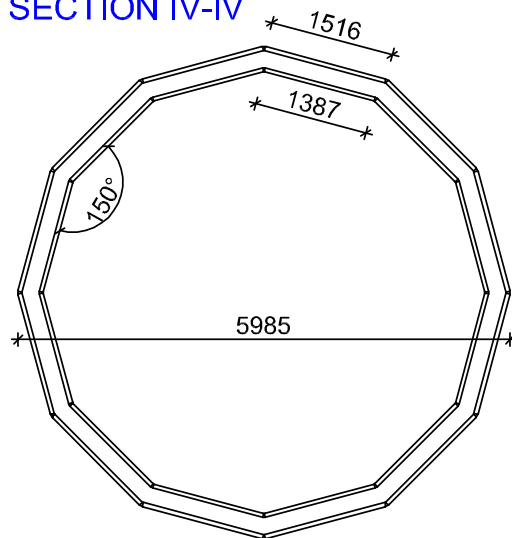


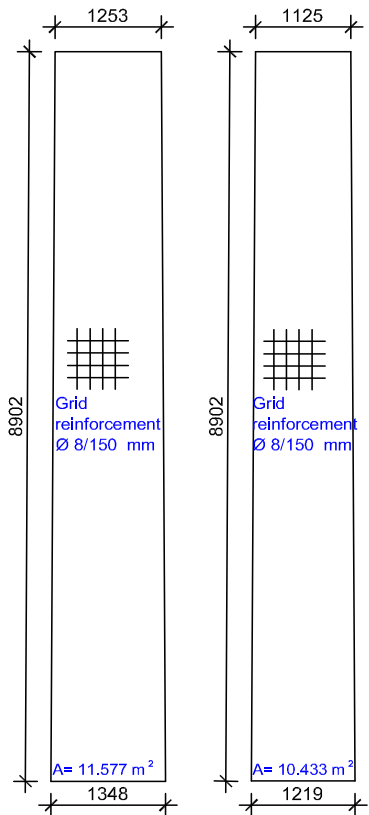
Figure 3.4: Top view of the prototype tower [mm]

The concrete slabs of the double walls are reinforced with a quadratic grid reinforcement on the mutual distance between the bars of 150 mm and with a rod diameter of 8 mm. The reinforced slabs are connected with 8 mm thick lattice girders over the whole length of the elements (Fig. 3.5). The distance between the girders in vertical direction is 600 mm.

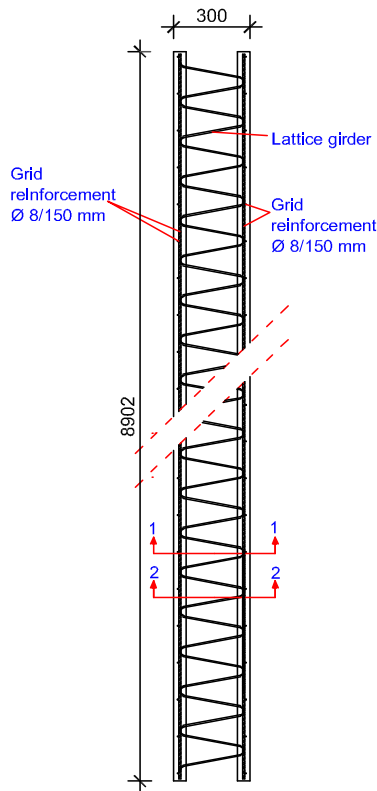
ELEMENT A

G = 330 kN

OUTER WALL ELEMET INNER WALL ELEMENT



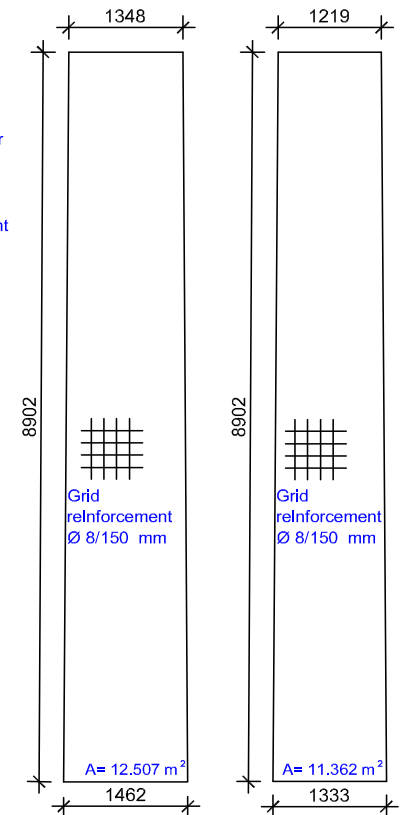
CROSS-SECTION



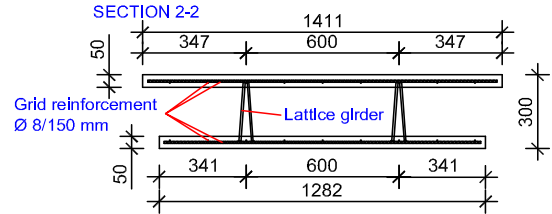
ELEMENT B

G = 358 kN

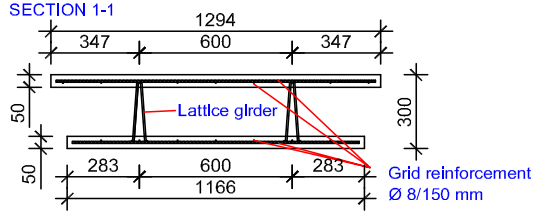
OUTER WALL ELEMET INNER WALL ELEMENT



SECTION 2-2



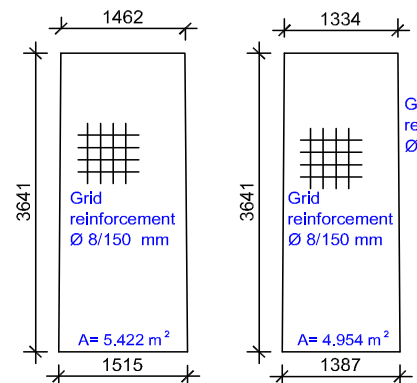
SECTION 1-1



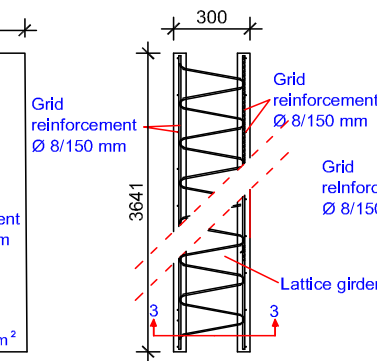
ELEMENT C

G = 13,0 kN

OUTER WALL ELEMET INNER WALL ELEMENT



CROSS-SECTION



SECTION 3-3

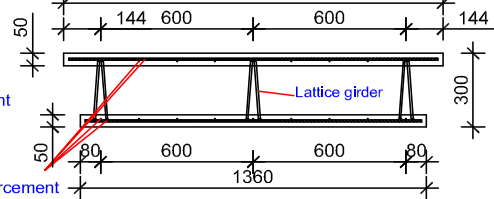


Figure 3.5: Double wall elements of the proposed prototype tower [mm]

For the prototype structure with an average element length of 1.35 m and three segments, following total length of the horizontal joints can be estimated:

- average length of the element \times number of elements \times number of horizontal joints \times 2 (for inner and outer shell)=
 $1.35 \times 12 \times 2 \times 2 = 64.8 \text{ m}$

For the tower height of 21.4 m, the total length of the vertical joints can be estimated:

- height \times number of joints \times 2 (for inner and outer shell)=
 $21.4 \times 12 \times 2 = 513.6 \text{ m}$

The comparison of joint lengths of the prototype structure shows that the vertical joints have a much greater total length than the horizontal joints. Therefore, a greater attention is dedicated to their design (further information is provided in Subsubsection 3.3.3.4).

3.3 Construction process and technological challenges

The claim on an easy and economical construction process arise certain technological challenges, which are discussed in this section. All those challenges can be assigned to the specific construction phases that are presented schematically in Fig. 3.6. Emphasis is given to the challenges that occur in the pre-assembly phase because solutions for these are tested and evaluated through the construction of a mock-up, see also Chapter 4.

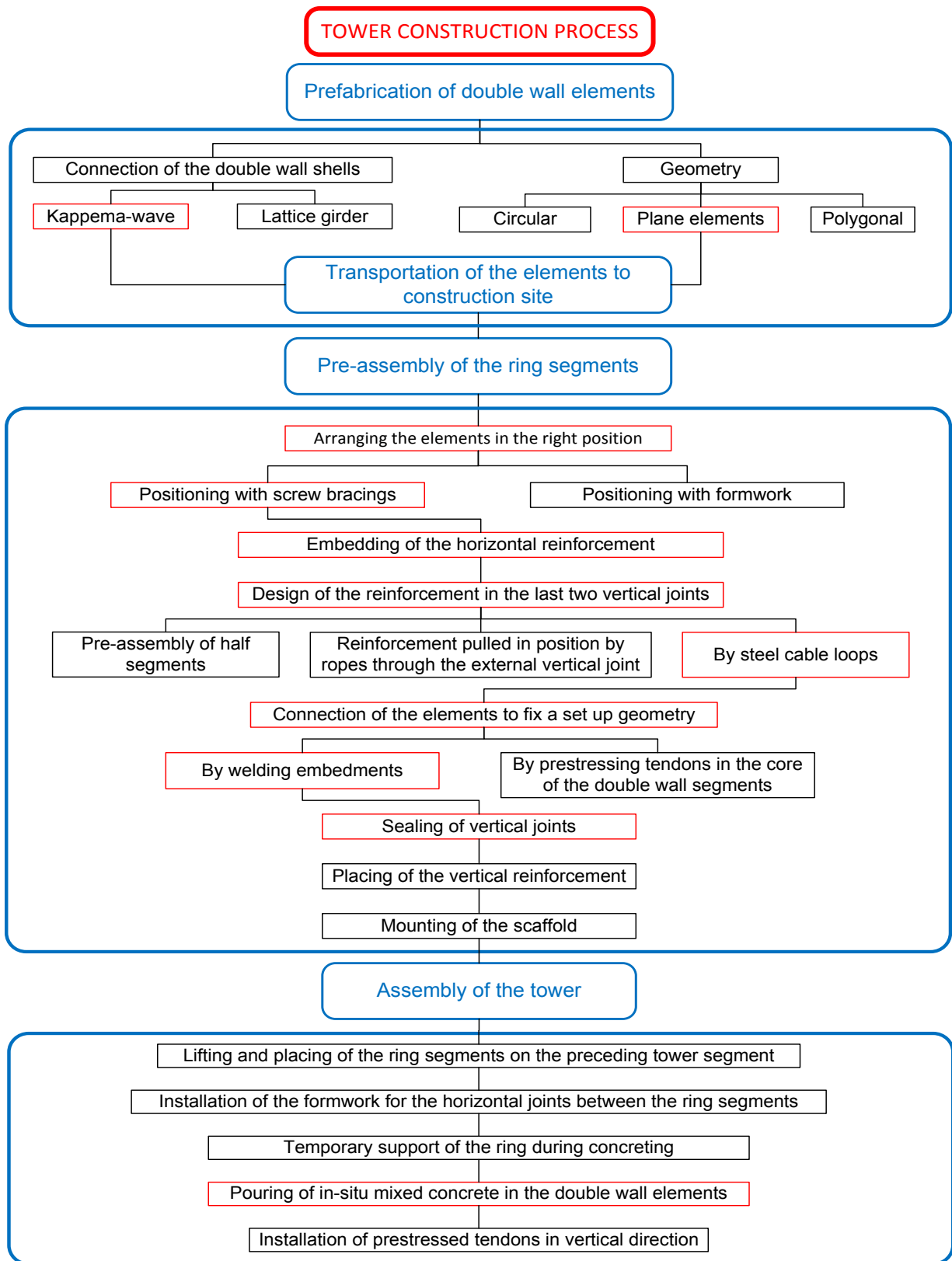


Figure 3.6: Schematic overview of the construction process and accompanying structural challenges. All solution that will be tested for the mock-up are highlighted red.

3.3.1 Technological challenges during prefabrication of double wall elements

Double wall elements are industrially precast concrete products manufactured under controlled factory conditions. The production of the elements consists of several mostly automated steps, which ensure a certain quality standard. The production process of these double wall elements is described in more detail in Section 4.3.

3.3.1.1 Common interconnections of double wall shells

The double wall elements consist of two slabs of reinforced concrete with a usual thickness of 5 to 7 cm, which are mutually connected by lattice girders (Fig. 3.7(a)) or Kappema elements (Fig. 3.7(b)) [36]. The concrete quality of the shells should be at least C25/30 wherein it is advisable to vibrate the concrete for 60% of filling time [37]. The thickness of the shells and the arrangement of the interconnections depends on the pressure during concreting.

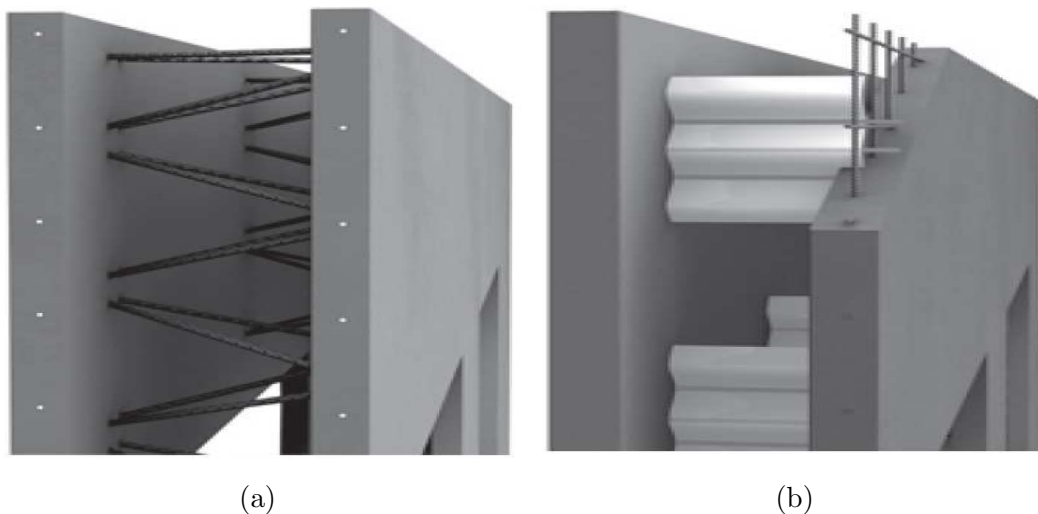


Figure 3.7: Double wall element with; (a) lattice girders; and (b) Kappema elements, taken from [36]

3.3.1.2 Geometry

A circular shape of the tower cross-section meets the requirements for stiffness and strength that have to resist wind loads. Therefore, the prototype is designed with a polygonal cross-section formed by plane double wall elements. These, polygonal shape, will result in a slightly unfavourable behaviour under wind loading, which is supposed to be negligible compared to the benefits gained by the usage of plane double wall elements.

3.3.2 Transportation

The double walls are semi-precast elements with a light weight of approximately 250 kg/m^2 for a slab thickness of $2 \times 5 \text{ cm}$, and therefore, they can be easily transported to the construction site. All elements are flat, so they can also be stacked vertically and horizontally to save space during transportation.

3.3.3 Pre-assembling of ring segments

The pre-assembling is performed on the ground in close proximity to the position of the future tower construction. Wherein, the main technological challenges are the arrangement of the elements in a desired geometry, placement of the horizontal reinforcement and the sealing of the vertical joints. Therefore, the discussion of stated challenges and proposals for technical solutions are described in the following subsections.

3.3.3.1 Arrangement of elements

During pre-assembling, the elements have to be arranged in the desired position and angled to form a polygonal and tapered ring segment.

There are two reasonable possibilities to secure the established position of the elements:

- by screw bracings
- by an auxiliary construction

The double wall elements can be precisely positioned by two screw bracings. A screw bracing consists of two hollow steel tubes that can be telescopically pulled out and adjusted with a thread to reach the desired length. In this method, elements are firstly placed in a vertical position and then they are slightly inclined until the specific angle is reached. The bracings are fixed to the foundation at one side and to the plastic anchors embedded in the double wall elements at the opposite side. The screw bracings have to remain until the geometry of the ring segment is secured by a mutual connection of the elements.

For the erection of tall ring segments with different heights and diameters, the usage of an adjustable auxiliary construction (e.g. a steel formwork) would be rational. This steel formwork out of hollow tubes should be expandable in horizontal and vertical direction in order to satisfy different ring diameters and heights. It could consist out of two interconnected frames that follow the polygonal geometry of the ring segment. The first frame is positioned at the bottom of the ring segment, while the second, narrower frame is placed at the top of the segment in order to provide the tapered geometry. Such a formwork is

accompanied with high initial investment costs, but it can be repeatedly used for different segment geometries.

3.3.3.2 Reinforcement in the last two vertical joints

The horizontal reinforcement in the core of the double wall elements has to be placed during the arrangement of each ring segment. The purpose of this reinforcement is to provide continuous reinforcement of the segments through the vertical joints between the elements.

All other common tower designs that use precast elements do not provide a continuous reinforcement over the whole section. One common solution for the connection of precast elements are steel embedments connected with bolts (Fig. 3.8).

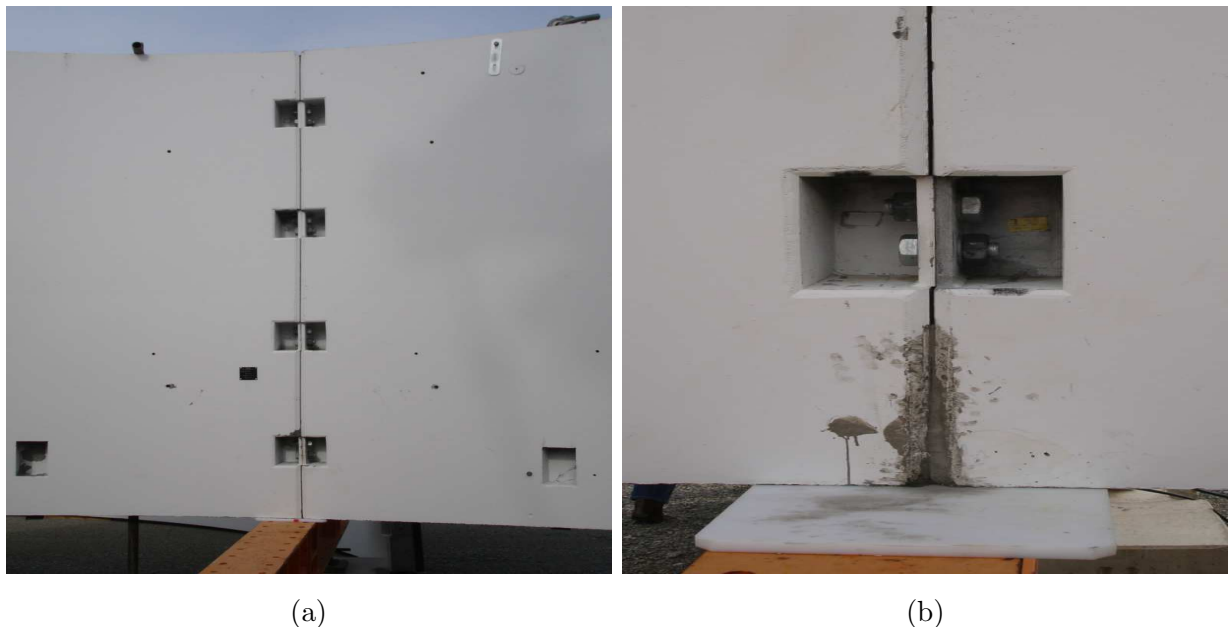
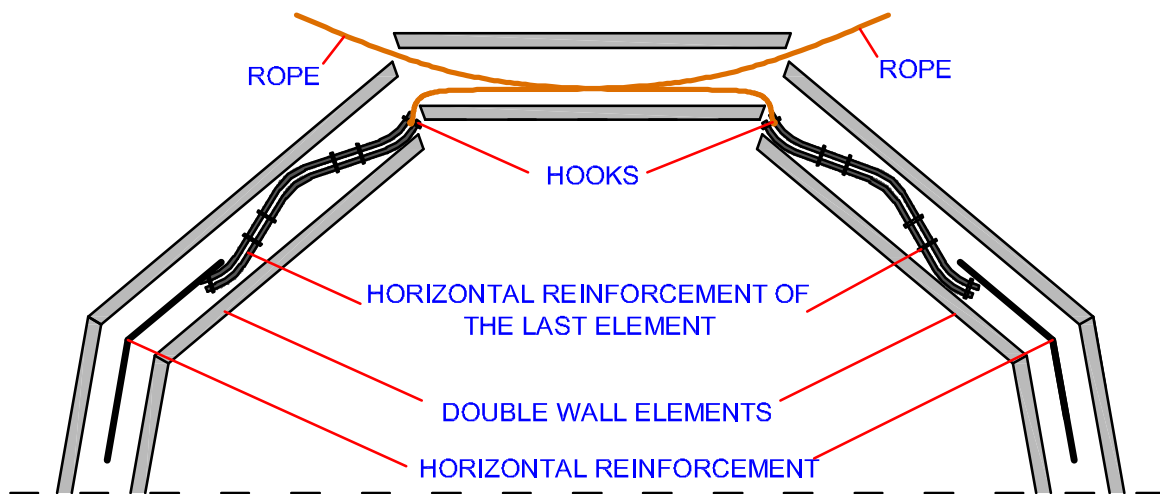


Figure 3.8: Connection of elements in a ring segment by embedments and bolts; (a) connection of two elements; and (b) enlarged view

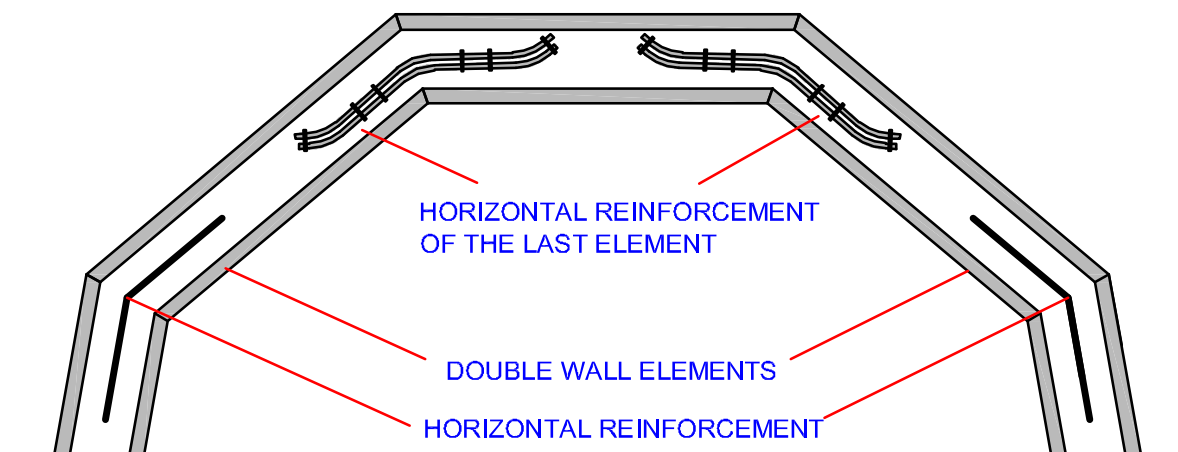
The positioning of the last element of the segment is accompanied by a collision problem of the reinforcement. Therefore, the horizontal reinforcement of the last two vertical joints can be placed by one of the following ways:

- Reinforcement pulled by ropes into the desired position through the external vertical joints
- Assembling together ring segment halves
- Embedding of horizontal reinforcement with steel cable loops

One possibility to place the horizontal reinforcement for the last double wall element is to position it in the adjacent elements from the left and right side, wherein the bars of the horizontal reinforcement have inbuilt hooks at their ends. When the last element is positioned close to the final position (Fig. 3.9), the reinforcement can be pulled from adjacent elements and moved by ropes into the last two vertical joints. After the reinforcement reaches the desired position, the ropes are cut and the element can be arranged in the final position.



(a)



(b)

Figure 3.9: Placing of the horizontal reinforcement by pulling it through external vertical joints with hooks; (a) phase 1; and (b) phase 2

Another way to solve the collision problem is to pre-assemble two half segments, which already contain the reinforcement for the vertical joints (Fig. 3.10). Afterwards, these two halves can be merged easily. Additionally, a connection in the vertical joints between the elements of each half has to be established in order to provide an unchangeable geometry during lifting and shifting. Each half contains reinforcement that sticks out from one side of the half-ring, and which is afterwards reaching into the second half-ring. In the final state, reinforcement protrudes through all corners of the ring segment.

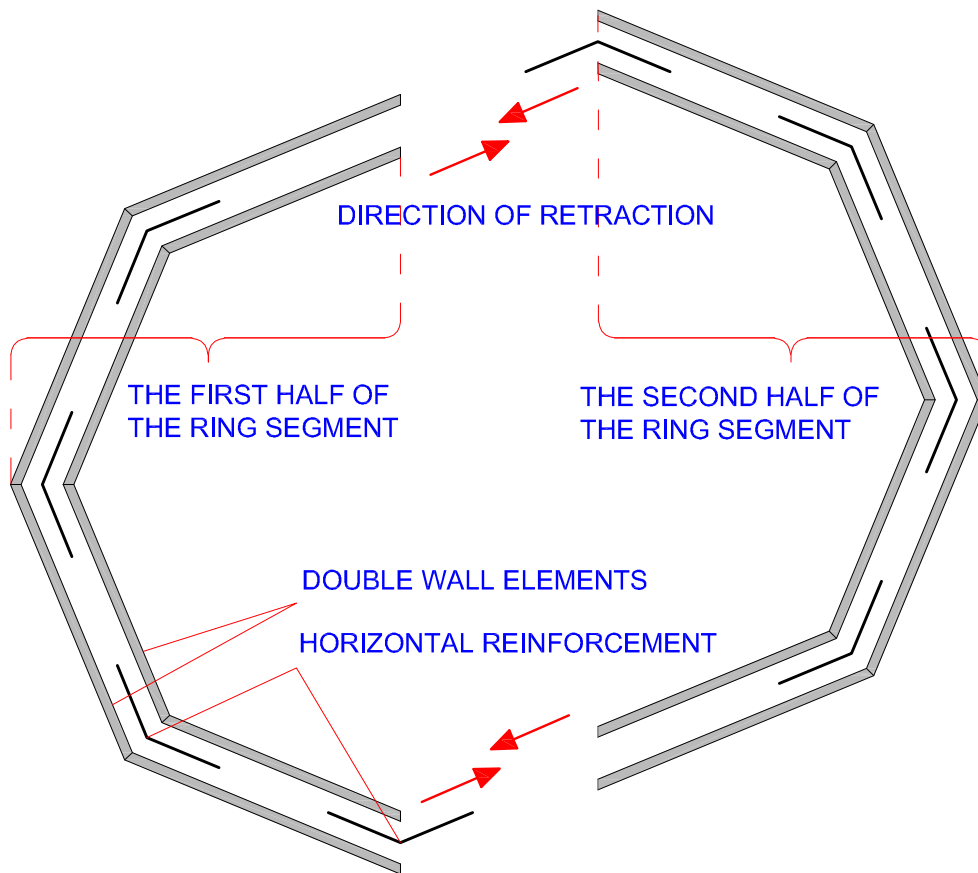
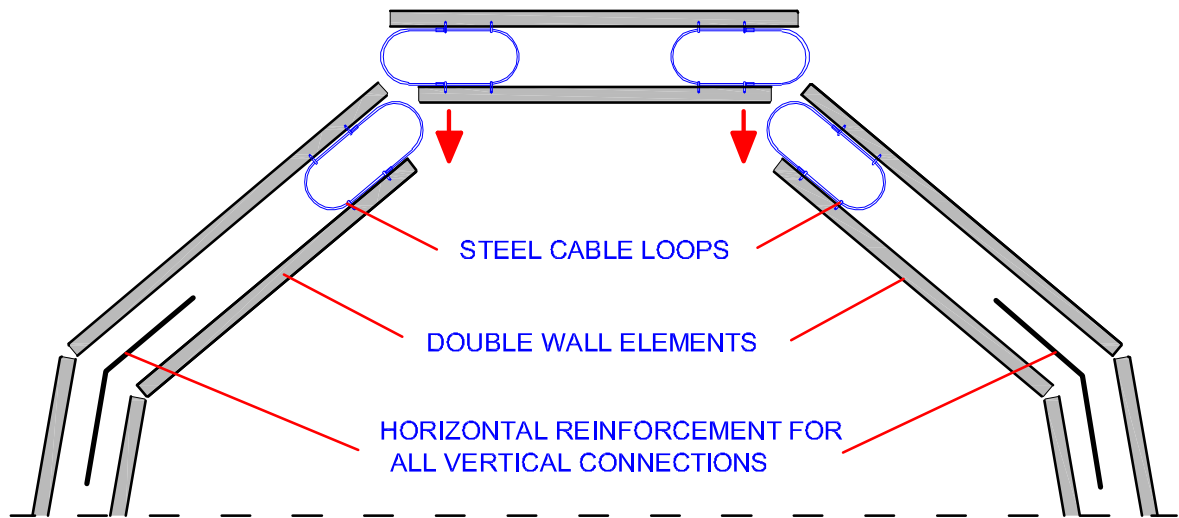
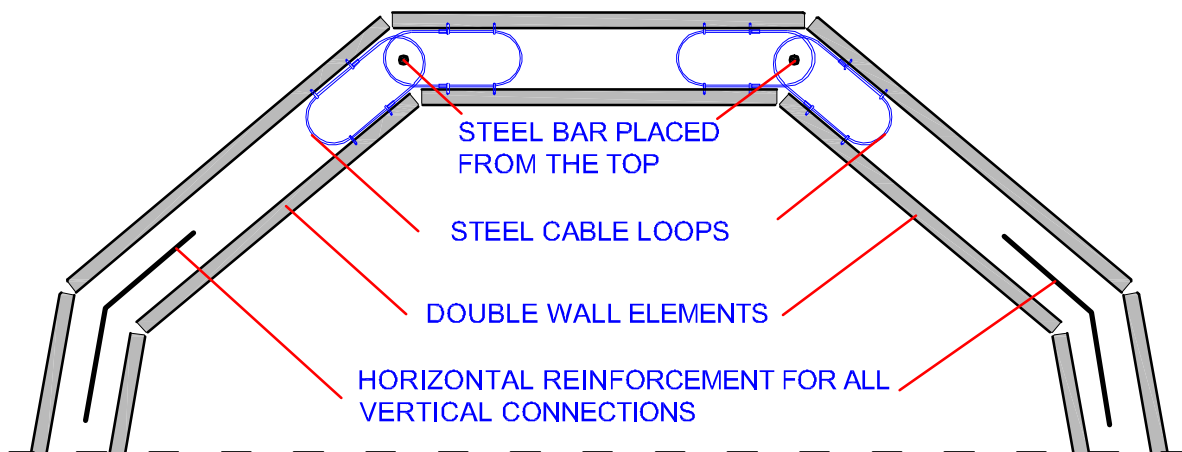


Figure 3.10: Pre-assembling of half segments in order to provide reinforcement in all vertical joints

A further approach to provide reinforcement in all vertical connections represent the usage of overlapping steel cable loops (Fig. 3.11). The loops are placed from the inner side of the double walls. Wherein, the element, which is positioned as last one, is equipped with cable loops on both sides, while the adjacent elements are equipped with cable loops from the side that is bordering the last element. Once the last element is in its final position, both cable loop pairs are mutually overlapped. In order to fix their position during all following construction phases, steel bars are inserted in the overlapping area of the loops.



(a)



(b)

Figure 3.11: Reinforcement of the last two vertical joints provided by steel cable loops; (a) positioning of the last element; and (b) installation of the vertical steel bars

3.3.3.3 Connection of elements in order to fix set up geometry

After all double wall elements are arranged in the accurate position it is necessary to mutually connect them in order to ensure the set up geometry during all following construction phases, like lifting and concreting.

Following connections are proposed:

- by welding embedments
- by prestressing tendons

The prestressed tendons, which are extended through the entire perimeter of the ring segments, are located in the hollow core of the double wall elements (Fig. 3.12). Therefore, the maximum radius of the tendon is limited to the radius of the inscribed circle in the regular polygon. Regarding to the height of the tower, the tendon has a shape of the three-dimensional helix curve which is the widest at the bottom of the tower and narrows to the top. The advantage of this system is that the prestressed tendon has the function of a horizontal reinforcement, so there is no need for additional horizontal reinforcement, which is described in Subsection 3.3.3.2.

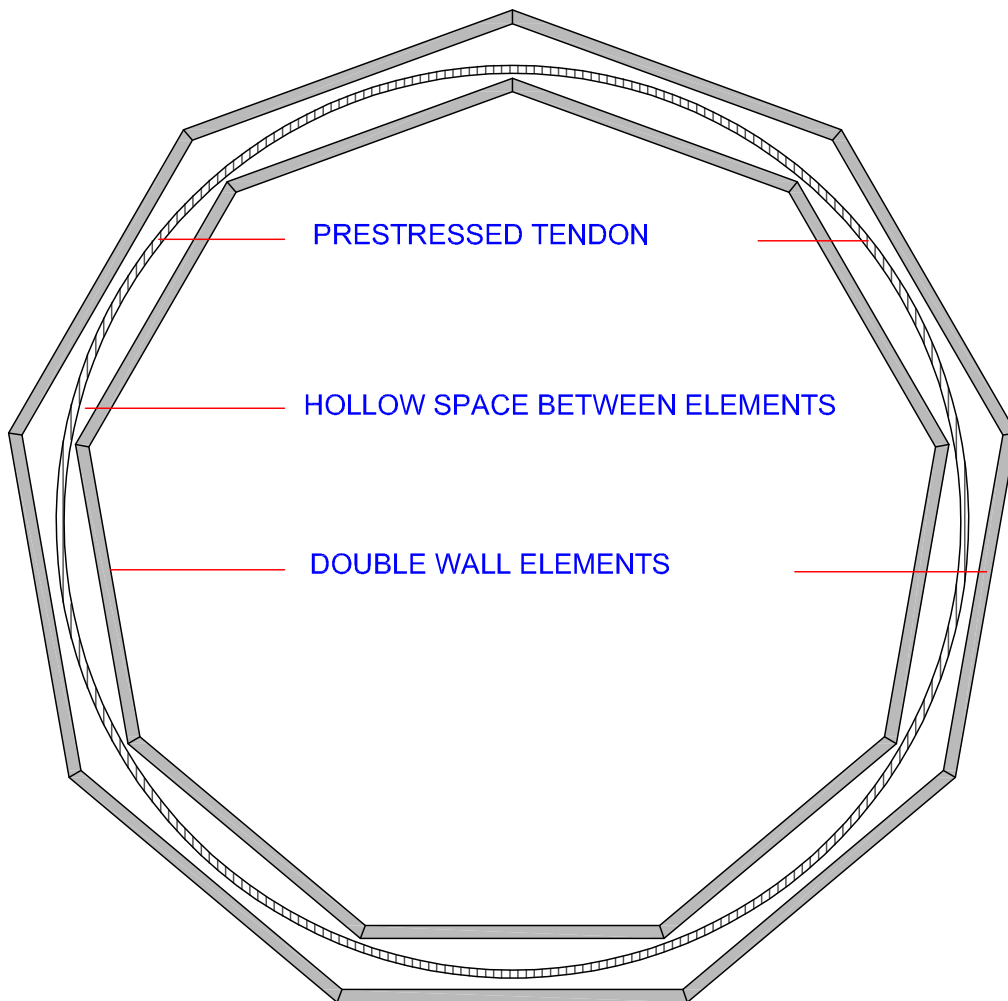


Figure 3.12: Arranging of prestressed tendons in order to secure the set up geometry and as alternative horizontal reinforcement

Another possibility to secure the set up geometry is by connecting the elements through steel embedments that are welded together (Fig. 3.13). A possible arrangement of embedments is to position them at least at the top and bottom of every outer shell flank. After positioning and arranging of the all elements in one ring segment, reinforcement bars are placed between the steel embedments and mutually welded to both neighbouring flanks. The reinforcement bars of different diameters can be used in order to compensate possible building tolerances. Afterwards, all vertical joints are sealed with mortar to provide an anti-corrosive protection and to function as formwork during concreting.

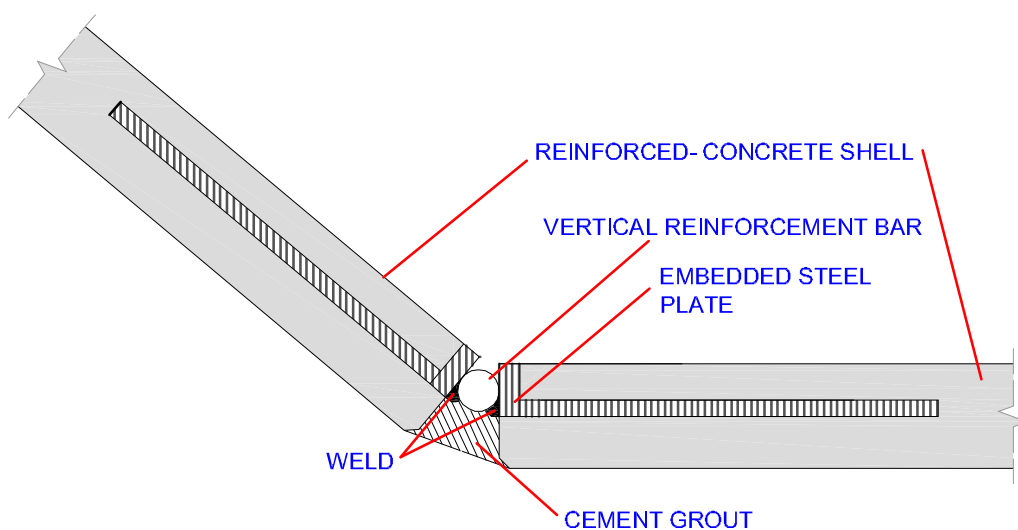


Figure 3.13: Outer shells of the elements with embedments connected by welds

3.3.3.4 Sealing of internal and external vertical joints

The inner and outer vertical joints need to be sealed in order to gain a closed mould for the concrete. As estimated in Subsection 3.2, the comparison between vertical and horizontal joints show that the vertical joints have a considerably greater length. Therefore, a cost-effective technology to seal the vertical joints is of greater importance.

The vertical joints are sealed when the required geometry of the ring segment is set up. According to their position in the construction, vertical joints are divided into internal and external vertical joints.

Following possible sealings of the vertical joints are proposed:

- flexible tubes that deform under concrete pressure and thus seal the joint (Fig. 3.14).
- mortar or cement grout (Fig. 3.15)
- vertical formwork (e.g. out of wood or foil) over the entire length of the joint (Fig. 3.16)

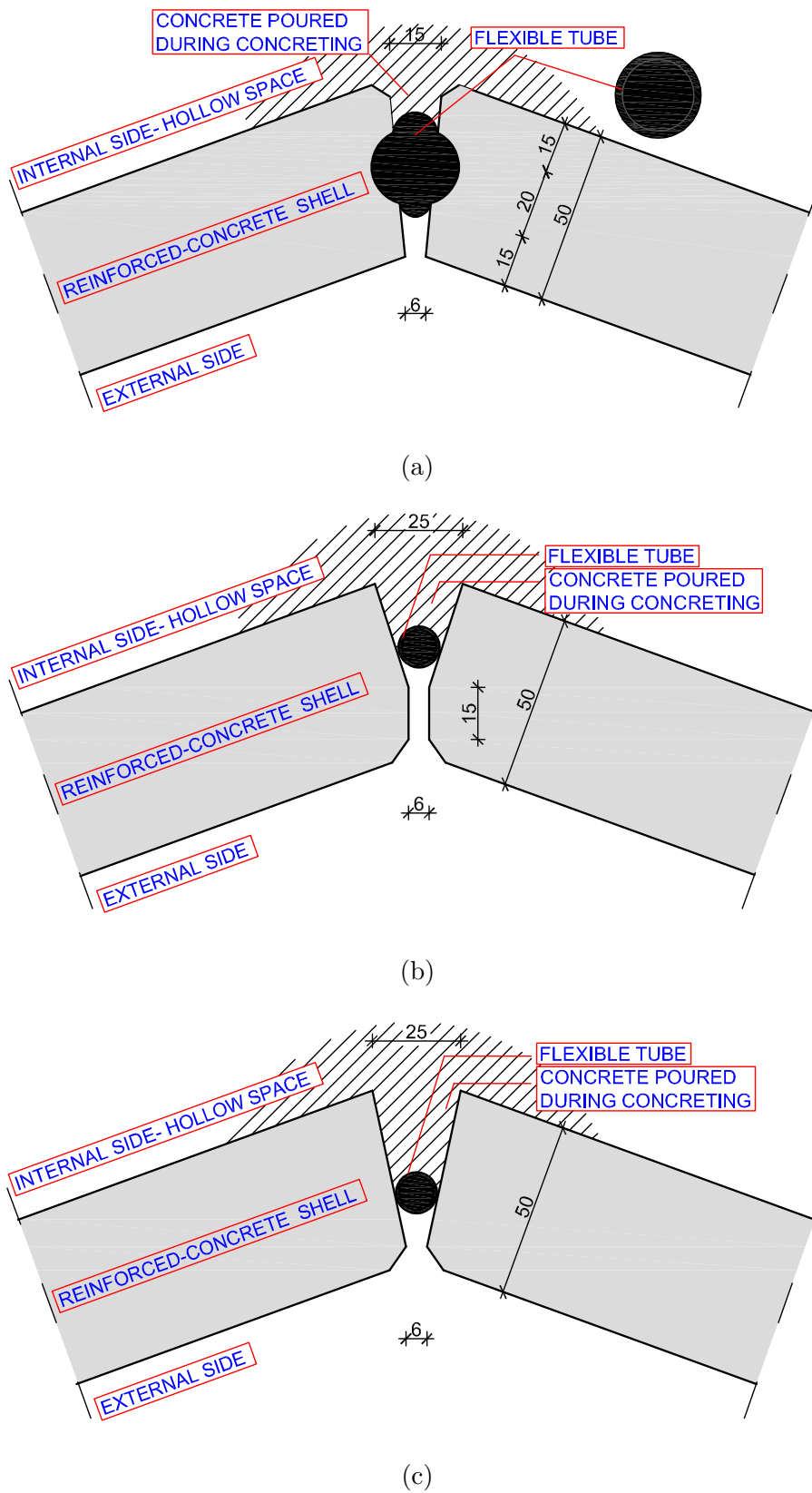


Figure 3.14: Flexible tubes as sealing for internal vertical joints; (a); (b); and (c) possible geometries of the joints [mm]

Similar sealing possibilities can be applied to the outer vertical joints (Fig. 3.17):

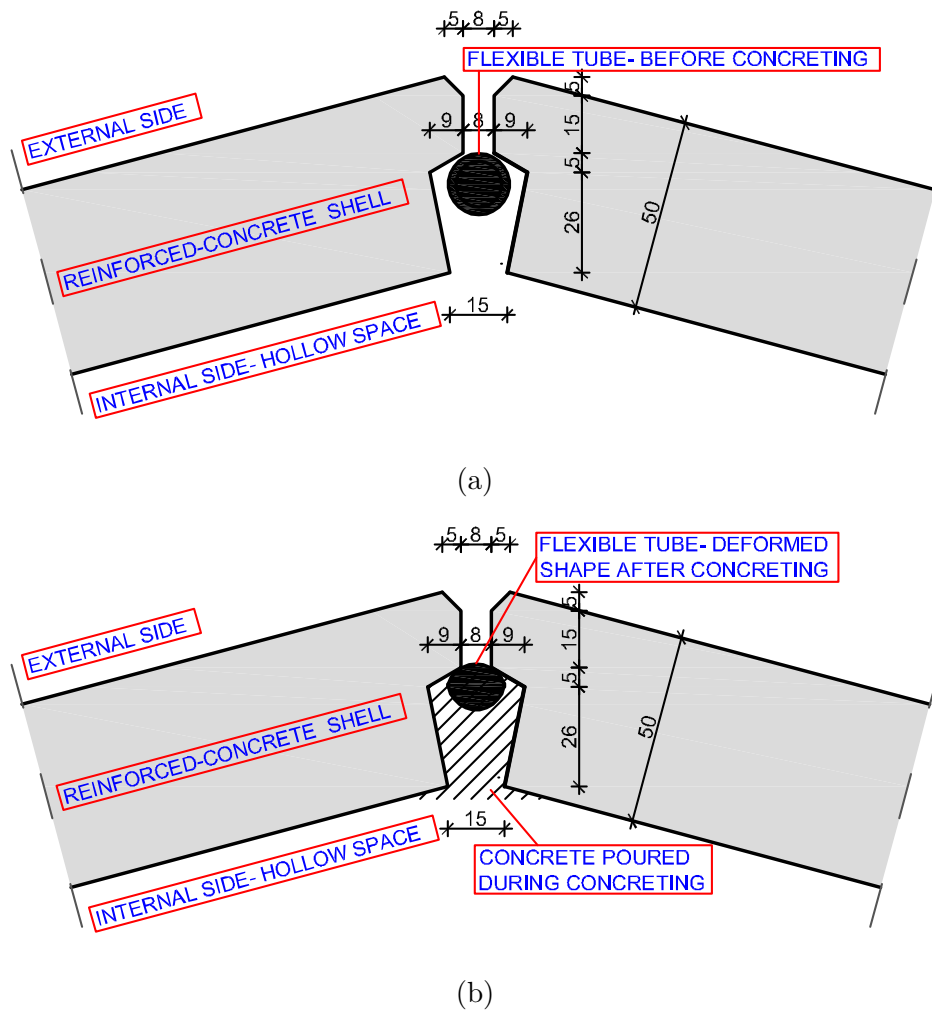


Figure 3.17: Flexible tubes as sealing for external vertical joints; (a) initial position of the pipe before concreting; and (b) deformed shape of the pipe due to concreting [mm]

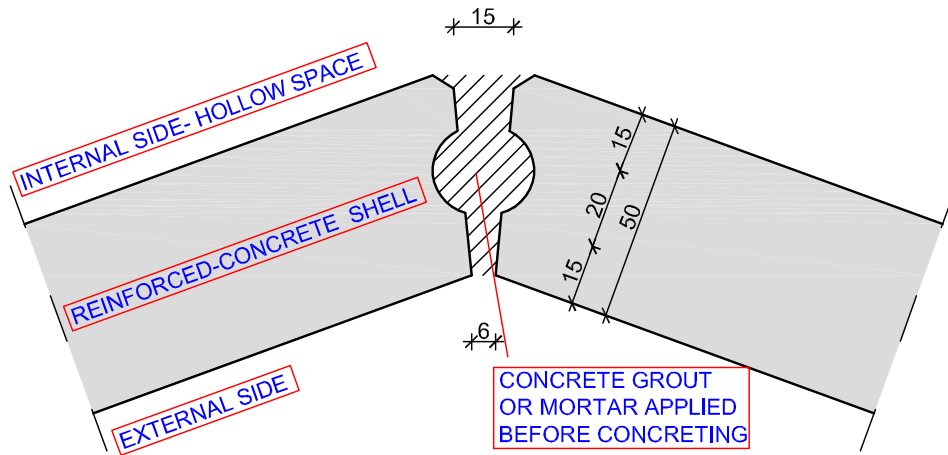


Figure 3.15: Concreting grout or mortar as sealing for inner vertical joint [mm]

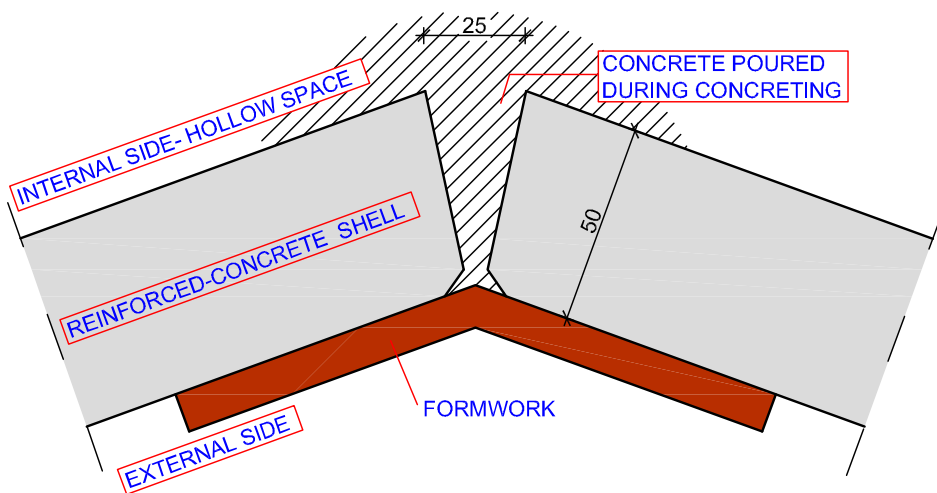
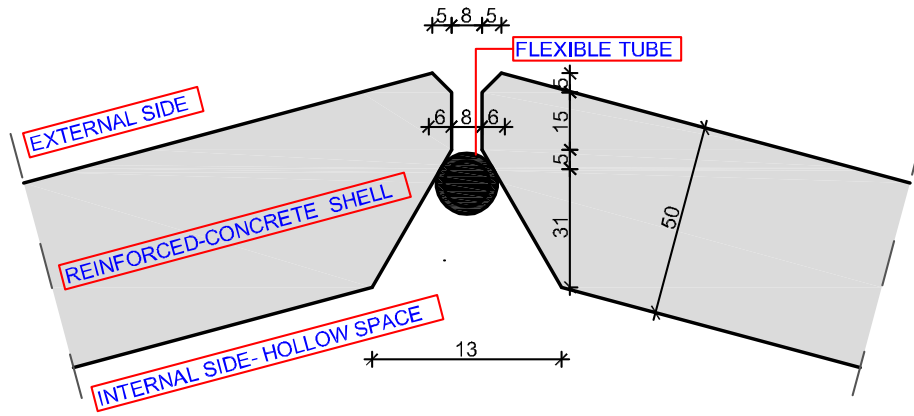
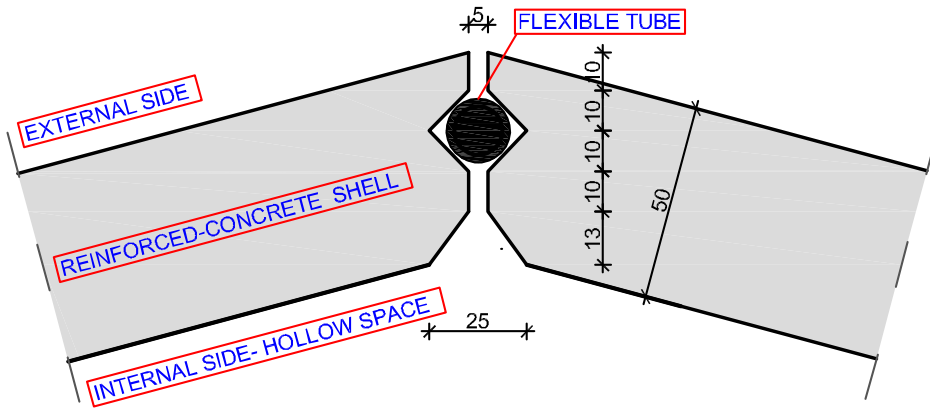


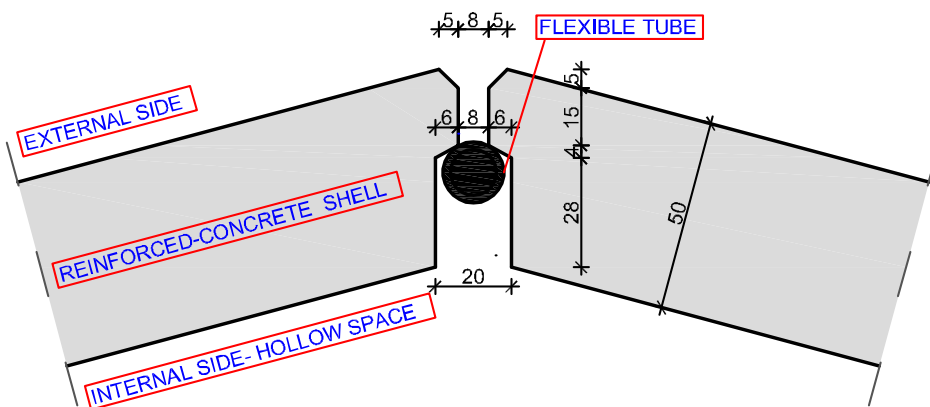
Figure 3.16: Formwork as sealing for inner vertical joints [mm]



(a)



(b)



(c)

Figure 3.18: Flexible tubes as sealing for external vertical joints; (a); (b); and (c) different geometries [mm]

The sealing of joints can also be designed as geometrically complicated halves mounted with a swelling tape (Fig. 3.19). Such geometries of joints can be used for both inner and outer vertical joints.

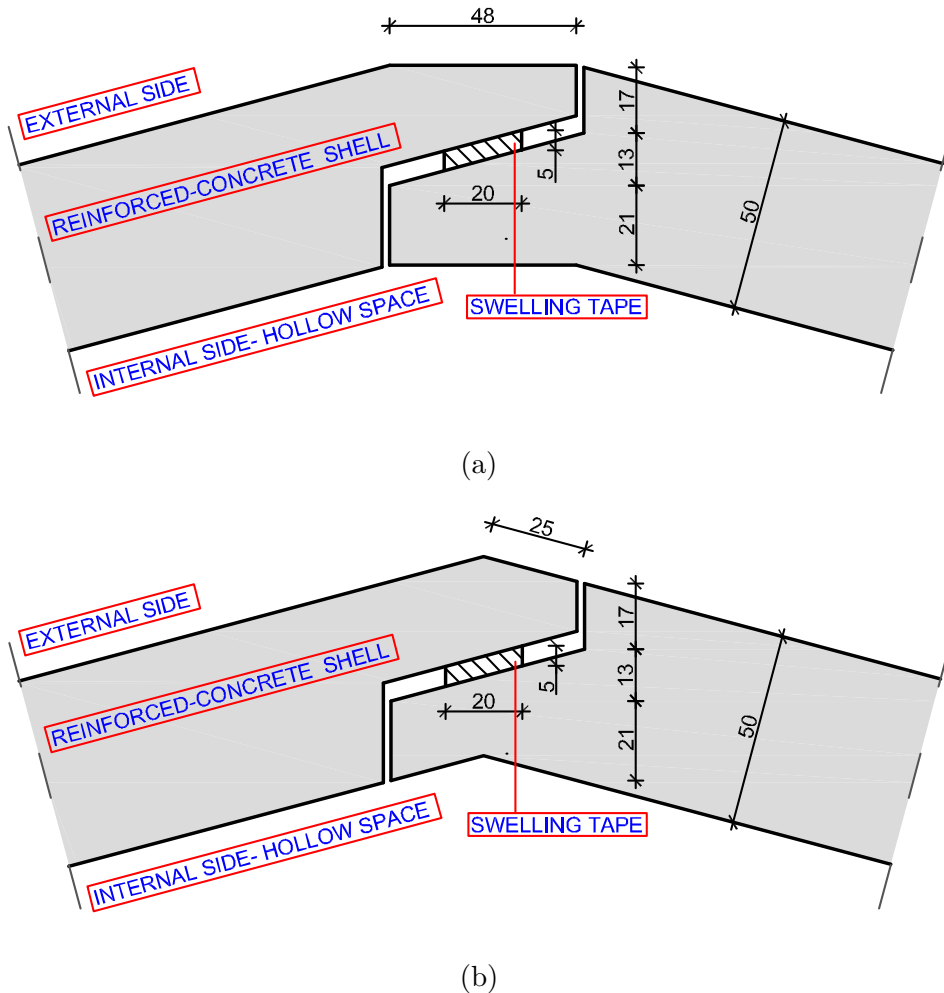


Figure 3.19: Sealing of external and internal vertical joints by halving; (a); and (b) different geometries sealed with swelling tape [mm]

3.3.4 Assembly of the tower

Once the foundation is built and the first two ring segments are pre-assembled, it is possible to start with the erection of the tower. In this phase, the segments can be lifted and placed upon the previous one and subsequently filled with concrete until the desired tower height is reached. Wherein, the entire process ends with vertical prestressing of the concrete structure.

The technological challenges that accompany the assembly phase are related to:

- lifting and arranging of the segments
- sealing of the horizontal joints
- concreting of the segments
- mounting of the scaffolding
- vertical prestressing of the whole tower

Therefore these challenges are further discussed in the following subsections.

3.3.4.1 Lifting and placing of the ring segment

In the assembly process each ring segment is lifted and placed on top of the previous segment. For the lifting of the ring segment it is useful to use lifting beam in order to load the segment only with vertical forces (Fig. 3.20).

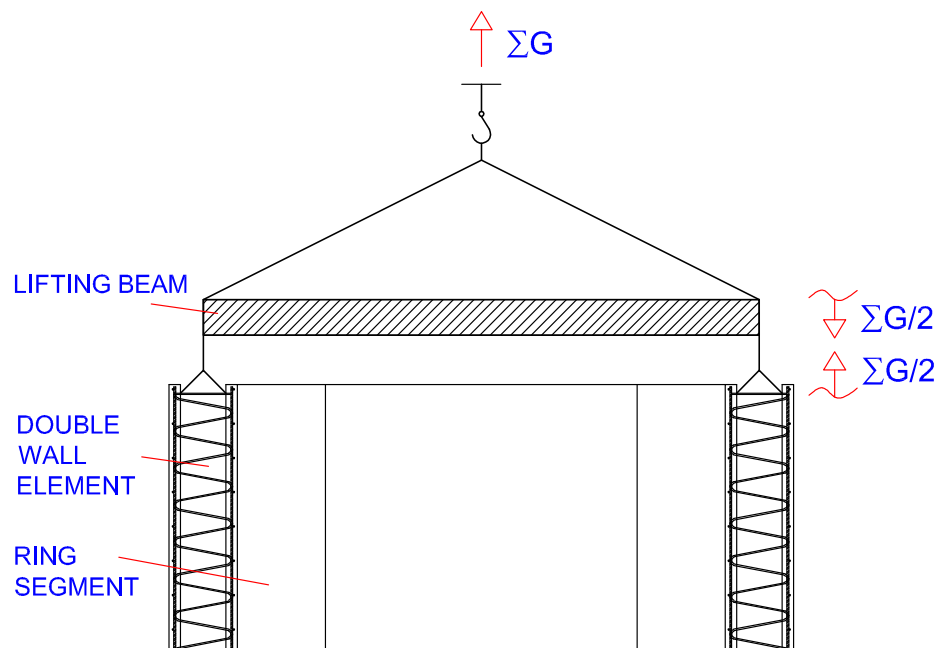


Figure 3.20: Lifting a segment with a lifting beam

An alternative method is to lift the segment without lifting beam by taking into account that the segment is loaded under an angle (α). However, this leads to an additional horizontal loading of the segment (Fig. 3.21).

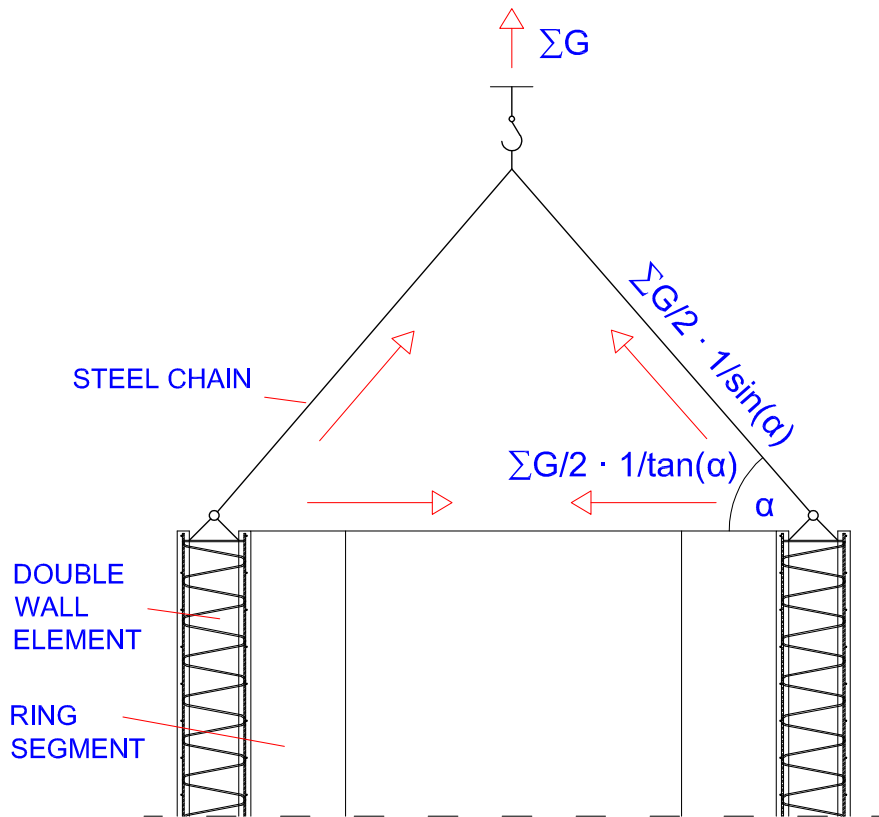


Figure 3.21: Lifting a segment with angled chains

3.3.4.2 Horizontal joints

The horizontal joints are the resulting gap of the vertical arranging of the ring segments. Its design has to enable an adjustment of minor tolerances that can be the consequence of imperfectly assembled ring segments and to provide an efficient transfer of compressive stresses between the segment shells. Therefore, the geometry of the joint has to ensure a gap of a certain size between segments during concreting.

After erection of one ring segment, a formwork is positioned at the horizontal joints so that the hollow space between the double walls can be concreted. The formwork consist of two wooden planks that are clamped with steel rods and anchors (Fig. 3.22). It is designed in a way that it is possible to remove the formwork from the inside of the tower, so that no external scaffolding is needed. Therefore, the formwork is at the outer side of the tower equipped with a rope that secures the formwork from falling down when the anchor rod is removed from the inside.

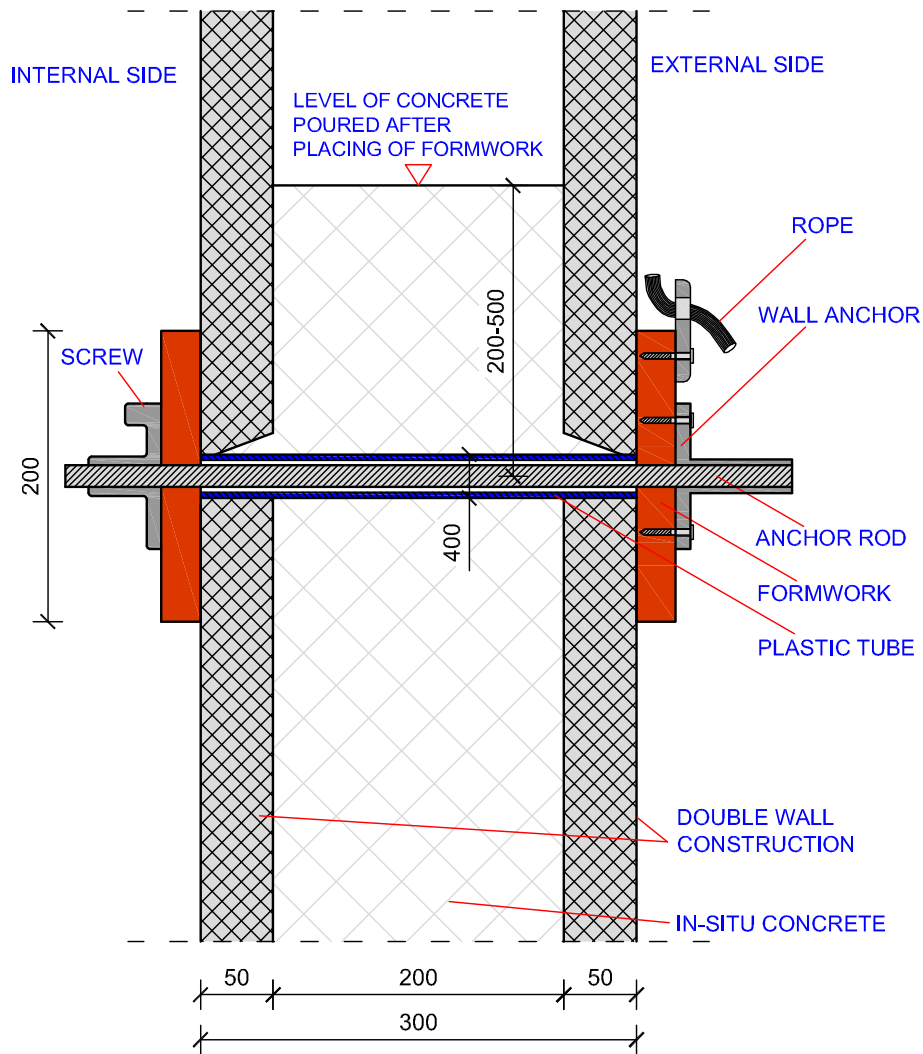


Figure 3.22: Proposal of formwork for horizontal joint [mm]

3.3.4.3 Proposal of scaffold and crane arrangement

The erection of the tower demands the usage of a scaffolding and a crane (Fig. 3.23). Ring segments, which are pre-assembled from double walls, are lightweight in comparison with conventional precast walls, and therefore it is possible to use a crane with a lower capacity. The lattice mast of the crane, which is used as part of the climbing scaffold, is connected by bracings to the tower to ensure its stability. A climbing scaffold can be used for all works at higher altitudes, like sealing of horizontal joints or concreting.

Alternatively, it is possible to perform the erection of the tower with a climbing formwork that is mounted with working platforms on the inner and outer side (Fig. 3.24). This formwork provides the accessibility of the tower from all sides. Moreover, there would be no need for an additional formwork of the horizontal segment joints.

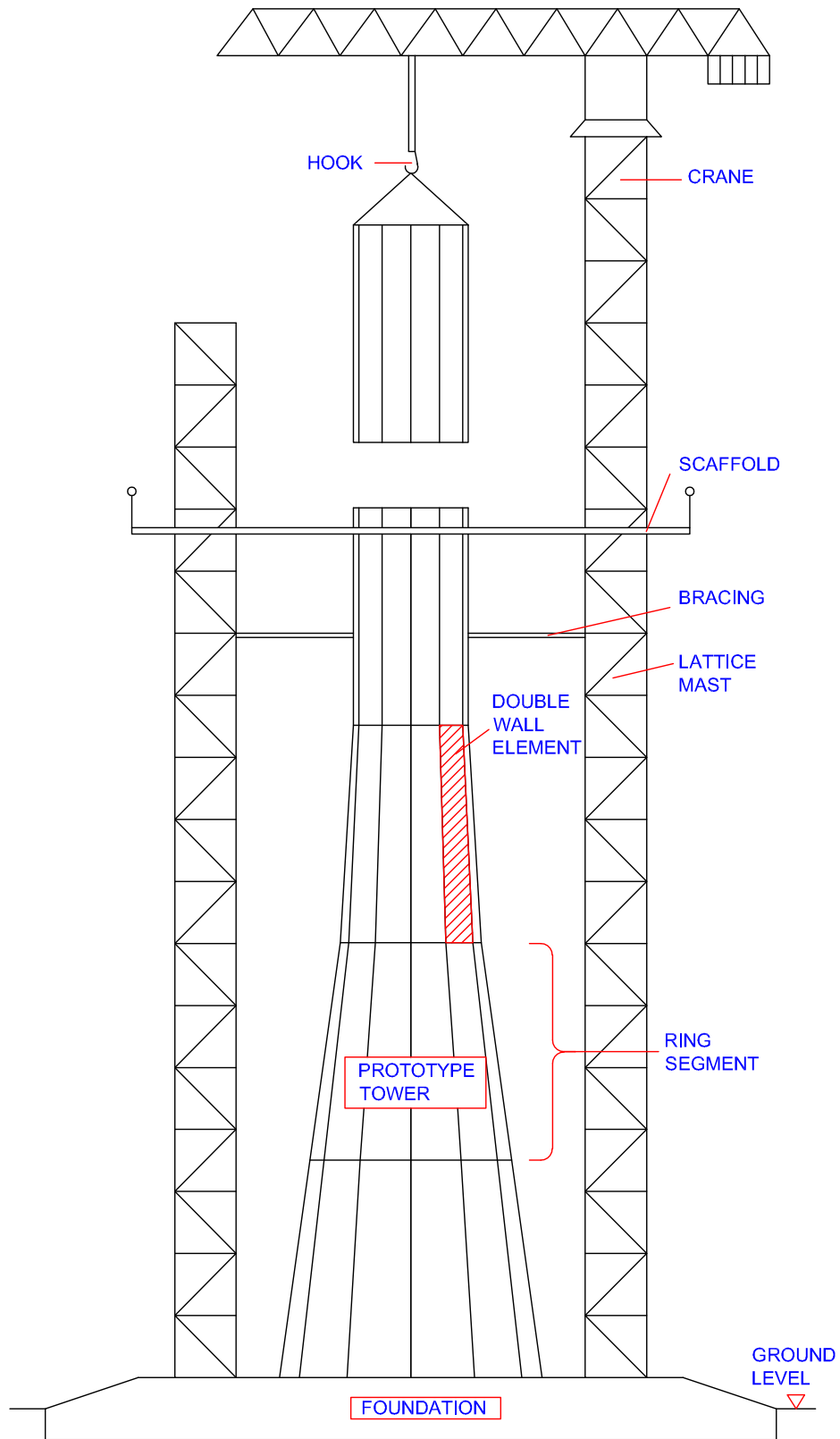


Figure 3.23: Proposal of scaffolding and crane arrangement used in Patent [34]

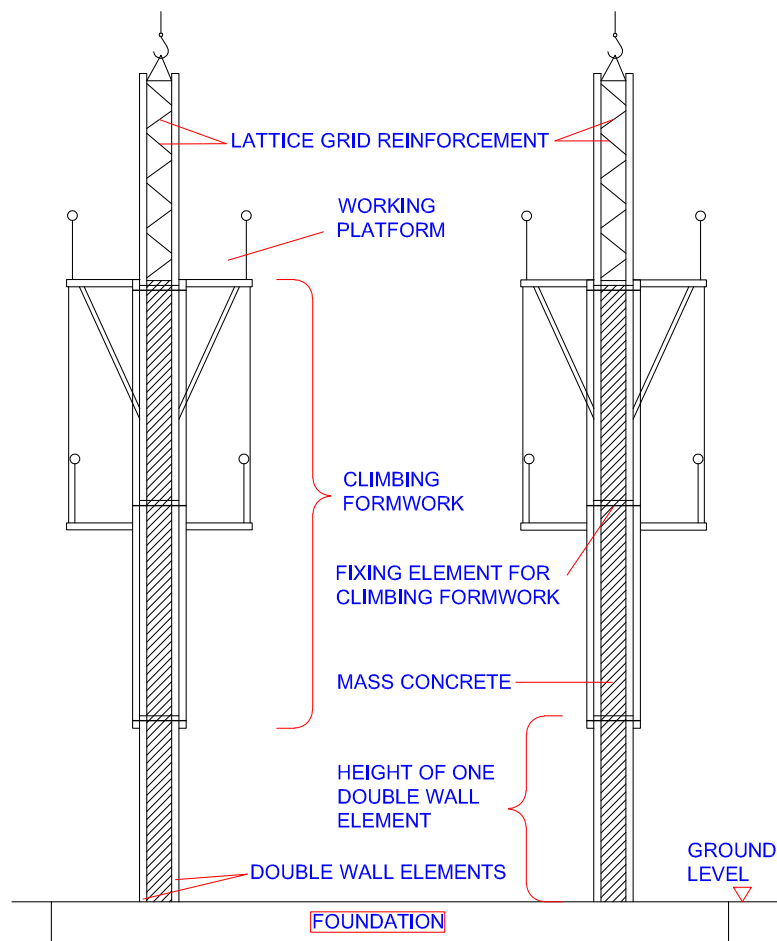


Figure 3.24: Proposal of climbing formwork used in Patent [34]

3.3.4.4 Installation of prestressed tendons in vertical direction

When the tower is completed, it has to be pre-stressed with tendons in the vertical direction. The vertical prestressing can be performed internally through the center of double wall elements or externally through the interior of the tower. An external prestressing has the advantage of an easier deconstruction of the tower, while internal prestressing ensures a better corrosion protection.

3.4 Innovations and comparison with conventional construction techniques

3.4.1 Advantages of the proposed construction method

- The elements can be easily transported because of their light weight. The tower segments are composed of flat double wall elements, and therefore they can be easily transported to construction site in comparison with conventional precast curved sections.
- The ring reinforcement is placed continuously in the core of the segment, which allows a higher load bearing capacity of the tower accompanied by thinner double wall elements and a reduced diameter of the ring segment. In contrast, conventional precast tower structures possess no reinforcement between two connected segments.
- It is assumed that the erection time can be reduced and the cost effectiveness can be increased.
- The weight of the double wall elements with a slab thickness of 2x5 cm is only 28.75% of the weight of the conventional precasted elements, and therefore, it is possible to lift almost four times higher tower elements with the same crane capacity.

Weight of one double wall element:

$$2 \cdot 0.05 \text{ m} \cdot 25 \text{ kN/m}^3 = 2.5 \text{ kN/m}^2$$

Weight of conventional precasted element (thickness is 35 cm):

$$0.35 \text{ m} \cdot 25 \text{ kN/m}^3 = 8.75 \text{ kN/m}^2$$

$$\text{Weight of double wall element} \div \text{Weight of conventional precasted element} = \\ 2.5 \text{ kN/m}^2 \div 8.75 \text{ kN/m}^2 = 0.2875 = 28.57\%$$

- Double wall elements are manufactured industrially in factories under controlled conditions with a high degree of accuracy and with low dimensional tolerances.
- The double wall elements of conventional manufactures can have a height of approximately 13 m, which is much larger than the height that is currently in use for conventional curved precast elements. This feature of the new method enables a faster progress in the erection and significantly smaller amount of the horizontal joints over the tower.
- The vertical joints can be created on the ground in a protected environment.

- The proposed construction method is more independent on the weather conditions in comparison to nowadays common ones. In conventional construction methods the horizontal joints sometimes need an equalizing layer out of epoxy resin which has to be applied at temperatures between +5 and +30°C.
- The mass concrete, which is in the double walls, is continuous along the whole height of the tower providing a monolithic structure of the tower.

3.4.2 Disadvantages of the proposed construction method

- The pre-assembling of the polygonal ring segment is complex and possibly require high initial capital investment for the production of a steel formworks.
- Large number of vertical joints.
- Polygonal cross-section of the tower may cause greater wind loads compared with circular cross-sections.

The comparison between advantages and disadvantages indicates that there could be more positive arguments of this proposed construction method. Summarizing, one could say that the presented construction method has a high chance to represent a lighter, taller and faster erected alternative to nowadays common wind tower construction methods.

Structural analysis, production and assembly of the mock-up tower segment

The technological challenges described and discussed in Chapter 3 are tested by the assembling of a *mock-up*. A mock-up is a real-size model of a structure or design that is used to study, test, evaluate and promote new designs. Whereby, a mock-up is a prototype if it provides at least a partial functionality of a tested design [38]. In this case the mock-up is one polygonal ring segment with the typical dimensions from the middle part of a 130 m high wind tower. The planning of the mock-up requires an analysis of the various boundary conditions, like environmental influences and the different construction phases that result in accompanying loadings. Therefore, the description and structural analysis of the ring segment are presented in the beginning of this chapter. This is followed by a description of the production process of double wall elements and their assembly into the mock-up tower segment.

4.1 Description of the mock-up

The mock-up is a tapered, 2.5 m high, tower segment with an average circumcircle diameter of 3.92 m. The geometry of the mock-up tower segment is chosen in order to simplify the erection and the observation of the most technological challenges that are related to the construction of the tower prototype, from Section 3.2. The segment is composed of nine

double wall elements that are arranged to form a regular nine sided polygon (Fig. 4.1). Each double wall element consists of two five centimeter thick concrete slabs with a strength of C30/37, which are interconnected by Kappema elements. This interconnection is chosen due to its cost effectiveness and to increase accuracy of the gained double wall element thickness. The standard element has an approximate weight of 800 kg, while the whole segment has a weight of 7200 kg.

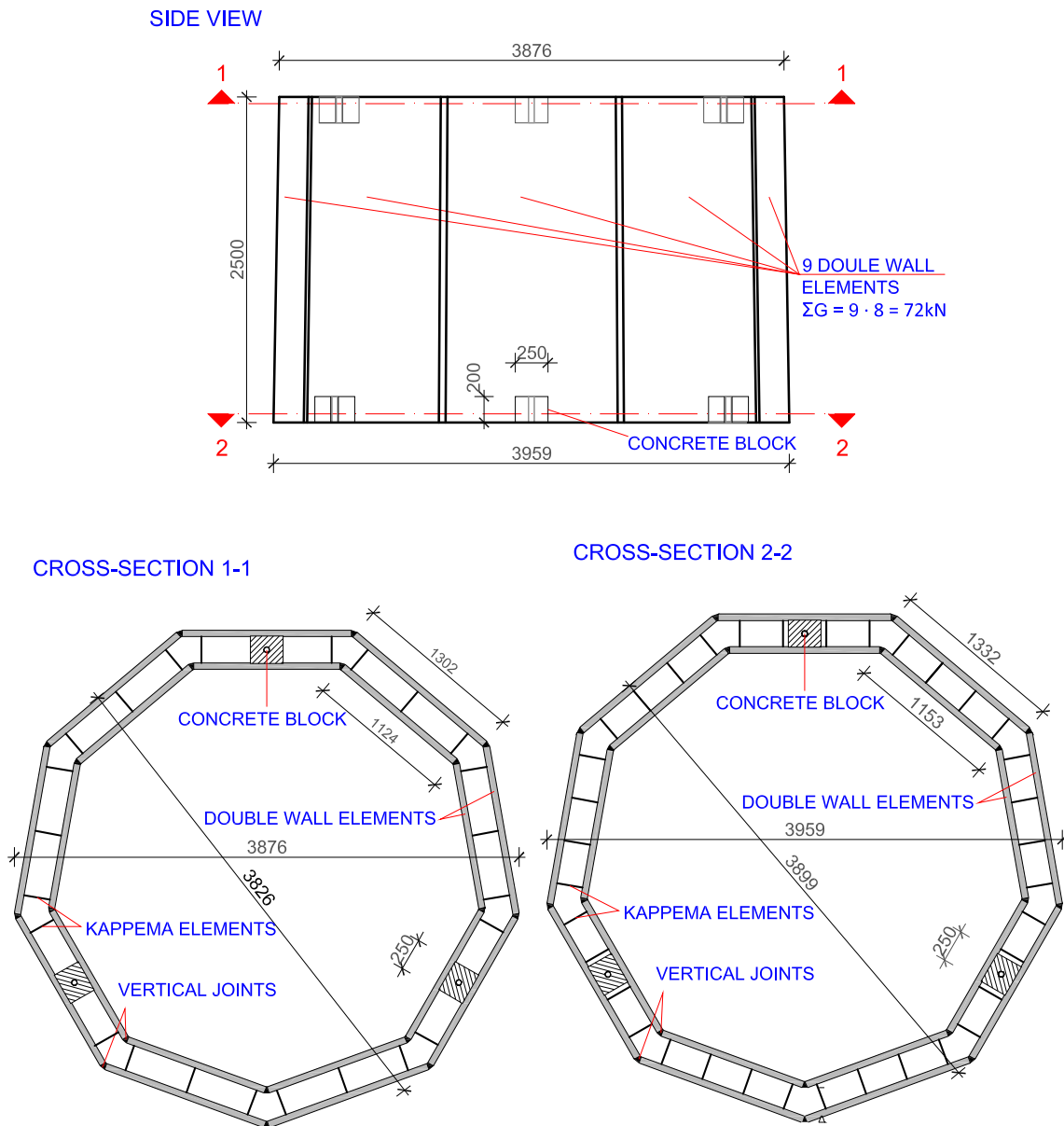


Figure 4.1: Mock-up segment: front elevation and characteristic cross-sections [mm]

The mock-up is set up by six different types of double wall elements. These different types account to the different function assigned to each element in the segment (Fig. 4.2). These functions as well as the according embedments are described next.

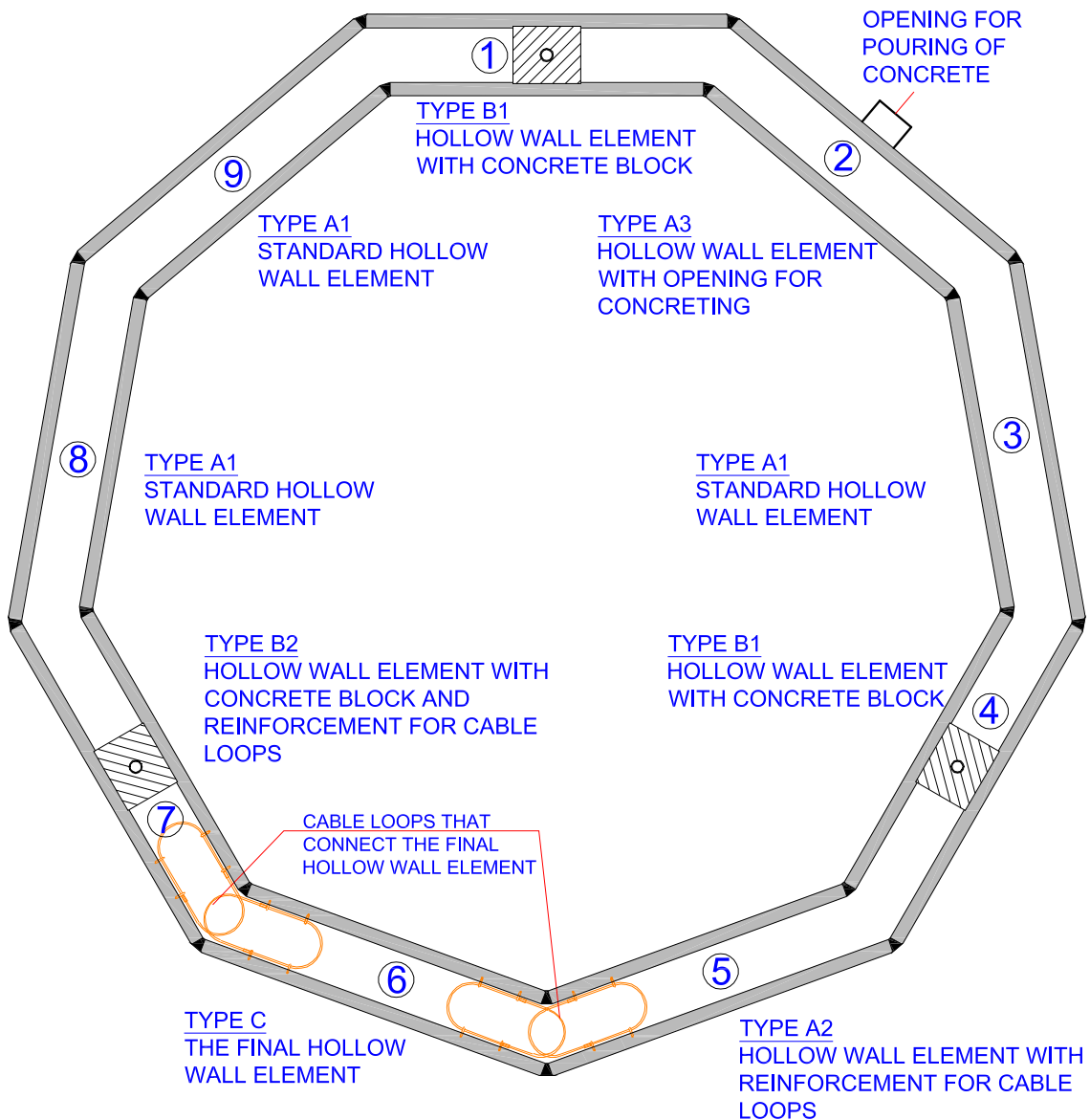


Figure 4.2: Overview of different element types

The element type A1 is the standard hollow double wall element without any special embedments, and consequently, it can be considered to be the cheapest compared to the others. Contrary to the type A1, the type C is more complex by having special embedments. The element type C is the last one that will be arranged during assembling of the segment, and therefore, it has embedded reinforcement hooks for the installation of cable loops

(Fig. 4.3). Whereby, the function of the cable loops is to substitute the stiff horizontal reinforcement that can not be placed into the element which is arranged as the last one. A certain yielding strength and diameter need to be chosen in order to connect the horizontal reinforcement of the concrete slabs between the elements.

The summed up tensile strength of the reinforcement of both shells can be estimated:

Diameter and number of bars: $n = 2 \cdot 17 \varnothing 8$

Steel quality: BSt 550 ($f_{yd} = 478 \text{ N/mm}^2$)

Area of stiff reinforcement: $\sum A_{\varnothing 8} = 2 \cdot 17 \cdot \frac{0.8^2 \cdot \pi}{4} = 17.10 \text{ cm}^2$

Tensile strength of cable loops:

Chosen number of steel cable loops: $n_{loop} = 6$

Chosen loop diameter: $\varnothing_{loop} = 9 \text{ mm}$

Chosen loop yield strength: $f_y = 1770 \text{ N/mm}^2$

Break normal force per one rope cross-section: $N_{break} = 75.3 \text{ kN}$, taken from [39]

$$N_{Rd,bar}^{tensile} = 17.1 \cdot 47.8 = 817.4 \text{ kN} < N_{Rd,loop}^{tensile} = 75.3 \cdot 6 \cdot 2 = 903.6 \text{ kN}$$

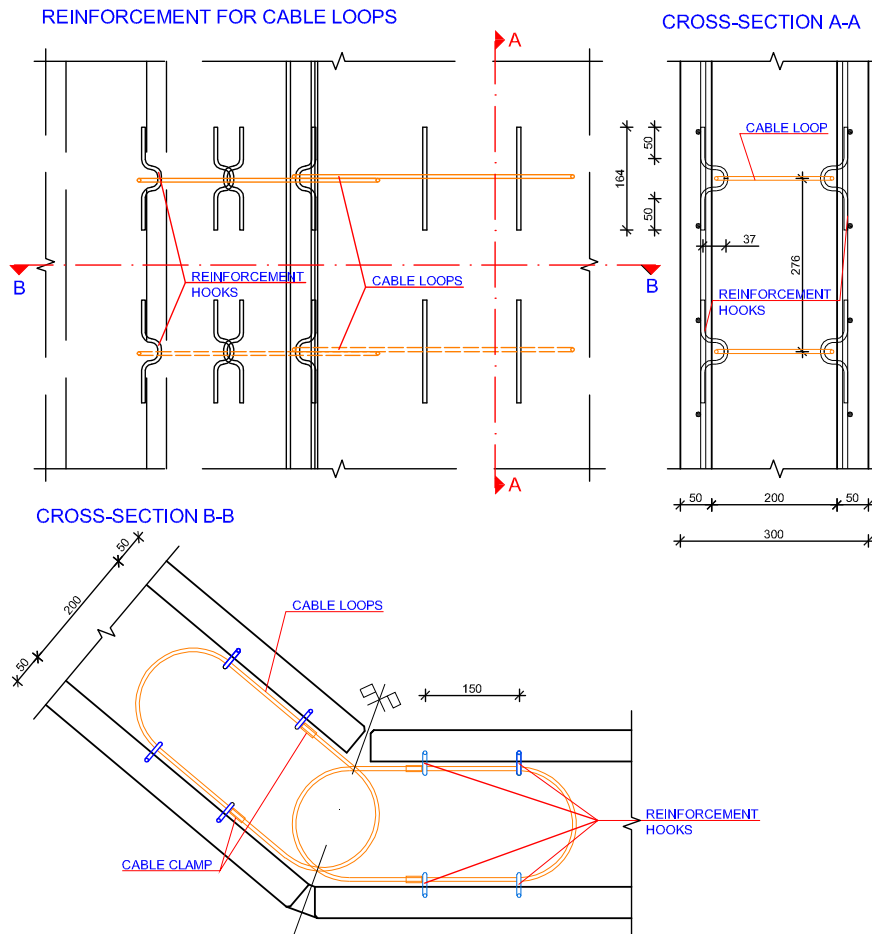


Figure 4.3: Arrangement of steel cable loops at the edge of the elements [mm]

One of the standard element types (A3) has an opening that is used to pump concrete into the segment (Fig.4.4 and 4.5). This opening is surrounded by four M16 steel threads that allow mounting of a steel adapter which is afterwards connected to a concrete pump.

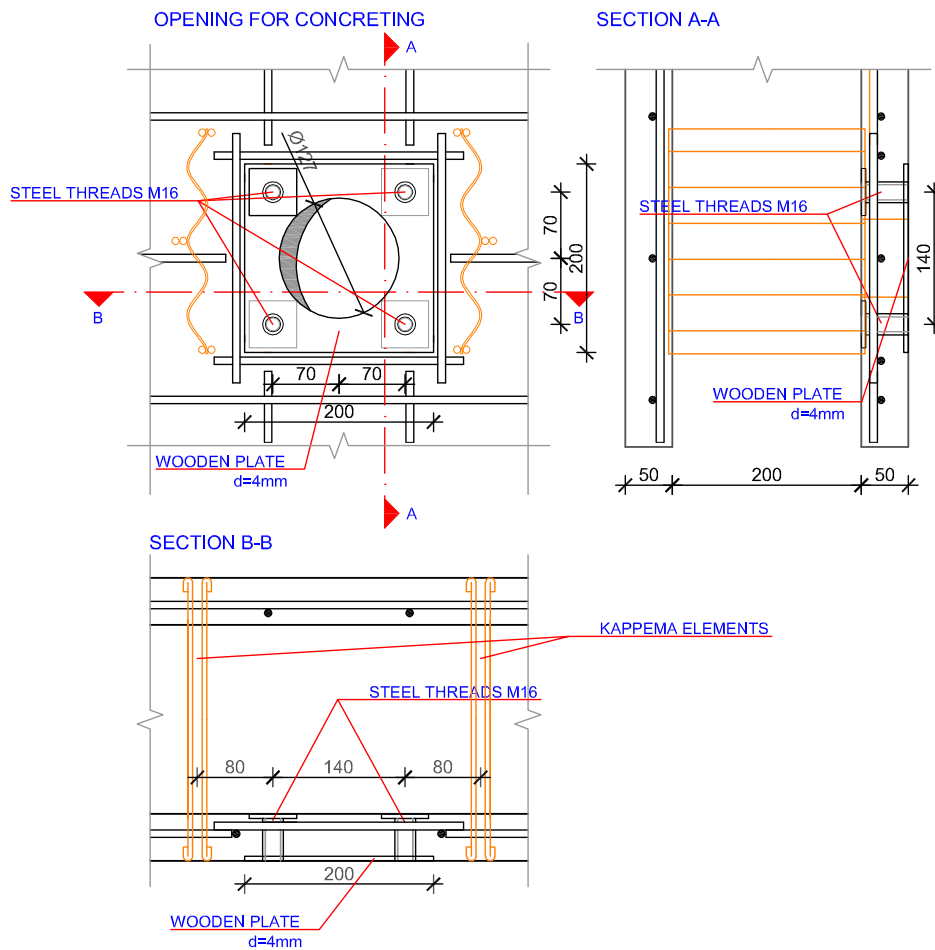


Figure 4.4: Detail of opening for concreting [mm]

The concrete slabs are reinforced by steel bars with a diameter of 8 mm and a grade of BSt 550, which is arranged in a quadratic grid with a mesh size of 150 mm. Whereby, the reinforcement is assembled by an automated welding machine. The connection of both shells is provided by 13 Kappema elements (Fig. 4.5).

The Kappema elements are arranged in four rows which are equally distributed over the segment height. The upper three rows contain three Kappema elements that are arranged symmetrically around the central vertical axis with a mutual distance of 500 mm. Only the elements which contain a concrete block, described in the following paragraphs, miss one connecting element in the top row. The lowest row contains four Kappema elements with a mutual distance of 333 mm, which attributes to the higher pressure while concreting (Fig. 4.5). Additionally, a pair of U-formed reinforcement is situated in all four corners of each double wall element. This provides the possibility to install an additional reinforcement at the top and bottom of the assembled segment in ring direction (Fig. 4.5 and 4.37(e)).

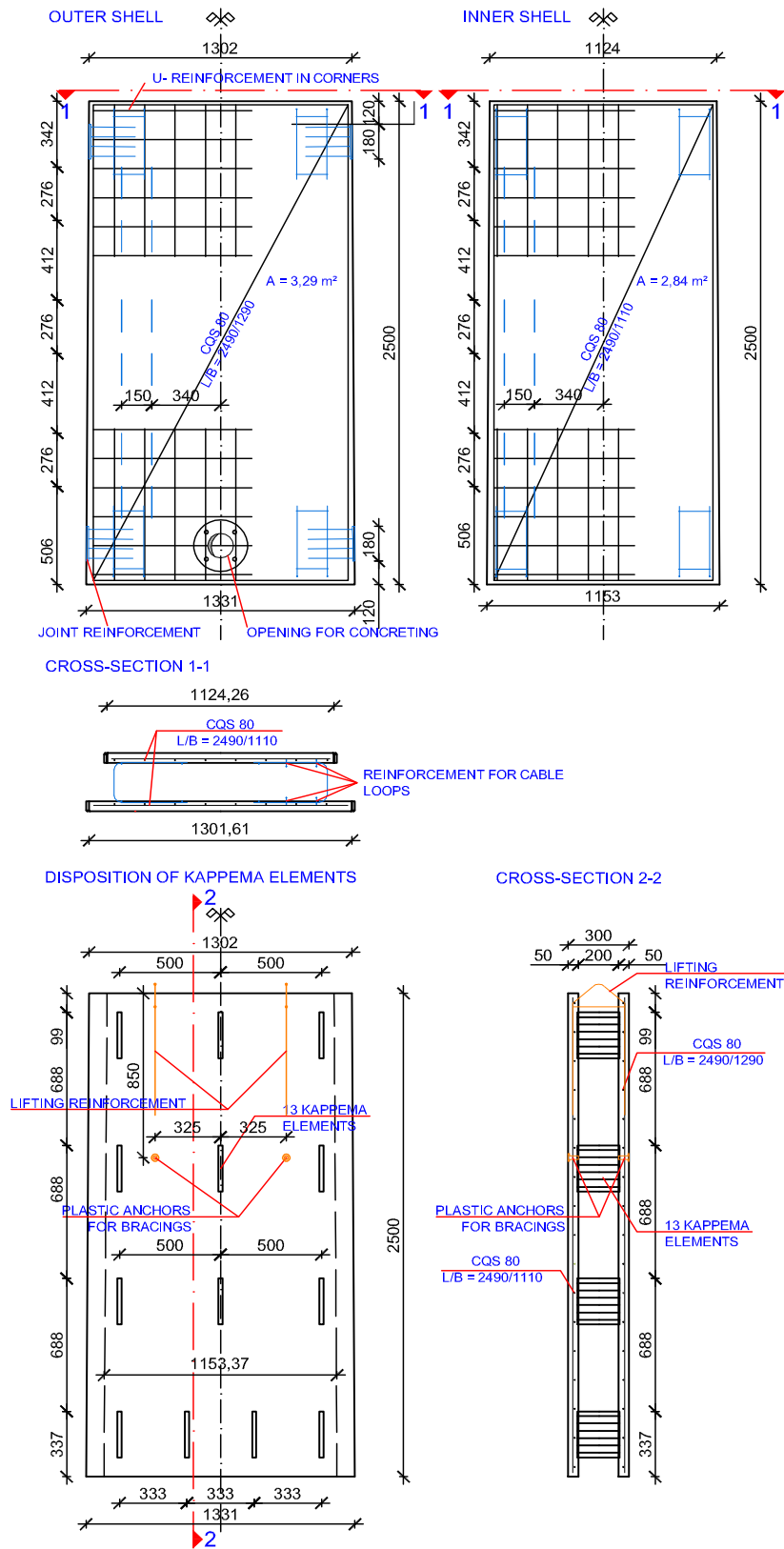


Figure 4.5: Characteristic arrangement of the reinforcement and Kappema waves in the elements [mm]

Every third double wall element (type B1 and B2) contains two concrete blocks that are situated centrally at the top and the bottom (Fig. 4.6). These blocks have two main functions. Firstly, they are used for the lifting of the assembled ring segment to its foreseen location at the tower. Secondly, the blocks are used to position one ring segment on the previous one. Wherein, this positioning by three points enable a precise adjustment of the segment and thus the correction of any inaccuracies. The concrete blocks are reinforced with glass fibre bars, which have a length of 300 mm and a diameter of 8 mm. The glass fibre material is used in order to enlarge the bonding length, because the usually required concrete cover can be neglected. This fibre glass reinforcement was produced by the company Schöck and they are called ComBAR [40].

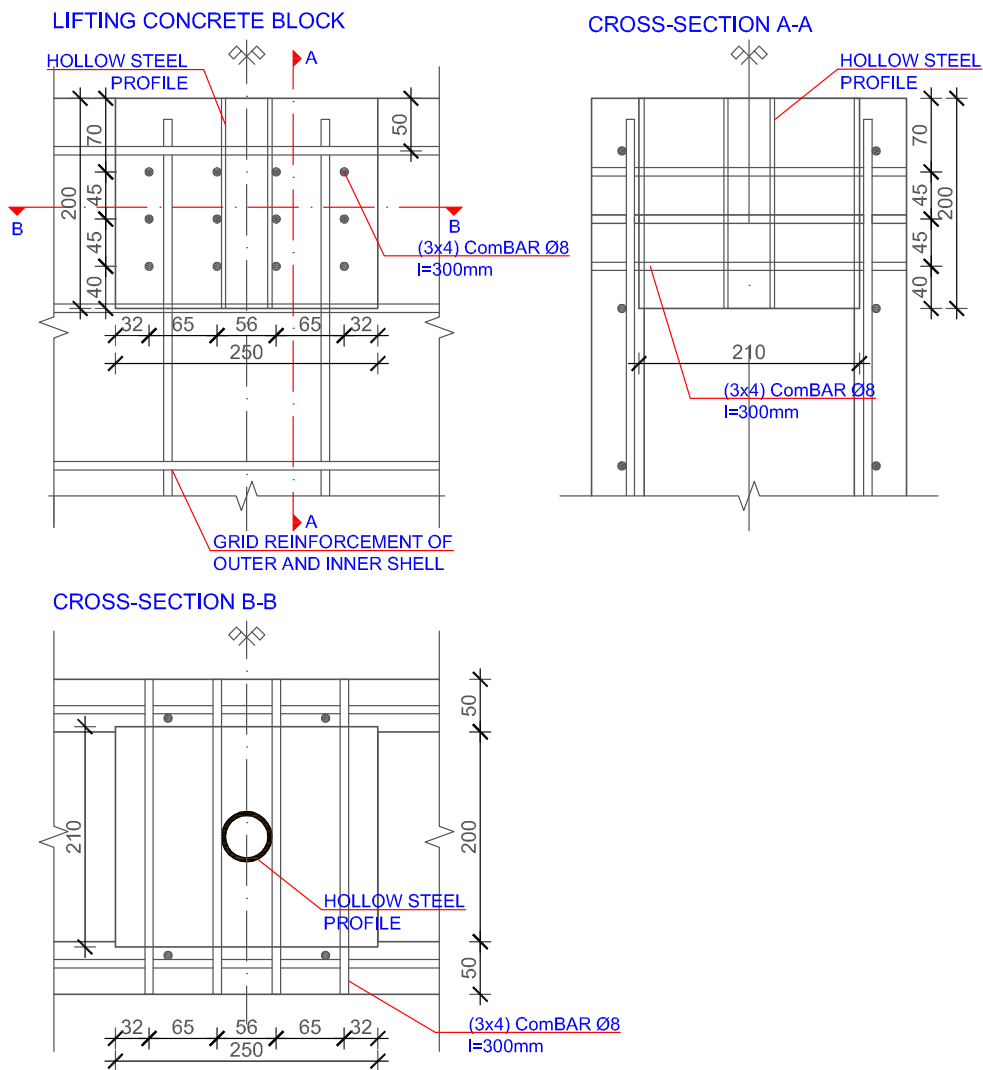


Figure 4.6: Detail of one concrete block [mm]

The joints between elements have to be sealed to prevent leakage during concreting. Therefore, different types of sealings are tested for the mock-up. Wherein, the joints of the outer and inner shells are treated differently. The outer edges of the element types A1 and A3 (for definition see Fig. 4.2) are formed with styrofoam formwork profiles in order to produce a rough surface, while the rest of the elements are formed by steel formwork profiles that result with a smooth edge surface. In that way, the joints with either smooth–smooth, rough–rough or smooth–rough surface are gained (Fig. 4.7). Such arrangement of the elements resulted with the following combinations of the joint surfaces: smooth–smooth, rough–rough or smooth–rough. These combinations are used to examine the flank adhesion with the mortar, which is filled into the joint to form a sealant.

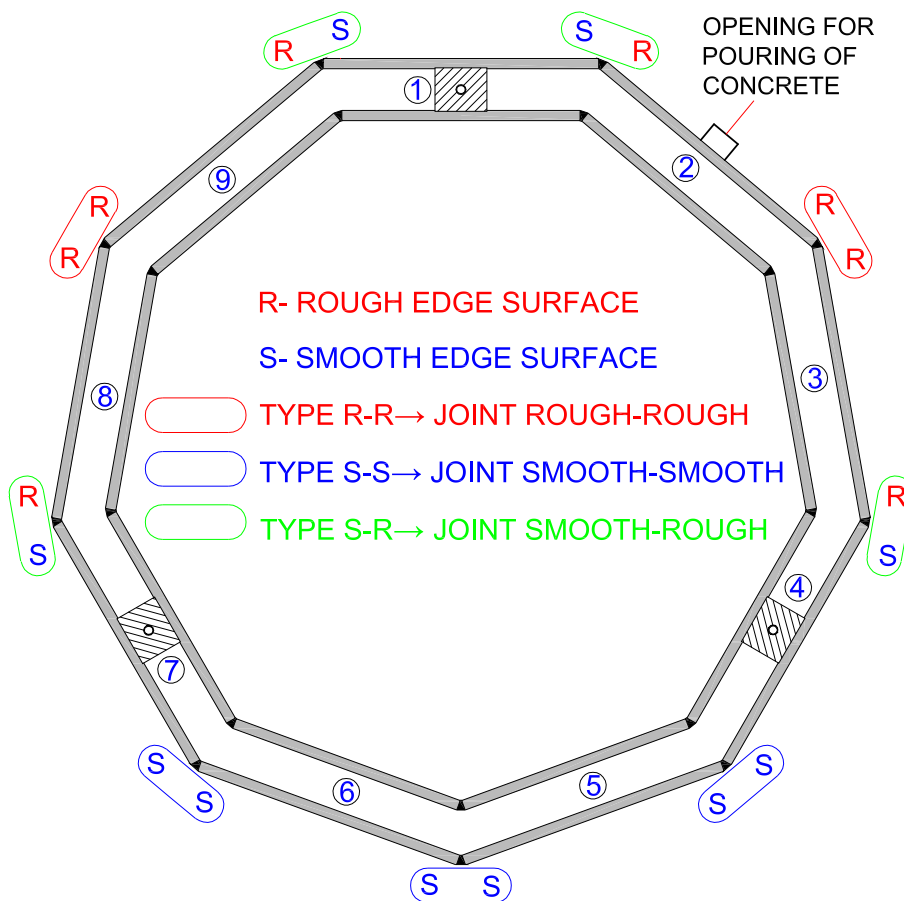


Figure 4.7: Schematic position of smooth and rough surface edges

The inner joints are sealed by two different construction types. The first type of the sealing is realized by foil that is glued over the entire height of the joint, while the second type consists of elastomer tubes clamped into the joint and so providing a sealing during concreting (Fig. 4.8).

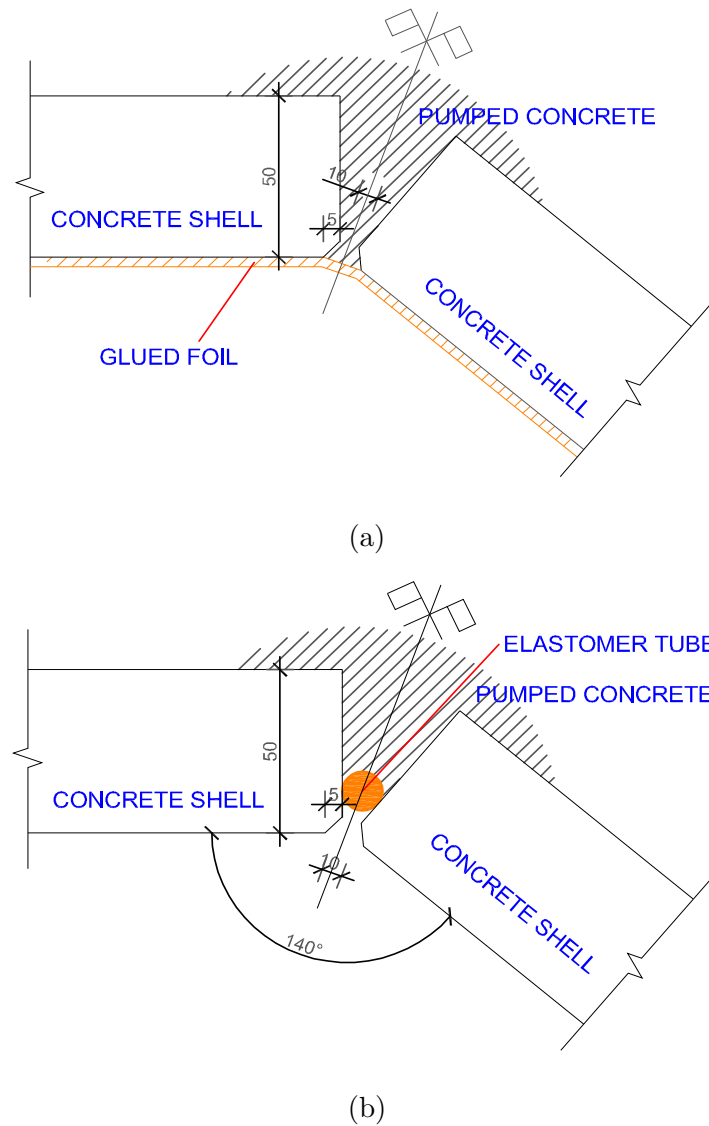


Figure 4.8: Detail of internal vertical joints; (a) glued foil as sealing; and (b) elastomer tube as sealing [mm]

After arrangement, all double wall elements have to be connected to ensure an unchangeable geometry during lifting of the whole segment. This connection is realised by steel embedments that are arranged at the top and the bottom of the outer shell (Fig. 4.9). The embedments consist of a 18 cm long steel plate with four on welded 20 cm long reinforcement bars, which are anchored in the outer shell. To connect two shells, reinforcement bars are placed between the embedments and mutually welded.

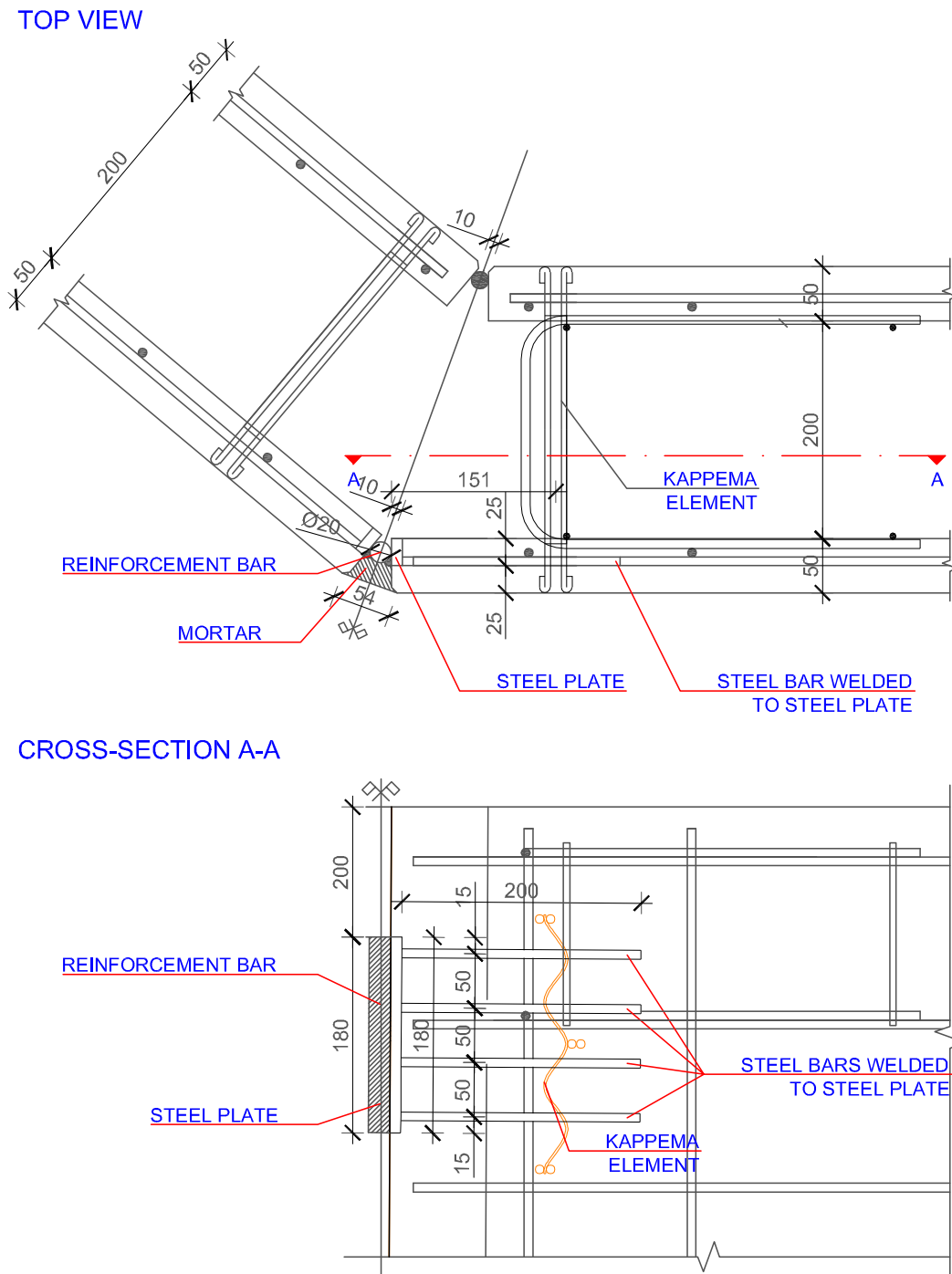


Figure 4.9: Detail of outer vertical joint [mm]

4.2 Structural analysis of the mock-up

An estimation of the structural strength of the chosen mock-up design from Section 4 can be obtained by performing a structural analysis. This analysis should contain considerations about the most important parameters like concrete cover, reinforcement, thickness of the double wall shells and the interconnections of the shells. Herein, one should also consider different load cases and construction phases, such as lifting of the segment and loading of the segment while concreting. All these observations and more are discussed in the following subsection.

4.2.1 Estimation of the required concrete cover

The herein proposed construction method is characterized by the usage of light weight double wall elements. Therefore, the estimation of the concrete cover of both double wall element shells is of high interest. While the inner shell is located under a controlled and rather protected environment, the outer shell is exposed to all corrosive influences of the surrounding environment, which occur over the whole height of approximately 130 m. With this in mind, the field of application for the proposed method is limited to the inland in order to exclude any possible contact with airborne chlorides from sea water. At the inland, it is assumed that the tower is located in a cyclic wet and dry environment, which is classified by the exposure class XC4 according to EN 1992-1-1 [41]. In contrast, the inner shell can be classified to be in a corrosive protected environment and therefore it is classified with exposure class XC0.

The concrete cover can be estimated according to EN 1992-1-1 [41], page 48, table 4.1.1.1 [41]:

$$c_{nom} = c_{min} + \Delta c_{dev} \quad (4.1)$$

where:

- c_{nom} nominal thickness of concrete cover
- c_{min} minimum concrete cover
- Δc_{dev} allowance in design for deviation

Estimation of minimum concrete cover c_{min}

The minimum concrete cover (c_{min}) can be estimated according to EN 1992-1-1, page 49, section 4.4.1.2 [41]:

$$c_{min} = \max \left\{ \begin{array}{c} c_{min,b} \\ c_{min,dur} + \Delta c_{dur,\gamma} - \Delta c_{dur,st} - \Delta c_{dur,add} \\ 10 \text{ mm} \end{array} \right\} \quad (4.2)$$

where:

$c_{min,b}$	minimum cover due to bond requirement
$c_{min,dur}$	minimum cover due to environmental conditions
$\Delta c_{dur,\gamma}$	additive safety element
$\Delta c_{dur,st}$	reduction of minimum cover due to use of stainless steel
$\Delta c_{dur,add}$	reduction of minimum cover due to use of additional protection

The minimum cover regarding the bonding requirements is defined by Table 4.2, page 50, and depends on the biggest used reinforcement bar diameter:

$$c_{min,b} = \text{diameter of bar (for separated bars)} = 8 \text{ mm}$$

The structural class has to be defined in order to determine the minimal concrete cover due to environmental conditions ($c_{min,dur}$). The structural classification as well as the amount of $c_{min,dur}$ is defined in the different national annexes. The recommended structural class for a design working life of 50 years and the exposure class XC4 is S4. Whereby, this recommendation can be adjusted as defined in Table 4.1 of the Eurocode. Due to slab geometry of the double wall elements and due to their production in a factory under controlled conditions with a special quality control, a reduction to class S2 is permitted. Having all the previously given information in mind, the estimated minimum cover for the outside of the tower, considering the environmental conditions according to Table 4.2, page 50, is:

$$c_{min,dur,outside} = 20 \text{ mm}$$

Table 4.1: Recommended structural classification adjustment, taken from EN 1992-1-1, page 50, Table 4.3N [41]

Structural Class							
Criterion	Exposure Class according to Table 4.1						
	X0	XC1	XC2 / XC3	XC4	XD1	XD2 / XS1	XD3 / XS2 / XS3
Design Working Life of 100 years	increase class by 2	increase class by 2	increase class by 2	increase class by 2	increase class by 2	increase class by 2	increase class by 2
Strength Class	≥ C30/37 reduce class by 1	≥ C30/37 reduce class by 1	≥ C35/45 reduce class by 1	≥ C40/50 reduce class by 1	≥ C40/50 reduce class by 1	≥ C40/50 reduce class by 1	≥ C45/55 reduce class by 1
Member with slab geometry (position of reinforcement not affected by construction process)	reduce class by 1	reduce class by 1	reduce class by 1	reduce class by 1	reduce class by 1	reduce class by 1	reduce class by 1
Special Quality Control of the concrete production ensured	reduce class by 1	reduce class by 1	reduce class by 1	reduce class by 1	reduce class by 1	reduce class by 1	reduce class by 1

Table 4.2: Values for the minimum cover regard to the durability of steel reinforcement steel in accordance with EN 10080, taken from EN 1992-1-1, page 51, Table 4.4N [41]

Environmental Requirement for $c_{min,dur}$ (mm)							
Structural Class	Exposure Class according to Table 4.1						
	X0	XC1	XC2 / XC3	XC4	XD1 / XS1	XD2 / XS2	XD3 / XS3
S1	10	10	10	15	20	25	30
S2	10	10	15	20	25	30	35
S3	10	10	20	25	30	35	40
S4	10	15	25	30	35	40	45
S5	15	20	30	35	40	45	50
S6	20	25	35	40	45	50	55

The construction class for the inner shell with the exposure class of XC0 can be defined to be S1. This results in an environmental required concrete cover of:

$$c_{min,dur,inside} = 10 \text{ mm}$$

The recommended values for the remaining parameters can be set to:

$$\Delta c_{dur,\gamma} = 0$$

$$\Delta c_{dur,st} = 0$$

$$\Delta c_{dur,add} = 0$$

Calculation of maximum construction deviation ($\Delta_{c_{dev}}$)

The recommended value of the deviation of reinforcement bars is defined in the Eurocode 1992. The recommended value amounts to be 10 mm, whereby, this value can be reduced under certain circumstances according to EN 1992-1-1, page 54, section 4.4.1.3:

$$10 \text{ mm} \geq \Delta_{c_{dev}} \geq 0 \text{ mm}$$

However, according to the Austrian National Annex ON B 1992-1-1 following recommendation for maximal deviation can be found to be:

$$\Delta_{c_{dev}} = 5 \text{ mm}$$

Nominal concrete cover (c_{nom})

Considering all the information given in the previous subsections allow to estimate the minimum required concrete cover for the outer and inner side of the tower structure:

$$\begin{aligned} c_{nom, outside} &= c_{min, outside} + \Delta_{dev} = 20 + 5 = 25 \text{ mm} \\ c_{nom, inside} &= c_{min, inside} + \Delta_{dev} = 10 + 5 = 15 \text{ mm} \end{aligned}$$

4.2.2 Estimation of normal forces in the concrete shells due to concrete pressure

To minimize the construction time of the tower it is desired to concrete a height of at least 2.5 to 3.5 m at one time. This means that care should be taken that the pre-assembled segment, which is placed on its foreseen position at the tower, is capable of bearing the pressure while concreting. Therefore, the following sections are dedicated to reveal if any normal forces in ring direction occur when that the polygon is loaded by a perpendicular pressure load.

In the first estimation a hexagon model is examined because it represents a simplification of the mock-up nine edged geometry. The hexagon model consists of two mutually interconnected rings with circumcircle diameters of 470 and 500 cm (Fig. 4.10). As a first estimation, the interconnections arranged in the corners of the polygon should represent girder beams or Kappema elements. Herein, all corners are fully hinged around the global z direction in order to transmit only forces and no moments.

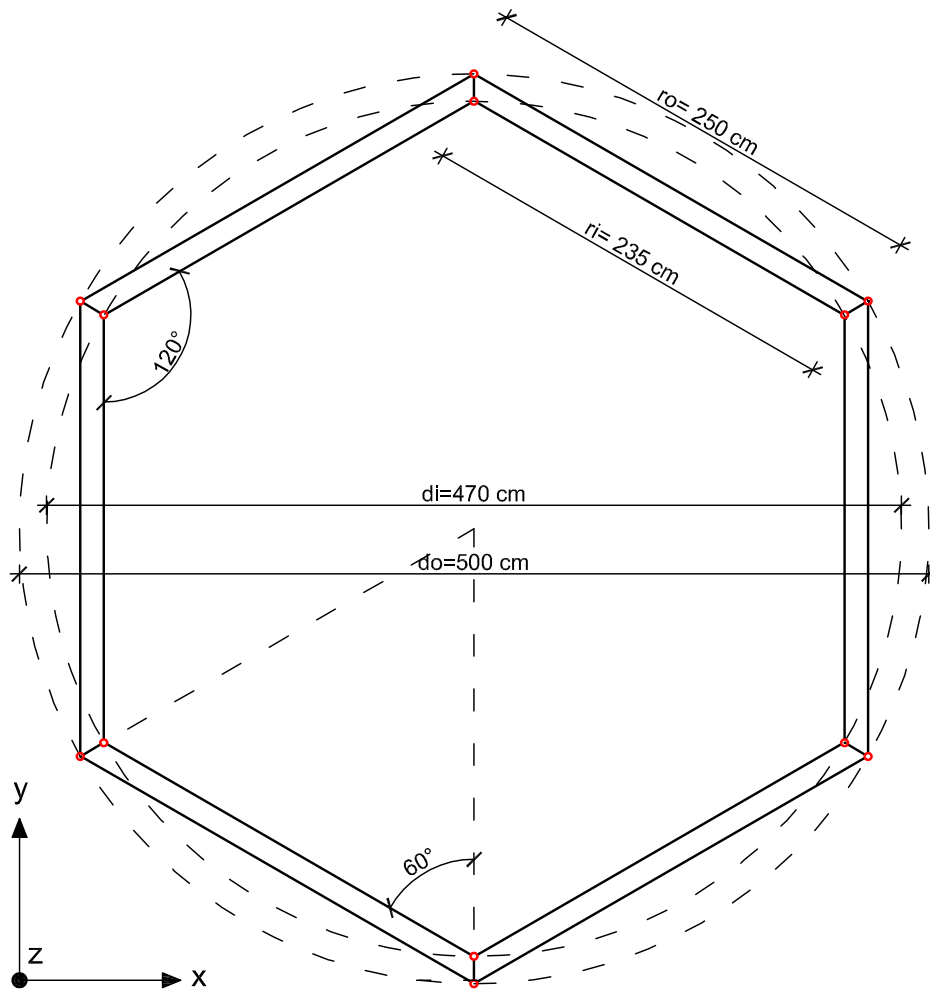


Figure 4.10: Proposed simplified mock-up geometry in the form of a double shell polygon, interconnected at the edges which are hinged around the global z direction

In the next step the geometrical constraints (e.g. support conditions) have to be defined so that the system is at least statically determined and able to reproduce the real state variables like forces, moments, deflections and rotations.

In the first considerations, one beam of the polygon is extracted out of the structure. Herein, the neighboring beams can be modeled as sliding supports, while the interconnections of the shells are neglected. The introduced support reactions are placed in a way to enable free expansion of the shell perpendicular to its axis. This extracted shell, loaded with a perpendicular linear distributed load, is shown in Fig. 4.11.

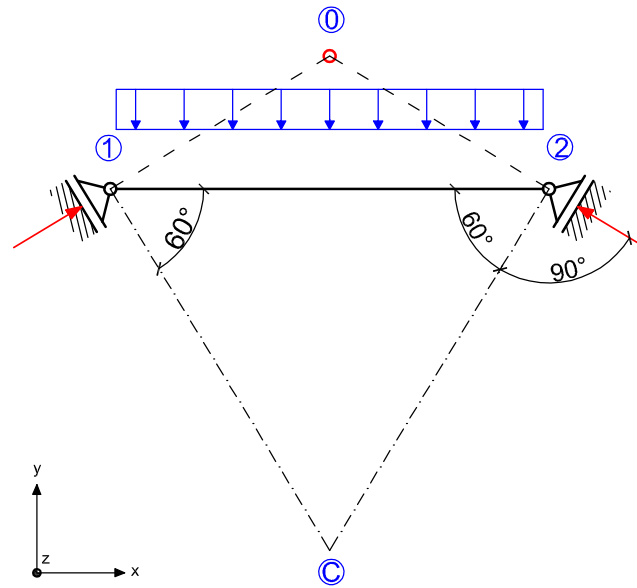


Figure 4.11: Extracted polygonal shell with suggested support conditions

It can be noticed that the proposed support reactions of this partial system are concurrent and therefore capable of rotating around the z axis located in the point O . Consequently, an additional boundary condition needs to be introduced in order to restrain this rotation. The now gained system with the restrained rotation at the center of the beam is presented in Fig. 4.12.

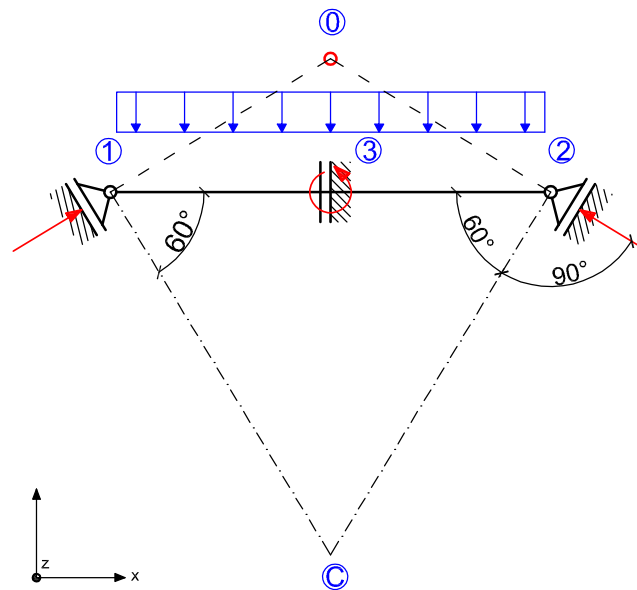


Figure 4.12: Extracted polygonal shell with restrained rotation

In the following step the outer and inner shells are merged together by using the previously defined support conditions. Whereby, both shells are loaded with linear distributed loads that press the elements from the inside to the outside (Figure 4.13). This partial system, which is a sixth of the hexagon, is capable to represent the whole structure in terms of the state variables.

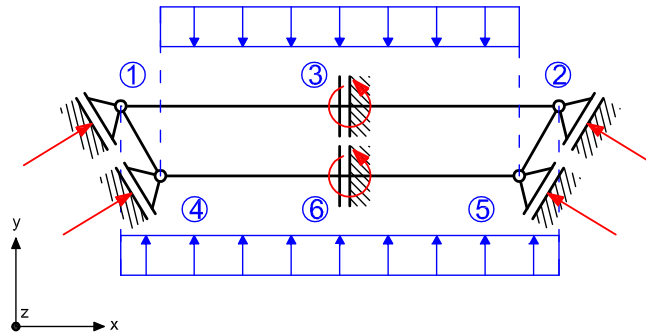


Figure 4.13: One sixth of a polygon with introduced supports reactions that represents the neighboring polygonal sides

Applying of the previously described boundary conditions to the whole hexagon result in the searched model for further investigations of any normal forces induced by concrete pressure (Fig.4.14).

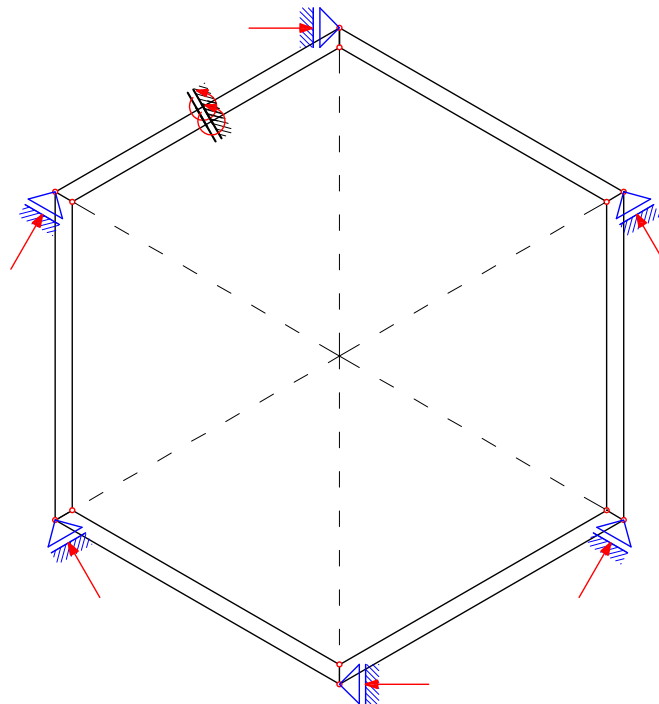


Figure 4.14: Support conditions of the hexagon model

4.2.2.1 Analytical analysis

The previously discussed hexagon model is now used to estimate the internal forces due to concrete pressure. The concrete pressure pushes the inner shells inside, while the outer one is pushed outside. The different lengths of the shells is an indicator for the appearance of the normal forces in the shells, because it is assumed that the greater length of the outer shell compared to the inner one results in an internal tension force. Additionally, the interconnections have to keep both shells together and thus also have to transmit normal forces.

To estimate these internal forces, an assumption of the bending and strain stiffness is needed. Therefore, it is assumed that the shells have a bending stiffness equal to infinite and a strain stiffness amounting to a finite value. Moreover, the interconnection of the shells is not only assumed, as former described, to be in the edges of the hexagon, but also continuously distributed about the whole hexagon perimeter (Fig. 4.15 and 4.16).

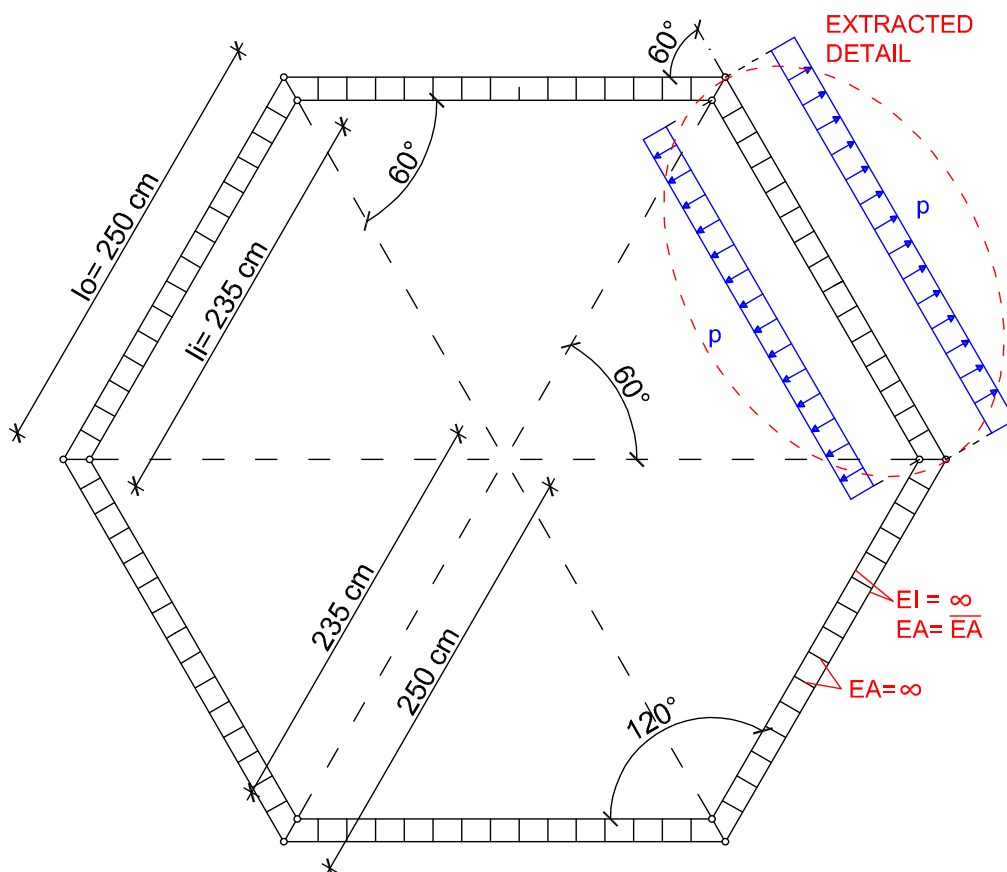


Figure 4.15: Hexagon model with concrete pressure load and simplified approximation for the bending and strain stiffness

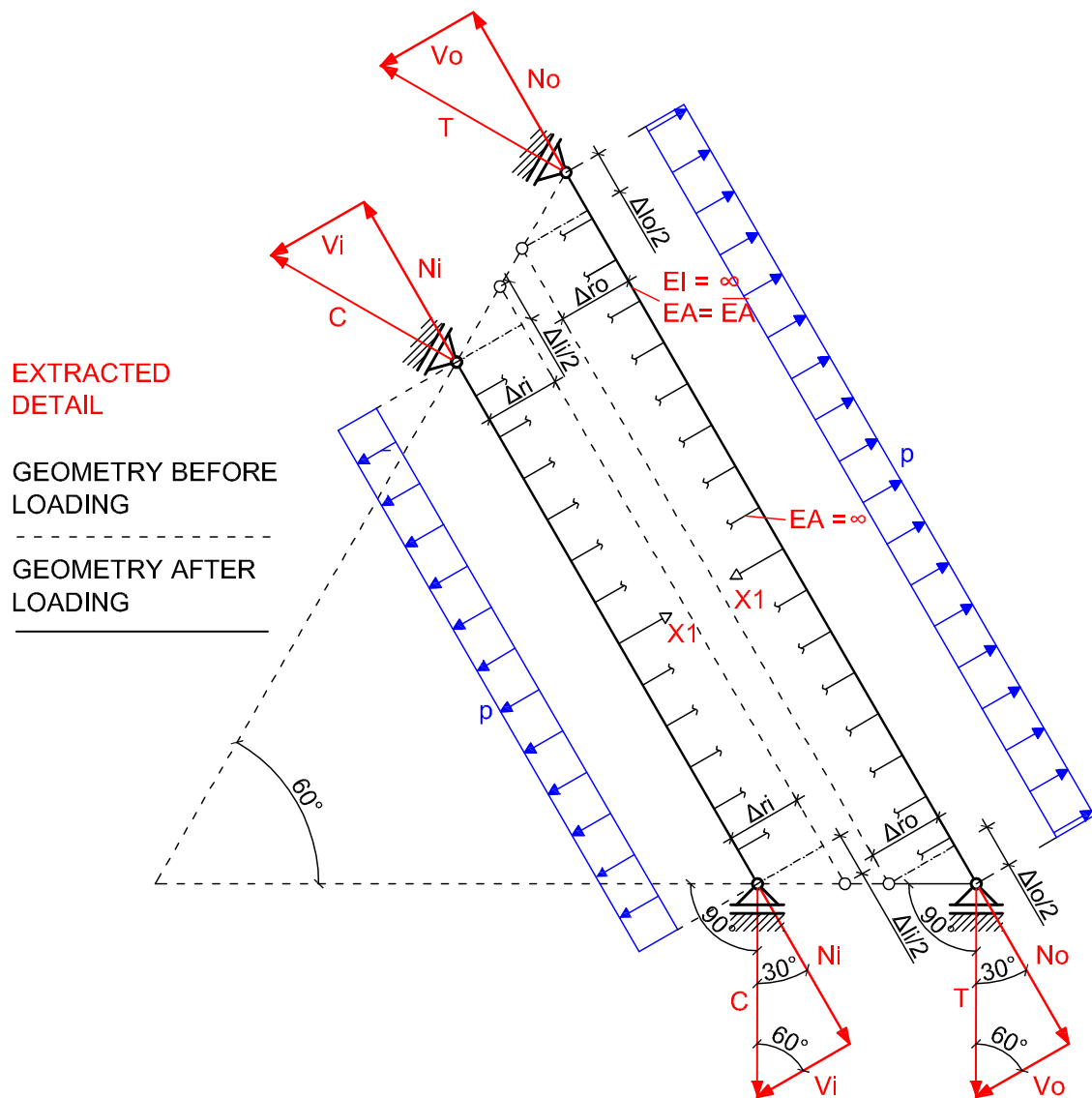


Figure 4.16: One sixth of the hexagon extracted from the whole model showing the geometrical relation between the elongation of length and radius, as well as the relation between normal force, shear force and the support reactions

Each concrete shell for itself is statically determined, but the connection of both results in a statically indeterminate system. Therefore, the flexibility method is used to estimate the state variables. Herein, the change of radius is used as the geometrically compatibility equation:

$$(\Delta r_{o,x1=1} + \Delta r_{i,x1=1}) \cdot X_1 + (\Delta r_{o,p} + \Delta r_{i,p}) = 0 \quad (4.3)$$

where:

$\Delta r_{o,x1=1}$	elongation of outer radius due to connection force
$\Delta r_{i,x1=1}$	elongation of inner radius due to connection force
$X_1 = 1$	connection force
$\Delta r_{o,p}$	elongation of outer radius due to concrete pressure
$\Delta r_{i,p}$	elongation of inner radius due to concrete pressure

This relation is applicable only if the interconnection strain stiffness is assumed to be infinite, so consequently, there is no change in the difference between the inner and outer radius.

The former needed elongation of radius (Δr) can be shown in dependence of the elongation of one member (Δl).

$$\Delta r = \frac{\Delta l}{2} \cdot \frac{1}{\tan(30)} \quad (4.4)$$

The elongation itself (Δl) can be expressed in dependence of the normal force (N), the total length (l) and the strain stiffness (EA) of the observed member:

$$\Delta l = \frac{N \cdot l}{EA} \quad (4.5)$$

For our special case the normal force of the beam can be estimated in dependence of the shear force (V) of the observed member:

$$N = V \cdot \frac{1}{\tan(30)} \quad (4.6)$$

If the equation for the static equilibrium of summed forces, which parallel to the shear force (V), are used separately for the loadings p and X_1 , the following relations for both shells are obtained (i ...inner, o ...outer):

$$V_{o,p} = \frac{p \cdot l_o}{2} \quad (4.7)$$

$$V_{i,p} = -\frac{p \cdot l_i}{2} \quad (4.8)$$

$$V_{o,X_1} = -\frac{X_1}{2} \quad (4.9)$$

$$V_{i,X_1} = \frac{X_1}{2} \quad (4.10)$$

If the former path of thinking is reversed, the searched elongation in radius can be expressed by already known values. As a first step, the equations 4.7 to 4.10 are inserted into 4.6:

$$N_{o,p} = \frac{p \cdot l_o}{2} \cdot \frac{1}{\tan(30)} \quad (4.11)$$

$$N_{i,p} = -\frac{p \cdot l_i}{2} \cdot \frac{1}{\tan(30)} \quad (4.12)$$

$$N_{o,X_1} = -\frac{X_1}{2} \cdot \frac{1}{\tan(30)} \quad (4.13)$$

$$N_{i,X_1} = \frac{X_1}{2} \cdot \frac{1}{\tan(30)} \quad (4.14)$$

Introducing the gained relations 4.11 to 4.14 into 4.5 enables to calculate the elongation of the shells in dependence of the loading:

$$\Delta l_{o,p} = \frac{p \cdot l_o^2}{2 \cdot EA} \cdot \frac{1}{\tan(30)} \quad (4.15)$$

$$\Delta l_{i,p} = -\frac{p \cdot l_i^2}{2 \cdot EA} \cdot \frac{1}{\tan(30)} \quad (4.16)$$

$$\Delta l_{o,X_1} = -\frac{X_1 \cdot l_o}{2 \cdot EA} \cdot \frac{1}{\tan(30)} \quad (4.17)$$

$$\Delta l_{i,X_1} = \frac{X_1 \cdot l_i}{2 \cdot EA} \cdot \frac{1}{\tan(30)} \quad (4.18)$$

Finally, the searched elongation of radius can be estimated for each shell:

$$\Delta r_{o,p} = \frac{p \cdot l_o^2}{2 \cdot 2 \cdot \tan(30)^2 \cdot EA} \quad (4.19)$$

$$\Delta r_{i,p} = -\frac{p \cdot l_i^2}{2 \cdot 2 \cdot \tan(30)^2 \cdot EA} \quad (4.20)$$

$$\Delta r_{o,X_1} = -\frac{X_1 \cdot l_o}{2 \cdot 2 \cdot \tan(30)^2 \cdot EA} \quad (4.21)$$

$$\Delta r_{i,X_1} = \frac{X_1 \cdot l_i}{2 \cdot 2 \cdot \tan(30)^2 \cdot EA} \quad (4.22)$$

After transforming the equation 4.3 by the expressing and inserting $X_{1=1}$ in the expressions for $\Delta r_{o,X_1}$ and $\Delta r_{i,X_1}$, the X_1 can be estimated by following transformations:

$$\begin{aligned}
 X_1 &= \frac{\Delta r_{o,p} + \Delta r_{i,p}}{\Delta r_{o,X_{1=1}} + \Delta r_{i,X_{1=1}}} \\
 &= \frac{p \cdot (l_o^2 + l_i^2) \cdot \frac{1}{4 \cdot EA \cdot \tan(30)^2}}{1 \cdot (l_o + l_i) \cdot \frac{1}{4 \cdot EA \cdot \tan(30)^2}} \\
 &= p \cdot \frac{l_o^2 + l_i^2}{l_o + l_i}
 \end{aligned} \tag{4.23}$$

Using a concrete pressure load of $p = 80 \text{ kN/m}$ and the former defined geometry of $l_o = 2.5 \text{ m}$ and $l_i = 2.35 \text{ m}$, the following values for the force in the connection and the normal force in the shells can be calculated:

$$\begin{aligned}
 N_o &= N_{o,p} + N_{o,X_1} \\
 &= \frac{p \cdot l_o}{2 \cdot \tan(30)} - \frac{X_1}{2 \cdot \tan(30)} \\
 &= \frac{p \cdot l_o}{2 \cdot \tan(30)} - \frac{p \cdot \frac{l_o^2 + l_i^2}{l_o + l_i}}{2 \cdot \tan(30)} \\
 &= \frac{p}{2 \cdot \tan(30)} \cdot \left(l_o - \frac{l_o^2 + l_i^2}{l_o + l_i} \right) \\
 &= \frac{80}{2 \cdot \tan(30)} \cdot \left(2.50 - \frac{2.5^2 + 2.35^2}{2.5 + 2.35} \right) \\
 &= 5.04 \text{ kN}
 \end{aligned}$$

$$\begin{aligned}
 N_i &= N_{i,p} + N_{i,X_1} \\
 &= -\frac{p \cdot l_i}{2 \cdot \tan(30)} + \frac{X_1}{2 \cdot \tan(30)} \\
 &= \frac{p}{2 \cdot \tan(30)} \cdot \left(-l_i + \frac{l_o^2 + l_i^2}{l_o + l_i} \right) \\
 &= 5.36 \text{ kN}
 \end{aligned}$$

$$X_1 = 80 \cdot \frac{2.5^2 + 2.35^2}{2.5 + 2.35} = 194.19 \text{ kN}$$

What stands out is the fact that both interconnected shells have to bear a rather small tension load compared to the tension force in the interconnection.

4.2.2.2 Approval of analytical solution using the FEM

To prove the previously gained analytical solution, a computer analysis is performed using the RFEM– finite element method software for structural analysis and design created by the company Dlubal. The same geometry as introduced in Fig. 4.15 is implemented in the program (Fig 4.17). Additionally, both shells are connected in each corner by 32 double hinged interconnections per hexagon sixth.

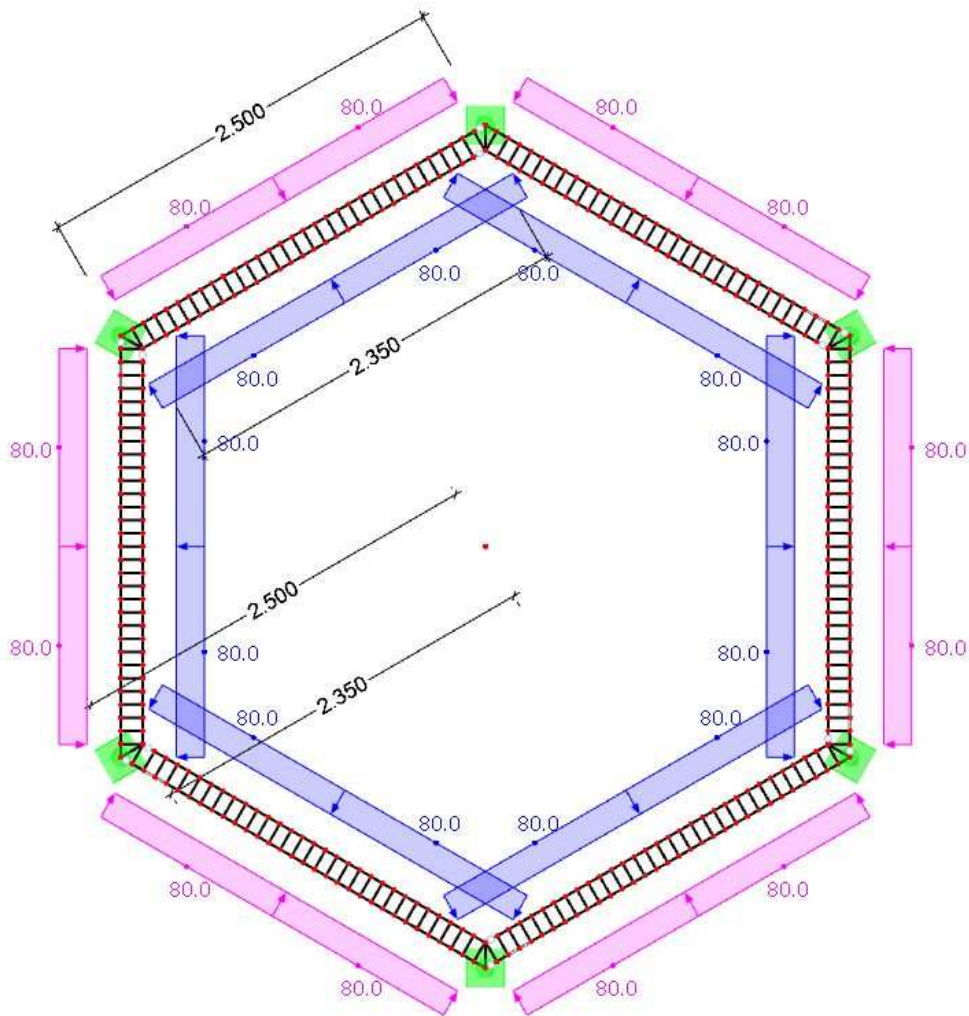


Figure 4.17: FEM model showing the hexagon model loaded by an assumed concrete pressure of 80 kN/m (dimensions in [m])

Comparing the gained internal normal forces of the shells with the analytical solution shows that they are nearly identical (Fig. 4.18). Both shells are loaded with a tensile force and the divergence is very small:

$$\Delta_i = 100 - \frac{N_{i,analytical}}{N_{i,FEM}} \cdot 100 = 100 - \frac{5.04}{5.05} \cdot 100 = 0.19\%$$

$$\Delta_o = 100 - \frac{N_{o,analytical}}{N_{o,FEM}} \cdot 100 = 100 - \frac{5.36}{5.35} \cdot 100 = 0.19\%$$

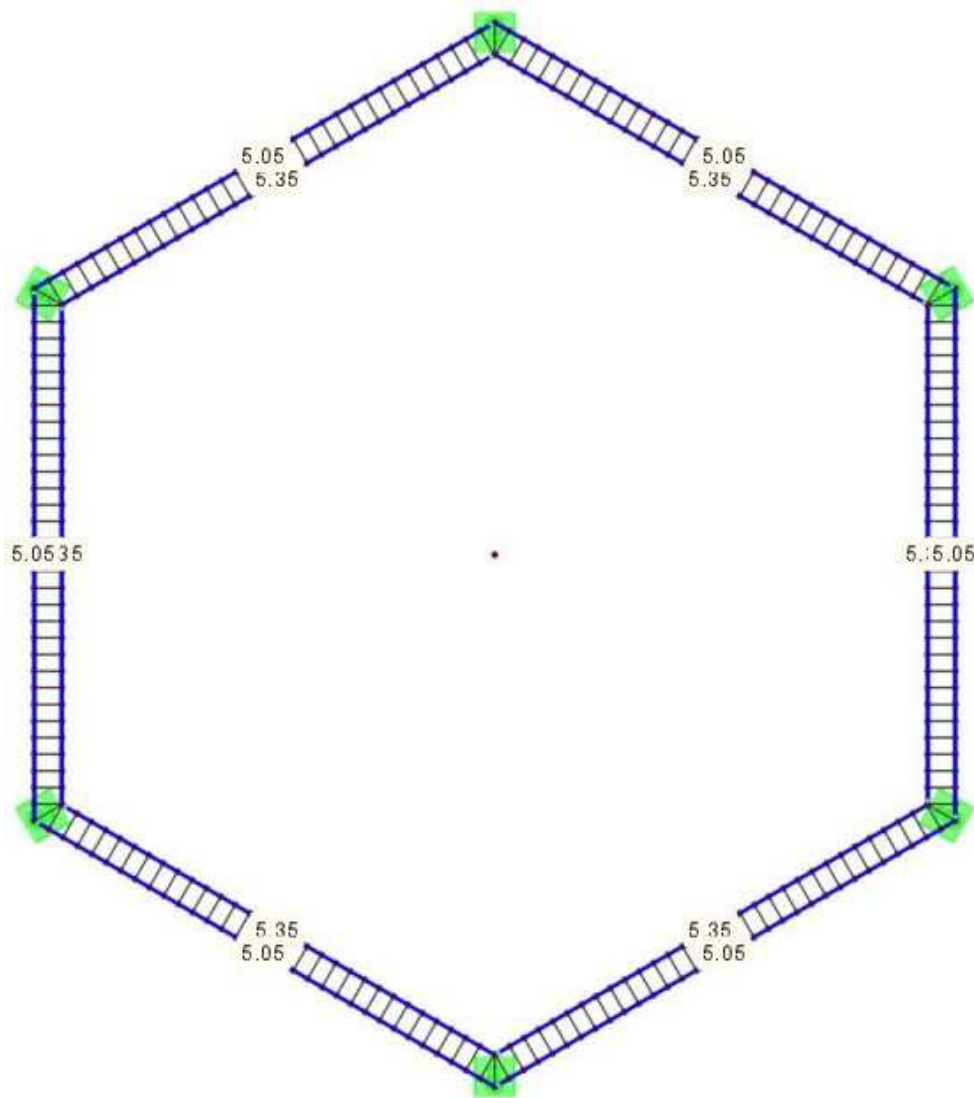


Figure 4.18: Plotted results of internal normal forces in the shells [kN]

Summing up the connection forces of all 32 interconnections in the sixth of the hexagon model shows that the analytical solution match with the one gained by the FEM

(Fig. 4.19). All interconnection together inherit a force of 194.16 kN, which is very close to the analytical solution of 194.19 kN.

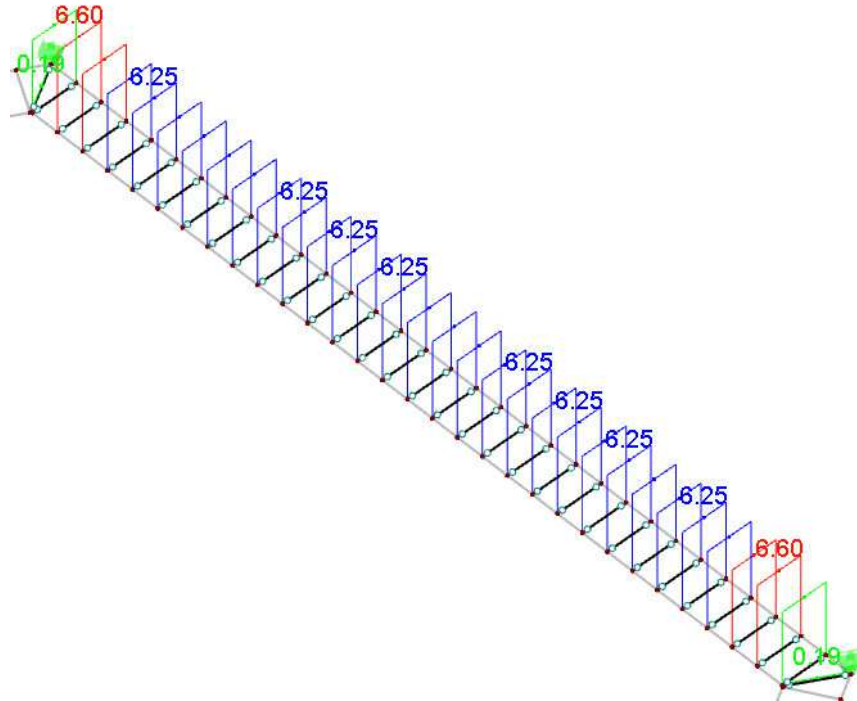


Figure 4.19: One sixth of the FEM model showing the internal forces in interconnection [kN]

As a conclusion, it can be stated that this investigation gives a better insight into the behaviour of a polygonal double ring segment loaded by a concrete pressure in the hollow space between both shells. This, so gained insight, is used in the further considerations for the mock-up with its real measurements and geometry of a nine sided polygon.

4.2.3 Structural analysis of the mock-up

To perform a fully structural analysis of the mock-up, all relevant load cases during construction stages have to be defined. In the planning phase the following load cases are recognized:

- loading of the pre-assembled segment through its self weight while lifting,
- loading of the pre-assembled segment by mounted scaffolding, and
- loading of the pre-assembled segment by the concrete pressure while concreting

There could be more than the three mentioned load cases, but until now these ones are identified. In the following, only the concrete pressure is investigated in order to define the needed reinforcement and the required concrete shell thickness.

4.2.3.1 Concrete pressure

The pressure caused by wet unhardened concrete is the matter of scientific investigations and codes like [42] and [43]. Certainly, the consistence of the used concrete has a big influence in a way that concrete with a high water percentage and additives, like flow improves and plasticisers, shows a higher lateral concrete pressure.

One of the mentioned works [42] recommend that an inner friction angle and the cohesion can be used to reduce the estimated pressure. In our case, an estimation on the safe side is used by stating that the pressure while concreting can never be higher than the hydrostatic pressure. Using a self defined safety factor of γ_s , the following concrete pressure (p_d) for the whole segment height ($h=2.5$ m) can be assumed:

$$p_d = \gamma_s \cdot \gamma_c \cdot h = 1.35 \cdot 24 \cdot 2.5 = 84.38 \text{ kN/m}^2$$

where:

- γ_s safety factor
- γ_c specified weight of fresh concrete
- h height of the mock-up

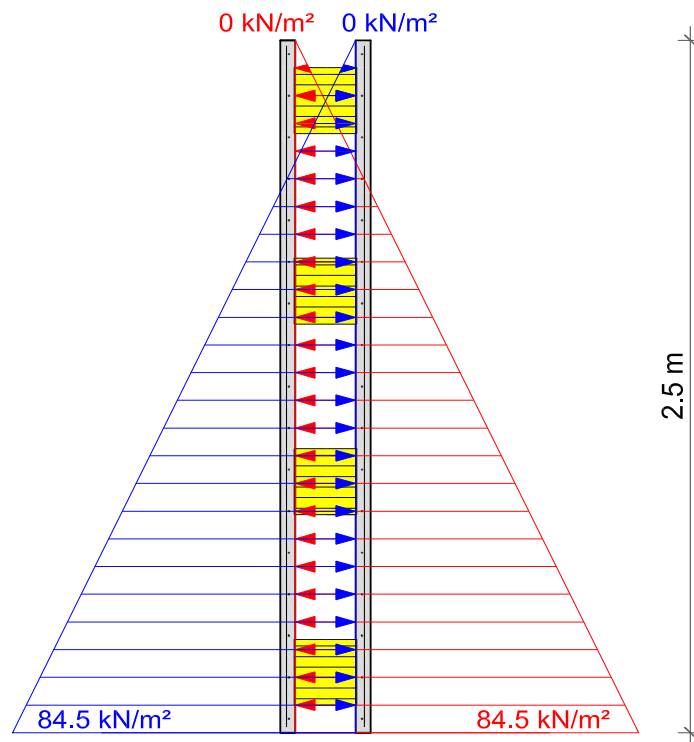


Figure 4.20: Concrete pressure on one double wall element when the whole height is concreted at once

4.2.3.2 Internal forces of vertical element strip

For the investigation of the internal forces in the mock-up segment, a 1 m wide vertical strip is extracted from the system and analysed. The internal forces are estimated for the shell sections that are cut through the Kappema elements. Each Kappema element, which consist of three sticks anchored in both concrete shells, is modeled as one support. These support forces calculated using RFEM are presented in Fig. 4.21.

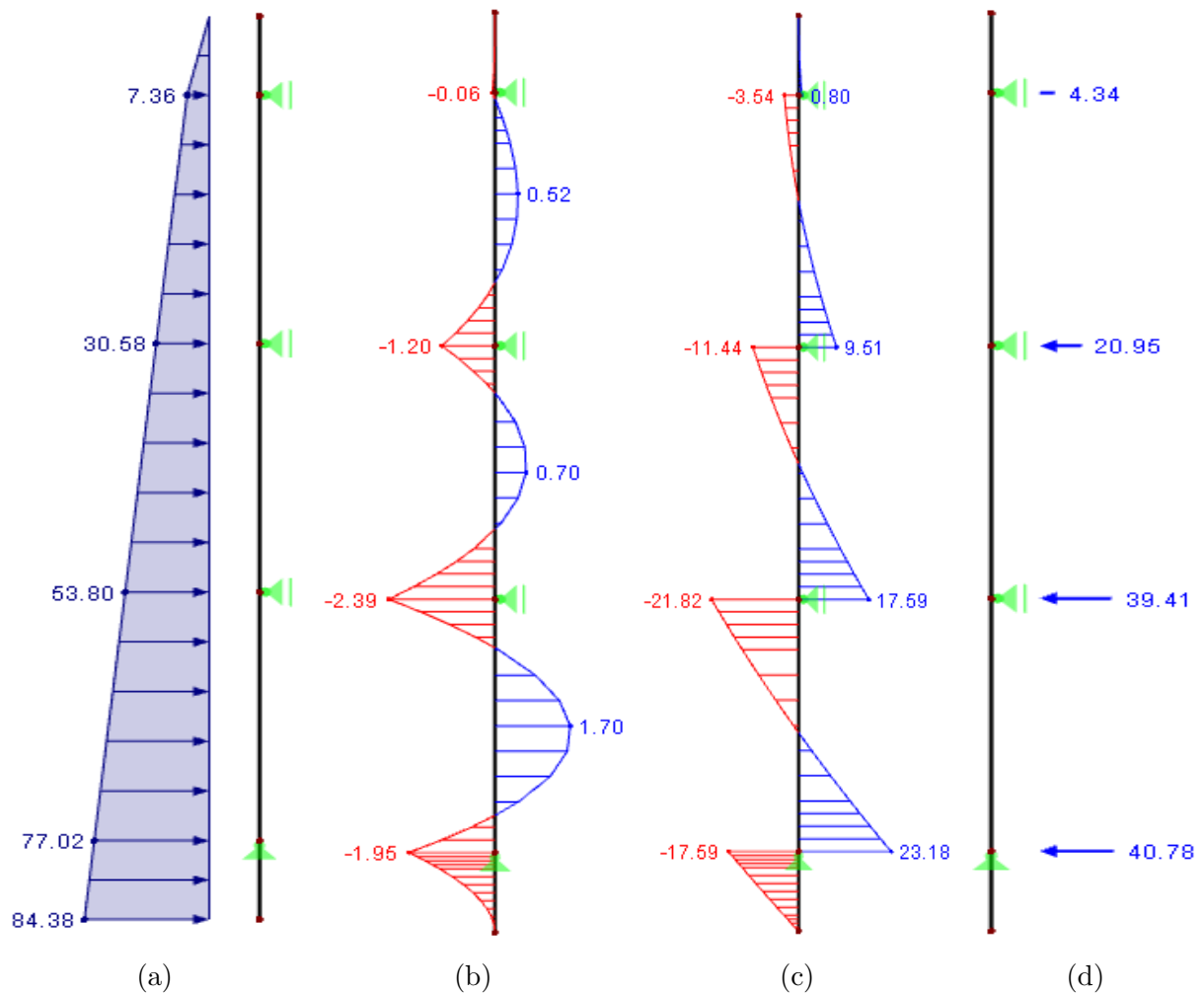


Figure 4.21: Modeled system with loading, internal forces and support reactions of a one meter wide element strip; (a) loading by concrete pressure [kN/m]; (b) moments [kNm]; (c) shear forces [kN]; and (d) reaction forces [kN]

Following relevant values were obtained from the analysis of the vertical strip:

Maximum positive moment:	1.70 kNm
Maximum negative moment:	2.39 kNm
Maximum reaction force:	40.78 kN
Maximum shear force:	23.18 kN

The analysis of the vertical strip shows that, as it is assumed, the cross-section positioned in the lowest row of the Kappema elements have the highest loading of a horizontal concrete strip. Therefore, this horizontal cross-section with a maximal loading of 40.78 kN/m is further investigated.

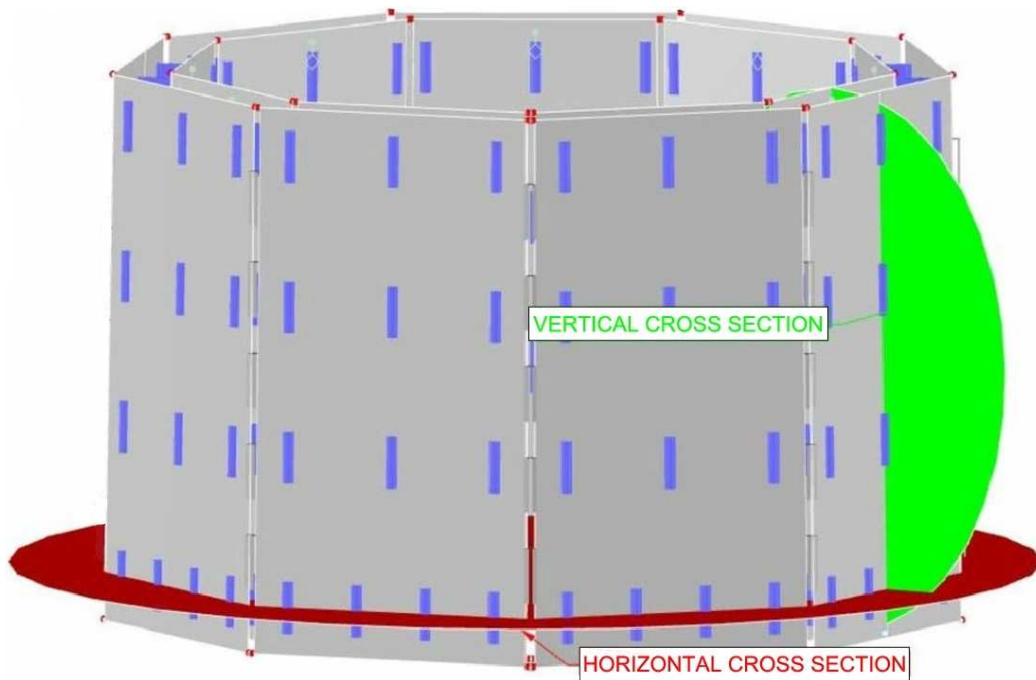


Figure 4.22: Relevant cross-section used in the structural analysis of the mock-up

4.2.3.3 Internal forces of the most loaded horizontal element strip

The horizontal cross-section through the bottom row of the Kappema elements with the loading estimated from the vertical strip is analyzed next. At first, it is necessary to estimate the relevant cross-section height that will be used in the analysis. This effective segment height can be calculated by the equilibrium of the lowest support force R_4 and the linear loading $p(h)$ (Fig. 4.23).

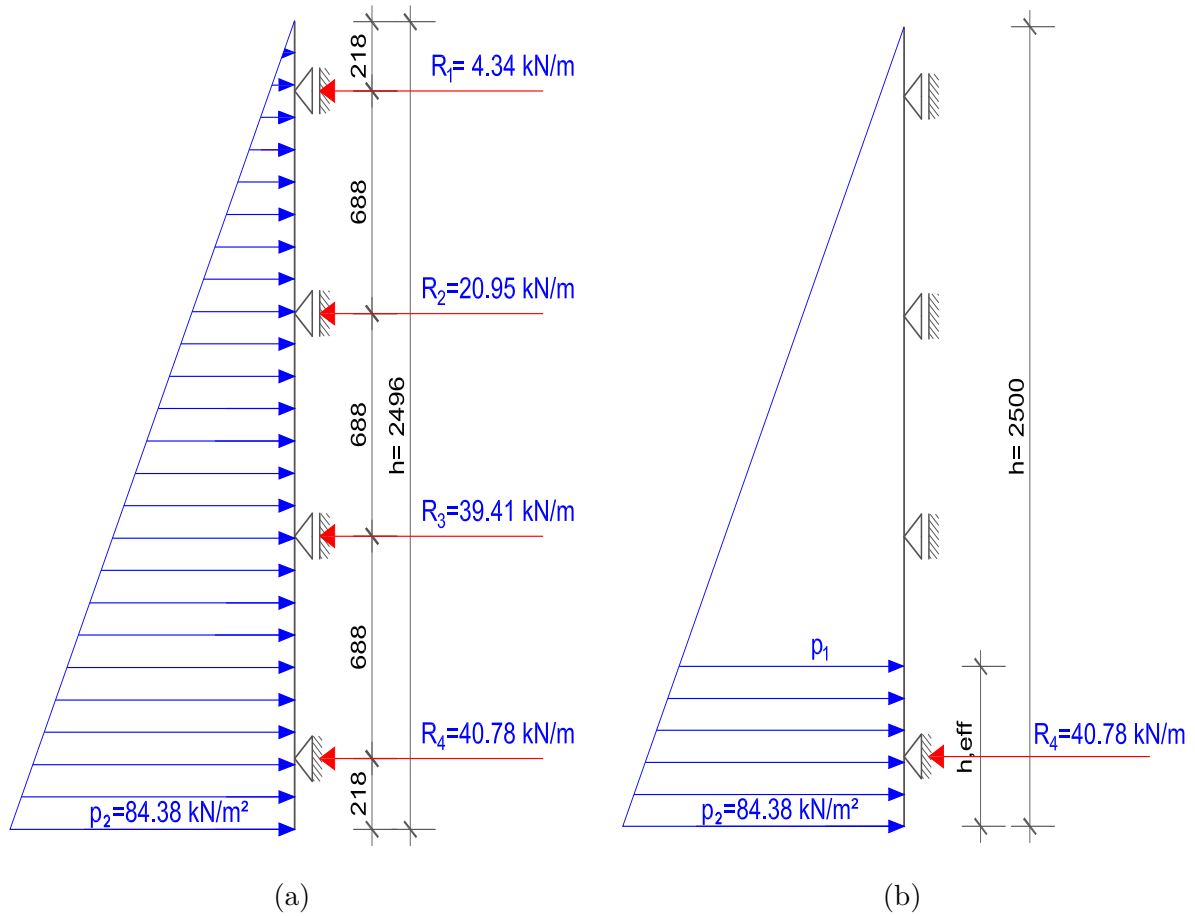


Figure 4.23: Estimation of effective pressure height; (a) support reaction forces; and (b) equilibrium of support reaction and linear load [cm]

Used notation:

- h height of the double wall element
- w width of the element
- h_{eff} estimated effective height
- R_4 reaction force in the lowest support
- p_1 pressure at the height h_{eff}
- p_2 maximal pressure

A force equilibrium between the bottom reaction force R_4 and the linear load $p(h)$ can be expressed in the following way:

$$\frac{p_2 + p_1}{2} \cdot w \cdot h_{eff} = R_4 \quad (4.24)$$

From the theorem of similarity of triangles the following relation can be stated:

$$\frac{p_2}{h} = \frac{p_1}{h - h_{eff}} \longrightarrow p_1 = \frac{p_2 \cdot (h - h_{eff})}{h} \quad (4.25)$$

Inserting equation 4.24 into the 4.25, the following quadratic equation for the effective height is obtained:

$$\frac{p_2 + \frac{p_2 \cdot (h - h_{eff})}{h}}{2} \cdot w \cdot h_{,eff} = R_4 \quad (4.26)$$

Simplifying equation 4.26 into the standard form of a quadratic equation, the following equation is gained:

$$h_{eff}^2 - 2 \cdot h_{eff} \cdot h + \frac{2 \cdot R_4 \cdot h}{p_2 \cdot w} = 0 \quad (4.27)$$

Therefore, the solution of the quadratic equation for the effective height of the bottom ring segment can be estimated by following expression:

$$h_{eff} = \frac{2 \cdot h \pm \sqrt{4 \cdot h^2 - \frac{8 \cdot R_4 \cdot h}{p_2 \cdot w}}}{2} \quad (4.28)$$

With the known values h_{eff} can be defined:

$$h_{eff} = \frac{2 \cdot 2.5 \pm \sqrt{4 \cdot 2.5^2 - \frac{8 \cdot 40.78 \cdot 2.5}{84.38 \cdot 1}}}{2} = 0.542 \text{ m}$$

The internal forces for the section through the bottom row of the Kappema elements with the loading estimated from the vertical strip are calculated further (Fig. 4.24 – 4.28).

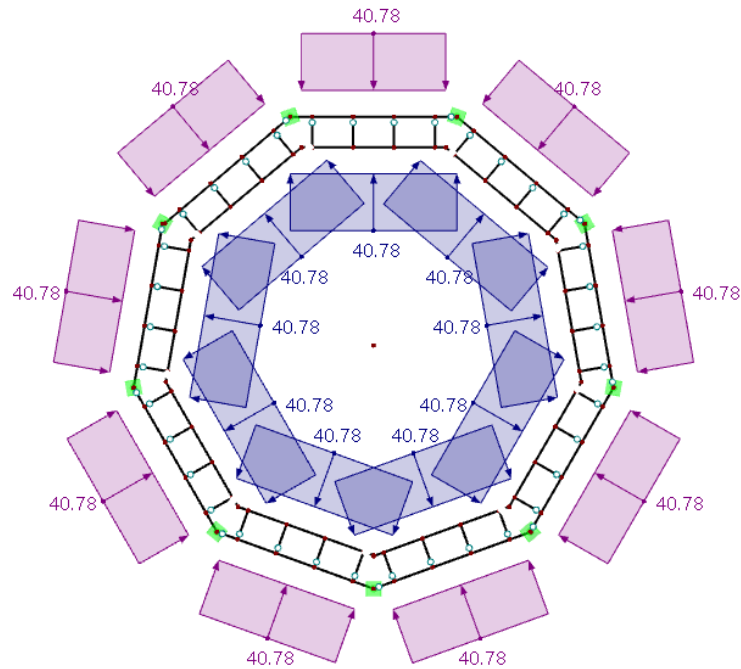


Figure 4.24: Geometry and loading of the relevant horizontal cross-section modelled in RFEM [kN/m]

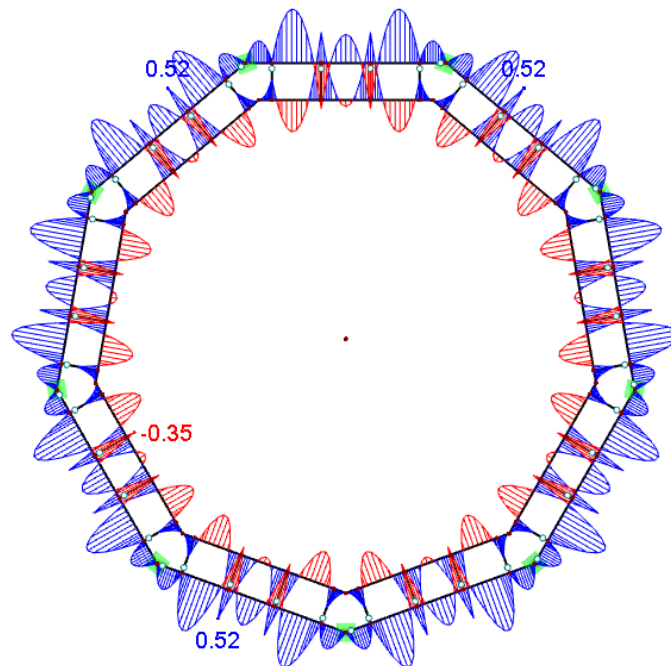


Figure 4.25: Resulting moments of the relevant horizontal cross-section modelled in RFEM [kNm]

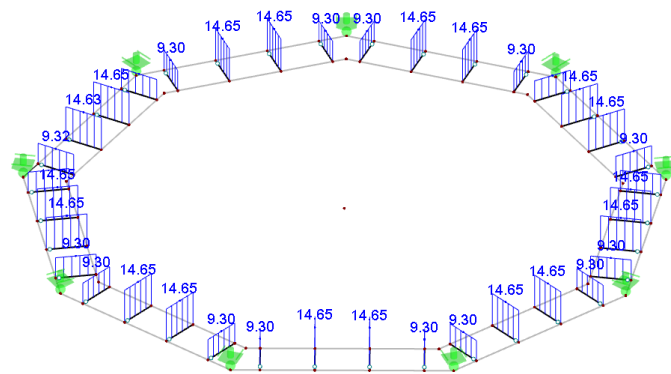


Figure 4.26: Resulting normal forces in Kappema elements [kN]

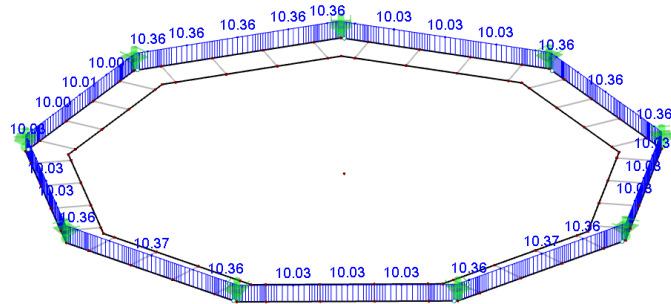


Figure 4.27: Resulting normal forces in concrete shells [kN]

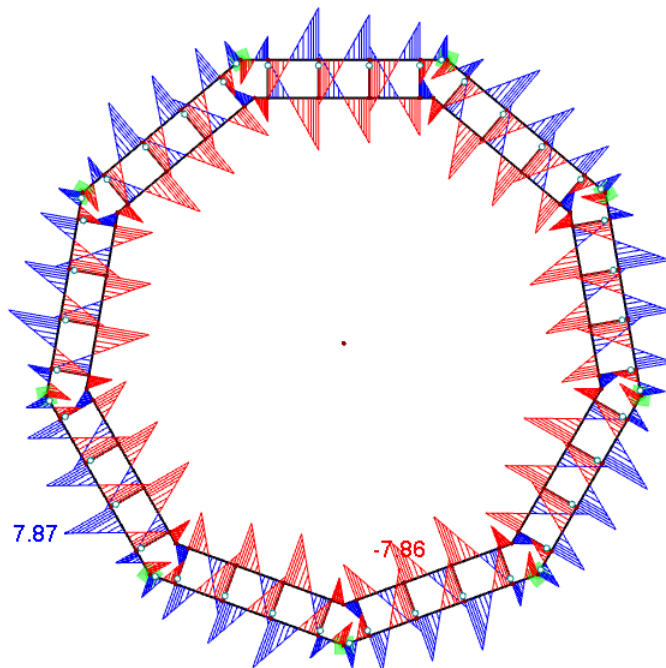


Figure 4.28: Resulting shear forces in concrete shells [kN]

The internal forces obtained from the computer analysis of the horizontal cross-section:

Maximum positive moment:	0.52 kNm
Maximum negative moment:	0.35 kNm
Maximum force in the Kappema elements:	14.65 kN
Maximum force in the outer ring elements:	10.36 kN
Maximum force in the inner ring elements:	0.00 kN
Maximum shear force:	7.87 kN

4.2.4 Proofs for reinforced-concrete shells

A concrete with the quality of C 30/37 and the reinforcement BSt 550 with a diameter of 8 mm arranged in a grid of 150 mm are used for the concrete shells of the mock-up (Tables 4.3 and 4.4).

Table 4.3: Strength and deformation characteristic of concrete C 30/37, according to [41]

Strength class	C 30/37
Characteristic compressive cylinder strength of concrete (f_{ck}) [MPa]	30
Characteristic compressive cube strength of concrete ($f_{ck,cube}$) [MPa]	37
Mean value of axial tensile strength of concrete (f_{ctm}) [MPa]	2.9
Secant modulus of elasticity of concrete (E_{cm}) [GPa]	33
Strain at reaching the maximum strength (ε_{c2})* [%]	2
Ultimate strain (ε_{cu2})* [%]	3.5

* for parabola-rectangle diagram of concrete under compression

Table 4.4: Partial factors for materials for ultimate limit state, according to [41]

Design situation	γ_c for concrete	γ_s for reinforcing steel
Persistent and transient	1.5	1.15

Design value of compressive strength for concrete class C 30/37:

$$f_{cd} = \alpha_{cc} \cdot \frac{f_{ck}}{\gamma_c} = 1 \cdot \frac{30}{1.5} = 20 \text{ MPa}$$

where:

- α_{cc} coefficient taking account of long term effects on the tensile strength and on unfavourable effects, resulting from the way the load is applied
- f_{ck} characteristic compressive cylinder strength of concrete at 28 days
- γ_c partial factor for concrete

Design yield strength of steel reinforcement BSt 550:

$$f_{yd} = \frac{f_{yk}}{\gamma_s} = \frac{550}{1.15} = 478.26 \text{ MPa}$$

where:

- f_{yd} Design yield strength of reinforcement
- f_{yk} Characteristic yield strength of reinforcement
- γ_s Partial factor for reinforcing

4.2.4.1 Concrete shells bending proof

The concrete bending bearing capacity for the ultimate limit state (ULS) is performed according to the linear elastic theory. For the analysis of bending capacity and the required reinforcement of the shells are used equations derived from a static equilibrium of a reinforced concrete cross-section:

$$\mu_{Ed} = \frac{M_{Ed}}{b \times d^2 \times f_{cd}} \quad (4.29)$$

$$A_{s,req} = \frac{M_{Ed}}{z \cdot f_{yd}} \quad (4.30)$$

$$z = \zeta \times d \quad (4.31)$$

where:

- M_{Ed} design value of bending moment
- b width of the cross-section
- d effective height of cross section
- z lever arm of internal forces
- ζ coefficient for lever arm of internal forces
- $A_{s,req}$ area of required tension reinforcement
- $A_{s,prov}$ area of provided tension reinforcement

Values μ_{Rd} , ε_c , ε_{s1} and ζ are determined according to the tables for the design of reinforced-concrete profiles [44]. The proofs are performed for the biggest negative and positive moment.

Bending bearing proofs for the vertical strip cross-section (Fig. 4.21)

Maximal positive bending moment:

$$M_{Ed} = 1.701 \text{ kNm (positive)}$$

$$d = 2.1 \text{ cm (Fig 4.29)}$$

$$b = 100.0 \text{ cm (for a 1 m strip of the concrete slab)}$$

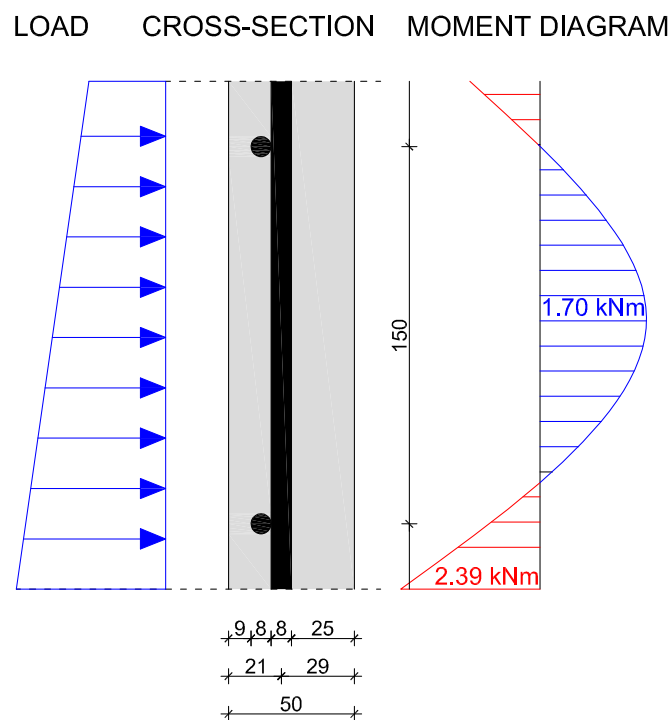


Figure 4.29: Closer view on the vertical strip loading with chosen reinforcement position [mm]

$$\mu_{Ed} = \frac{1.70 \cdot 100}{100 \cdot 2.1^2 \cdot 2} = 0.192$$

$\mu_{Ed} = 0.192 < 0.296 \rightarrow$ compression reinforcement is not required

$$\mu_{Rd} = 0.194 \Rightarrow \begin{cases} \varepsilon_c & = -3.5\text{‰} \\ \varepsilon_{s1} & = 9.5\text{‰} \\ \zeta & = 0.888 \end{cases}$$

$$A_{s,req} = \frac{1.70 \cdot 100}{0.888 \cdot 2.1 \cdot 47.83} = 1.91 \text{ cm}^2 < A_{s,prov} = 3.35 \text{ cm}^2 \checkmark$$

Maximal negative bending moment:

$$M_{Ed} = 2.39 \text{ kNm (negative)}$$

$$d = 2.9 \text{ cm}$$

$$b = 100.0 \text{ cm}$$

$$\mu = \frac{2.39 \cdot 100}{100 \cdot 2.9^2 \cdot 2} = 0.142$$

$\mu = 0.142 < 0.296 \rightarrow$ compression reinforcement is not required

$$\mu_{Rd} = 0.145 \Rightarrow \begin{cases} \varepsilon_c & = -3.5\text{‰} \\ \varepsilon_{s1} & = 14.5\text{‰} \\ \zeta & = 0.919 \end{cases}$$

$$A_{s,req} = \frac{2.39 \cdot 100}{0.919 \cdot 2.9 \cdot 47.83} = 1.87 \text{ cm}^2 < A_{s,prov} = 3.35 \text{ cm}^2 \checkmark$$

Bending bearing proofs for the horizontal strip cross-section (Fig. 4.24- 4.28))

Maximal positive bending moment:

$$M_{Ed} = 0.52 \text{ kNm (positive)}$$

$$d = 2.1 \text{ cm (Fig. 4.29)}$$

$$h_{eff} = 54.2 \text{ cm}$$

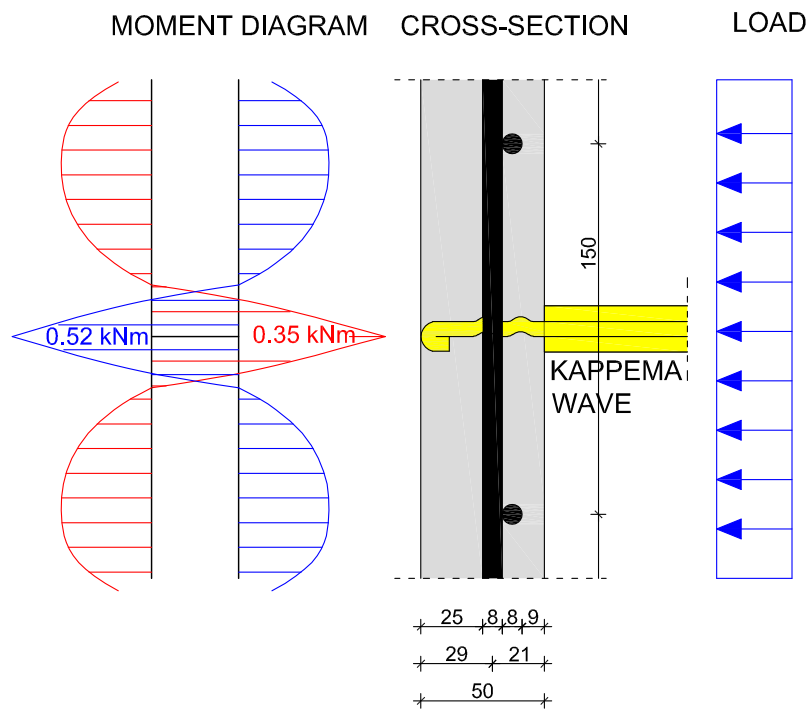


Figure 4.30: Closer view on the horizontal strip loading with chosen reinforcement position [mm]

$$\mu_{Ed} = \frac{0.52 \cdot 100}{54.2 \cdot 2.1^2 \cdot 2} = 0.109$$

$\mu_{Ed} = 0.109 < 0.296 \rightarrow$ compression reinforcement is not required

$$\mu_{Rd} = 0.110 \Rightarrow \begin{cases} \varepsilon_c & = - 3.4\text{‰} \\ \varepsilon_{s1} & = 20.0\text{‰} \\ \zeta & = 0.940 \end{cases}$$

$$A_{s,req} = \frac{0.54 \cdot 100}{0.940 \cdot 2.1 \cdot 47.83} = 0.57 \text{ cm}^2 < A_{s,prov} = 3.35 \text{ cm}^2 \checkmark$$

Maximal negative bending moment:

$$M_{Ed} = 0.35 \text{ kNm (negative)}$$

$$d = 2.9 \text{ cm}$$

$$h_{eff} = 54.2 \text{ cm}$$

$$\mu = \frac{0.35 \cdot 100}{54.2 \cdot 2.9^2 \cdot 2} = 0.038$$

$\mu = 0.038 < 0.296 \rightarrow$ compression reinforcement is not required

$$\mu_{Rd} = 0.038 \Rightarrow \begin{cases} \varepsilon_c & = -1.5\text{‰} \\ \varepsilon_{s1} & = 20.0\text{‰} \\ \zeta & = 0.975 \end{cases}$$

$$A_{s,req} = \frac{0.35 \cdot 100}{0.975 \cdot 2.9 \cdot 47.83} = 0.25 \text{ cm}^2 < A_{s,prov} = 3.35 \text{ cm}^2$$

4.2.4.2 Shear resistance

Slabs do not require design shear reinforcement if the design value for the shear resistance $V_{Rd,c}$ is greater than the design value of the applied shear force V_{Ed} according to EC2 [41]:

$$V_{Rd,c} > V_{Ed}$$

The design value for the shear resistance $V_{Rd,c}$ is:

$$V_{Rd,c} = [C_{Rd,c} \cdot k \cdot (100 \cdot \rho_l \cdot f_{ck})^{1/3} + k_1 \cdot \sigma_{cp}] \cdot b_w \cdot d \quad (4.32)$$

with a minimum of:

$$V_{Rd,c} = (v_{min} + k_1 \cdot \sigma_{cp}) \cdot b_w \cdot d \quad (4.33)$$

where:

k size factor, $k = 1 + \left(\sqrt{\frac{200}{d}}\right) \leq 2.0$, with d in mm

f_{ck} characteristic concrete compressive strength [MPa]

ρ_l longitudinal reinforcement ratio, $\rho_l = \frac{A_{s,l}}{b_w \cdot d} \leq 0.02$

$A_{s,1}$ area of the tensile reinforcement

b_w is the smallest width of the cross-section in the tensile area [mm]

σ_{cp} concrete compressive stress at centroidal axis due to axial loading or prestressing, $\sigma_{cp} = \frac{N_{Ed}}{A_c} < 0.2f_{cd}$

$C_{Rd,c}$ coefficient derived from tests, $C_{Rd,c} = \frac{0.18}{\gamma_c} = \frac{0.18}{1.5} = 0.12$

k_1 coefficient

$$v_{min} = 0.035 \cdot k^{3/2} \cdot f_{ck}^{1/2}$$

Shear resistance of vertical strip cross-section

Using the parameters for the vertical strip cross-section, the following values that are needed for the equations 4.32 and 4.33 are determined:

$$k = 1 + \left(\frac{200}{21}\right)^{1/2} = 4.09 > 2 \rightarrow k = 2$$

$$\rho_l = \frac{3.35}{100 \cdot 21} = 0.0016 \leq 0.02$$

$$f_{ck} = 30 \text{ MPa}$$

$$b_w = 100 \text{ cm}$$

$$v_{min} = 0.035 \cdot 2^{3/2} \cdot 30^{1/2} = 0.542$$

Introducing the gained values into the equations 4.32 and 4.33, the design value for the shear resistance of the vertical strip can be calculated to be:

$$V_{Rd,c} = [0.12 \cdot 2 \cdot (100 \cdot 0.0016 \cdot 30)^{1/3} + 0] \cdot 100 \cdot 2.1 = 85.01 \text{ kN}$$

with a minimum of:

$$V_{Rd,c} = (0.542 + 0) \cdot 100 \cdot 2.1 = 113.82 \text{ kN}$$

Shear force proof for the vertical strip:

$$V_{Rd} = 113.82 \text{ kN} > V_{Ed} = 23.18 \text{ kN} \checkmark$$

Shear resistance of horizontal strip cross-section:

The parameters used in calculation of vertical cross-section differ only in the width of the horizontal strip cross-section:

$$h_{eff} = 54.2 \text{ cm}$$

Introducing the gained values into the equations 4.32 and 4.33, the design value for the shear resistance of the horizontal strip can be calculated to be:

$$V_{Rd,c} = [0.12 \cdot 2 \cdot (100 \cdot 0.0016 \cdot 30)^{1/3} + 0] \cdot 54.2 \cdot 2.1 = 46.07 \text{ kN}$$

with a minimum of:

$$V_{Rd,c} = (0.542 + 0) \cdot 54.2 \cdot 2.1 = 61.69 \text{ kN}$$

Shear force proof for horizontal strip:

$$V_{Rd} = 61.69 \text{ kN} > V_{Ed} = 7.87 \text{ kN} \checkmark$$

4.2.5 Proofs for interconnection of concrete shells

Care has to be taken that the interconnection of the concrete shells is able to bear the load of the concrete pressure. The interconnection is provided by Kappema elements anchored with three sticks into the concrete shell. The technical approval for these Kappema elements states that a pull out strength per stick, while using a concrete slab thickness of at least 5.5 cm, amount to 9.5 kN [45]. In our case, contrary to the recommended, concrete shells with a thickness of 5 cm should be used. Therefore, already performed investigations in the pullout strength of the Kappema element sticks were used. These investigations have been carried out by the TU Graz and they are documented in [46]. The experiments were performed on two different samples of concrete shells: concrete shell with one stirrup and concrete cover of 2.5 cm (Type 1), and concrete shell with two stirrups and grid reinforcement $\varnothing 6/150$ mm (Type 2). The obtained test results for the 5 cm thick concrete shells are presented in the Table 4.5.

Table 4.5: Pull out strength of Kappema sticks form experiments performed at TU Graz [46]

Type	Examination after	Compressive strength of concrete cube [MPa]	Pull out strength of one Kappema stick [kN]
1	24 h	23.00	7.94
	48 h	32.50	12.67
2	48 h	30.00	11.17
	7 d	35.41	14.08
	28 d	49.00	14.55

For the mock-up construction a grid reinforcement $\varnothing 8/150$ mm is used, so the results of the Type 2 are chosen as representative because they had a similar grid reinforcement.

Pull out strength of one Kappema element stick after 28 days:

$$F_p = 14.55 \text{ kN}$$

Design value of pull out strength:

$$F_{pd,1} = \frac{F_{p,1}}{\gamma} = \frac{14.55}{1.5} = 9.70 \text{ kN}$$

where:

- $F_{p,1}$ pull out strength of one Kappema stick obtained in the experiment
 γ concrete safety factor

Every Kappema element consists of three sticks, therefore, the design pull out resistance of the whole Kappema wave is:

$$F_{R,pd} = 3 \cdot 9.70 = 29.1 \text{ kN}$$

The maximum applied force on one Kappema element obtained in the numerical analysis of the horizontal strip is:

$$F_{E,pd} = 14.65 \text{ kN}$$

Proof of bearing capacity of one Kappema element:

$$F_{E,pd} = 14.65 \text{ kN} < F_{R,pd} = 29.1 \text{ kN}$$

The utilization of the interconnection amount to:

$$\frac{F_{R,pd}}{F_{E,pd}} = 50.34 \%$$

4.3 Production of double wall elements

The production of double wall elements is performed in a factory under controlled conditions and with the assistance of automated machines. Consequently, such organized process provides a certain accuracy in the geometry of the end products. The double wall elements used for the construction of the mock-up were produced by the company Oberndorfer in their factory in Herzogenburg, Austria. This factory operates with specialized steel formwork pallets that ensure flat and smooth surfaces. Whereby, the pallets are transported through all stages of the production by using roller blocks, friction wheels and cross-lifting trucks. When one stage is completed safety railings are lifted up and the pallet is transported to the next station. The whole process is organized in six production phases, which should last 12 minutes for an optimum production output. This production process of double wall elements is described in detail in the following paragraphs.

4.3.1 Positioning of formwork

The lateral formwork steel profiles are automatically positioned by robots on the working pallets (Fig. 4.31). In the forefront the robot receives and processes all geometrically required CAD/CAM data and aligns the lateral formwork profiles on the pallet by means of magnets (Fig. 4.32). These magnets, which are integrated in the formwork profiles, are subsequently activated by the robot gripper so that they can not be shifted during the remaining production process (Fig. 4.33). Additionally, the formwork robot is equipped with a plotting unit that marks the position for special embedments on the pallets.

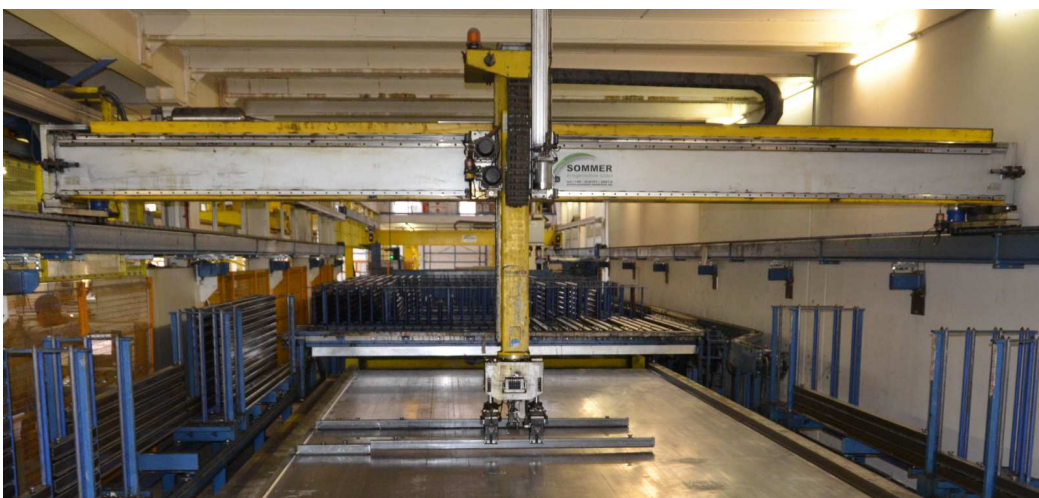


Figure 4.31: Formwork robot



Figure 4.32: Forwork robot placing the lateral formwork profiles

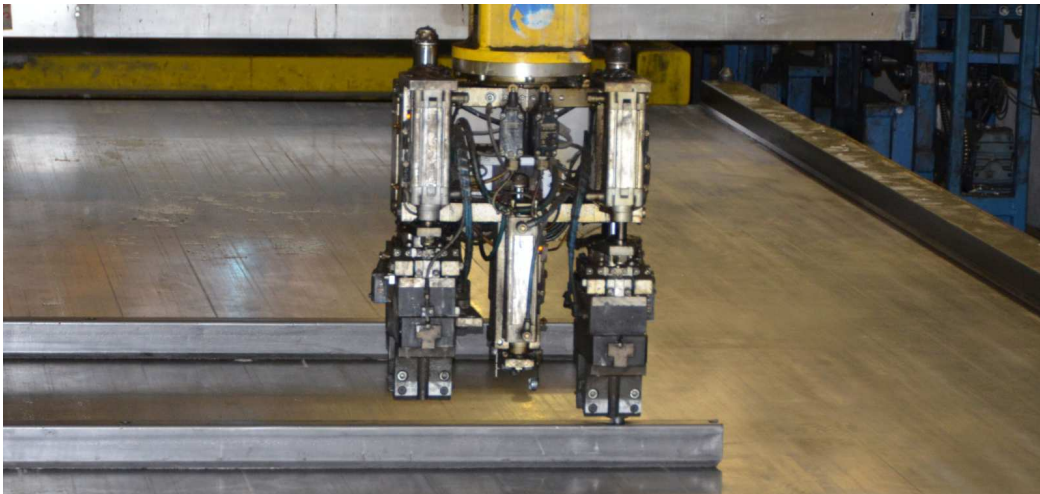


Figure 4.33: Forwork robot activating the fixing magnets

The lateral formwork steel profiles only provide standard lengths and shapes. Therefore, if a random geometry is needed, additional formwork has to be placed manually in the remaining opening between standard profiles. Once the formwork robot placed the lateral formwork profiles, the working pallet is moved to the next station. This station is equipped with rotating optical lasers which are capable of marking every desired geometry. With assistance of the lasers all additional formwork, which usually consists of styrofoam profiles, is manually glued on the pallets (Fig. 4.34).

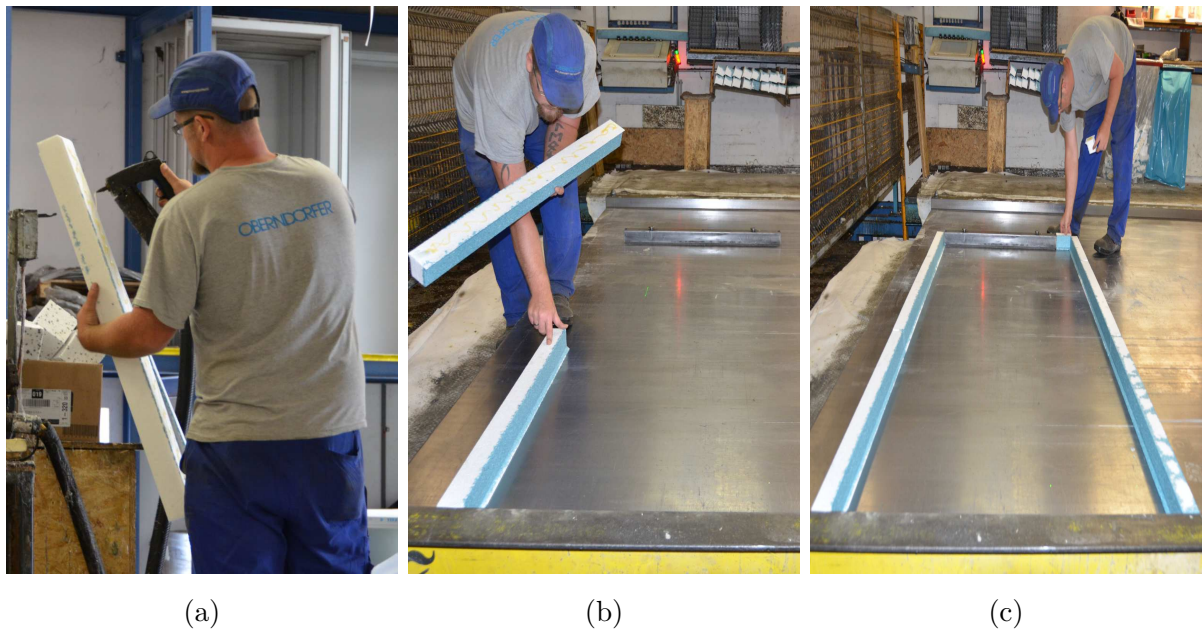


Figure 4.34: Manually placing of styrofoam profiles; (a) gluing; (b) arranging of the glued profiles; and (c) finished formwork

When the formwork is assembled, workers are placing plastic spacers that secure a concrete cover of 2.5 cm (Fig. 4.35(a)). Before relocation of the working station a layer of oil is sprayed on the pallet (Fig. 4.35(b)).

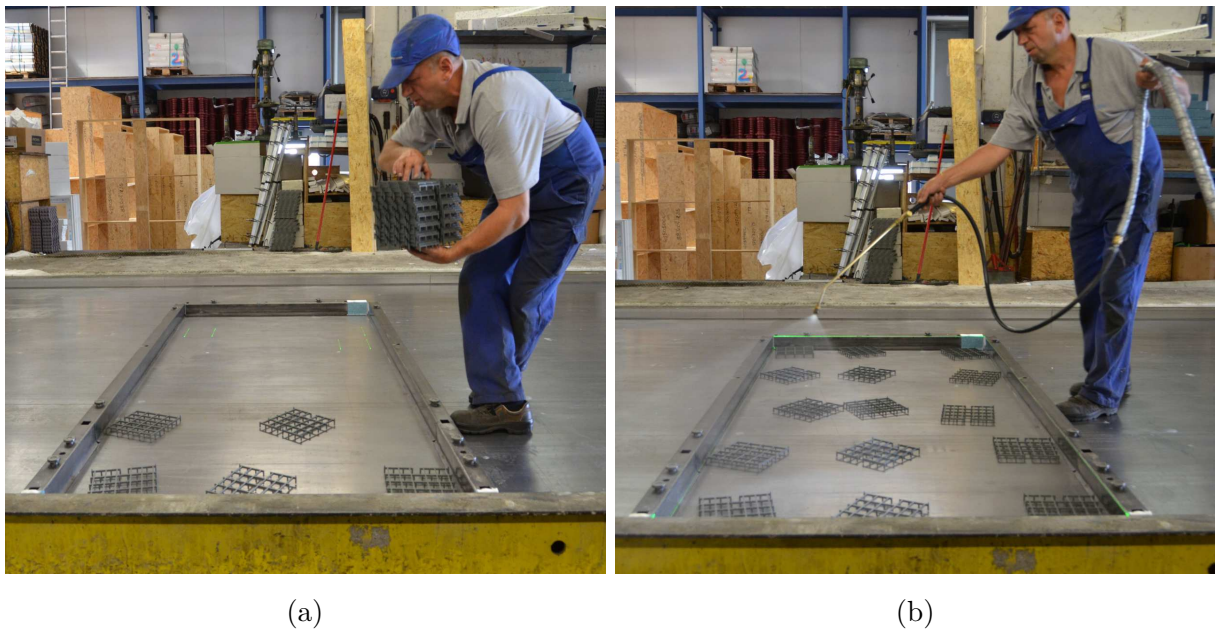


Figure 4.35: Placing of the spacers and spraying of oil layer on working pallet; (a) placing of plastic spacers; and (b) oiling of the pallet

4.3.2 Placing of the reinforcement

In this production step the pallet is transported to the reinforcement station where a previously welded mesh reinforcement is automatically laid into the pallet (Fig. 4.36). The reinforcement meshes are welded and cut automatically according to the in forefront defined CAD data.

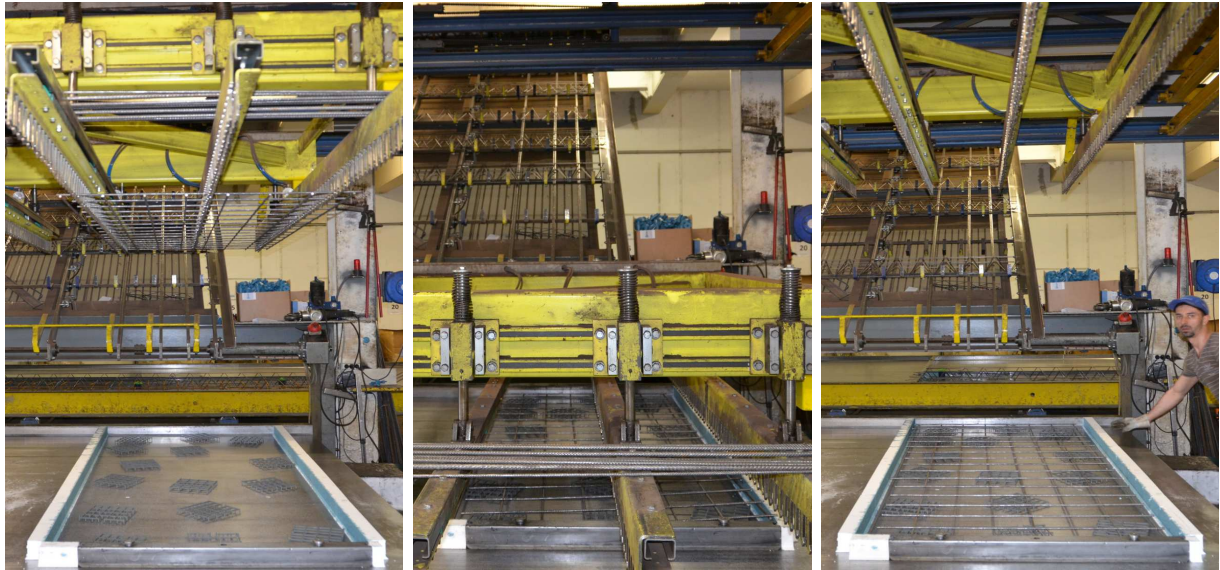


Figure 4.36: Automated placing of the reinforcement

Once the mesh reinforcement is automatically placed in the right position it is possible to manually place additional reinforcement and special embedments. The additional reinforcement and embedments that are exemplary described here are used for production of the elements for the mock-up and they are not part of standard double wall elements.

In this stage following elements are installed:

- plastic anchors that are used to attach screw bracings during pre-assembly (Fig. 4.37(a))
- opening for concreting (Fig. 4.37(b))
- welding embedments for the connection of arranged elements in ring segment during pre-assembling (Fig. 4.37(c))
- standard lifting hooks in order to lift the element during arrangement (Fig. 4.37(d))
- U-reinforcement at the bottom and top of the elements (Fig. 4.37(e))
- reinforcement that enables attachment of the cable loops (Fig. 4.37(e))
- and finally, Kappema elements that connect both shells (Fig. 4.37(e))

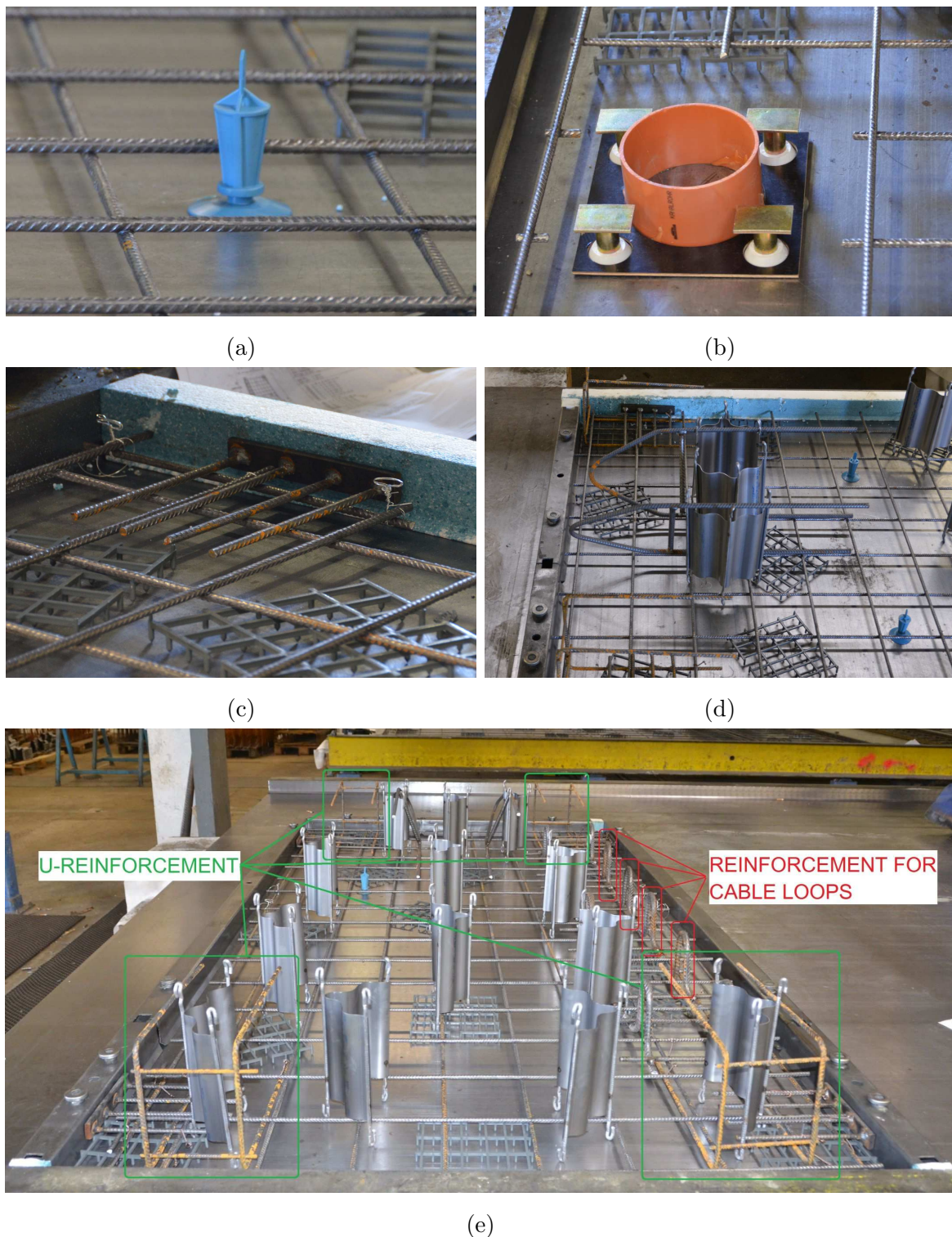


Figure 4.37: Reinforcement and embedments placed in the outer shell of the elements used for mock-up; (a) plastic anchors that are used to attach screw bracings; (b) opening for concreting; (c) welding embedments for the connection of arranged elements; (d) standard lifting hooks; and (e) finished formwork of the first shell prepared for following stage

4.3.3 Concreting and aftertreatment

After the reinforcement is placed and fixed in position, the pallet is transported into the station of the concrete spreader where the concrete is poured on the pallet (Fig. 4.38). The concrete spreader can operate automatically or manually, which depends on the requirements and complexity of the formwork. When the concrete is poured into the formwork, workers manually distribute the concrete and level the surface.



Figure 4.38: Concreting of the elements; (a) side view of the concrete spreader; (b) bottom view of the concrete spreader; and (c) formwork filled with concrete

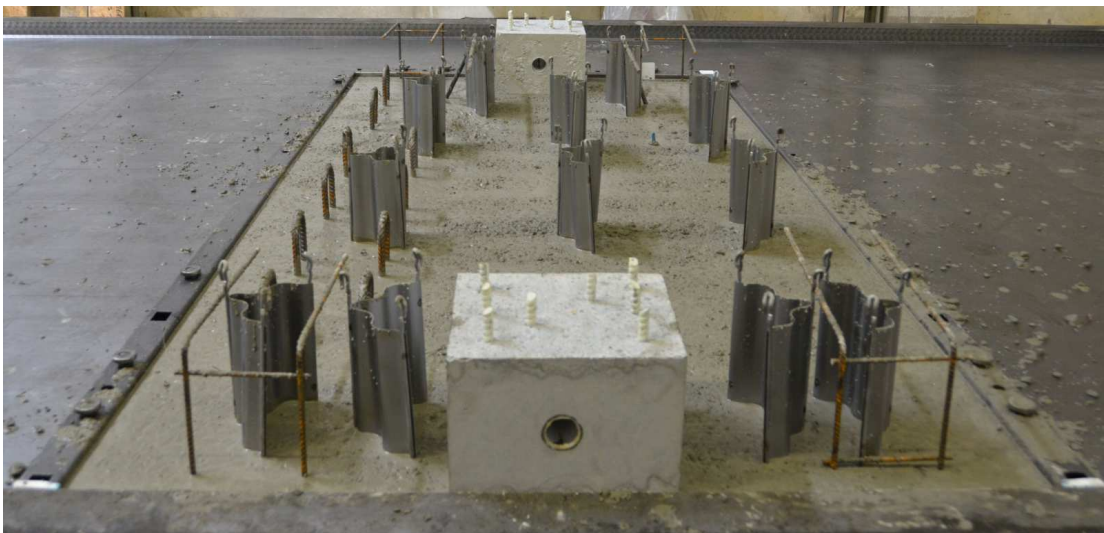
In the next step the whole pallet relocated to the vibration station where the first shell is vibrated. The vibration process provides a smooth and plain surface of the concrete shell while securing a certain strength and quality of the concrete. The applied frequencies

have to be adjusted to the thickness of the shells and the consistency of the used concrete.

After vibrating, previously prepared concrete blocks with embedded glass fiber reinforcement are manually placed in every third double wall element of the mock-up segment (Fig.4.39). In the last step of the production of the first shell, the whole pallet is stored for 24 hours under controlled conditions, like temperature, humidity etc.



(a)



(b)

Figure 4.39: Concrete blocks arranged in every third element of the mock-up segment; (a) concrete blocks; (b) positioning of the blocks; and (c) concreted blocks positioned in vibrated concrete shell

4.3.4 Connection of both shells

Once the first shell is hardened enough and the second one is reinforced and concreted, both shells are merged. The production of the second shell is similar to the first one, with the exception that this shell is not stored before it is connected to the first shell. The first shell is fixed to the turning device by means of tensioning steel arms and pneumatically operated clamps. When the steel arms are inserted through openings in the frame of the pallets, pneumatic clamps are tightened and thus ensure a fixed position of the first shell during rotation (Fig. 4.40).



Figure 4.40: Fixing of the first shell in the turning device; (a) hardened concrete shell; and (b) concrete shells fixed in turning device by steel arms

Afterwards, the turning device with first pallet is lifted with pneumatic jacks and rotated by 180° (Fig. 4.41). While this working station raises and rotates, the second pallet, with the recent concreted shells, is positioned right under its counter part so that both inner sides of the shells are facing each other (Fig. 4.42 and 4.43). When the first and second pallets are aligned in an accurate position, the rotated working station of the first shell goes down and pushes itself into the fresh concrete of the second shell (Fig. 4.44 and 4.45).



Figure 4.41: Lifting of the pallet with the first shells from the day before



Figure 4.42: Positioning of the pallet with the recent concreted second shells

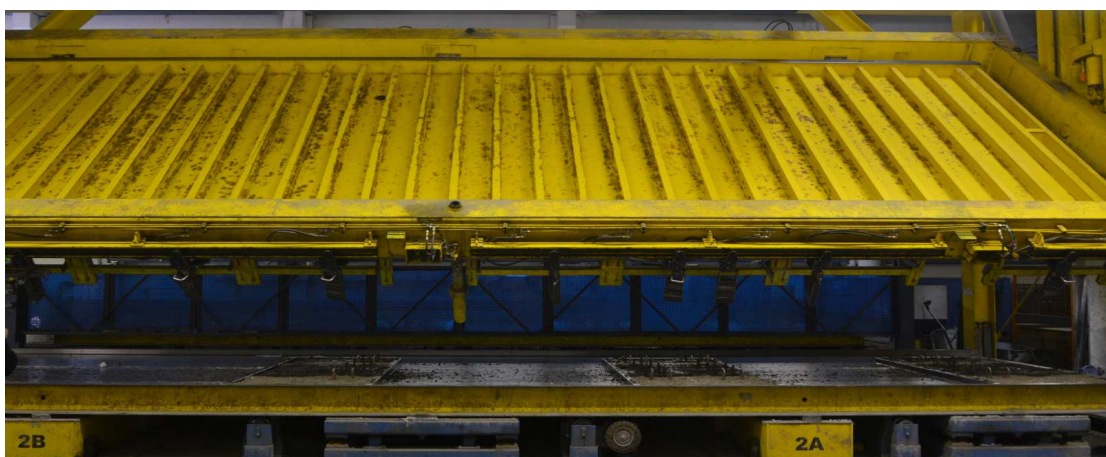


Figure 4.43: Rotation of the upper pallet by 180°



Figure 4.44: Descending of the upper shell into the lower one



Figure 4.45: Merged double wall elements

While the both shells are merged, the bottom pallet is vibrated in order to prevent any aggregate jamming, what would cause a larger element thickness. After vibration, the pneumatic clamps are released and tensioning arms are removed and placed in the special holders. When both shells are merged and vibrated, the upper pallet is removed (Fig. 4.46) and freed from remains of styrofoam and concrete. The integrated magnets in the lateral formwork are also manually deactivated and placed on a pallet frame.



Figure 4.46: Double wall elements after merging

4.3.5 Concrete curing and storage of the double wall elements

When the both shells have been successfully merged, the empty pallets are moved in the cleaning station so that they can be returned in the new production cycle (Fig. 4.47). The double wall elements are stored in the curing chamber where they are preserved under controlled conditions. After approximately one day all elements are finished and ready for the transport to the construction site (Fig. 4.48).



Figure 4.47: Storage and curing area of the double wall elements



Figure 4.48: All nine double wall elements transported to the building site and ready to be put together to form a mock-up segment

4.4 Assembly of the mock-up

The double wall elements were transported to the building site where they were prepared for the assembly into a real size segment. The construction site was provided by the company Oberndorfer at their factory in Gars am Kamp, Austria. In the first step the foundation in the range of a gantry crane was built. Then the lower cross-section geometry of the segment was marked on the foundation, which enabled the start of the segment erection.

4.4.1 Foundation

In order to arrange the elements with a certain accuracy a flat and horizontal levelled surface was needed. This surface was provided by a not reinforced concrete foundation with dimensions of 8×8 m. The foundation was built on an asphalt layer with a minimum thickness of 10 cm and a quality of C 30/37. The concrete was placed by a concrete truck with a pump and subsequently polished (Fig. 4.49(a) and 4.49(b)). When the concrete had hardened to a certain degree, the wooden formwork was removed and the foundation was ready for the assembly process (Fig. 4.49(c)).



(a)



(b)



(c)

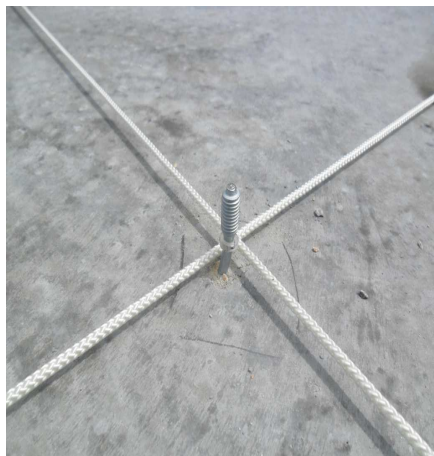
Figure 4.49: Foundation of the mock-up; (a) concreting by a concrete truck (b) polishing of the concrete; and (c) finished foundation

4.4.2 Marking and measuring of the bottom ring segment geometry

In order to arrange the elements on their foreseen positions, the bottom section of the ring segment was marked on the ground. Therefore, the first step was to mark the center of the foundation that was used as a reference point for all following stages of the assembly process. This point was estimated as the intersection of two diagonal ropes that were spanned between the foundation corners (Fig. 4.50(a)). Subsequently, the point was marked with a nail that was shot from the nail gun Hilti DX 460 (Fig. 4.50(b) and 4.50(c)).



(a)



(b)



(c)

Figure 4.50: Determination of the foundation centre; (a) diagonally positioned ropes; (b) central- reference nail; and (c) nail gun Hilti DX 460

Once the reference point was defined, the bottom inner and outer circumcircle of the nine sided double wall segment was marked. The circumcircles were marked with the assistance of a wooden plank that had one hole for the centre and a hole for each radius that needed to be labelled on the ground (Fig. 4.51(a)). This plank was on one end attached to the nail at the foundation enter, while on the other end a regular pencil was attached through the remaining two holes (Fig. 4.51(b)). The plank was then rotated around the central nail marking the both circumcircle radiuses of 2015 mm and 1696 mm. As next, the polygons were marked by measuring the side length of 1378.5 mm for the outer and 1160.1 mm for the inner circumcircle.



(a)



(b)

Figure 4.51: Marking of the circumcircles; (a) wooden plank; and (b) marking pencil attached to the hole in the plank

Finally, wooden planks with a thickness of 5 mm were placed at the outer marked polygon in order to simplify the arrangement in terms of inclination (Fig. 4.52). The planks were placed on the outer sides of the polygon, beneath the outer shells of the double wall elements to ensure a slight inclination of the elements. These 5 mm thick wooden planks were fixed to the foundation by silicone adhesive.



Figure 4.52: Wooden planks for the easier arranging of the elements

4.4.3 Arrangement of the double wall elements

The double wall elements were positioned on the foundation by the gantry crane (Fig. 4.53(a)). Whereby, the elements were hooked to the crane by textile ropes that were wrapped around two embedded lifting loops in the upper zone of the elements. When the elements were near to the foundation, the workers manually positioned them according to the previously marked polygons (Fig. 4.53(b) and 4.54(a)). After positioning, the element was able to stand independently at a slight angle and with no need of any support (Fig. 4.54(b)).

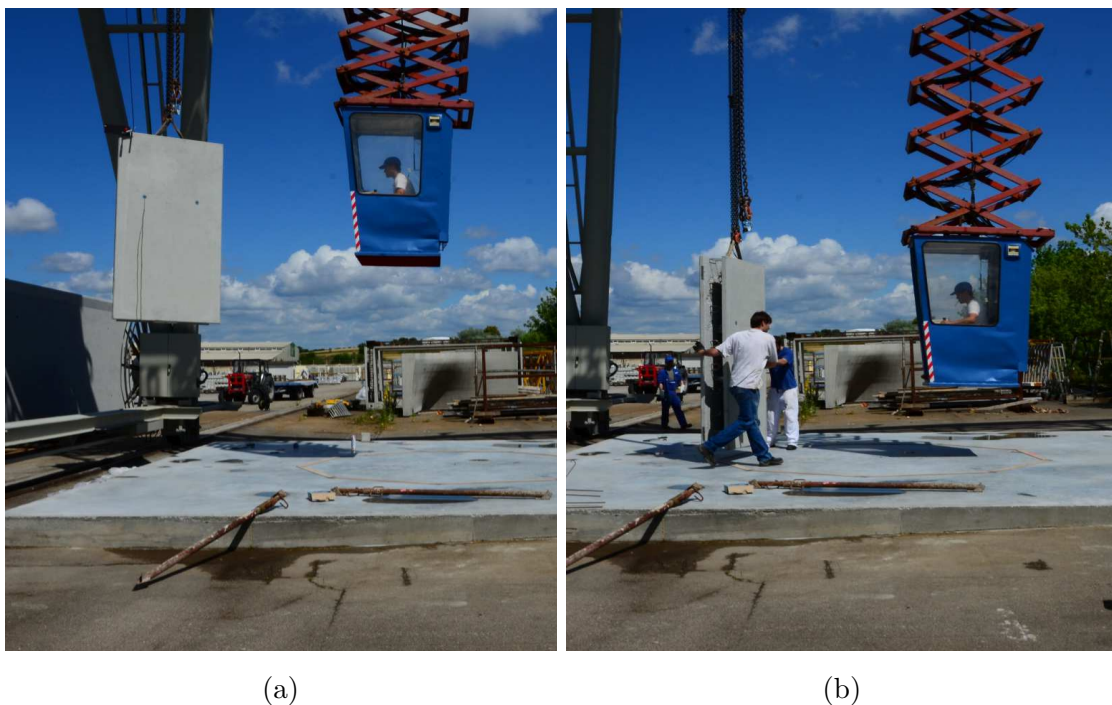


Figure 4.53: Positioning of one double wall element; (a) transport of the element with the crane; and (b) manually positioning of the elements while landing

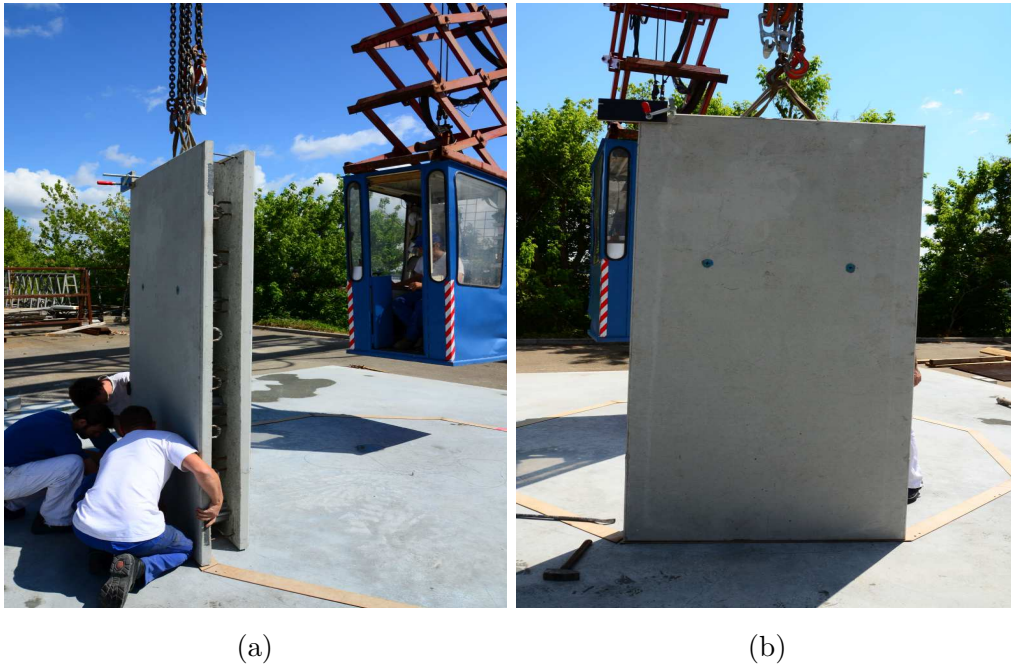


Figure 4.54: Arrangement of one double wall element; (c) adjustment of the element; and (d) positioned element prepared for inclination

The elements were arranged along two steel L-profiles, wherein the centre of the elements was used as a reference point. Before the elements were placed, each side of the outer polygon marked on the ground had installed two steel L-profiles fixed by expanding anchors (Fig. 4.55(a)). These profiles, used as falsework, simplified the arrangement of the elements at the bottom. Additionally, the centre of the elements and the centre of the polygon sides on the ground were marked (Fig. 4.55(b)). These allowed precise positioning of the elements and distribute any possible errors equally on each side.

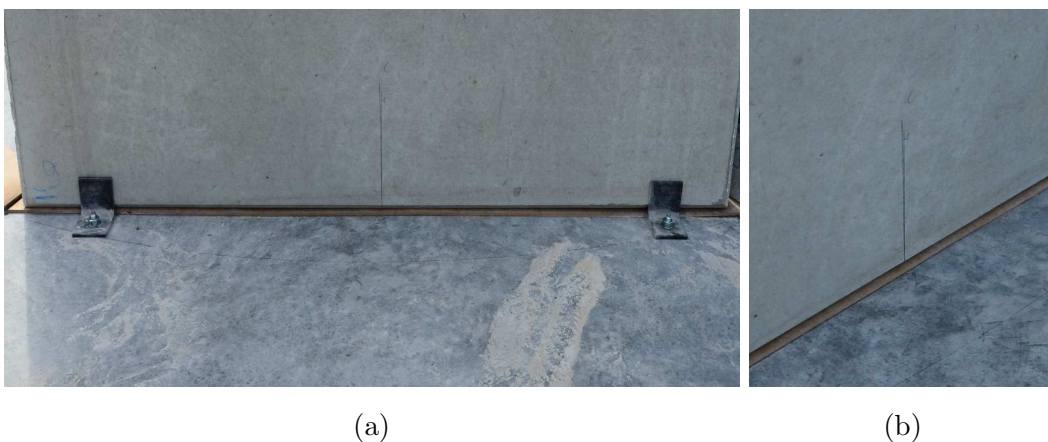


Figure 4.55: Aids at the element arrangement; (a) steel L-profiles; and (b) marked middle point on the foundation and the element

In the following stage the expendable bracings were used to secure the elements. The screw bracings were placed outside of the segment to avoid their mutual collision. Herein, the angle of the bracings should range between 45° and 60° . On one end the bracings were fixed by bolts screwed into the plastic threaded sleeving embedded in the element (Fig. 4.56(a)), while the other end was fixed by expanding anchors drilled into the foundation (Fig. 4.56(b)). The screw bracing consists of two steel pipes inserted into each other and connected by a thread. This thread enables a fine adjustment of the bracing length, which is used to adjust the accurate inclination of the elements. For easier adjustment, two screw bracings were used for each element (Fig. 4.56(c)).



Figure 4.56: Installation of the screw bracings; (a) into the element; (b) into the foundation; and (c) placed bracings

The upper left corner of each element was equipped with a wooden board which was used to angle the element in planned position (Fig. 4.57(a)). Before the elements were positioned, the board with a hole at a specific point was fixed with hot glue on each upper left corner of the the outer shell.

The board was positioned so that the hole represents the intersection of the horizontal upper edge of the segment and the associated vertical edge. The element inclination was measured as a distance of a steel wire between the nail in the centre of the segment and an inner side of the hole in the wooden plank (Fig. 4.57(b)). This distance, which was marked on the steel wire, was estimated to be 3184.3 mm. The wire was pulled through the hole in

the wooden board and the length of the screw bracings, as described before, was adjusted until the elements had the desired inclination.

This kind of measurement was favoured in comparison to any direct measurements of the angle because a small error in the measurement of the previously describe length result in a very small error in the desired angle. On the contrary, a small error of a directly measured angle would result in a big shift of the upper edge of the element.



(a)

(b)

Figure 4.57: Measuring of the inclination; (a) wooden plate in the upper left corner; and (b) measuring of the rope distance by using a steel wire

After the positioning of each element, horizontal reinforcement was placed in the core of the double wall elements. The horizontal reinforcement consist of 12 horizontal bars that are bent under angle of 40° to follow the ring segment geometry. These horizontal bars were welded to two vertical reinforcement bars that ended with hooks at the top (Fig. 4.58(a)). The hooks were used to hang the horizontal reinforcement on the existing U-reinforcement at the top of the double wall elements. In order to avoid collision with Kappema elements, the horizontal bars were grouped into four at different altitudes. Before arranging of the following double wall elements, one half of the horizontal bars was located in the elements, while the other half was sticking out of the element (Fig. 4.58(b) and 4.58(c)).

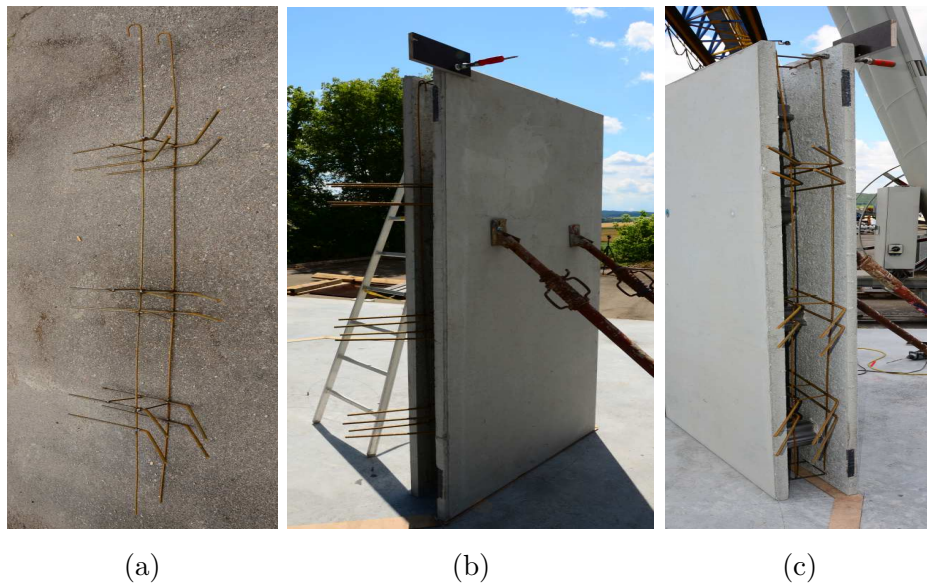


Figure 4.58: Horizontal reinforcement in the ring segment direction; (a) welded to vertical bars; (b) placed into one element; and (c) hooked to the U-reinforcement at the top of the element

Simultaneously with placing of the horizontal reinforcement, the second double wall element was prepared for arrangement. This element had to be shifted in from the side where the reinforcement was sticking out of the previously placed element. Therefore, the second element was firstly lowered slightly above the ground and then horizontally pushed toward the first element (Fig. 4.59). Afterwards, this element was arranged and secured by screw bracings as previously described.

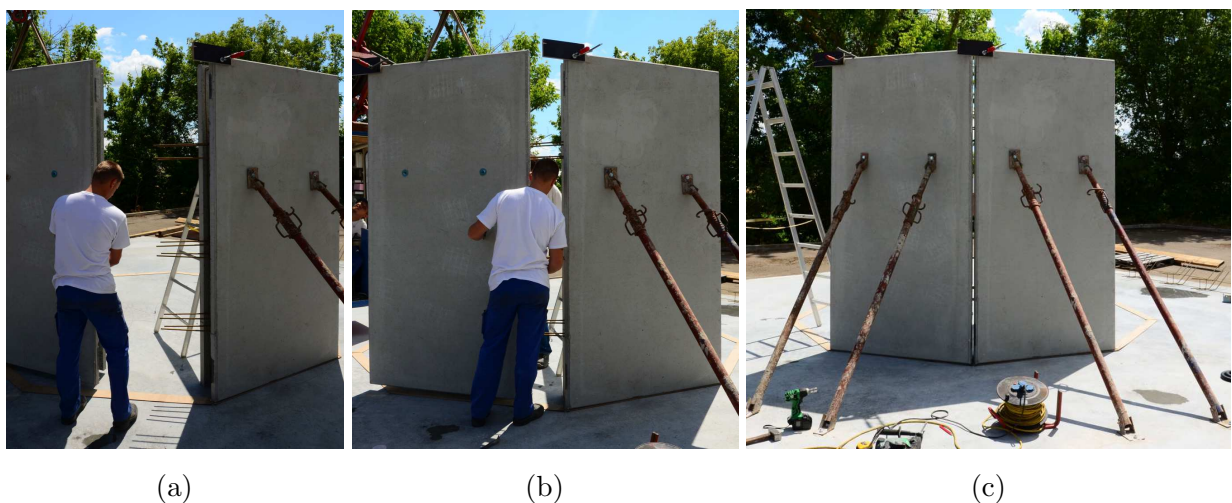


Figure 4.59: Positioning of the second element; (a) element hovers above ground; (b) horizontal pushing of the element toward the first one; and (c) two arranged elements

All other elements, except of the last one, were arranged in the same way (Fig. 4.60, 4.61 and 4.62).



Figure 4.60: Arranged and supported half ring segment- view from inside



Figure 4.61: Arranged and supported half ring segment- view from outside



Figure 4.62: Assembled ring segment without the last element

The last element was surrounded from both sides with neighboring elements, and consequently, it was not possible to place the horizontal reinforcement as in the preceding elements (Fig. 4.63(a) and 4.63(b)). Therefore instead of horizontal reinforcement, the last two vertical joints were reinforced with steel cable loops.



(a)

(b)

Figure 4.63: Positioning of the last double wall element; (a) positioning of the last element with the crane; and (b) last element at its foreseen position

The steel cables were mounted in the special reinforcement hooks that were positioned in the elements around the two last vertical joints. These loops were hidden in the last and neighboring elements in order to allow uninterrupted placement of the last element (Fig. 4.64(a)). The cable loops had tied thin steel wires on itself so that it is possible to easily pull them out when the last element is arranged. As last, a steel bar with a hook at the top was placed in an overlapping area of the loops to secure their position (Fig. 4.64(b) and 4.64(c)).



(a)

(b)



(c)

Figure 4.64: Steel cable loops; (a) loops hidden in the elements; (b) pulled out loops; and (c) reinforcement bar placed in the overlapping of the loops

Once all elements of the ring segments were arranged and secured by bracings, the elements had to be mutually connected. Herein, only the outer shells of the elements were mutually connected in order to participate in the transfer of loads, while the inner shells were unconnected. The outer shells had at each flank embedded two 18 cm long steel plates that were used to connect the elements by welds. After the elements were aligned, a vertical reinforcement bar was placed between two steel plates and welded to both concrete shells and so connecting the elements (Fig. 4.65). Once the connection of all elements was finished the structural integrity of the segment was provided and the bracings were no longer required.

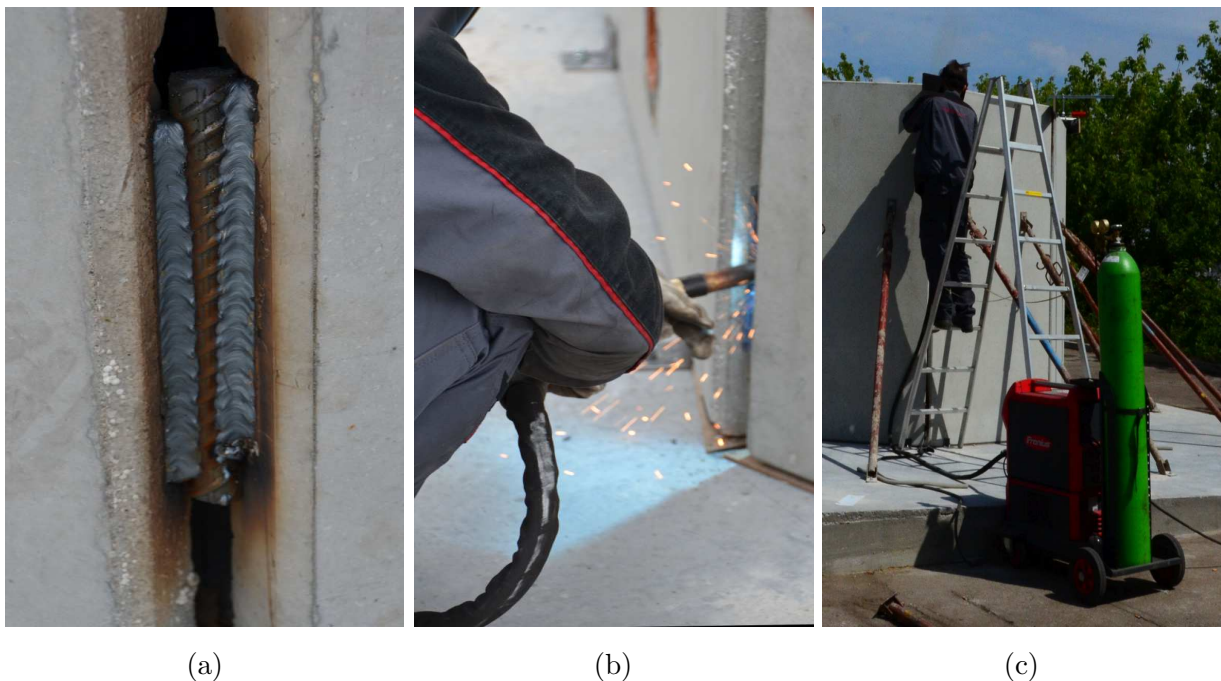


Figure 4.65: Structural connection of the elements; (a) reinforcement bar welded to the steel plate embedments of the outer shell; (b) bottom connection; and (c) top connection

To prevent leakage of the concrete during filling of the hollow space the outer vertical joints needed to be sealed. These joints were sealed with mortar, which except sealing had to provide a corrosion protection of previously produced weld connections. Before the mortar itself could be applied, sponge tubes had been positioned along the joint, so that no mortar can fall into the hollow space of the elements. Afterwards, the mortar was manually filled into the joint by a trowel (Fig. 4.66).

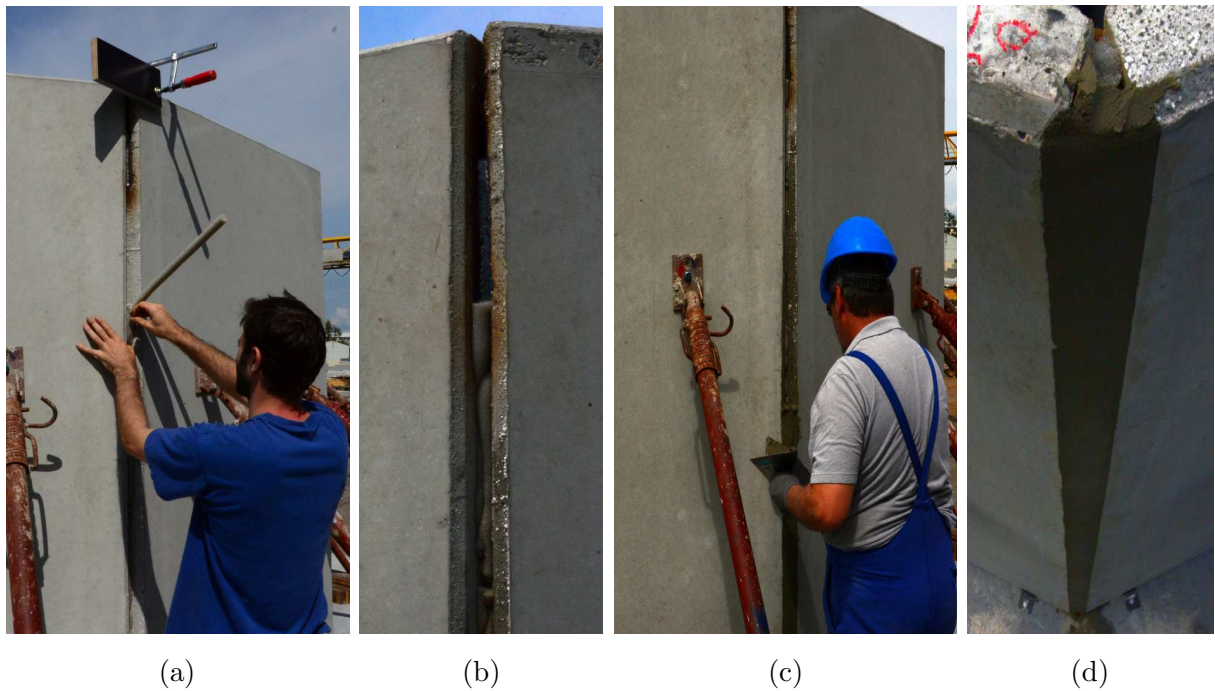


Figure 4.66: Sealing of the outer vertical joints with mortar; (a) placing of sponge tubes to prevent mortar leakage; (b) placed sponge tubes; (c) manually filling of the joints with mortar; and (d) top view of filled joint

The inner vertical joints were sealed simultaneously. For the internal joints the two types of sealant were tried in order to test their performance:

- ethylene propylene diene monomer (EPDM) tubes (SX Knock-in Profile)
- glued foil (Polyfleece SX 1000)

The used sealing material was provided by the company StekoX [47].

The EPDM tubes with a diameter of 30 mm were manually installed with the assistance of tied wires, which were used to pull the tubes from the top to the bottom of the joint (Fig. 4.67). When the tube was installed in planned position, the wires were spanned and tied to the screws drilled in the concrete shell to secure the position of the tube during all following construction phases (Fig. 4.67(b)). This kind of sealing was applied to six of nine inner vertical joints.



Figure 4.67: Vertical joints with embedded EPDM tubes; (a) installed tubes; (b) wires tied to screws; and (c) top view

The other three inner vertical joints were sealed with a glued water-resistant foil (Fig.4.68). Therefore, a special glue was applied by an ordinary paint roller to the neighboring edges of the vertical joints. Afterwards, the foil was applied by pressing it against the glue.

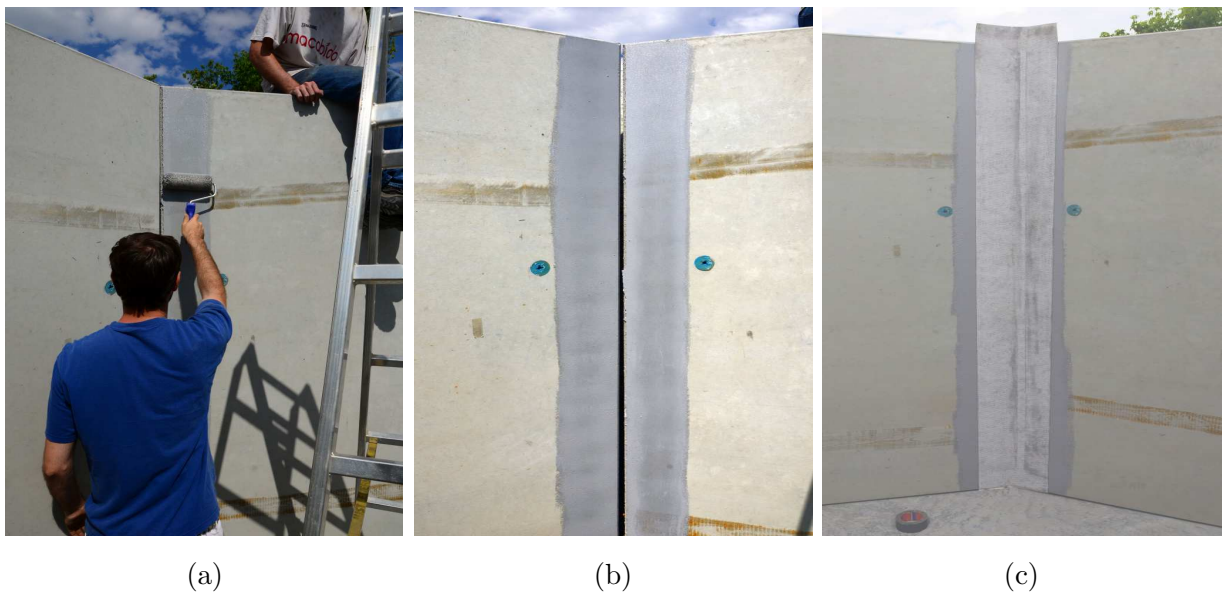


Figure 4.68: Inner vertical joints with glued water-resistant foil; (a) application of the glue; (b) glued concrete surface; (c) joint with glued foil

In the meantime, a special steel adapter for the concreting was mounted by 4 M16 bolts at its foreseen position (Fig. 4.69). This adapter allowed mounting of additional equipment for the concrete pump.

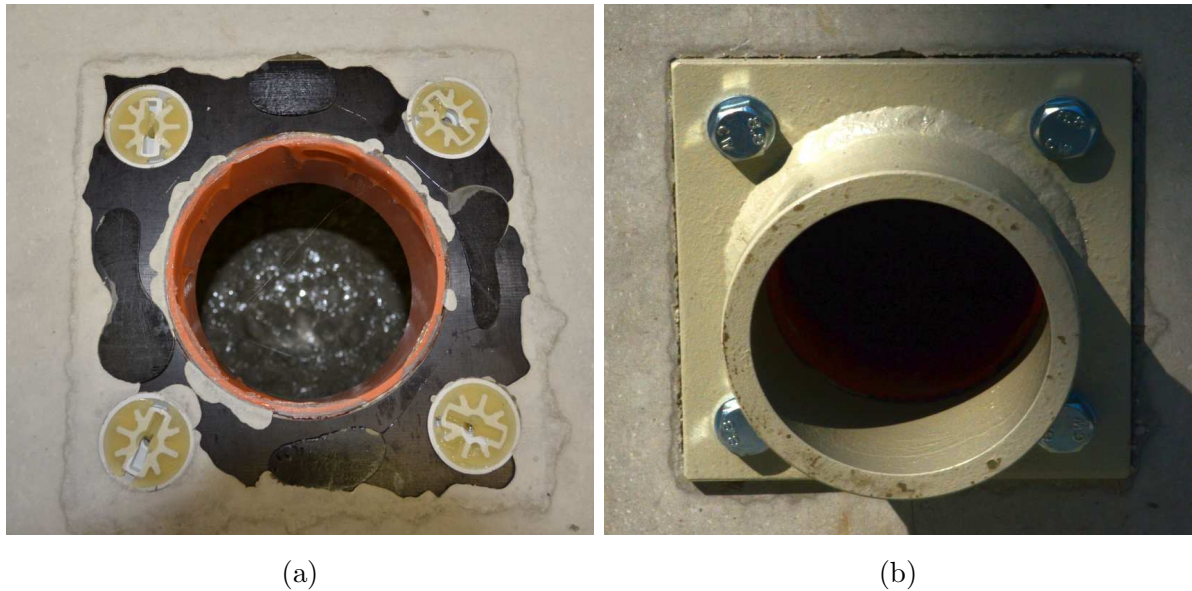


Figure 4.69: Steel adapter for the concreting; (a) embedment in concrete element with threaded sleeves; and (b) adapter fixed at the segment

In this stage screw bracings were removed and the assembly of the mock-up was completed (Fig. 4.70 and 4.72).



Figure 4.70: Assembled mock-up with bracings



Figure 4.71: Assembled mock-up without bracings



Figure 4.72: Top view of the assembled mock-up

4.5 Lifting and concreting of the mock-up

In order to determine the structural response of the ring segment at different load cases, it was lifted and partially filled with concrete. Results and observations obtained from these tests are presented in the Chapter 5.

The ring segment was lifted with the assistance of two lifting beams, which purpose was to minimize the horizontal loading of the test segment (Fig. 4.73). When the segment was lifted to the altitude of approximately 1 m, a plastic foil was attached to its bottom (Fig. 4.74). Whereby, the function of the foil was:

- to prevent leakage of concrete underneath the segment during concreting and
- to separate the poured concrete from the foundation surface



Figure 4.73: Lifting set up; (a) top view of the segment with lifting set up; and (b) side view of the segment with lifting set up



(a)

(b)



(c)

Figure 4.74: Lifting of the ring segment; (a) segment in the air; (b) lifted segment with placed plastic foil; and (c) lifting beam ($l = 240$ cm)

As safety precautions a 10 cm high layer of concrete was poured at the bottom of the segment. This layer sealed the segment so that no concrete could leak at the bottom while concreting of the whole segment. Herein, a concrete with strength C 30/37 was used. The concrete was filled in by a wooden slide and a concrete bucket that was lifted by the crane (Fig. 4.75). These works for the sealing of the segment at the bottom were needed only for the mock-up and they are not relevant for the real tower structure.



(a)



(b)

Figure 4.75: Concreting of a 10 cm high layer of concrete C 30/37; (a) lifting of the basket; and (b) pouring of the concrete from basket

The concreting of the segment could start when the introduced concrete layer at the bottom of the segment was hardened enough. The segment was filled with concrete C 30/37

by the usage of a pump connected to the adapter that was fixed to the opening in one of the elements (Fig. 4.76). This adapter consisted of following components:

- previously mounted steel adapter for the panel closure tool,
- filler neck,
- panel closure tool with clamps and
- steel pipe connector for connection to the concrete pump

The filler neck and panel closure toll were provided by the company Doka [48].



(a)



(b)

Figure 4.76: Adapters and additional equipment for connection of the concrete pump; (a) adapter and connection equipment without the concrete pump connector; and (b) assembled connection

Firstly, the ring segment was concreted from below (Fig. 4.77(a)), as previously described, while later the concreting from above was also tried (Fig. 4.77(b)). The segment was filled with 5.8 m^3 of concrete with the strength C 30/37. Thereby, only 2.1 m of the segment was concreted in approximately 45 minutes.



Figure 4.77: Concreting of the mock-up; (a) under pressure from below; and (b) from above

When the segment was filled with concrete, the concrete pump set up was closed by using the panel closure tool. After the pump was removed, the spiral bar of the filler neck was attached and screwed into the opening, while the panel closure tool was opened again (pay attention to the different position of the closure panels and length of the screwed bar in Fig. 4.78(a) and 4.78(b)).



(a)



(b)

Figure 4.78: Concrete pump set up equipped with spiral bar that pushes the fresh concrete out of the adapter; (a) closed panel and prepared bar of the filler neck; and (b) open panel and screwed bar of the filler neck

When the concrete is hardened the whole pump set up was removed and cleaned (Fig. 4.79).



Figure 4.79: Concrete pump opening after concreting

During concreting, the free space had to be left around the concrete blocks, and therefore, the mock-up could only be filled with concrete until a certain height of around 2.20 m (Fig. 4.80). This was necessary to lift the mock-up by placing of the lifting ropes around the blocks and to use the blocks as foundation during the erection of further towers segments.



Figure 4.80: Top view of concreted ring segment showing the accessibility of the concrete blocks

Chapter 5

Evaluation and discussion

To evaluate the achieved performance of the assembled structure and to improve its design and implementation for the further segments, the measurements of the mock-up segment are taken. This assessment has to provide a verification of aforementioned claims and identification of further technological challenges that will be confronted to the construction of the prototype, described in the Section 3.2. For this purpose, measurements of the prefabricated double wall elements and assembled mock-up structure are collected and analysed. Furthermore, structural details and their response during the application of former identified loads are examined and evaluated. The presentation and analysis of the obtained results are the objects of this chapter.

5.1 Comparison of planned and achieved geometry of the double wall elements

The acceptable construction tolerances are very limited for tower structures with a great height, and therefore, the basic tower components have to be constructed with a certain accuracy. To determine the degree of accuracy in the production of double walls, all nine elements used for the mock-up are measured. These measurements include characteristic geometrical values that are of relevance for one element and for the gained segment weight, which is of interest for the used crane capacity and transportation vehicle (Fig 5.1).

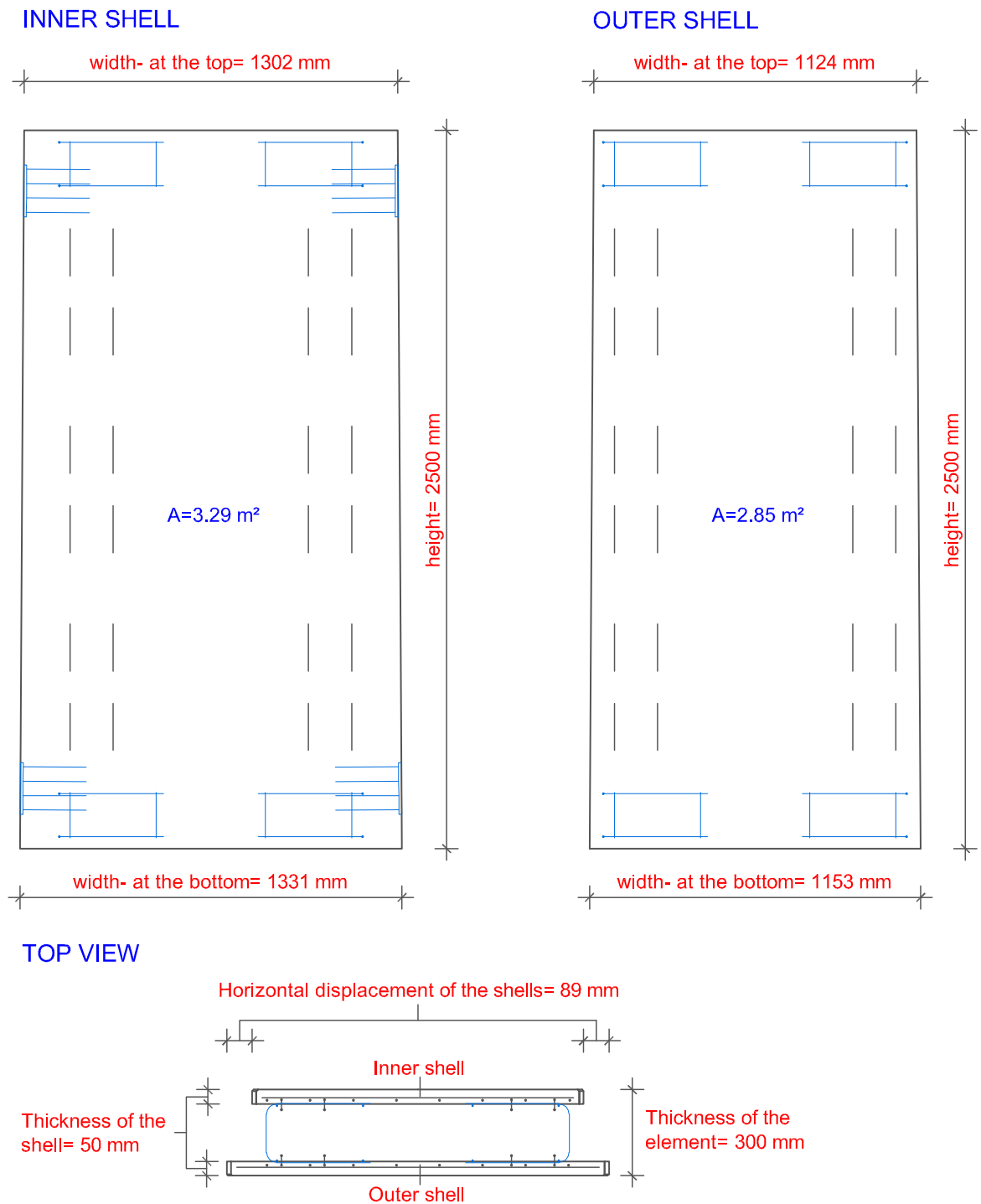


Figure 5.1: Planned dimensions of the double wall element

5.1.1 Element width

The gained joint size depends on the accuracy of the element width at the top and bottom of the neighbouring shells. This means that even a small deviation in the width of the element results in a significant deviation in the width of the vertical joints. The comparison of planned and achieved width of the elements revealed a very small deviation of maximum 7 mm or 0.6% of the planned width (Table 5.1), which is still very big regarding to the planned joint size of 10 mm. However, because the elements are arranged according to their centre, such deviations are distributed over both neighbouring joints. Consequently, it can be stated that the gained tolerances are in the expected range.

Table 5.1: Comparison of the planned and measured element widths

		Width of the elements							
Element	Shell	Bottom section				Top section			
		Planned (mm)	Measured (mm)	Deviation (mm)	Deviation (%)	Planned (mm)	Measured (mm)	Deviation (mm)	Deviation (%)
1	inner	1153.0	1160.0	7.0	0.6	1124.0	1123.0	-1.0	0.1
	outer	1331.0	1325.0	-6.0	0.5	1302.0	1297.0	-5.0	0.4
2	inner	1153.0	1155.0	2.0	0.2	1124.0	1126.0	2.0	0.2
	outer	1331.0	1330.0	-1.0	0.1	1302.0	1306.0	4.0	0.3
3	inner	1153.0	1155.0	2.0	0.2	1124.0	1125.0	1.0	0.1
	outer	1331.0	1334.0	3.0	0.2	1302.0	1304.0	2.0	0.2
4	inner	1153.0	1157.0	4.0	0.3	1124.0	1126.0	2.0	0.2
	outer	1331.0	1328.0	-3.0	0.2	1302.0	1300.0	-2.0	0.2
5	inner	1153.0	1157.0	4.0	0.3	1124.0	1127.0	3.0	0.3
	outer	1331.0	1330.0	-1.0	0.1	1302.0	1298.0	-4.0	0.3
6	inner	1153.0	1158.0	5.0	0.4	1124.0	1125.0	1.0	0.1
	outer	1331.0	1328.0	-3.0	0.2	1302.0	1299.0	-3.0	0.2
7	inner	1153.0	1156.0	3.0	0.3	1124.0	1125.0	1.0	0.1
	outer	1331.0	1330.0	-1.0	0.1	1302.0	1298.0	-4.0	0.3
8	inner	1153.0	1150.0	-3.0	0.3	1124.0	1122.0	-2.0	0.2
	outer	1331.0	1325.0	-6.0	0.5	1302.0	1303.0	1.0	0.1
9	inner	1153.0	1151.0	-2.0	0.2	1124.0	1122.0	-2.0	0.2
	outer	1331.0	1325.0	-6.0	0.5	1302.0	1300.0	-2.0	0.2
Total average	inner		1155.4	2.4	0.3		1124.6	0.6	0.1
	outer		1328.3	-2.7	0.3		1300.6	-1.4	0.2

5.1.2 Element height

Since the elements are arranged regarding to the horizontally levelled surface, any deviation in the element height can result in a geometrically collision at the top of two neighbouring elements. For this reason, the effective produced double wall element heights are documented in the Table 5.2. The maximum deviation of the height amounts to 5 mm or 0.2% of the planned height, which indicates a relatively small deviation in comparison with planned values, but shows a similar maximum value of the absolute error as for the element widths.

Table 5.2: Comparison of the planned and measured height of the elements

		Height of the elements			
Element	Shell	Planned (mm)	Measured (mm)	Deviation (mm)	(%)
1	inner	2500.0	2498.0	-2.0	0.1
	outer	2500.0	2499.0	-1.0	0.0
2	inner	2500.0	2497.0	-3.0	0.1
	outer	2500.0	2500.0	0.0	0.0
3	inner	2500.0	2500.0	0.0	0.0
	outer	2500.0	2499.0	-1.0	0.0
4	inner	2500.0	2498.0	-2.0	0.1
	outer	2500.0	2499.0	-1.0	0.0
5	inner	2500.0	2499.0	-1.0	0.0
	outer	2500.0	2499.0	-1.0	0.0
6	inner	2500.0	2499.0	-1.0	0.0
	outer	2500.0	2499.0	-1.0	0.0
7	inner	2500.0	2500.0	0.0	0.0
	outer	2500.0	2499.0	-1.0	0.0
8	inner	2500.0	2500.0	0.0	0.0
	outer	2500.0	2495.0	-5.0	0.2
9	inner	2500.0	2499.0	-1.0	0.0
	outer	2500.0	2499.0	-1.0	0.0
Total	inner		2498.9	-1.1	0.0
average	outer		2498.7	-1.3	0.1

5.1.3 Shell thickness

Even small imperfections in the shell thickness would either result in: elements heavier than planned if they are too thick, or insufficient anchored embedments if they are too

thin. The concreting process should be automatically performed, however, it happens that some areas, like corners of the shells, are not supplied with enough concrete. For this reason these areas are additionally concreted manually, what inevitably results in thicker shells than planned. Mentioned in passing, it is known that the inner side (facing the hollow space) of each shell has a rough surface (± 5 mm), so this addition was considered while measuring the shell thickness. The comparison of the planned and average measured values shows a maximum deviation of 14.5 mm or 29 % of the planned thickness (Tables 5.3 and 5.4). These results indicate large deviations from planned values that will have an influence on weight and thickness of the double wall elements (see further Subsections 5.1.4 and 5.1.6).

Table 5.3: Comparison of the planned and measured shell thicknesses- measured at the bottom section

		Thickness of the shells					
		At the bottom					
Element	Shell	Planned	Measured		Average	Deviation	
		(mm)	left (mm)	right (mm)	(mm)	(mm)	(%)
1*	inner	50.0	51.5	50.0	50.8	0.8	1.5
	outer	50.0	56.5	56.0	56.3	6.3	12.5
2	inner	50.0	55.0	59.0	57.0	7.0	14.0
	outer	50.0	55.0	60.0	57.5	7.5	15.0
3	inner	50.0	51.0	55.0	53.0	3.0	6.0
	outer	50.0	50.0	48.0	49.0	-1.0	2.0
4*	inner	50.0	55.0	53.0	54.0	4.0	8.0
	outer	50.0	51.0	50.0	50.5	0.5	1.0
5	inner	50.0	52.0	55.0	53.5	3.5	7.0
	outer	50.0	55.0	59.0	57.0	7.0	14.0
6	inner	50.0	55.0	56.0	55.5	5.5	11.0
	outer	50.0	55.0	55.0	55.0	5.0	10.0
7*	inner	50.0	57.0	57.0	57.0	7.0	14.0
	outer	50.0	55.0	60.0	57.5	7.5	15.0
8	inner	50.0	54.0	54.0	54.0	4.0	8.0
	outer	50.0	50.0	51.0	50.5	0.5	1.0
9	inner	50.0	55.0	52.0	53.5	3.5	7.0
	outer	50.0	50.0	50.0	50.0	0.0	0.0
Total	inner		53.9	54.6	54.3	4.3	8.5
average	outer		53.1	54.3	53.7	3.7	7.8

* double wall element with embedded concrete blocks

Table 5.4: Comparison of the planned and measured thickness of the shells-measured at the top section

		Thickness of the shells					
		At the top					
Element	Shell	Planned	Measured		Average	Deviation	
		(mm)	left (mm)	right (mm)	(mm)	(mm)	(%)
1*	inner	50.0	59.0	59.0	59.0	9.0	18.0
	outer	50.0	56.0	55.5	55.8	5.8	11.5
2	inner	50.0	60.0	63.0	61.5	11.5	23.0
	outer	50.0	54.0	55.0	54.5	4.5	9.0
3	inner	50.0	57.0	58.0	57.5	7.5	15.0
	outer	50.0	52.0	49.0	50.5	0.5	1.0
4*	inner	50.0	55.0	60.0	57.5	7.5	15.0
	outer	50.0	49.0	48.0	48.5	-1.5	3.0
5	inner	50.0	59.0	60.0	59.5	9.5	19.0
	outer	50.0	56.0	55.0	55.5	5.5	11.0
6	inner	50.0	62.0	64.0	63.0	13.0	26.0
	outer	50.0	58.0	54.0	56.0	6.0	12.0
7*	inner	50.0	64.0	65.0	64.5	14.5	29.0
	outer	50.0	51.0	51.0	51.0	1.0	2.0
8	inner	50.0	60.0	58.0	59.0	9.0	18.0
	outer	50.0	53.0	50.0	51.5	1.5	3.0
9	inner	50.0	50.0	61.0	55.5	5.5	11.0
	outer	50.0	61.0	54.0	57.5	7.5	15.0
Total	inner		58.4	60.9	59.7	9.7	19.3
average	outer		54.4	52.4	53.4	3.4	7.5

* double wall element with embedded concrete blocks

5.1.4 Element thickness

Any deviations from the planned element thickness result in an offset between two neighbouring elements. Therefore, the elements in the segment are aligned according to the outer shell so that any possible offsets are accumulated in the interior of the tower. Generally, it can be stated that measured element thicknesses are in an acceptable range, except of element 7, which has a deviation of 7.5 mm or 2.5 % compared to the planned thickness. This deviation can stem from the fact that element 7 contains concrete blocks, so it is assumed that some error was made while placement or production of the blocks.

Consequently following sources for the element thickness deviation are detected:

- the blocks are placed so that a concrete aggregate could jam between the formwork and the 30 cm long fibre glass reinforcement bars (ComBar), and/or
- the ComBar reinforcement are too long

For these reasons, it is recommended that in future special attention is devoted to the placement and production of the concrete blocks.

Table 5.5: Comparison of the planned and measured thickness of the elements

		Thickness of the element				
Element	Section	Planned	Measured		Average	Deviation
		(mm)	left (mm)	right (mm)	(mm)	(mm) (%)
1*	bottom	300.0	300.0	302.0	301.0	1.0 0.3
	top	300.0	302.0	298.5	300.3	0.3 0.1
2	bottom	300.0	306.0	301.0	303.5	3.5 1.2
	top	300.0	300.0	299.0	299.5	-0.5 0.2
3	bottom	300.0	301.0	301.0	301.0	1.0 0.3
	top	300.0	301.0	302.0	301.5	1.5 0.5
4*	bottom	300.0	303.0	302.0	302.5	2.5 0.8
	top	300.0	302.0	300.0	301.0	1.0 0.3
5	bottom	300.0	302.0	301.0	301.5	1.5 0.5
	top	300.0	300.0	300.0	300.0	0.0 0.0
6	bottom	300.0	301.0	300.0	300.5	0.5 0.2
	top	300.0	299.0	300.0	299.5	-0.5 0.2
7*	bottom	300.0	306.0	306.0	306.0	6.0 2.0
	top	300.0	306.0	309.0	307.5	7.5 2.5
8	bottom	300.0	302.0	301.0	301.5	1.5 0.5
	top	300.0	300.0	300.0	300.0	0.0 0.0
9	bottom	300.0	303.0	306.0	304.5	4.5 1.5
	top	300.0	300.0	303.0	301.5	1.5 0.5
Total	bottom		302.7	302.2	302.4	2.4 0.8
average	top		301.1	301.3	301.2	1.2 0.5

* double wall element with embedded concrete blocks

5.1.5 Horizontal displacement between shells

Since the elements are arranged according to the centre of outer shell, any horizontal shift between both shells can result in too narrow or too wide inner joints. The comparison of planned and measured horizontal displacement of the shell shows a maximum deviation of 6.5 mm or 7.3 % of the planned displacement (Table 5.6). Such deviation can be considered

to be high, because during the planning, the maximum acceptable value was set to amount to the half planned joint width (5 mm). The reason for this unacceptable value could be that in the production process, at the point where outer and inner shells are merged, some reinforcement jammed and shifted the shells. Therefore, care must be taken that possible collisions of reinforcement between both shells are prevented.

Table 5.6: Comparison of the planned and measured horizontal displacement of the shells

		Horizontal displacement of the shells					
Element	Section	Planned (mm)	Measured		Average (mm)	Deviation	
			left (mm)	right (mm)		(mm)	(%)
1	bottom	89.0	85.5	85.0	85.3	-3.8	4.2
	top	89.0	91.0	85.0	88.0	-1.0	1.1
2	bottom	89.0	84.0	89.0	86.5	-2.5	2.8
	top	89.0	86.0	91.0	88.5	-0.5	0.6
3	bottom	89.0	81.0	85.5	83.3	-5.8	6.5
	top	89.0	88.0	84.5	86.3	-2.8	3.1
4	bottom	89.0	85.0	85.0	85.0	-4.0	4.5
	top	89.0	87.0	85.0	86.0	-3.0	3.4
5	bottom	89.0	80.0	85.0	82.5	-6.5	7.3
	top	89.0	82.0	89.0	85.5	-3.5	3.9
6	bottom	89.0	86.0	85.0	85.5	-3.5	3.9
	top	89.0	84.0	85.0	84.5	-4.5	5.1
7	bottom	89.0	87.0	85.0	86.0	-3.0	3.4
	top	89.0	83.0	87.0	85.0	-4.0	4.5
8	bottom	89.0	90.0	85.0	87.5	-1.5	1.7
	top	89.0	92.0	90.0	91.0	2.0	2.2
9	bottom	89.0	85.0	85.0	85.0	-4.0	4.5
	top	89.0	85.0	90.0	87.5	-1.5	1.7
Total	bottom		84.8	85.5	85.2	-3.8	4.3
	average top		86.4	87.4	86.9	-2.1	2.8

5.1.6 Element weight

The previously compared shell thicknesses from Subsection 5.1.3 imply that the weight of the elements is higher than planned. It is important to determine the weight of the elements, and consequently of the ring segment, so that is possible to establish whether its weight meets the limitations of maximum crane capacity. Therefore, the weight of the elements is a factor that affecting the cost effectiveness. In the first step the planned weight is estimated for the reinforced elements with and without lifting concrete blocks, while afterwards, the theoretical weight is compared with the real measured one.

5.1.6.1 Theoretical weight of the elements

The weight of the double wall elements without embedded concrete blocks can be estimated to be:

$$\begin{aligned}
 \text{Area of the inner shell:} & \quad A_i = 2.85 \text{ m}^2 \\
 \text{Area of the outer shell:} & \quad A_o = 3.29 \text{ m}^2 \\
 \text{Planned thickness of the shells:} & \quad d = 0.05 \text{ m} \\
 \text{Specific weight of the shells:} & \quad \gamma = 25 \text{ kN/m}^3
 \end{aligned}$$

Weight of the double wall elements:

$$W_E = (A_i + A_o) \cdot d \cdot \rho = (2.85 + 3.29) \cdot 0.05 \cdot 2500 = 767.50 \text{ kg}$$

The weight of the double wall elements with embedded concrete blocks can be estimated to be:

$$\begin{aligned}
 & \text{Specific weight of the} \\
 & \text{block with ComBAR} \quad \gamma = 24.50 \text{ kN/m}^3 \\
 & \text{reinforcement:} \\
 & \text{Concrete block dimensions: } 0.2 \times 0.25 \times 0.3 \text{ (l} \times \text{w} \times \text{h) in [m]} \\
 & \text{Weight of the concrete} \quad W_B = (l \cdot w \cdot h) \cdot \rho \\
 & \text{block:} \quad \quad \quad = (0.2 \cdot 0.25 \cdot 0.3) \cdot 2450 = 36.80 \text{ kg}
 \end{aligned}$$

Weight of the double wall elements with embedded concrete blocks:

$$W_{E+B} = 767.50 + 2 \cdot 36.8 = 841.10 \text{ kg}$$

5.1.6.2 Measuring of the element weight

The weight of the elements was measured by four pressure cells that were placed on steel plates in order to ensure a flat surface underneath the cells (Fig. 5.2(a) and 5.2(b)). The cells were connected to a converter unit that converts their electrical signal into data that is evaluated on a computer. Afterwards, a wooden panel is laid on the cells to ease the positioning of the double wall elements by crane, as well as to distribute the weight equally and to prevent any destructive pressure on the concrete surface (Fig. 5.2(c)). The double wall elements were lifted using textile ropes in order to prevent any damaging of the element edges during lifting.



(a)



(b)



(c)

Figure 5.2: Measuring of the element weight; (a) set up for the measuring of the weight; (b) pressure cells with underlying steel plate and data cable; and (c) positioning of the elements

A comparison of the calculated and measured weight is presented in the Table 5.7 and it shows that a majority of the elements are heavier than desired. The maximum weight exceeding is noted at element 6 with an amount of 164 kg or 21 % of the planned value, which is in correlation with an excessive thickness of this element.

Table 5.7: Comparison of the planned and measured weight of the elements

Weight of the elements				
Element	Planned	Measured	Deviation	
	(kg)	(kg)	(kg)	(%)
1*	841.1	922.3	81.2	9.7
2	767.5	906.5	139.0	18.1
3	767.5	809.5	42.0	5.5
4*	841.1	906.0	64.9	7.7
5	767.5	890.5	123.0	16.0
6	767.5	946.0	178.5	23.3
7*	841.1	980.0	138.9	16.5
8	767.5	821.0	53.5	7.0
9	767.5	839.0	71.5	9.3
Total average			99.2	12.5
Total weight			892.5	12.5

* double wall element with embedded concrete block

The evaluation of the compared planned and achieved geometry indicates that the dimensions which depend on the automated work of the robot show little tolerance, while the dimensions that depend on manual work are subject to human errors and thus show significant deviations. According to that, the maximum deviations of average values were obtained from the evaluation of the shell thickness (19.3 %) and consequently the element weight (12.2 %). Therefore, such large deviations require a further attention during the production of elements for the following ring segments.

5.2 Evaluation of the achieved mock-up segment geometry

One of the main technological challenges confronted to the feasibility of the proposed construction method is achieving and securing of the planned segment geometry during all construction phases. First of all, the performed assembly process, described in Section 4.4, has to prove that the desired ring segment geometry can be achieved. Secondly, the pre-assembled segment, secured by the interconnections of the elements, has to demonstrate its unchangeable geometry through different construction phases, like lifting and concreting. Therefore, measurements of certain geometries were taken at aforementioned construction phases in order to evaluate the achieved geometry and interconnection of the elements.

In this context it must be mentioned that two major complications occurred at the erection of the mock up:

- the foundation surface did not provide the needed planarity of the horizontal surface
- the produced double wall elements had greater tolerances than expected

The superposition of the mentioned problems, caused difficulties during inclination, and thus greater deviations in the geometry of the mock-up.

5.2.1 Segment geometry before lifting, after lifting and after concreting

Due to the complexity and the workload associated with the complete measurement of the segment geometry, only several representative values or sub-geometries were gathered manually. These values are compared with the planned dimensions and observed through the construction process.

5.2.1.1 Observation of the deformation between concrete blocks

To evaluate the ring segment geometry at all construction phases, the distance between three reference points is measured and compared (Fig. 5.3). Whereby, these points are defined as the centre of the three concrete blocks that are embedded in every third double wall element. The concrete blocks at the top of the segment were observed, because this section is easy accessible. The distances between these points, which are measured before lifting, after lifting and after concreting of the ring segment, are compared and presented in the Table 5.8.

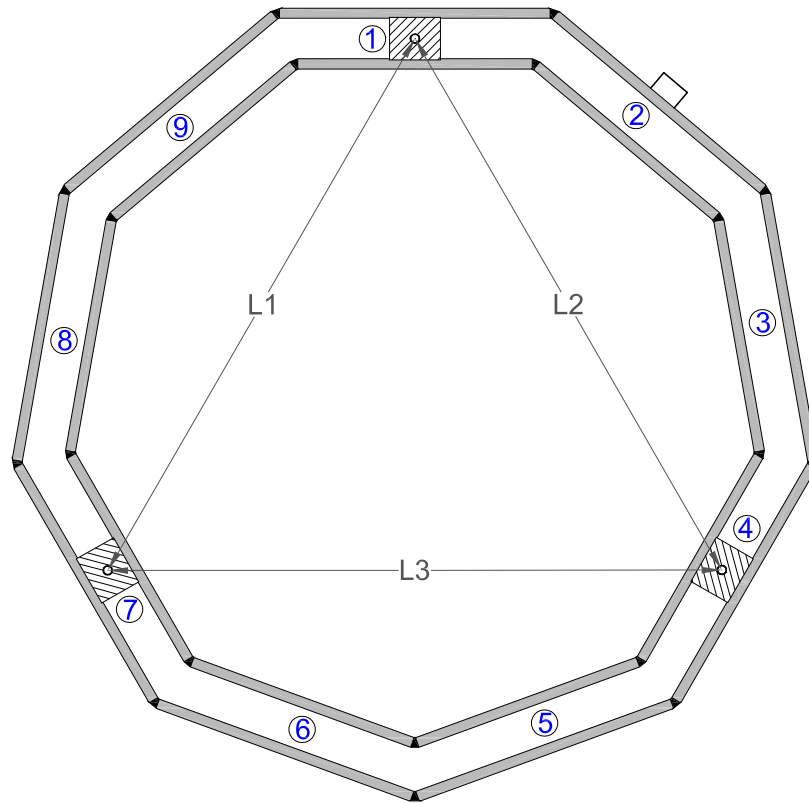


Figure 5.3: Top section of the mock-up segment with marked distances L1, L2 and L3 measured at all relevant construction phases (assembly, lifting and concreting)

Table 5.8: Comparison of planned and measured distances L1, L2 and L3, as defined in Fig. 5.3, between the three reference points

Distances between the observed reference points										
Distance	Planned (mm)	Measured			Deviation					
		Before lifting (mm)	After lifting (mm)	After concreting (mm)	Planned-before (mm)	(%)	Before-after (mm)	(%)	After lifting-concreting (mm)	(%)
L1	2951.0	2920.0	2925.0	2925.0	31.0	1.1	-5.0	0.2	0.0	0.0
L2	2951.0	2925.0	2920.0	2920.0	26.0	0.9	5.0	0.2	0.0	0.0
L3	2951.0	2920.0	2925.0	2928.0	31.0	1.1	-5.0	0.2	-3.0	0.1
Total average		2921.7	2923.3	2924.3	29.3	1.0	-1.7	0.2	-1.0	0.0

The comparison of the measured values of L1, L2 and L3 through the aforementioned construction phases demonstrated the largest divergence in comparison of planned and

assembled geometry, which amount to 31 mm or 1.1% of planned distance. The change in geometry after lifting and concreting shows a quite smaller divergence that amount to 5 mm or 0.2% and 3 mm or 0.1% of planned value.

5.2.1.2 Deformation of the segment after concreting

Another approach to evaluate the finally gained geometry of the segment is to measure the upper inner polygon of the segment. This polygon section of the segment is chosen because of its accessibility, which provides the possibility to fix a projection of two points per polygon side on the foundation by using a plumb. The distances between the centre reference point and the former marked points as well as the distances between the marked point itself are used to reconstruct the desired geometry on the foundation surface (Fig. 5.4). This measuring method proved to be practical because a small error of only 9.3 mm (0.1%) is gained over a length of approximately 10.2 m.

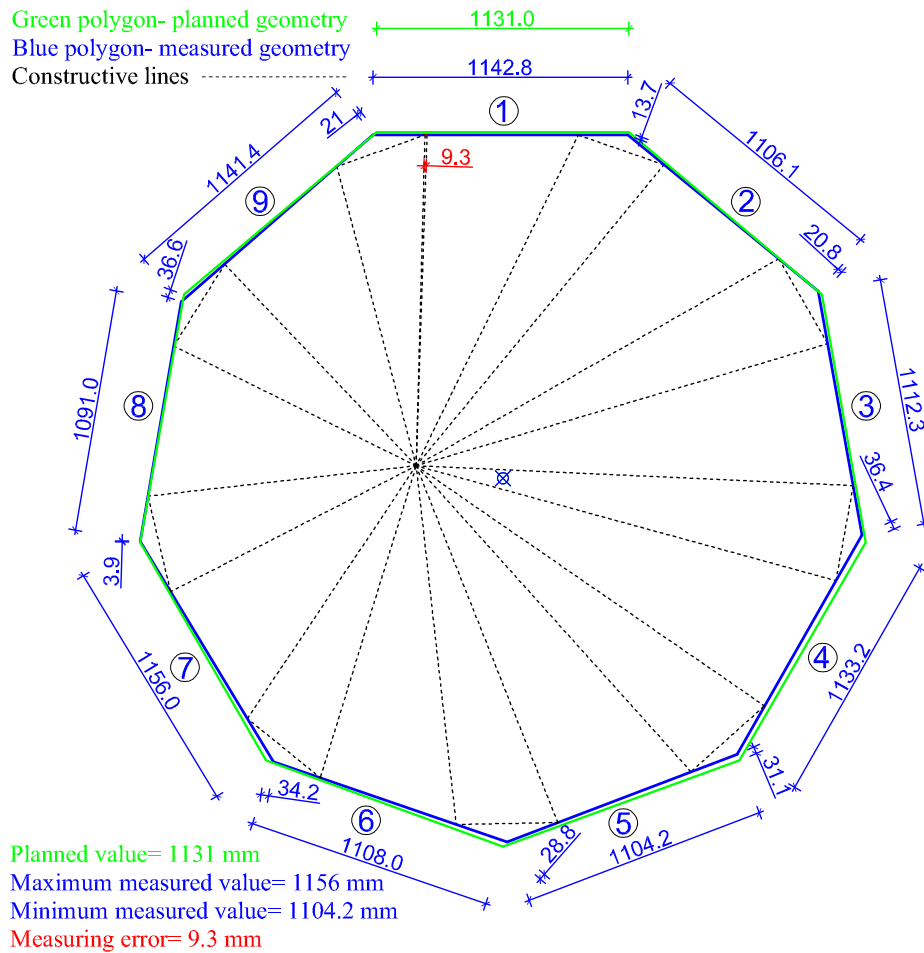


Figure 5.4: Comparison of planned and achieved upper inner polygon of the segment section [mm]

To provide easier comparison of the planned and achieved polygon lengths, the obtained measures are presented in Table 5.9. The comparison of the planned and measured geometry shows that the upper inner polygon is smaller than planned. This can be a result of the assembly process where the elements are arranged according to the outer polygon geometry, so all imperfections, like element width, element thickness and horizontal displacement of the shells, have an influence on the inner polygon geometry. Another possibility is that inclination was set up bigger than it should have been.

Table 5.9: Comparison of the planned and measured length of polygon sides of the upper inner segment section

Lenght of polygon sides				
Element	Planned (mm)	Measured (mm)	Deviation	
			(mm)	(%)
1	1131.0	1142.8	11.8	1.0
2	1131.0	1106.1	-24.9	2.2
3	1131.0	1112.3	-18.7	1.7
4	1131.0	1133.2	2.2	0.2
5	1131.0	1104.2	-26.8	2.4
6	1131.0	1108.0	-23.0	2.0
7	1131.0	1156.0	25.0	2.2
8	1131.0	1091.0	-40.0	3.5
9	1131.0	1141.4	10.4	0.9
Total average		1121.7	-9.3	1.8

To estimate the deviations of the outer outline of the ring segment geometry, the measured thicknesses of the double wall elements have to be added to the inner one. However, as previously stated, the maximum deviation of the shell thickness is 7.5 mm (see Subsection 5.1.3), which is a small value in comparison with the previously obtained deviation of the inner upper geometry of 40 mm. Therefore, it can be stated that the outer geometry is not considerably affected by element thickness deviation.

5.2.2 Joint widths before lifting, after lifting and after concreting

The structural response during lifting of the ring segment, and thus obtained results from this experiment, mostly depend on the lifting conditions. As previously described in the section 4.5, the mock-up is lifted at three points by lifting ropes and two beams (Fig. 5.5). The ropes were at the one end tied to the concrete blocks and at the another end hooked

to the two lifting beams. The 240 cm long steel beams were used to reduce the inclination angle of the chains. Otherwise, lifting with more inclined chains and without lifting beams would result in a horizontal loading of the segment. However, due to the chain length of 335 cm and a deflection between the hooks and the blocks axis of 31 cm, the segment was lifted with a relatively small angle of elements of approximately 5.33° .

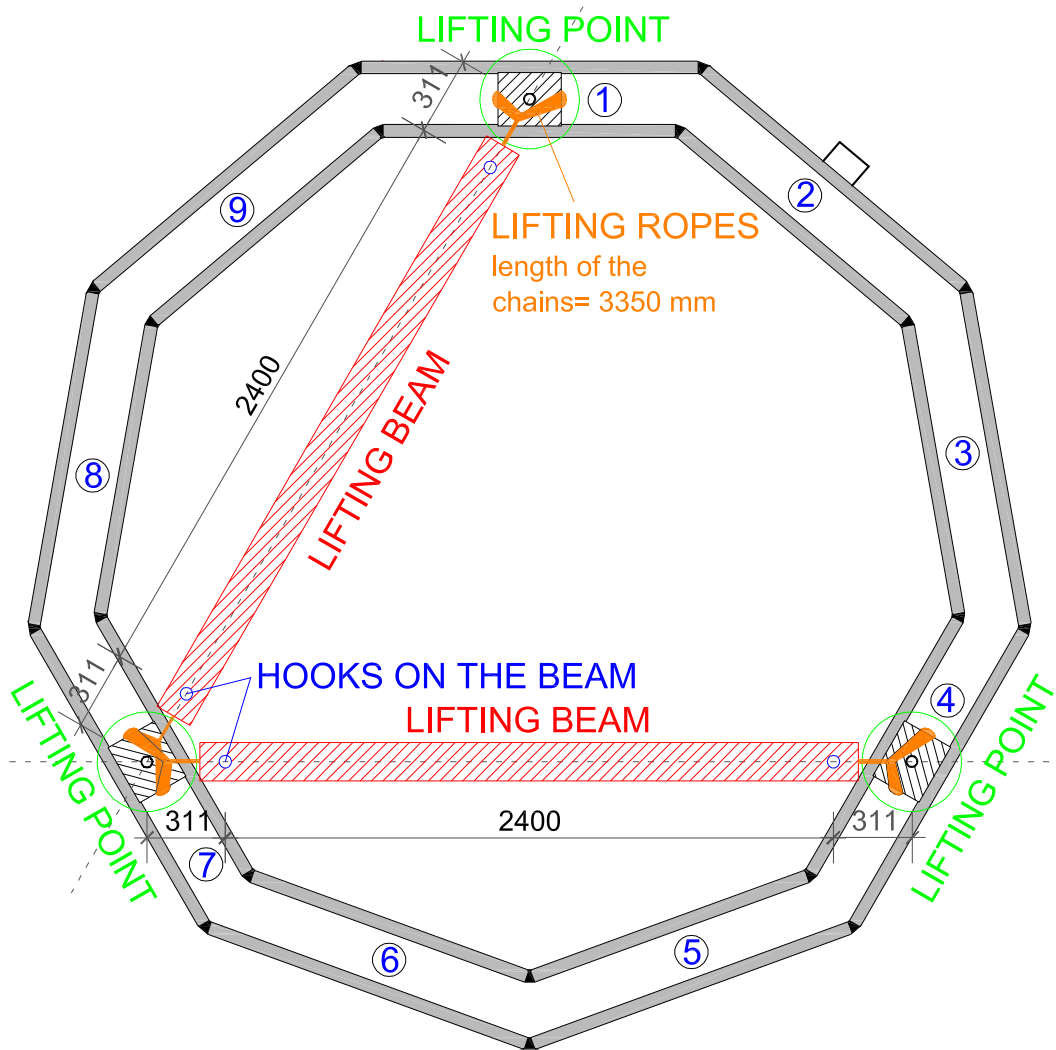


Figure 5.5: Position of lifting beams and points [mm]

The widths of the internal vertical joints were measured at the bottom and top section of the ring segment (Fig. 5.6). Herein, it should be considered that due to different joint geometries, as a result of the former described production deflections as well as erection deviations, the presented values are approximative. A well-arranged comparison of the inner vertical joint measurements is provided in Table 5.10.

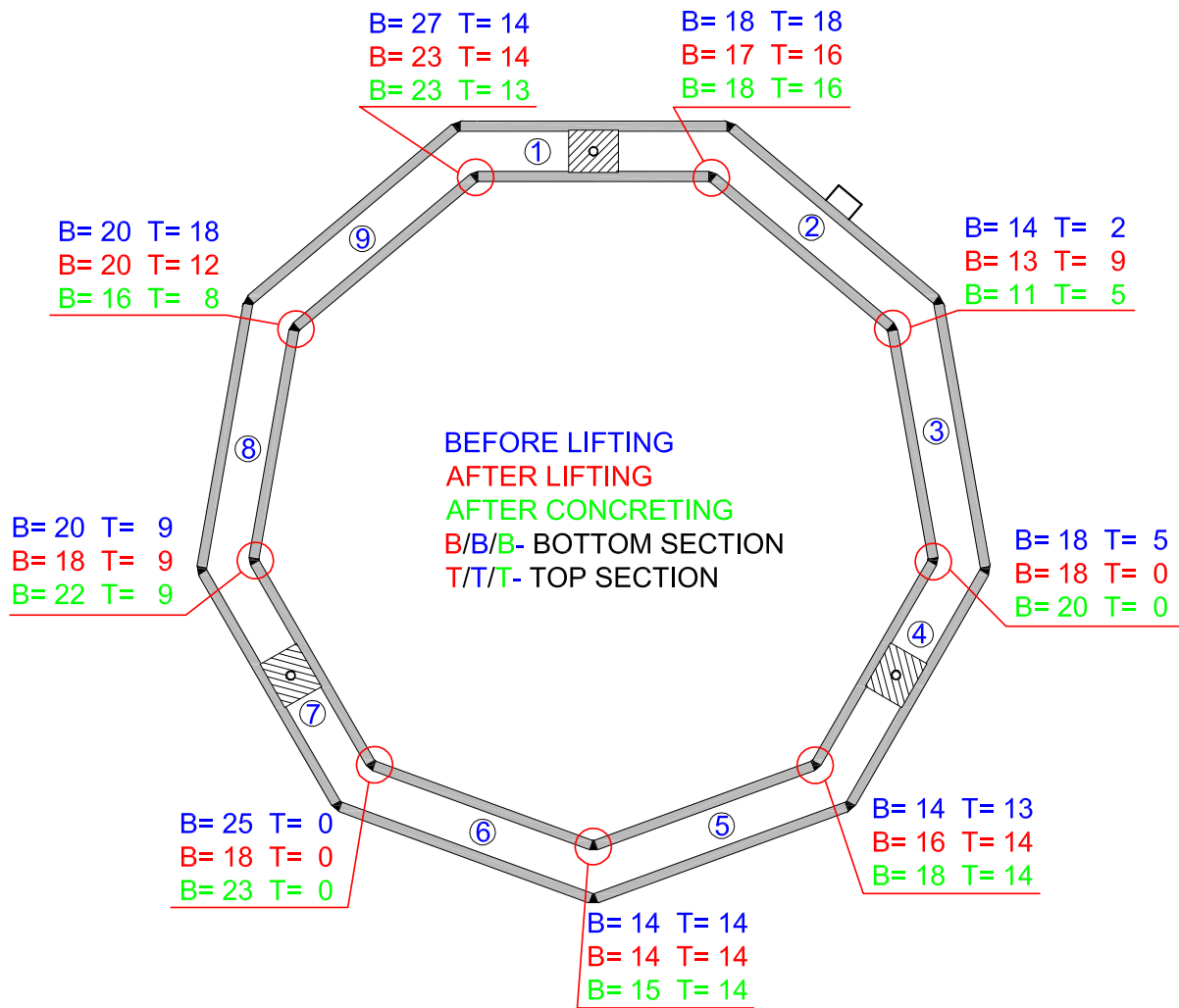


Figure 5.6: Width of the internal vertical joints before lifting, after lifting and after concreting of the ring segment [mm]

Table 5.10: Comparison of internal vertical joint widths before and after lifting of the mock-up

Width of the joints of planned, assembled, after lifting and after concreting geometry											
Joint between elements	Section	Planned (mm)	Before lifting (mm)	After lifting (mm)	After concreting (mm)	Displacement					
						Planned- before lifting		Before- after lifting		After lifting- after concreting	
						(mm)	(%)	(mm)	(%)	(mm)	(%)
1-2	bottom	10.0	18.0	17.0	18.0	8.0	80.0	-1.0	0.1	1.0	0.1
	top	10.0	18.0	16.0	16.0	8.0	80.0	-2.0	0.1	0.0	0.0
2-3	bottom	10.0	14.0	13.0	11.0	4.0	40.0	-1.0	0.1	-2.0	0.2
	top	10.0	2.0	9.0	5.0	-8.0	80.0	7.0	3.5	-4.0	0.4
3-4	bottom	10.0	18.0	18.0	20.0	8.0	80.0	0.0	0.0	2.0	0.1
	top	10.0	5.0	0.0	0.0	-5.0	50.0	-5.0	1.0	0.0	0.0
4-5	bottom	10.0	14.0	16.0	18.0	4.0	40.0	2.0	0.1	2.0	0.1
	top	10.0	13.0	14.0	14.0	3.0	30.0	1.0	0.1	0.0	0.0
5-6	bottom	10.0	14.0	14.0	15.0	4.0	40.0	0.0	0.0	1.0	0.1
	top	10.0	14.0	14.0	14.0	4.0	40.0	0.0	0.0	0.0	0.0
6-7	bottom	10.0	25.0	18.0	23.0	15.0	150.0	-7.0	0.3	5.0	0.3
	top	10.0	0.0	0.0	0.0	-10.0	100.0	0.0	0.0	0.0	0.0
7-8	bottom	10.0	20.0	18.0	22.0	10.0	100.0	-2.0	0.1	4.0	0.2
	top	10.0	9.0	9.0	9.0	-1.0	10.0	0.0	0.0	0.0	0.0
8-9	bottom	10.0	20.0	20.0	16.0	10.0	100.0	0.0	0.0	-4.0	0.2
	top	10.0	18.0	12.0	8.0	8.0	80.0	-6.0	0.3	-4.0	0.3
9-1	bottom	10.0	27.0	23.0	23.0	17.0	170.0	-4.0	0.1	0.0	0.0
	top	10.0	14.0	14.0	13.0	4.0	40.0	0.0	0.0	-1.0	0.1
Average			14.6	13.6	13.6	4.6	72.8	-1.0	0.3	0.0	0.1

As previously stated, the biggest divergence between planned and measured values is found to be after the assembly of the ring segment and right before lifting. The test lifting caused small deformations of the ring segment, which are caused by lifting conditions. In other words, the inclination of the lifting chains resulted in horizontal load components that caused deformations of the ring segment. Additionally, lifting caused the biggest cracks in the vertical joints. The measured average deviation of the reference joint widths before and after lifting is 7 mm or 3.5 %, while the comparison of measures after lifting and after concreting shows maximum deviation of 5 mm or 0.3 %.

Comparing the measured values for the width of the joints after lifting and after concreting it is obvious that the joints at the bottom are spreading, while joints at the top are tapering. This could be the consequence of the concrete pressure that has estimated a triangle distribution over the height with a resultant force in the bottom area of the segment.

5.3 Evaluation of vertical joints

At the construction of the mock-up, one type of external and two types of internal vertical joints were tested (Fig. 5.7). Whereby, all nine outer joints were connected by welding and afterwards filled with mortar. The three inner vertical joints were sealed with a glued foil, while the remaining six joints were sealed by elastomer tubes. After the concrete in the double wall elements was hardened, all joints were thoroughly inspected.

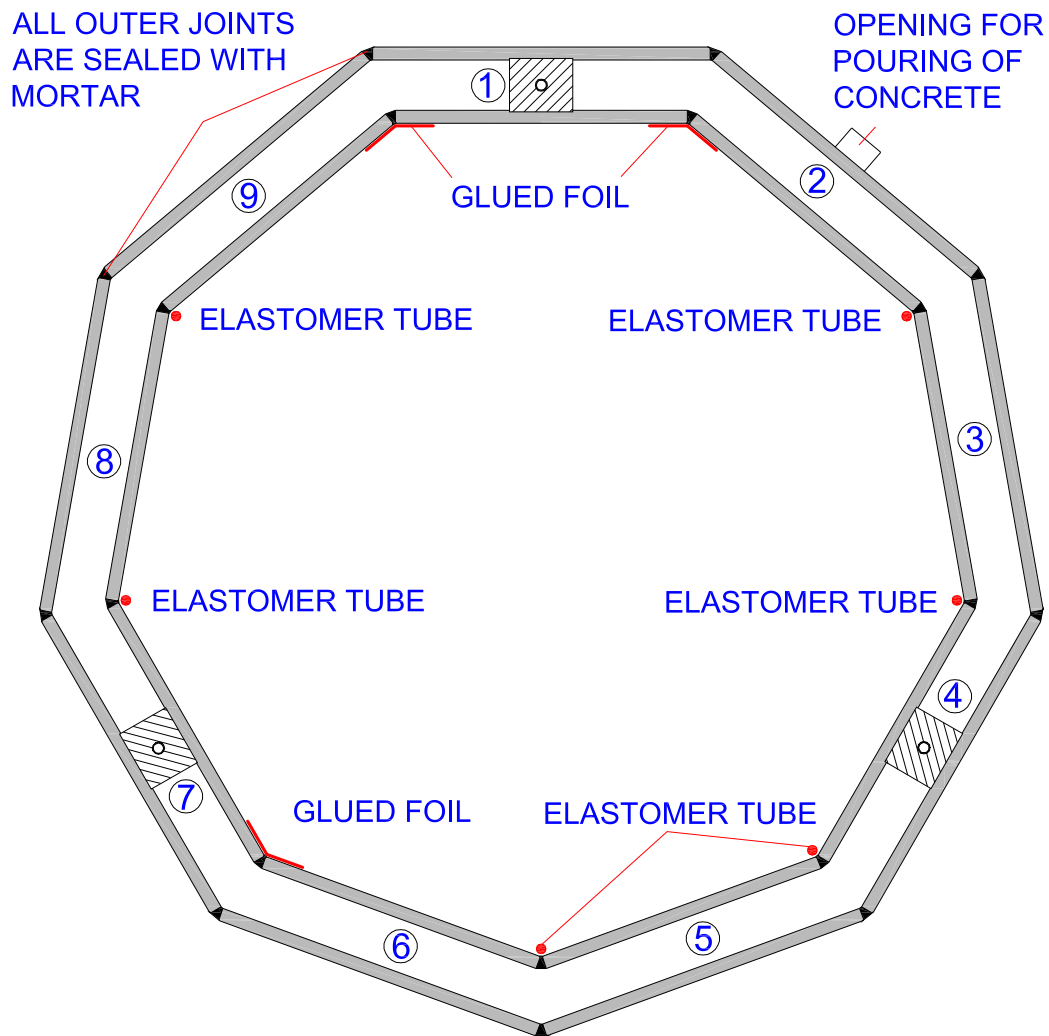


Figure 5.7: Position of the different inner and outer sealing types tested in the mock-up

5.3.1 Evaluation of different joint types

All tested sealing types fulfilled its function to prevent concrete leakage while concreting, which can be highlighted positively. Whereby some performed better than others.

It is observed that the glued foil formed bubbles in the lower area of certain joints (Fig. 5.8 and 5.9). Wherein, the foil located between the elements 1-2 showed the largest bubbles, while the foil located between the elements 1-9 showed smaller ones. The foil positioned between the elements 6-7 showed no sign of bubbles at all.

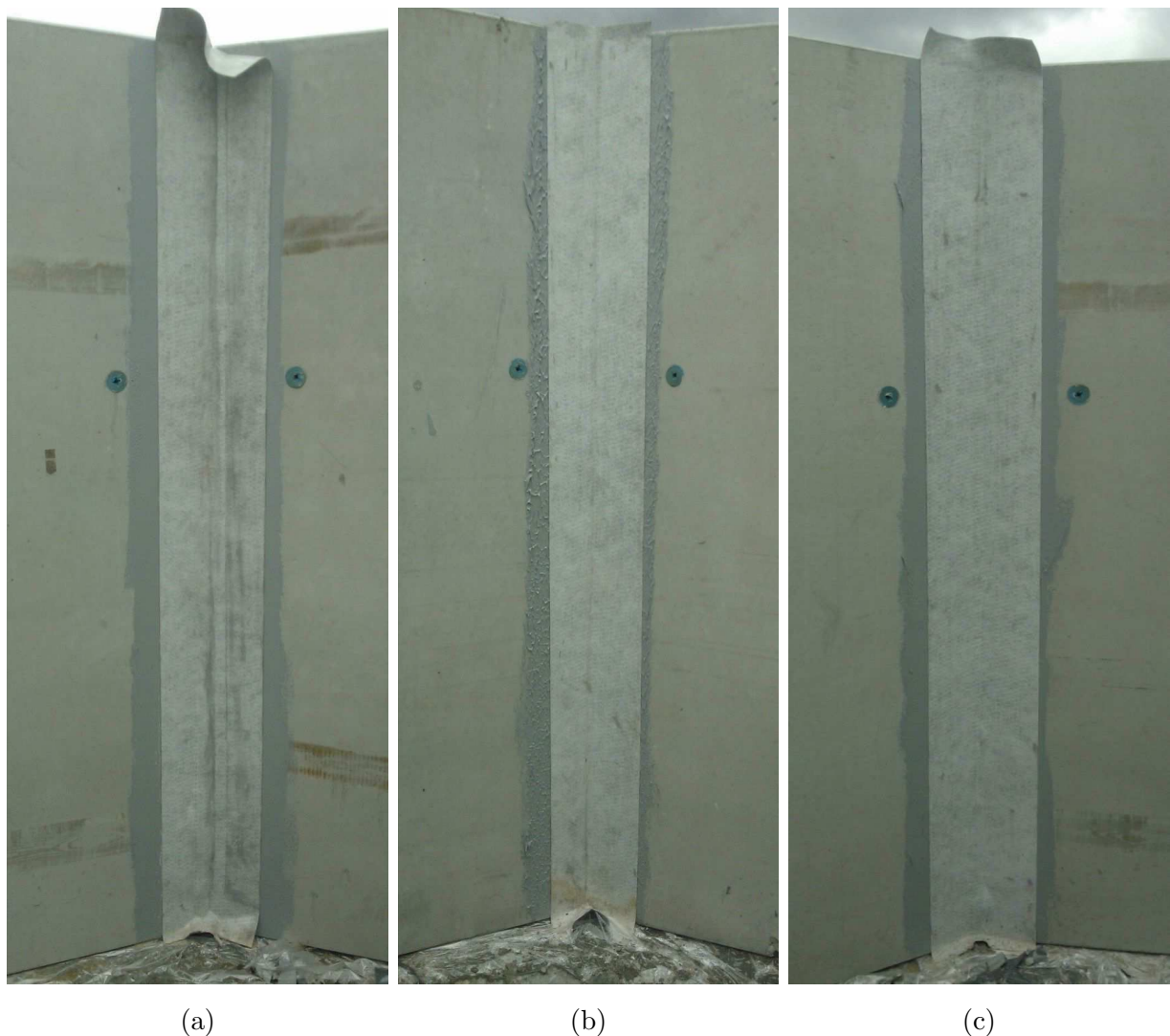


Figure 5.8: Inner vertical joints sealed by glued foil; (a) between elements 1-2; (b) between elements 1-9; and (c) between elements 6-7



Figure 5.9: Characteristic top view of inner vertical joints sealed by glued foil

Once the foil was removed to examine the result of the sealing, it is noticed that the observed bubbles are formed by concrete (Fig. 5.10). The reasons for this behaviour can be determined as one or the combination of the following:

- too wide joints between the elements
- too less or not properly applied glue
- too big concrete pressure near the opening for concreting

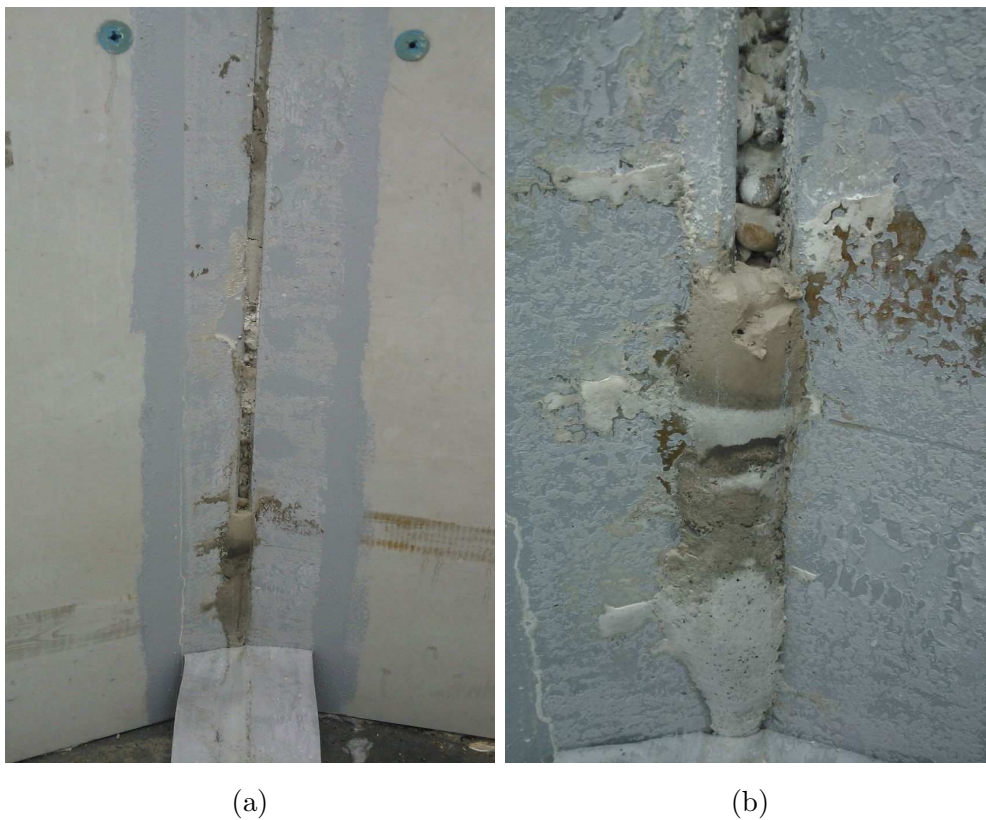


Figure 5.10: Vertical joint sealed by foil between the elements 1-2: (a) after removing of the foil; and (b) enlarged view of the bottom area

Due to the observed correlation of the position and bubble appearance it can be stated that the two sealings that are in close proximity to concreting opening were target of high concrete pressure, which can be concluded because at these joints the largest bubbles occurred. This assumption is strengthened by the fact that the same sealing type at the joint 6-7, which is the opposite to the concreting opening, showed no signs of concrete bubbles. One improvement could be that the sealing located next to the concreting opening should be pressed and fixed further into the joint, especially if the large joint width is encountered.

The remaining six joints, which were sealed by using elastomer tubes (EPDM) with a diameter of 30 mm (further described in Section 4.4), demonstrated no unexpected behaviour. The only downside which accompanies this sealing type is the relatively lengthy introduction of the tubes into the joints. Using a smaller diameter of the tube can probably solve this issue.



Figure 5.11: Inner vertical joint sealed by elastomer tube; (a) view from inside; and (b) top view

On the outside all joints were sealed with mortar. The mortar should provide a transmission of compression and shear forces between the element shells while providing the same visual appearance as the double wall elements. Both goals are observed through all tested construction stages, wherein, the influence of the joint flange roughness on the mortar adhesion is tested as well and further described in Subsection 5.3.2. The disadvantages of this sealing type can be encountered with the time consuming applying of the mortar and with the unfavourable cracking behaviour. The appearance of cracks is found to be of interest for evaluation of this type, and because of that, it is further discussed also in Subsection 5.3.2. Additionally, all joint sealing types are compared by highlighting their advantages and disadvantages in Table 5.11.

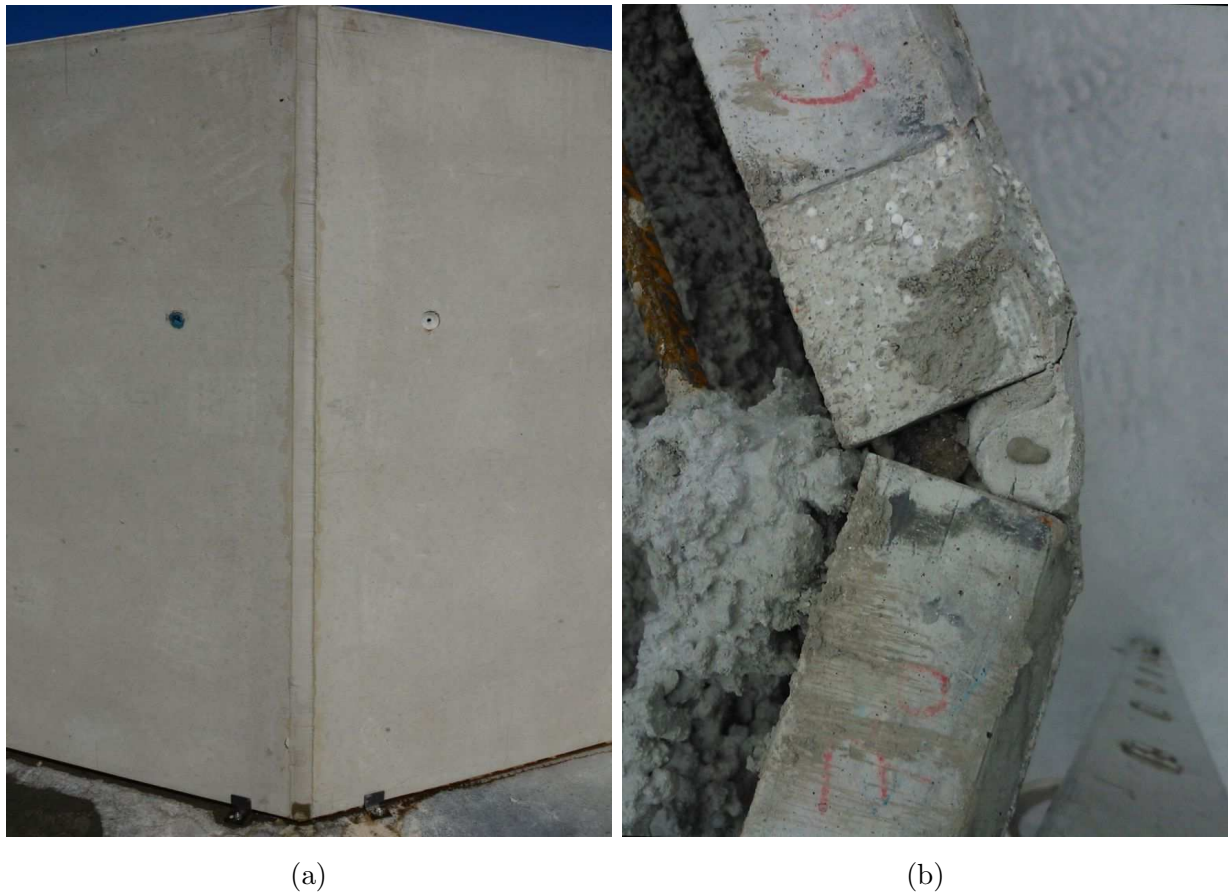


Figure 5.12: Outer vertical joint sealed by mortar; (a) front view from outside; and (b) top view

Table 5.11: Comparison of the tested sealings for inner and outer vertical joints

Type	Advantages	Disadvantages
Glued foil (inner)	<ul style="list-style-type: none"> • installation is independent of the joint width • quick installation 	<ul style="list-style-type: none"> • it is necessary to use glue, which is only applicable under certain environmental conditions (e.g. temperature) • under great pressure the foil can be easily deformed and cause concrete bubbles • glue hardening time has to be taken into account
Elastomer tube (inner)	<ul style="list-style-type: none"> • easy positioning • installation is independent of weather conditions • tubes are not visible from the outside • enable sealing immediately after installation 	<ul style="list-style-type: none"> • various joint widths require different tube sizes • tubes have to be fixed (by e.g. wires and screws) to avoid displacement during all construction phases • afterwards, wires and screws have to be removed
Mortar (outer)	<ul style="list-style-type: none"> • application for all joint widths • mortar is able to conceal imperfections in joint geometry • dried mortar acquires concrete colour of the neighbouring elements (joints are merged in construction design) • mortar enables limited force transmission • once applied, no working steps are necessary after the segment concreting 	<ul style="list-style-type: none"> • rigid sealing is accompanied by the appearance of cracks • long-time performance in comparison to other types • application depends on the weather conditions • it requires a time consuming application • a mortar hardening time has to be taken into account

5.3.2 Evaluation of mortar cracks in joints

During the lifting and concreting of the segment cracks formed in the mortar that is used to seal the outer shell joints. As already described in Subsection 4.1, the flank adhesion of the mortar was tested by using smooth and rough surfaces at the outer shell edges. Such arrangement of the surface pattern was used to examine the force transmission through the joints, which can be identified by studying the crack formations induced by different loads. These crack formations have been recorded through all test phases and the documented in Table 5.12.

Table 5.12: Width of cracks before lifting, after lifting and after concreting.

Table corresponds with crack distribution presented in Fig, 5.13. The used abbreviations S-S, R-R and S-R represent the neighbouring joint properties where S is a smooth and R represents a rough surface.

		Width of cracks					
Joint between elements	Joint type	Before lifting		After lifting		After concreting	
		Width (mm)	Comment	Width (mm)	Comment	Width (mm)	Comment
1-2	S-R	0.0	no cracks	0.2	at the bottom	0.2	no change
2-3	R-R	0.1	thin shrinkage cracks	0.5	along whole height	1.3	cracks growth, same pattern
3-4	R-S	0.0	no cracks	0.7	new cracks along E 4	1.3	cracks growth, same pattern
4-5	S-S	0.0	no cracks	0.0	thin hor. cracks	0.5	new crack along E 4
5-6	S-S	0.1	thin shrinkage cracks	0.2	thin cracks	0.3	cracks growth
6-7	S-S	0.0	no cracks	0.2	new thin cracks	0.4	cracks growth, same pattern
7-8	S-R	0.1	thin shrinkage cracks	0.5	crack growth along E 7	1.3	cracks growth, same pattern
8-9	R-R	0.0	no cracks	0.2	new thin cracks	0.3	cracks growth and new cracks
9-1	R-S	0.0	no cracks	0.0	no cracks	0.2	new cracks
Marked (on figures)		in blue		in red		in green	

To properly assess the influence of the cracks on the structure it is not enough just to provide the width of cracks, but also their distribution over the entire width and height

of the joints. With this in mind, the schematic illustration of the crack disposition due to different load cases is provided in Fig. 5.13.

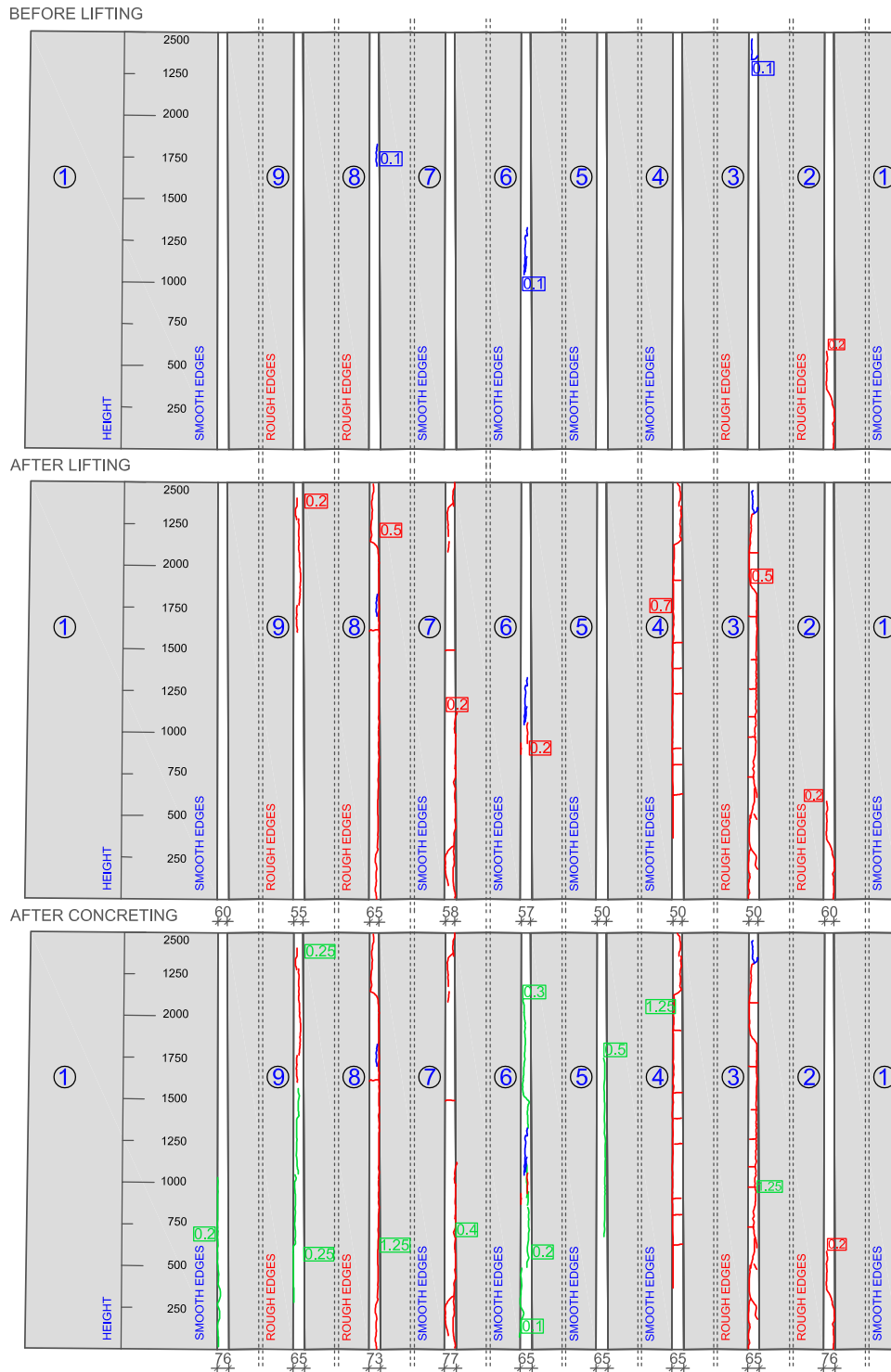


Figure 5.13: Schematic overview of crack distribution along the mortar in the vertical joints before lifting, after lifting and after concreting [mm]

The first significant appearance of the cracks was formed while the test lifting of the segment. The concreting also resulted in the development of new cracks, but the biggest effect was noticed in the growth of already existing ones. One of the most interesting facts is an occurrence of the biggest cracks of both joints around element 3, as well as the one between elements 7 and 8. Comparing these results with the measurements from Subsection 5.2 it can be stated that in these three joints were developed plastic hinges caused by a horizontal loading, which was induced by an imperfect vertical alignment of the lifting chains (Fig. 4.73). For this reason, it is recommended to lift the future segments so that no horizontal loadings occur or to change the design of interconnections of the outer element shells in a way that no hinges can develop. The latter possibility can be realised by using a interconnection that connects both outer and inner shells, instead of only outer ones.

The other issue concerning the mortar flank adhesion revealed not a complete insight, and therefore, mostly tendencies can be stated. Observations of the joints between element 5-6 and 8-9 (presented in Fig. 5.13 and 5.14) indicate that in the joints with flanks of the same roughness, cracks in mortar tend to rise somewhere in-between the flanks. Contrary to that, the joints with different edge surface tend to form the cracks grow along the smooth flank (e.g. joints between elements 3-4 and 7-8 presented in Figures 5.13 and 5.14). In this context it has to be highlighted that at the position of the welded interconnection at the bottom and the top of the elements, the cracks tended to change their path and sometimes switched the flank side.



Figure 5.14: Cracks pattern for different edges surfaces of outer shell; (a) type R-R: joint between elements 3-2; (b) type S-R: joint between elements 4-3; and (c) type S-S: joint between elements 6-5

5.3.3 Joint deformation measurement during the concreting of the segment

To estimate the effects of concrete pressure on the mock-up geometry, the joint deformation during concreting is measured at three vertical joints. These joints were chosen to be positioned symmetrically around the segment (Fig. 5.15). Wherein, each of the joints, located between elements 3-4, 6-7 and 1-9, were equipped with five LVDT sensors over the segment height. The LVDT (Linear Variable Differential Transformer) is an electromechanical transducer that converts a linear displacement into a corresponding electrical signal. These sensors were distributed over the height so that the top and the bottom sensors were positioned over the centre of the welded interconnections, while the residual three sensors were equally distributed in between (Fig. 5.16).

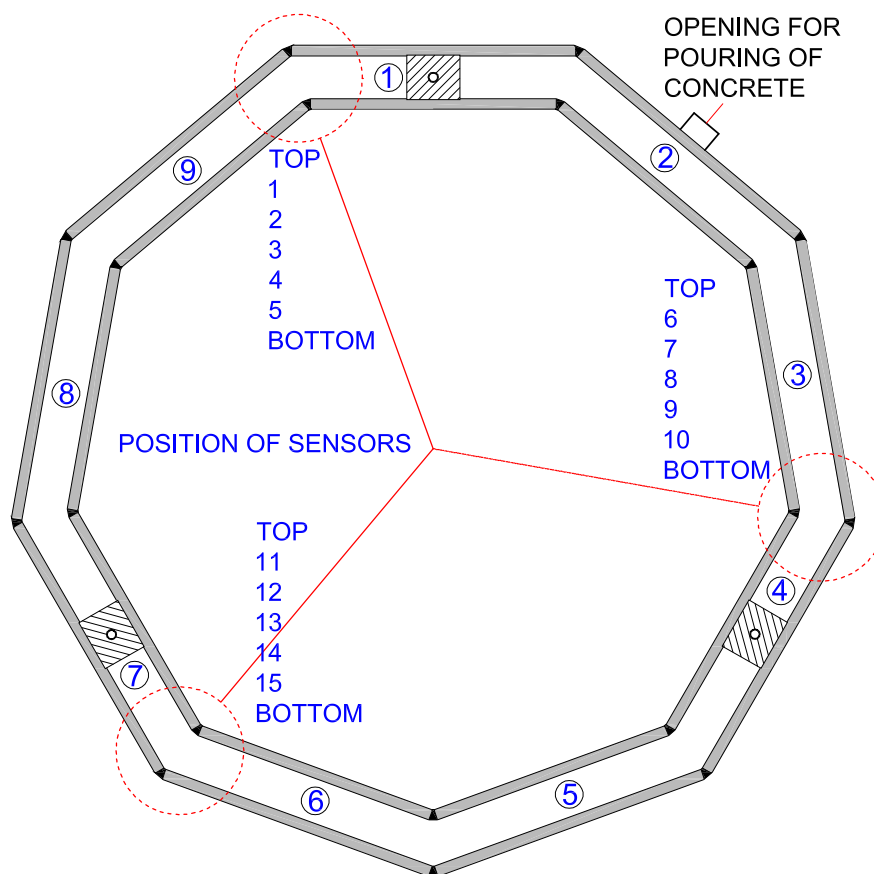


Figure 5.15: Arrangement of the LVDT sensors- top view

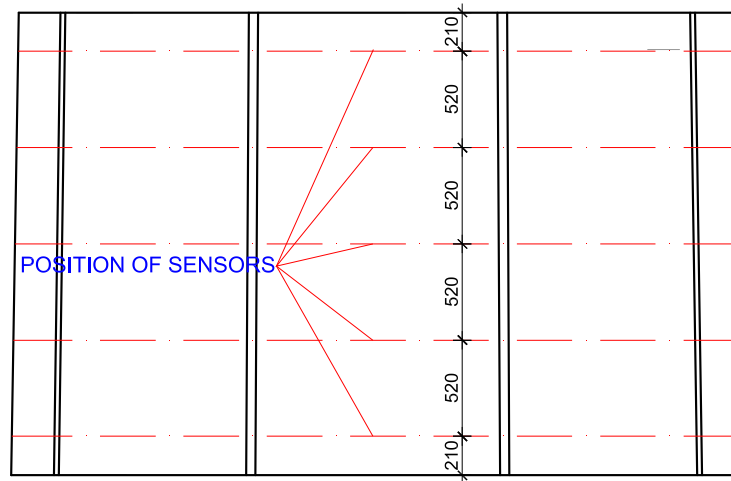


Figure 5.16: Arrangement of the LVDT sensors over the ring segment height [mm]

The sensors were glued to wooden pieces, so that deformation in tangential direction of the outer circumference can be measured (Fig. 5.17). A hot glue is used because it is very brittle and show nearly no deformation, and therefore, its influence on the measurement is minimized. While placing, the sensors have to be pre-tensioned to provide the observation of the deformations in all directions. Once all sensors are placed they are connected to a converter unit which send converted displacement data to a computer (Fig. 5.18).

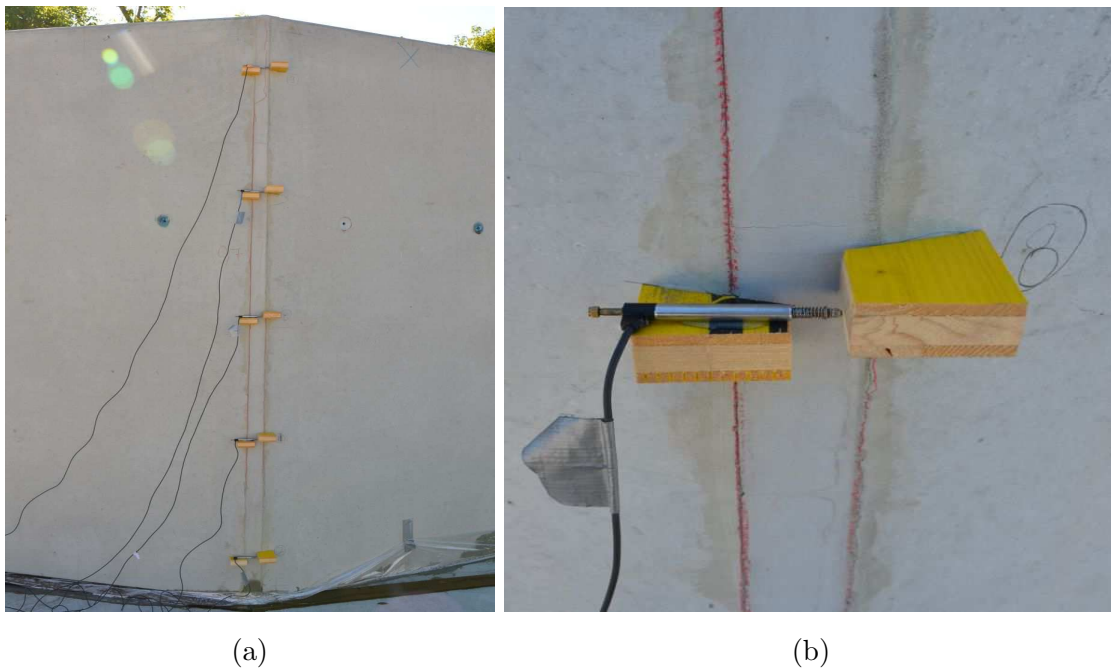


Figure 5.17: LVDT sensors; (a) arrangement over the height of a vertical joint; and (b) detail view of one sensor



Figure 5.18: Installed and connected measuring equipment

The measuring of the tangential deformation of each joint as a function of time during concreting is recorded and illustrated in the following graphs (Fig. 5.19-5.21). During the measurement, two sensors (LVDT 7 and 12) failed due to malfunction in the data cable and an electrical overload of the data cable because it got wet. The values in the presented diagrams represent a shrinkage if they are positive and an expansion if they are negative.

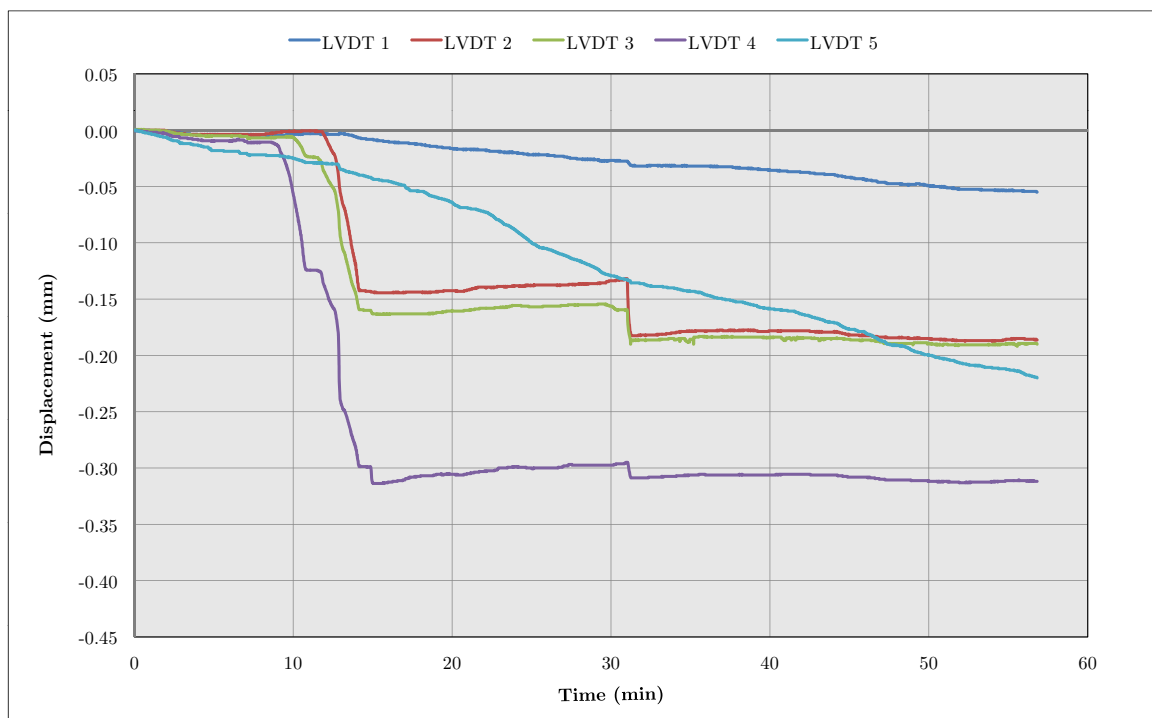


Figure 5.19: Displacement of the vertical joints between elements 1-9

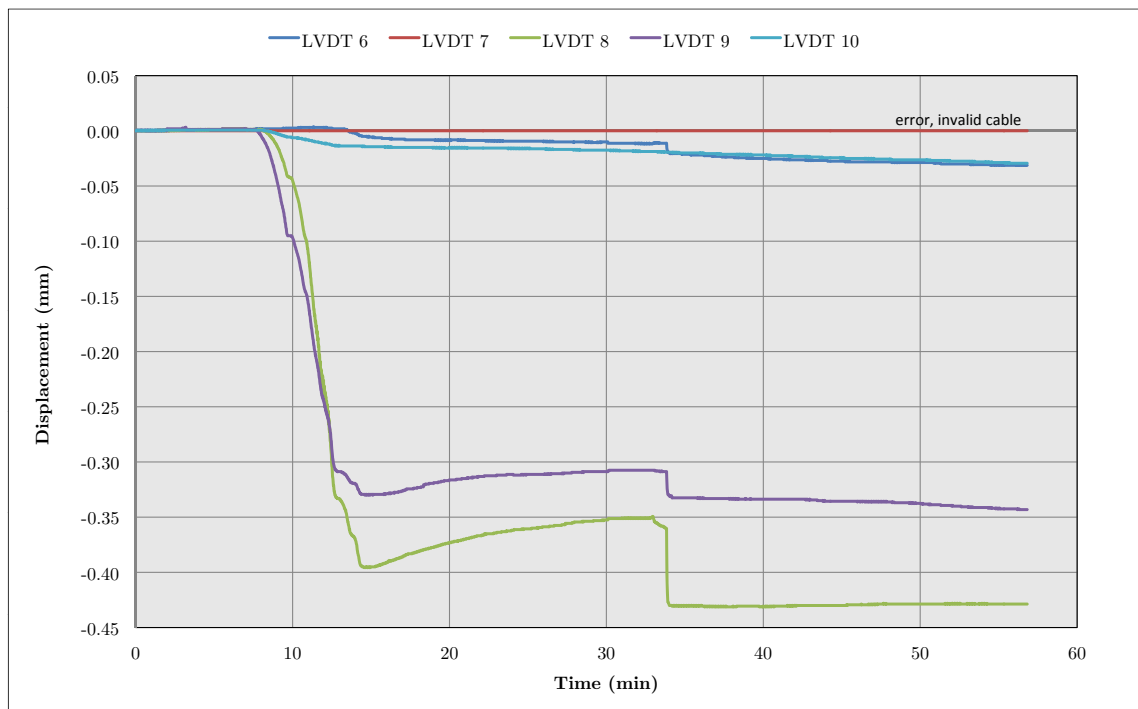


Figure 5.20: Displacement of the vertical joints between elements 3-4

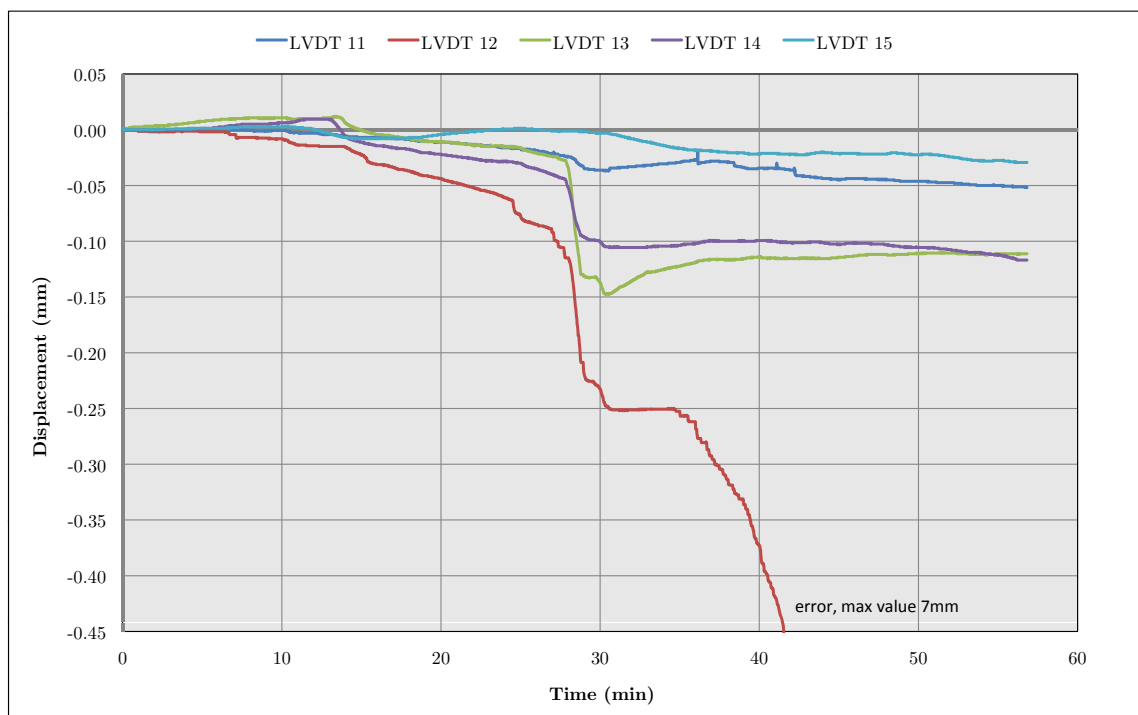


Figure 5.21: Displacement of the vertical joints between elements 6-7

The presented results (Fig. 5.19, 5.20 and 5.21) show the concreting history:

- Phase 1: from minute 10-15 the concrete was pumped under pressure through the opening in the element 2 (first jump in the diagrams 5.19- 5.21)
- Phase 2: afterwards, concrete was poured from the top (second jump in the diagrams)

Herein, it can be seen that the joints between elements 1-9 and 3-4 (near the concrete opening) were rapidly exposed to the pressure, while the joint 6-7 (opposite to the concrete opening) was gradually loaded with pressure because of the time that was needed for concrete to reach that part of the ring. If self-compacting concrete had been used, pressure would be more equally distributed on all vertical joints. Moreover, the biggest displacements are obtained in the middle area of the joint, although the pressure is the highest at the bottom of the segment (Fig. 5.22). This could be the outcome of boundary conditions, because the welded connections between the elements at the bottom do not permit the deformation of the joints, while at the middle area there is no connection to resist the concrete pressure.

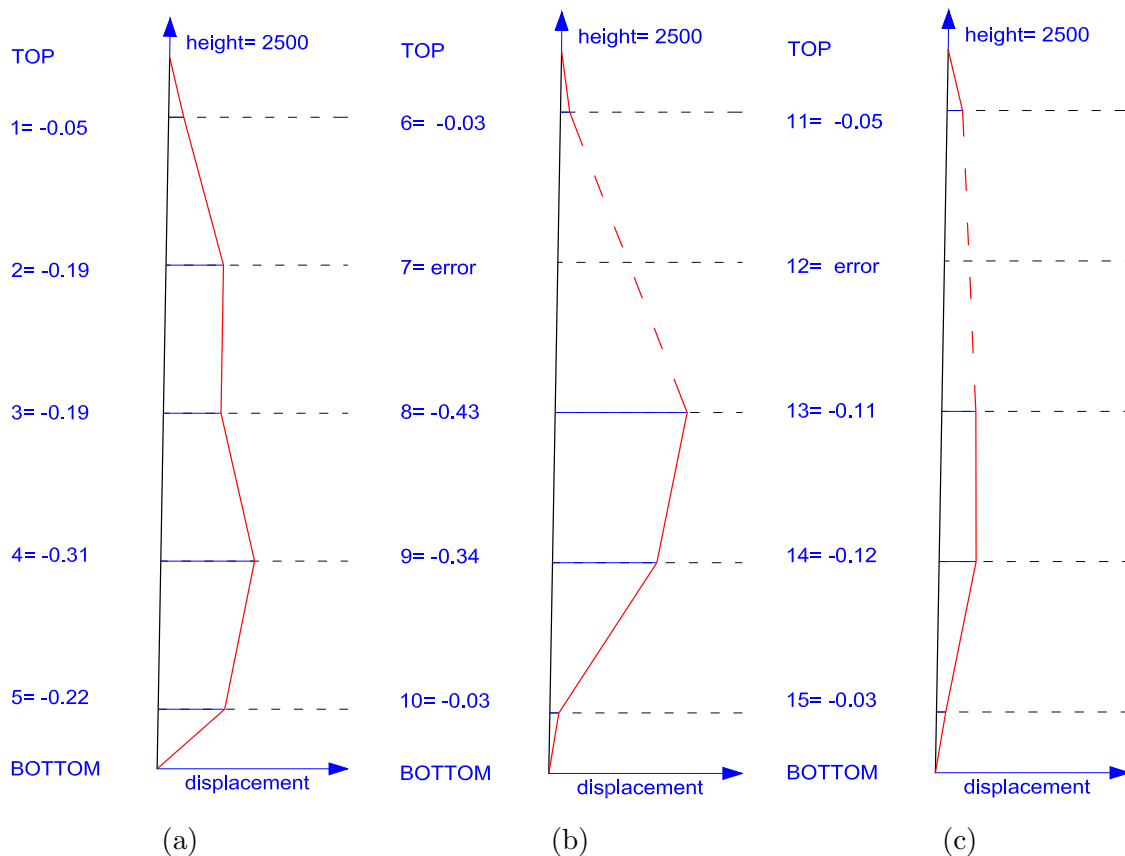


Figure 5.22: Deformation of final displacement after concreting of the mock-up [mm]; (a) joint between elements 1-9; (b) joint between elements 3-4; and (c) joint between elements 6-7

With respect to the maximum intensity of the measured pressure, it can be noted that the displacement of the joints that are located around the concreting opening is almost three times larger than for the joint that is situated on the opposite side (Table 5.13). Based on these results one can conclude that the maximum pressure is applied on the vertical joints that are in close proximity to the concreting opening, despite to the fact that the concrete should be equally spreading around the ring segment during concreting.

Table 5.13: Maximum tangential displacement of the vertical joints after concreting regarding the location of concreting opening

Joint between elements	Maximum displacement of the joints (mm)	Position regarding to the concreting opening
1-9	0.31	right
3-4	0.43	left
6-7	0.12	opposite

Chapter 6

Summary, conclusions and outlook

This thesis presents a study about a new construction method to build concrete wind towers out of double wall elements developed at the Institute for Structural Engineering at Vienna University of Technology. The aim is to examine the constructability of the proposed building technique and to identify resulting technological challenges that oppose to the construction of a prototype wind tower.

The rising demands for wind energy led to the development of precast concrete wind towers that demonstrated better structural properties and a higher cost-effectiveness in comparison to formerly common steel towers. The nowadays conventional precast solutions are confronted with a complicated transportation of long elements to construction sites that are difficult to reach. In contrast, the herein proposed wind tower design out of double wall elements combines the advantages of lightweight precast elements and in-situ concrete. This approach tries to offer a sustainable and more economical tower structure in comparison with present wind tower designs out of full bodied precast concrete elements.

In order to evaluate the aforementioned claims about the feasibility and sustainability of the prototype, the mock-up ring segment is built, tested and analysed for certain load cases. Herein, emphasis is given on the tolerances of the produced double wall elements and the achieved mock-up segment geometry. In addition, a variety of technical solutions has been tested and evaluated.

The presented results in the Section 5 imply that the tested mock-up in general meet the desired aforementioned claims about the functionality of the proposed tower structure and feasibility of the new construction method. However, the performance of certain technological solutions showed the defects that have to be considered in the future.

Taking a detailed look at the performance of the single elements, following judgements and suggestions of improvement can be made:

- Some elements were equipped with special embedments which are accompanied by several downsides. The number of these partly individual embedments need to be minimized in order to accelerate the production process and so making it cheaper. This could be managed when embedments are merged without any increase of reinforcement volume.

Moreover, the embedments are capable of interfering the merging process of the concrete shells, which results in a bigger element thickness and a possible horizontal shift between shells. Both consequences are encountered at the elements by causing too big or too narrow vertical joints. Especially the concrete blocks in every third element jammed and caused a greater element thickness than planned. Therefore, a quality planning and survey needs to be established to ensure that no embedment get in the way while merging of the concrete shells.

- It is determined that all elements are heavier than planned. A closer look on the production process shows that the required concrete volume is generally placed by an automated concrete bucket. However, any blank spots with insufficient concrete (e.g. corners) are filled manually, which increase the concrete volume. This results in too thick concrete shells and consequently in too heavy elements that have an influence on the transport vehicles and the crane capacity at the building site. One suggestion to avoid this overweight is to reduce the initially planned amount of concrete that is placed automatically by approximately 12% (see also Table 5.7).

The evaluation of the erection process and the gained test segment revealed new technological challenges which can be opposed by following suggestions of improvement:

- One of the most complicated tasks in the assembly process is to arrange the elements in the right position and to angle them as planned while providing a certain accuracy, which is vital for high tower structures. This task was confronted by several difficulties. At first, the foundation did not provide the desired horizontal planar surface which is needed in order to avoid any collision problems at the vertical joints

between the elements. Although the foundation was produced properly, the uneven shrinkage of the concrete resulted in valleys that formed on the surface. This can be improved by the use of concrete containing additives which minimise the shrinkage and a proper aftertreatment. Alternatively, the horizontal plain can be provided by a steel construction which usually provides a much higher accuracy compared to concrete. The second big difficulty encountered at the assembly was that the measuring of the inclination at the building site is a very complex venture. It could be that some deviations had their root in imperfect measurement of the element angle.

- The evaluation of the shell interconnection showed that the designed welding connection is capable of keeping the segment together during lifting and concreting. Nevertheless, deformations in an unexpected range are encountered. These deviations are formed mostly during the lifting process and made themselves most of all visible by the crack growth in the outer mortar fillings of the joints. To avoid this effect in the future it is suggested to either lift the segment perfectly vertically or if horizontal loading can not be excluded while lifting, the interconnection of the elements has to be redesigned in order to bear this loading.
- The vertical joints between the elements are sealed by three different sealing types. All three types fulfilled their function although some specialities can be emphasized. The outer sealing out of mortar was on the one hand confronted with time consuming applying and tendency to accumulate cracks if it is loaded too high. On the other hand this sealing type transmits shear and normal force and a uniform visual appearance of the segment without visible joints is gained.

A closer look on the foil sealing reveals that the application is simple and allows to bridge joints with unexpected large widths. Nevertheless, it was observed that joints loaded with a high pressure, as the one near to the concreting opening, formed concrete bubbles. Therefore, a better attachment of the foil in such sections has to be assured.

The last tested sealing type using elastomer tubes sealed the joints properly. The only downside is the lengthy introduction of the tubes into the joints, which probably can be resolved by using an anti-friction agent.

List of Figures

2.1	Growth in the size of the wind turbines since 1985, taken from [2]	4
2.2	Components of a horizontal-axis wind turbine, taken from [3]	5
2.3	Configuration of the most important tower designs	6
2.4	Relation between height and output capacity of a wind turbine, taken from [5]	7
2.5	Steel tower; (a) bolt connection between segments, taken from [7]; and (b) rolled 40 mm thick steel sheet, taken from [8]	8
2.6	Transportation of a steel tower segment, taken from [9]	8
2.7	Guyed steel towers; (a) with a tubular design, taken from [10]; or (b) with a lattice design, taken from [11]	9
2.8	Steel lattice towers; (a) Fuhrländer Wind Turbine Laasow, taken from [12]; and (b) one bolted connection in Wind Turbine Laasow, taken from [13] . .	10
2.9	Fuhrländer Wind Turbine Laasow in Germany, taken from [14]	11
2.10	In-situ slip form method, taken from [17]; (a) concrete tower; (b) slip formwork; and (c) working platform in slip formwork	13
2.11	Inneo towers, taken from [18]; (a) transportation of precast elements; (b) erection of precast elements; and (c) the first assembly phase of a concrete tower	14
2.12	Inneo towers in assembly process, taken from [18]; (a) working environment; (b) tower erection; and (c) assembled wind turbine	14
2.13	Enercon market share, taken from [19]; (a) in Germany 2013; and (b) worldwide 2013	15
2.14	Enercon E-126, taken from [22]	16
2.15	Enercon E-126 during construction, taken from [18]; (a) concrete ring segments from the air; (b) assembly process; and (c) erection of the nacelle . .	17
2.16	ATS wind tower during construction, taken from [18]; (a) assembling process; (b) placing of the nacelle; and (c) assembled tower	18

2.17	Prefabricated modular tower, taken from [29]; (a) element with strut; (b) pre-assembled tower segment; and (c) tower assembling	24
2.18	Prefabricated modular tower, taken from [30]; (a) and (b) proposed details of vertical joint; (c) assembled tower; and (d) cross-section	25
2.19	Prefabricated modular tower, taken from [31]; (a) longitudinal cross-section; (b) and (c) proposed horizontal cross-sections of ring segment	26
2.20	Method for producing concrete pre-finished parts, taken from [32]; (a) milling head in operation; (b) working platform for the polishing; and (c) tower assembly process	27
2.21	Tower structure, taken from [33]; (a) cross-section of a ring segment; and (b) longitudinal section of the tower	28
3.1	Horizontal section through a schematic polygonal ring segment	30
3.2	Model for prototype- 130 m tall wind tower	31
3.3	Front elevation of the prototype [mm]	32
3.4	Top view of the prototype tower [mm]	33
3.5	Double wall elements of the proposed prototype tower [mm]	34
3.6	Schematic overview of the construction process and accompanying structural challenges. All solution that will be tested for the mock-up are highlighted red.	36
3.7	Double wall element with; (a) lattice girders; and (b) Kappema elements, taken from [36]	37
3.8	Connection of elements in a ring segment by embedments and bolts; (a) connection of two elements; and (b) enlarged view	39
3.9	Placing of the horizontal reinforcement by pulling it trough external vertical joints with hooks; (a) phase 1; and (b) phase 2	40
3.10	Pre-assembling of half segments in order to provide reinforcement in all vertical joints	41
3.11	Reinforcement of the last two vertical joints provided by steel cable loops; (a) positioning of the last element; and (b) installation of the vertical steel bars	42
3.12	Arranging of prestressed tendons in order to secure the set up geometry and as alternative horizontal reinforcement	43
3.13	Outer shells of the elements with embedments connected by welds	44
3.14	Flexible tubes as sealing for internal vertical joints; (a); (b); and (c) possible geometries of the joints [mm]	45

3.17	Flexible tubes as sealing for external vertical joints; (a) initial position of the pipe before concreting; and (b) deformed shape of the pipe due to concreting [mm]	46
3.15	Concreting grout or mortar as sealing for inner vertical joint [mm]	47
3.16	Formwork as sealing for inner vertical joints [mm]	47
3.18	Flexible tubes as sealing for external vertical joints; (a); (b); and (c) different geometries [mm]	48
3.19	Sealing of external and internal vertical joints by halvings; (a); and (b) different geometries sealed with swelling tape [mm]	49
3.20	Lifting a segment with a lifting beam	50
3.21	Lifting a segment with angled chains	51
3.22	Proposal of formwork for horizontal joint [mm]	52
3.23	Proposal of scaffolding and crane arrangement used in Patent [34]	53
3.24	Proposal of climbing formwork used in Patent [34]	54
4.1	Mock-up segment: front elevation and characteristic cross-sections [mm] . .	58
4.2	Overview of different element types	59
4.3	Arrangement of steel cable loops at the edge of the elements [mm]	61
4.4	Detail of opening for concreting [mm]	62
4.5	Characteristic arrangement of the reinforcement and Kappema waves in the elements [mm]	63
4.6	Detail of one concrete block [mm]	64
4.7	Schematic position of smooth and rough surface edges	65
4.8	Detail of internal vertical joints; (a) glued foil as sealing; and (b) elastomer tube as sealing [mm]	66
4.9	Detail of outer vertical joint [mm]	67
4.10	Proposed simplified mock-up geometry in the form of a double shell polygon, interconnected at the edges which are hinged around the global z direction	72
4.11	Extracted polygonal shell with suggested support conditions	73
4.12	Extracted polygonal shell with restrained rotation	73
4.13	One sixth of a polygon with introduced supports reactions that represents the neighboring polygonal sides	74
4.14	Support conditions of the hexagon model	74
4.15	Hexagon model with concrete pressure load and simplified approximation for the bending and strain stiffness	75

4.16	One sixth of the hexagon extracted from the whole model showing the geometrical relation between the elongation of length and radius, as well as the relation between normal force, shear force and the support reactions	76
4.17	FEM model showing the hexagon model loaded by an assumed concrete pressure of 80 kN/m (dimensions in [m])	80
4.18	Plotted results of internal normal forces in the shells [kN]	81
4.19	One sixth of the FEM model showing the internal forces in interconnection [kN]	82
4.20	Concrete pressure on one double wall element when the whole height is concreted at once	83
4.21	Modeled system with loading, internal forces and support reactions of a one meter wide element strip; (a) loading by concrete pressure [kN/m]; (b) moments [kNm]; (c) shear forces [kN]; and (d) reaction forces [kN]	84
4.22	Relevant cross-section used in the structural analysis of the mock-up	85
4.23	Estimation of effective pressure height; (a) support reaction forces; and (b) equilibrium of support reaction and linear load [cm]	86
4.24	Geometry and loading of the relevant horizontal cross-section modelled in RFEM [kN/m]	88
4.25	Resulting moments of the relevant horizontal cross-section modelled in RFEM [kNm]	88
4.26	Resulting normal forces in Kappema elements [kN]	89
4.27	Resulting normal forces in concrete shells [kN]	89
4.28	Resulting shear forces in concrete shells [kN]	89
4.29	Closer view on the vertical strip loading with chosen reinforcement position [mm]	92
4.30	Closer view on the horizontal strip loading with chosen reinforcement position [mm]	94
4.31	Formwork robot	100
4.32	Formwork robot placing the lateral formwork profiles	101
4.33	Formwork robot activating the fixing magnets	101
4.34	Manually placing of styrofoam profiles; (a) gluing; (b) arranging of the glued profiles; and (c) finished formwork	102
4.35	Placing of the spacers and spraying of oil layer on working pallet; (a) placing of plastic spacers; and (b) oiling of the pallet	102
4.36	Automated placing of the reinforcement	103

4.37	Reinforcement and embedments placed in the outer shell of the elements used for mock-up; (a) plastic anchors that are used to attach screw bracings; (b) opening for concreting; (c) welding embedments for the connection of arranged elements; (d) standard lifting hooks; and (e) finished formwork of the first shell prepared for following stage	104
4.38	Concreting of the elements; (a) side view of the concrete spreader; (b) bottom view of the concrete spreader; and (c) formwork filled with concrete	105
4.39	Concrete blocks arranged in every third element of the mock-up segment; (a) concrete blocks; (b) positioning of the blocks; and (c) concreted blocks positioned in vibrated concrete shell	106
4.40	Fixing of the first shell in the turning device; (a) hardened concrete shell; and (b) concrete shells fixed in turning device by steel arms	107
4.41	Lifting of the pallet with the first shells from the day before	108
4.42	Positioning of the pallet with the recent concreted second shells	108
4.43	Rotation of the upper pallet by 180°	108
4.44	Descending of the upper shell into the lower one	109
4.45	Merged double wall elements	109
4.46	Double wall elements after merging	110
4.47	Storage and curing area of the double wall elements	110
4.48	All nine double wall elements transported to the building site and ready to be put together to form a mock-up segment	111
4.49	Foundation of the mock-up; (a) concreting by a concrete truck (b) polishing of the concrete; and (c) finished foundation	112
4.50	Determination of the foundation centre; (a) diagonally positioned ropes; (b) central- reference nail; and (c) nail gun Hilti DX 460	113
4.51	Marking of the circumcircles; (a) wooden plank; and (b) marking pencil attached to the hole in the plank	114
4.52	Wooden planks for the easier arranging of the elements	115
4.53	Positioning of one double wall element; (a) transport of the element with the crane; and (b) manually positioning of the elements while landing	115
4.54	Arrangement of one double wall element; (c) adjustment of the element; and (d) positioned element prepared for inclination	116
4.55	Aids at the element arrangement; (a) steel L-profiles; and (b) marked middle point on the foundation and the element	116
4.56	Installation of the screw bracings; (a) into the element; (b) into the foundation; and (c) placed bracings	117

4.57	Measuring of the inclination; (a) wooden plate in the upper left corner; and (b) measuring of the rope distance by using a steel wire	118
4.58	Horizontal reinforcement in the ring segment direction; (a) welded to vertical bars; (b) placed into one element; and (c) hooked to the U-reinforcement at the top of the element	119
4.59	Positioning of the second element; (a) element hovers above ground; (b) horizontal pushing of the element toward the first one; and (c) two arranged elements	119
4.60	Arranged and supported half ring segment- view from inside	120
4.61	Arranged and supported half ring segment- view from outside	120
4.62	Assembled ring segment without the last element	121
4.63	Positioning of the last double wall element; (a) positioning of the last element with the crane; and (b) last element at its foreseen position	121
4.64	Steel cable loops; (a) loops hidden in the elements; (b) pulled out loops; and (c) reinforcement bar placed in the overlapping of the loops	122
4.65	Structural connection of the elements; (a) reinforcement bar welded to the steel plate embedments of the outer shell; (b) bottom connection; and (c) top connection	123
4.66	Sealing of the outer vertical joints with mortar; (a) placing of sponge tubes to prevent mortar leakage; (b) placed sponge tubes; (c) manually filling of the joints with mortar; and (d) top view of filled joint	124
4.67	Vertical joints with embedded EPDM tubes; (a) installed tubes; (b) wires tied to screws; and (c) top view	125
4.68	Inner vertical joints with glued water-resistant foil; (a) application of the glue; (b) glued concrete surface; (c) joint with glued foil	125
4.69	Steel adapter for the concreting; (a) embedment in concrete element with threaded sleeves; and (b) adapter fixed at the segment	126
4.70	Assembled mock-up with bracings	126
4.71	Assembled mock-up without bracings	127
4.72	Top view of the assembled mock-up	127
4.73	Lifting set up; (a) top view of the segment with lifting set up; and (b) side view of the segment with lifting set up	128
4.74	Lifting of the ring segment; (a) segment in the air; (b) lifted segment with placed plastic foil; and (c) lifting beam (l= 240 cm)	129
4.75	Concreting of a 10 cm high layer of concrete C 30/37; (a) lifting of the basket; and (b) pouring of the concrete from basket	130

4.76	Adapters and additional equipment for connection of the concrete pump; (a) adapter and connection equipment without the concrete pump connector; and (b) assembled connection	131
4.77	Concreting of the mock-up; (a) under pressure from below; and (b) from above	132
4.78	Concrete pump set up equipped with spiral bar that pushes the fresh concrete out of the adapter; (a) closed panel and prepared bar of the filler neck; and (b) open panel and screwed bar of the filler neck	133
4.79	Concrete pump opening after concreting	134
4.80	Top view of concreted ring segment showing the accessibility of the concrete blocks	134
5.1	Planned dimensions of the double wall element	136
5.2	Measuring of the element weight; (a) set up for the measuring of the weight; (b) pressure cells with underlying steel plate and data cable; and (c) positioning of the elements	144
5.3	Top section of the mock-up segment with marked distances L1, L2 and L3 measured at all relevant construction phases (assembly, lifting and concreting)	147
5.4	Comparison of planned and achieved upper inner polygon of the segment section [mm]	148
5.5	Position of lifting beams and points [mm]	150
5.6	Width of the internal vertical joints before lifting, after lifting and after concreting of the ring segment [mm]	151
5.7	Position of the different inner and outer sealing types tested in the mock-up	153
5.8	Inner vertical joints sealed by glued foil; (a) between elements 1-2; (b) between elements 1-9; and (c) between elements 6-7	154
5.9	Characteristic top view of inner vertical joints sealed by glued foil	155
5.10	Vertical joint sealed by foil between the elements 1-2: (a) after removing of the foil; and (b) enlarged view of the bottom area	155
5.11	Inner vertical joint sealed by elastomer tube; (a) view from inside; and (b) top view	156
5.12	Outer vertical joint sealed by mortar; (a) front view from outside; and (b) top view	157
5.13	Schematic overview of crack distribution along the mortar in the vertical joints before lifting, after lifting and after concreting [mm]	160

5.14	Cracks pattern for different edges surfaces of outer shell; (a) type R-R: joint between elements 3-2; (b) type S-R: joint between elements 4-3; and (c) type S-S: joint between elements 6-5	162
5.15	Arrangement of the LVDT sensors- top view	163
5.16	Arrangement of the LVDT sensors over the ring segment height [mm] . . .	164
5.17	LVDT sensors; (a) arrangement over the height of a vertical joint; and (b) detail view of one sensor	164
5.18	Installed and connected measuring equipment	165
5.19	Displacement of the vertical joints between elements 1-9	165
5.20	Displacement of the vertical joints between elements 3-4	166
5.21	Displacement of the vertical joints between elements 6-7	166
5.22	Deformation of final displacement after concreting of the mock-up [mm]; (a) joint between elements 1-9; (b) joint between elements 3-4; and (c) joint between elements 6-7	167

List of Tables

2.1	Embodied mass of CO ₂ by mass of material kgCO ₂ /t, taken from [15] . . .	21
2.2	Embodied mass of CO ₂ for 70 m tall tower, taken from [15]	21
2.3	Comparison of steel and concrete tower designs, taken from [4]	22
4.1	Recommended structural classification adjustment, taken from EN 1992-1-1, page 50, Table 4.3N [41]	70
4.2	Values for the minimum cover regard to the durability of steel reinforcement steel in accordance with EN 10080, taken from EN 1992-1-1, page 51, Table 4.4N [41]	70
4.3	Strength and deformation characteristic of concrete C 30/37, according to [41]	90
4.4	Partial factors for materials for ultimate limit state, according to [41] . . .	90
4.5	Pull out strength of Kappema sticks form experiments performed at TU Graz [46]	98
5.1	Comparison of the planned and measured element widths	137
5.2	Comparison of the planned and measured height of the elements	138
5.3	Comparison of the planned and measured shell thicknesses- measured at the bottom section	139
5.4	Comparison of the planned and measured thickness of the shells- measured at the top section	140
5.5	Comparison of the planned and measured thickness of the elements	141
5.6	Comparison of the planned and measured horizontal displacement of the shells	142
5.7	Comparison of the planned and measured weight of the elements	145
5.8	Comparison of planned and measured distances L1, L2 and L3, as defined in Fig. 5.3, between the three reference points	147
5.9	Comparison of the planned and measured length of polygon sides of the upper inner segment section	149

5.10	Comparison of internal vertical joint widths before and after lifting of the mock-up	152
5.11	Comparison of the tested sealings for inner and outer vertical joints	158
5.12	Width of cracks before lifting, after lifting and after concreting. Table corresponds with crack distribution presented in Fig, 5.13. The used abbreviations S-S, R-R and S-R represent the neighbouring joint properties where S is a smooth and R represents a rough surface.	159
5.13	Maximum tangential displacement of the vertical joints after concreting regarding the location of concreting opening	168

Bibliography

- [1] European Commission- Climate Action.
http://ec.europa.eu/clima/policies/brief/eu/index_en.htm, accessed 26 of July.
- [2] International Renewable Energy Agency. *Renewable Energy Technologies- Cost Analysis Series*. 2012. Volume 1, Power Sector, Issue 5/5, Wind Power.
- [3] Vertical Axis Wind Turbine.
<http://adamslegion.com/wind-power-advantages/vertical-axis-wind-turbine/>, accessed 14 of April, 2014.
- [4] Eric Hau. *Wind Turbines: Fundamentals, Technologies, Application, Economics*. Springer, 2nd edition, 2006.
- [5] Concrete wind towers: a low-tech innovation for a high-tech sector.
<http://www.thisisxy.com/pt/node/58>, accessed 14 of April, 2014.
- [6] World Steel Association. Steel solutions in the green economy: Wind turbines, 2012.
- [7] Manufacturing/installing towers.
http://mstudioblackboard.tudelft.nl/du/wind/Wind%20energy%20online%20reader/Static_pages/manufacture_in_stall_towers.htm, accessed 10 of April, 2014.
- [8] Denmark's Newes Offshore Wind Array.
<http://wagengineering.blogspot.co.at/2011/12/denmarks-newest-offshore-wind-array.html>, accessed 10 of April, 2014.
- [9] National Renewable Energy Laboratory.
http://www.nrel.gov/news/features/feature_detail.cfm/feature_id=1927?print, accessed 6 of April,, 2014.
- [10] Small-WindTurbine.com.
<http://www.small-windturbine.com/Wind-Turbine-Generator-News.htm>, accessed 11 of April, 2014.

-
- [11] Jane's Apple Farm- Wilson NY.
<http://www.cec-energy.com/jane-s-apple-farm-wilson-ny/>, accessed 11 of April, 2014.
- [12] Turbines of the year- Turbines 2.1-3.5 MW.
<http://www.w2e-rostock.de/en/news>, accessed 10 of April, 2014.
- [13] Photos: Is GE's Space Frame Tower the Future of Wind Power?.
<http://theenergycollective.com/hermantrabish/351156/photos-ges-space-frame-tower-future-wind-power>, accessed 10 of April, 2014.
- [14] Wikipedia. *http://en.wikipedia.org/wiki/Fuhrländer_Wind_Turbine_Laa_sow*, accessed 10 of April, 2014.
- [15] The Concrete Centre. *Concrete Towers for Onshore and Offshore Wind Farms*. 2007.
- [16] The Concrete Centre- Slip Form.
http://www.concretecentre.com/technical_information/building_solutions/formwork/slip_form.aspx, accessed 3 of April, 2014.
- [17] The Concrete Centre. *Concrete Wind Towers: Concrete solutions for offshore and onshore wind farms*. 2005.
- [18] Inneo- Precast Concrete Wind Towers. *<http://www.inneotorres.com/web/iConcWind>*, accessed 6 of April, 2014.
- [19] Enercon. *<http://www.enercon.de/en-en/247.htm>*, accessed 6 of April, 2014.
- [20] Enercon. *<http://www.enercon.de/en-en/755.htm>*, accessed 6 of April, 2014.
- [21] Wikipedia. *http://en.wikipedia.org/wiki/Enercon_E-126*, accessed 6 of April, 2014.
- [22] Enercon E-126: The world's largest wind turbine.
<http://subscribe.ru/archive/travel.towatch.construction/201203/19094122.html>, accessed 6 of April, 2014.
- [23] Jürgen Grünberg and Joachim Göhlmann. *Concrete Structures for Wind Turbines*. 2013.
- [24] Close up- the E126 still the world's biggest turbine.
<http://www.windpowermonthly.com/article/1138562/close-e126-worlds-biggest-turbine>, accessed 6 of April, 2014.

- [25] E-126 in Action: Enercon's Next-Generation Power Plant. <http://www.renewableenergyworld.com/rea/news/article/2009/09/e-126-in-action-enercons-next-generation-power-plant>, accessed 6 of April, 2014.
- [26] Prefabricated DYWIDAG Tendons Secure Innovative ATS Hybrid Wind Tower. <http://www.dywidag.co.uk/references/commercial-buildings/innovative-ats-hybrid-wind-tower-germany.html>, accessed 6 of April, 2014.
- [27] Advanced Tower Systems. Concrete-Steel Hybrid Tower from ATS. *Renewable Energy World*, 2009.
- [28] Jorge Jimeno. Concrete Towers for Multi-Megawatt Turbines, February 2012.
- [29] Miguel A. Fernandez Gomez and Jose E. Jimeno Chueca. Patent EP1889988A2. Assembly structure and procedure for concrete towers used in wind turbines, 2008.
- [30] Alfons O. Krautz. Patent D4US5038540. Sectional smokestack, 1991.
- [31] Fragüet J. Montaner and Bernat A. Ricardo Mari. Patent EP 1876316 A1. Prefabricated modular tower, 2008.
- [32] Norbert Hölscher. Patent WO2009/121581A2. Method for producing concrete pre-finished parts, 2009.
- [33] Hans-Peter Andrae, Wolfhart Andrae, Bernhard Goehler, Wilhelm Zellner, and Martin Dipl Ing Krone. Patent DE4023465A1. Tower structure, 1992.
- [34] Johann Kollegger and Maria Charlotte Schönweger. Patent WO2014067884A1. Method for producing a tower construction from reinforced concrete, 2013.
- [35] Johann Kollegger and David Wimmer. Bridge girders made of double walls erected by balanced lift method. *BFT International*, Issue 02, 2014.
- [36] BVT Rausch: Product range. <http://www.bvtrausch.com/>, accessed 6 of April, 2014.
- [37] Kerkstoel double walls- Reinforced concrete double walls. <http://www.kerkstoel2000.be/en/>, 2014.
- [38] Mockup definition. <http://en.wikipedia.org/wiki/Mockup>, accessed 29 of April, 2014.
- [39] <http://www.kr-industriebedarf.at/>, accessed 6 of August, 2014.
- [40] Schöck. <http://www.schoeck-combar.com/>, accessed 7 of July, 2014.

-
- [41] *Eurocode 2: Design of concrete structures- Part 1-1: General rules and rules for buildings*, 2004.
- [42] Reported by ACI Committee 347. *Guide to Formwork for Concrete*, 2014.
- [43] Deutsche Normen (DIN). *Frischbetondruck auf lotrechte Schalugen*, 1980.
- [44] Tomislav Kišiček, Zorislav Sorić, and Josip Galić. Tables for the design of reinforced-concrete profiles. *Gradjevinar 62 (2010) 11, 1001-1010*, 2010.
- [45] Deutsches Institut für Bautechnik. *Halbfertigwand mit Kappema-Bewehrungselementen aus Stahl als Verbindungselement*. Technical report, 2011.
- [46] TU Graz. *Bericht über die Untersuchung von Stahlankern hinsichtlich des Ausziehstandes aus Beton*. Technical report, 2008.
- [47] StekoX. <http://www.stekox.de/start-en.html>, accessed 15 of July, 2014.
- [48] Doka. <http://www.doka.com/web/home/index.en.php>, accessed 15 of July, 2014.